LOAD TESTING DETERIORATED SPANS OF THE HAMPTON ROADS BRIDGE-TUNNEL FOR LOAD RATING RECOMMENDATIONS

James J. Reilly

Thesis submitted to the faculty of
Virginia Polytechnic Institute and State University
in partial fulfillment of the requirements for the degree of

Masters of Science
In
Civil Engineering

Matthew Hardy Hebdon, Chair
Carin L. Roberts-Wollmann
Ioannis Koutromanos

November 29, 2016
Blacksburg, Virginia

Keywords: Deteriorated Prestressed Concrete Girders, Live Load Test, Live Load Distribution Factors, Bridge-Tunnel, Offshore Deflection Measurement System

LOAD TESTING DETERIORATED SPANS OF THE HAMPTON ROADS BRIDGE-TUNNEL FOR LOAD RATING RECOMMENDATIONS

James J. Reilly

ABSTRACT

The Hampton Roads Bridge-Tunnel is one of the oldest prestressed concrete structures in the United States. The 3.5 mile long twin structure includes the world's first underwater tunnel between two man-made islands. Throughout its 60 years in service, the harsh environment along the Virginia coast has taken its toll on the main load carrying girders. Concrete spalling has exposed prestressing strands within the girders allowing corrosion to spread. Some of the more damaged girders have prestressing strands that have completely severed due to the extensive corrosion. The deterioration has caused select girders to fail the necessary load ratings. The structure acts as an evacuation route for the coast and is a main link for the local Norfolk Naval Base and surrounding industry. Because of these constraints, load posting is not a viable option.

Live load testing of five spans was performed to investigate the behavior of the damaged spans. Innovative techniques were used during the load test including a wireless system to measure strains. Two different deflection systems were implemented on the spans, which were located about one mile offshore. The deflection data was later compared head to head. From the load test results, live load distribution factors were developed for both damaged and undamaged girders. The data was also used by the local Department of Transportation to validate computer models in an effort to help pass the load rating. Overall, this research was at the forefront of the residual strength of prestressed concrete girders and the testing of in-service bridges.

LOAD TESTING DETERIORATED SPANS OF THE HAMPTON ROADS BRIDGE-TUNNEL FOR LOAD RATING RECOMMENDATIONS

James J. Reilly

GENERAL AUDIENCE ABSTRACT

According to Federal law, each bridge across the United States must be inspected by a licensed engineer on a biennial cycle – meaning every two years. Roughly every ten years, or when major work is performed such as a bridge widening, a load rating must be performed. During a load rating, licensed structural engineers analyze every structural component of a bridge under various loads. These loads include general traffic loads, heavy design loads, as well as special permit truck loads. For each of these loadings, it is proven whether each structural component has enough strength to withstand the load entering the member. Inspection reports are incorporated into the load rating analysis to account for any deterioration in the members which will lower its strength.

Recently, a load rating was performed on the Hampton Roads Bridge-Tunnel. The Bridge-Tunnel is a 3.5 mile long twin structure located in Southeastern Virginia. Throughout its 60 years in service, the harsh coastal environment has caused extensive deterioration to some of its main load carrying girders. The deterioration has caused the Bridge-Tunnel to fail its load ratings meaning load posting may have to be imposed. This means signs, and possibly security guards, would have to be implemented before the approach ramps preventing trucks over a certain weight limit from entering. The structure acts as an evacuation route for the coast and is a main link for the local Norfolk Naval Base and surrounding industry. Because of these constraints, load posting is not a viable option.

The Bridge-Tunnel is one of the oldest structures of its type so the effects of the deterioration are not well understood causing conservative assumptions to be used within the load rating. This research describes load testing that was performed on the structure to understand the performance and deterioration effects of the bridge. The results and recommendations from this research were used by the load rating engineers to justify assumptions made and help pass the load rating.

Acknowledgements

I would like to extend my gratitude to everyone who has helped and supported me throughout this research project. First, I would like to thank Dr. Hebdon for bringing me onto the project. I am extremely grateful for your confidence in me during the load test preparation. I really enjoyed the freedom to operate throughout the project. To my committee members, Dr. Roberts-Wollmann and Dr. Koutromanos, thank you for your experience and guidance throughout the project.

I would like to extend my deepest gratitude to Ezra Arif Edwin for his relentless effort throughout the project. Thank you for the countless late nights spent preparing for the load tests and helping with the data analysis. Without your assistance, we would have never been ready in time for the load tests. It was a joy having a Kiwi on the research team.

To Carrie Field, Dr. Mokarem, and Uncle Brett, I am extremely grateful for each of you taking the time out of your busy schedules to help during the load test. The extra hands made the instrumentation possible and each of you definitely added to the comic relief of the trips. Thank you to my fellow Hokies who were always around to help with classes: Isaac Groshek, Trevor Szabo, Adrian Tola, and Brandon Gulledge.

Most importantly, I would like to thank my family for their love and support not only through this research, but through my entire life. Without their motivation, I would have never started on the engineering path. Lastly, a special thank you was earned by VDOT for funding the project and for their attention to detail during the load test planning.

TABLE OF CONTENTS

LIST OF FIGURES

LIST OF TABLES

CHAPTER 1 – INTRODUCTION

According to the 2013 American Society of Civil Engineers (ASCE) Report Card on America's Infrastructure, there are 607,380 bridges across the country with an average age of 42 years. Current bridges in service have a typical design life of 50 years. Through their lifetime, these bridges must be inspected, maintained, and load rated to comply with federal laws such as the National Bridge Inspection Standards (NBIS). These laws are set in place to protect the life safety of the American people and to ensure the nation's ability to compete in the global marketplace. Without these bridges, the major metropolitan areas across the nation could not be linked by land which would severely hinder the movement of the millions of commuters and freight that forms the backbone of the American economy.

Routine bridge inspections occur on a biennial cycle, meaning once every two years, while bridges labelled as structurally deficient are inspected every year. Structurally deficient bridges have critical load carrying elements in poor condition due to deterioration or damage, and require significant maintenance, rehabilitation or merit replacement (ASCE 2013). Special inspections can also be scheduled by an owner due to structural, environmental, or human factors such as after hurricanes or vehicular collisions. These types of events may have compromised the integrity of the structure.

Load ratings are another countermeasure to prevent bridge collapse. They are implemented to determine the live load carrying capacity of an existing bridge (AASHTO 2011). Load ratings are performed roughly every ten years or when major work is performed to a bridge. Major work is considered the alteration of a structure that will change the loads or ability to support traffic, such as a widening or partial replacement. Ratings are currently performed in accordance with the 2nd Edition of the Manual for Bridge Evaluation (MBE) which is developed by the American Association of State Highway and Transportation Officials (AASHTO). The MBE requires the most up-to-date inspection findings to be incorporated into the load rating to account for the decreased resistance of the bridge due to damage and deterioration. For various live loads, either design, legal, and permit loads, the load rating will analyze every structural component of the bridge to develop its respective rating factor. A rating factor is essentially a ratio of the factored resistance to the factored load and must be greater than 1 to be satisfactory.

After all components of the bridge are rated for each of the live loads, recommendations for the entire bridge are given to describe the integrity of the structure. Depending on the rating

of the members for the various live load types, load posting may need to be implemented or rehabilitation may be performed to help increase the rating so posting is not required. Typically, as the bridge age increases, the load resistance of the structure will decrease due to deterioration of the members and the loads increase as trucks get larger and design codes change. Load ratings are a quantitative measure to determine what loads the structure is able to withstand in its present state.

Live load tests are sometimes performed in conjunction with a load rating. This testing may reinforce the assumptions made when modelling the bridge during the load rating process, or justify the use of different assumptions. It is common for bridge load ratings based solely on theoretical calculations and modelling to be overly conservative because of the assumptions made in the models (Chajes and Shenton, 2005). These field diagnostic tests act as a means of supplemental procedures in determining the live load capacity of the bridge (AASHTO 2011). In some situations, a controlled live load test can be employed to quantify the response of the bridge and used in conjunction with simple beam line models to better assess the structural integrity of the bridge. In these situations, the load test is more accurate and realistic than high end modelling. This can make it a better allocation of DOT funds since it will most likely be a cheaper alternative. More often, the live load test is used to calibrate the model based on the test results (Chajes and Shenton, 2005). This allows for more data points to be analyzed than just the test data from the field at discrete locations along the bridge.

1.1 Hampton Roads Bridge-Tunnel

The Hampton Roads Bridge-Tunnel (HRBT) is located along the southeastern coast of Virginia and carries I-64 and US-60 over Hampton Roads from Norfolk, VA to Hampton, VA. Hampton Roads is a large natural roadstead (also known as a harbor) fed by the mouths of the Elizabeth River, Nansemond River, and James River and empties into the Chesapeake Bay as shown in Figure 1.

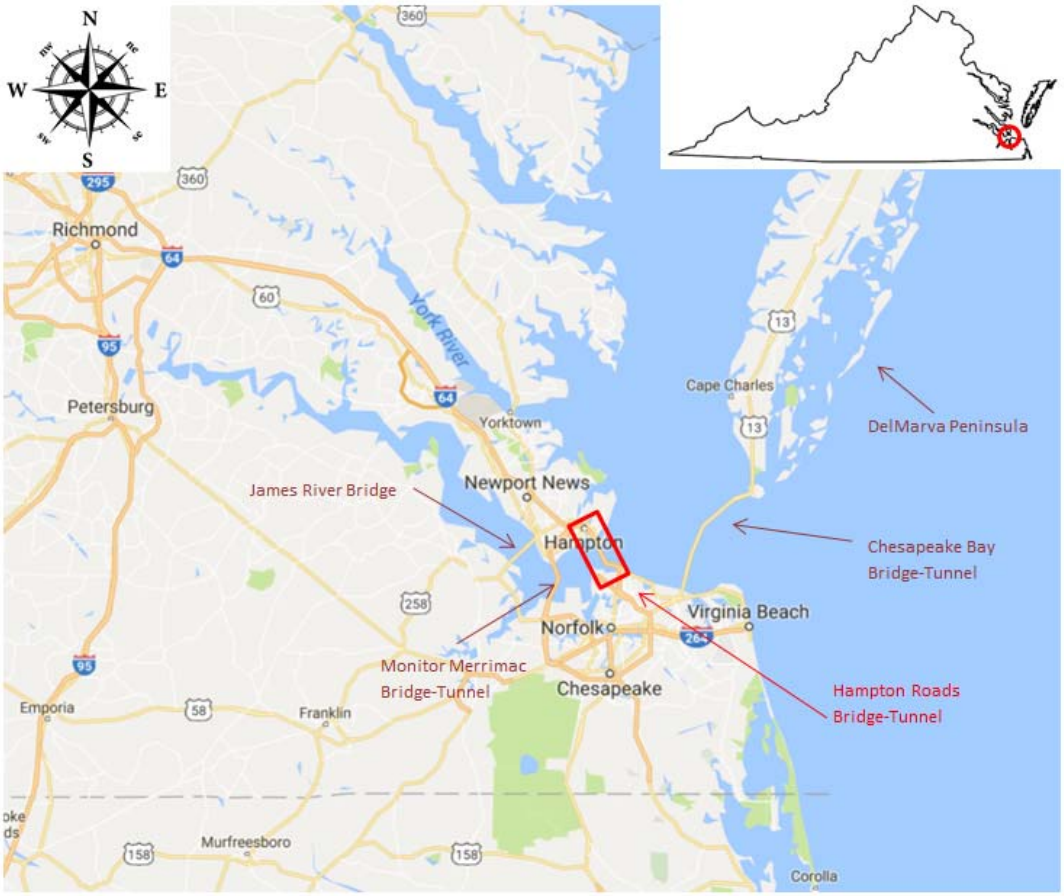

Figure 1: Project Location (Map via GoogleMaps, Images via Google Images)

The roadstead is shielded from ocean swells and rip currents and has relatively deep channels making it a prime location for ships to anchor safely while waiting to enter port. These characteristics allowed Norfolk Naval Base, the largest U.S. naval base, to flourish. As the surrounding areas grew in population, a permanent Hampton Roads crossing became necessary, but the Navy feared an enemy assault on the proposed bridge. The debris from the bridge would block all navigable channels and cripple the US Navy. The solution was a tunnel under the primary navigation channel with approach bridges leading to either end; hence a Bridge-Tunnel

was built. The Hampton Roads Bridge-Tunnel is a 3.5 mile long twin structure. The original crossing was built in 1956 and the second was completed in 1976. In 1995, the original crossing, which is today's westbound structure, was widened by 10 ft on its eastern side. The cross section is shown in Figure 2 looking South from Hampton towards Norfolk.

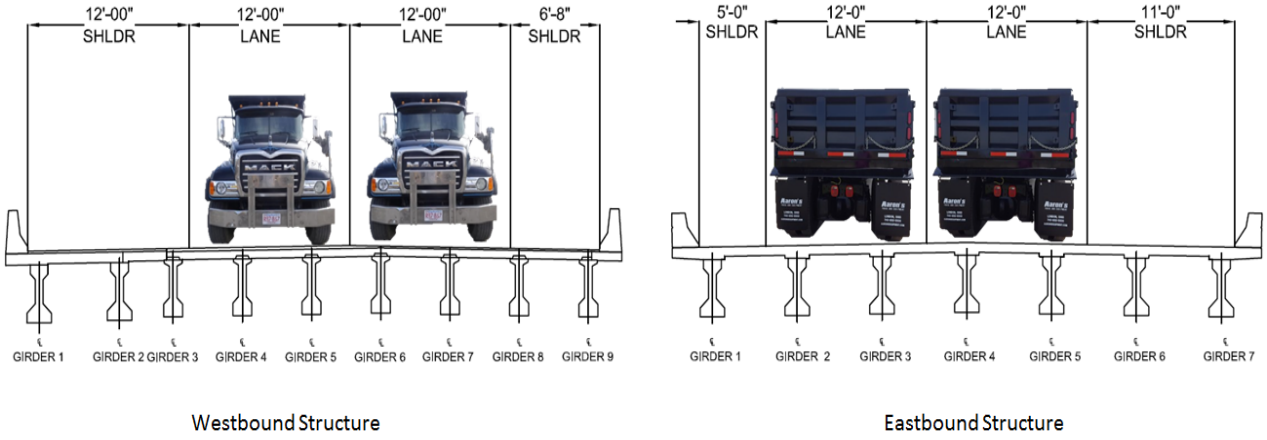

Figure 2: Twin Structure Cross Section

The Bridge-Tunnel is comprised of three main sections: the south approach bridge from the Willoughby Spit to the South Artificial Island; the Tunnel; and the north approach bridge from the North Artificial Island to Hampton, VA. The surrounding area of the Bridge-Tunnel is shown in Figure 3. Each approach bridge is a low level trestle type bridge comprised of simply supported prestressed concrete girders and a concrete deck. It was the world's first underwater tunnel connecting two man made islands. It paved the way for constructing later bridge-tunnels, including the famous Chesapeake Bay Bridge-Tunnel which was constructed just seven years after the HRBT was completed.

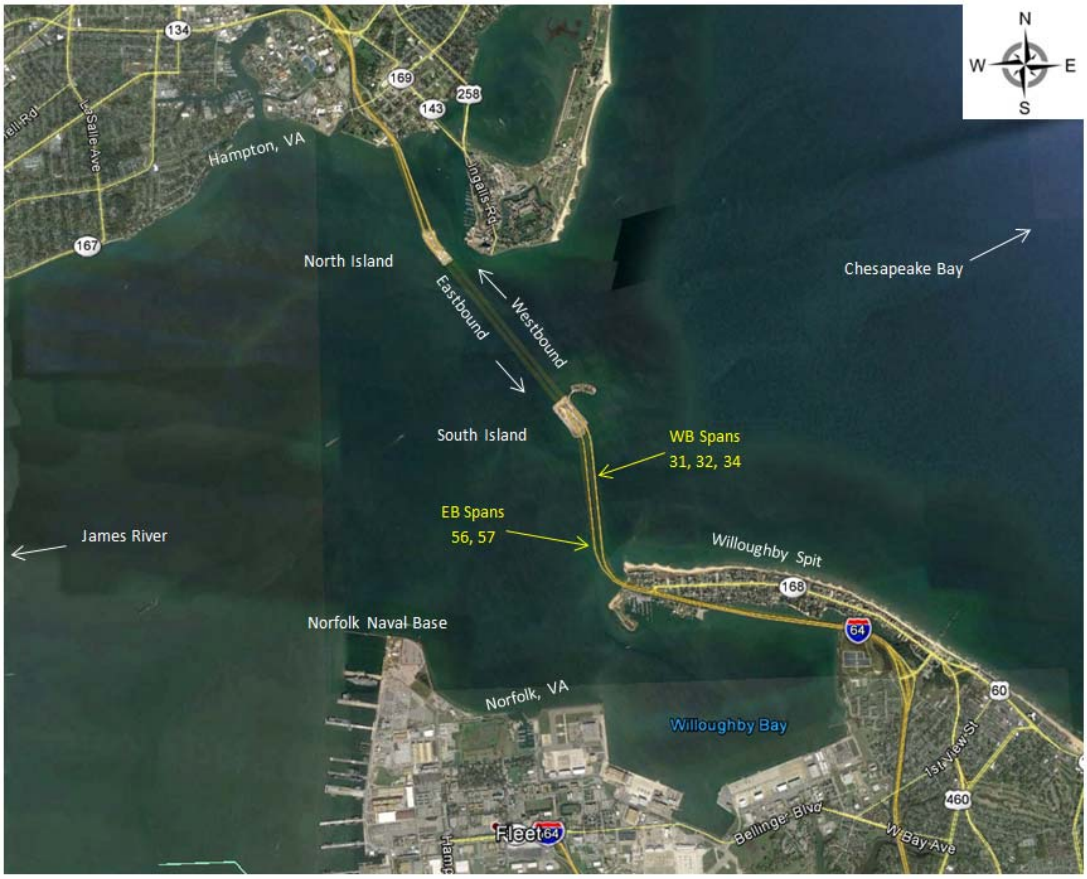

Figure 3: Hampton Roads Bridge-Tunnel (Image Via Google Earth)

The approach spans of the Bridge-Tunnel are showing signs of significant deterioration to its prestressed concrete girders. Signs of deterioration include concrete cracking and spalling along with exposed prestressing strands experiencing corrosion and loss of cross sectional area. Some of the more damaged girders have severed strands due to the excessive deterioration. Within damaged spans, some girders appear to be in good condition while others are heavily deteriorated so the damage is intermittent not only between spans, but also between girders. Because of the damage, select spans do not pass the necessary load ratings and truck posting may have to be imposed. The Bridge-Tunnel is subject to heavy vehicles from the shipyard and surrounding industry and, more importantly, is part of the coastal evacuation route. For these reasons, it would be extremely difficult to enforce a load posting on this structure.

1.2 Purpose and Scope

To help pass the rating, the Hampton Roads District of the Virginia Department of Transportation (VDOT) requested live load testing of select spans of the approach trestles. The

objective of the load test was to gain a more in-depth understanding of the behavior of the deteriorated girders as well as their ability to resist loads. The test results from the load test helped VDOT and their consultants validate detailed models used in the load rating.

Researchers from University of Virginia (UVA) and Virginia Tech performed the live load testing. The scope of the project included measuring strains and displacements of the girders at midspan as well as at select girder locations with significant damage. Five spans were selected for testing; each them is part of the south approach bridge. In the south approach, spans are numbered sequentially starting at the South Island and ending at the Willoughby Spit. The eastbound (EB) structure has 75 ft spans and girders are numbered from left to right when looking in direction of traffic (east to west) as shown previously in Figure 2. The westbound (WB) structure has 50 ft spans and girders are numbered right to left when looking in the direction of traffic (east to west). The numbering system used in this research maintains the convention used in previous inspection reports for the structure.

In the eastbound structure, span 56 was tested by Virginia Tech and span 57 was tested by University of Virginia. Both spans were tested on the night of April 29, 2016. Span 56 had one girder with extensive damage to its bottom layer of prestressing strands and minor damage to the other girders, whereas span 57 showed no signs of significant deterioration. Span 57 was intended to be used as a baseline for comparison to the span with extensive deterioration (56). In the westbound structure, Virginia Tech tested spans 31 and 32 the night of June 20, 2016. The following night, the University of Virginia tested span 34. Span 31 showed extensive damage to two of its girders whereas span 32 was considered to be in fairly good condition. Span 34 had significant damage on one of its girders near the bearing. In all, five spans were tested of which two spans were designated as good condition, two spans had girders damaged in flexure critical regions and one span had girder damage in a shear critical region.

The collected data was used to develop live load distribution factors for the different spans of the Bridge-Tunnel. Comparisons were then made between the experimental distribution factors and current code equations to investigate the accuracy of the code for this damaged and geometrically irregular bridge cross section.

1.3 Thesis Organization

This thesis is organized into seven chapters. A literature review is performed in Chapter 2 reporting relevant background information on prestressed concrete, residual strength of

prestressed concrete girders, live load distribution factors, and various deflection measurement systems. Chapter 3 describes the development and implementation of the experimental procedures used in the live load test. The live load test results and major findings are presented in Chapter 4. From the results, experimental live load distribution factors were calculated and compared to theoretical live load distribution factors determined from current design specifications. The final experimental and theoretical values are reported in Chapter 5. Chapter 6 includes an in-depth comparison of the two deflection measurement systems used during the bridge testing. Finally, Chapter 7 reports the conclusions reached throughout the research project as well as recommendations for future research and the remaining life of the Bridge-Tunnel.

CHAPTER 2 – LITERATURE REVIEW

2.1 History of Prestressed Concrete Design

Prestressing is the act of inducing permanent stresses into a structure to counteract stresses the structure will experience while in service. Today, the idea can be seen in bucksaws which have initially tensioned blades to counteract any compressive stresses developed during cutting. This prevents the blade from buckling while in use. This idea of prestressing traces back thousands of years to Egyptian ship hulls which were prestressed by twisting ropes to prevent upward curvature of the hull due to buoyancy differences, known as "hogging" (Gasparini, 2006). The process is shown in Figure 4. The Wright Brothers even used prestressing in their biplane wings which were basically three dimensional Pratt trusses. Turnbuckles were used to introduce permanent stresses into the wire diagonals (tension) and wood struts (compressive) to increase structural stability of the wings.

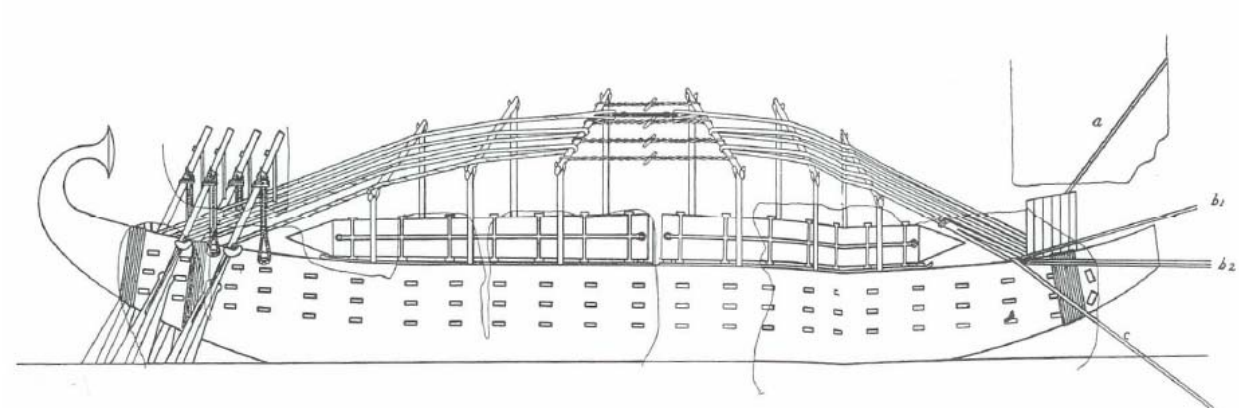

Figure 4: Egyptian Barge Prestressed to Prevent Hogging (Gasparini, 2006)

Concrete is known to have low tensile strength compared to its compressive strength, which is why it is typically reinforced with steel reinforcing bars. Prestressed concrete, on the other hand, uses high strength steel as prestressing strands to compress the concrete and prevent high tensile stresses from forming in the concrete section when loads are applied.

Prestressed concrete was first developed by Eugene Freysinnet in the late 1920's through his work with tied arches and concrete creep (Billington, 2004). Due to the economic depression of the era, it was difficult to implement the idea in industry and it wasn't until after World War II when prestressed concrete was widely used in Europe. A market developed due to the worldwide shortage in steel and the need to rebuild entire nations out of the ashes of World War II.

Just before the beginning of the War, Gustave Magnel became enthralled with Freysinnet's work and began researching prestressed concrete at the University of Ghent in Belgium (Billington, 2004). By the end of the War, Magnel had used his exceptional teaching skills and practical mindset to write "the first comprehensive design and analysis text ever written" named Le Béton Précontraint, which is French for "Prestressed Concrete" (Zollman 1978). Charles Zollman, a previous student of Magnel, translated the text into English and published it in England in 1948 with the assistance of Magnel. The book even made the trip across the Atlantic Ocean to Canada and America (Zollman, 1978).

Around the same time, a new arch bridge was being designed for Fairmount Park in Philadelphia, Pennsylvania where aesthetics was the driving force of the design. After all contractor bids came in above the engineer's estimate, the bids were rejected and the design was altered (Billington, 2004). A prestressed concrete bridge was the result, and after some help from Zollman acting as a liaison, Magnel became the lead designer. The structure is known today as the Walnut Lane Memorial Bridge. The design was completed using European codes which were developed by Magnel. The prestressing hardware and wire was developed by none other than the John Roebling & Sons Company. During construction, an extra prestressed beam was manufactured and was used to perform a full scale destructive test on October 25, 1949. The test was opened to engineers around the country and was attended by over 300 engineers from 17 states and five countries (Zollman, 1978). The beam, which was the typical 160 ft length for the bridge, was successfully loaded to over ten times it working load. One of the engineers at the proof test was William "Bill" Dean who later became instrumental in developing prestressed concrete in the USA. Dean became the bridge engineer of the State of Florida shortly after the proof test. In Florida, he pushed for prestressed concrete and soon implemented it on the Sunshine Skyway Trestle (FDOT 2015).

The Walnut Lane Memorial Bridge was completed in 1951 and the Sunshine Skyway was completed in 1954. Prestressed concrete continued to gain traction due to its aesthetic benefits, the worldwide shortage of steel, economy compared to other systems, and durability. Years prior, word of Freysinnet's work had surfaced in the United States and lead to the formation of the ACI-ASCE Joint Committee 323 (later becomes 423) in 1944 (D'Arcy, et. al 2003). It wasn't until 1954 that the Prestressed Concrete Institute (PCI) was formed. In the same year, two design publications were developed – the first two for the United States. The Bureau of

Public Roads (later became the FHWA) released “Criteria for Prestressed Concrete Bridges”, shown in Figure 5, which started the movement to recommend prestressed concrete to bridge designers (D’Arcy, et. al 2003). The precasters of the PCI wanted their own “code provisions” that were practical and more detailed on construction practices so they released “Specifications for Pretensioned Bonded Prestressed Concrete” which became active in November 1954 (D’Arcy, et. al 2003). These two documents were the backbone design specifications used to by Parson Brinckerhoff Hall and MacDonald when designing the westbound structure of the Hampton Roads Bridge-Tunnel as shown on the design drawings dated 1954.

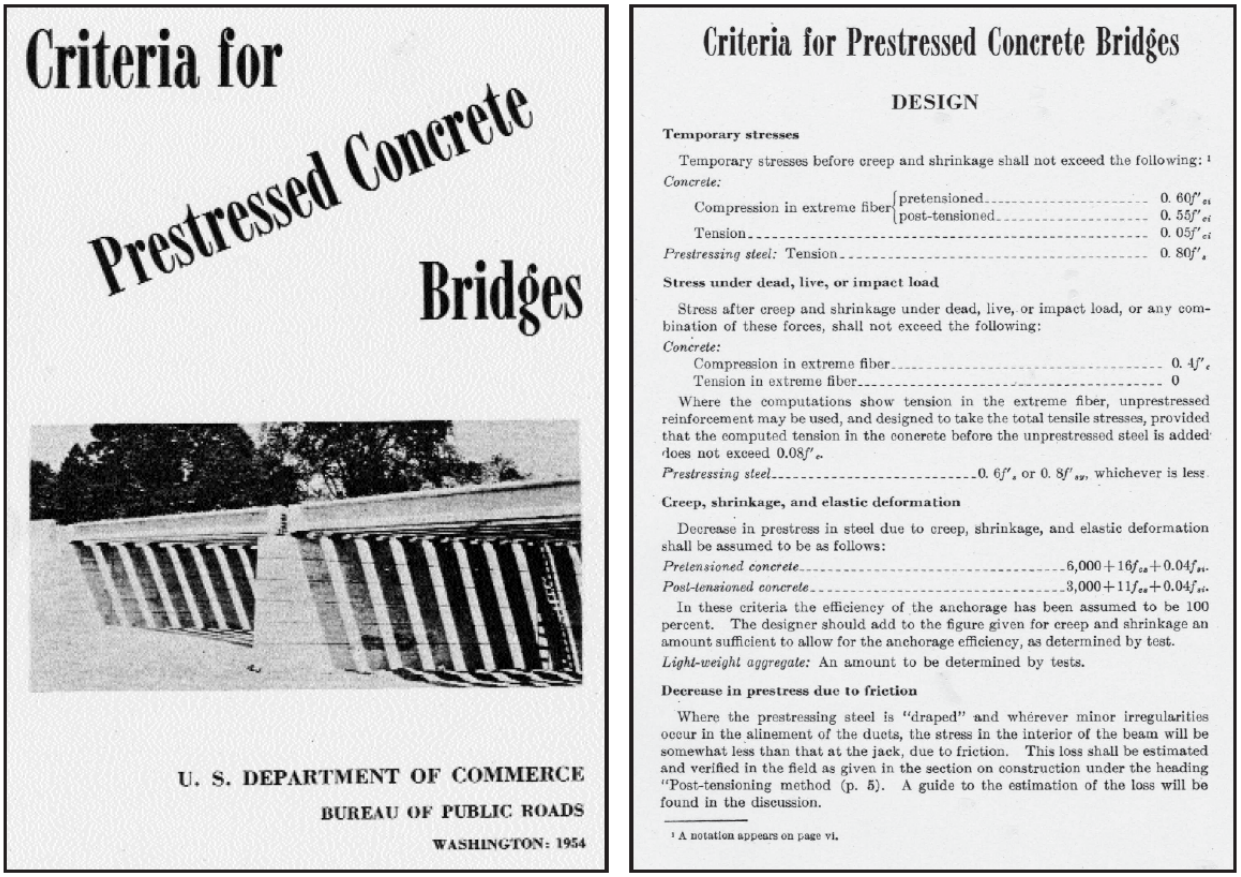

Criteria for Prestressed Concrete Bridges

U. S. DEPARTMENT OF COMMERCE
BUREAU OF PUBLIC ROADS
WASHINGTON: 1954

Criteria for Prestressed Concrete Bridges

DESIGN

Temporary stresses

Temporary stresses before creep and shrinkage shall not exceed the following: [1]

Concrete:

Compression in extreme fiber	pretensioned	$0.60f'_{ci}$
	post-tensioned	$0.55f'_{ci}$
Tension		$0.05f'_{ci}$
Prestressing steel: Tension		$0.80f'_s$

Stress under dead, live, or impact load

Stress after creep and shrinkage under dead, live, or impact load, or any combination of these forces, shall not exceed the following:

Concrete:

Compression in extreme fiber	$0.4f'_c$
Tension in extreme fiber	0

Where the computations show tension in the extreme fiber, unprestressed reinforcement may be used, and designed to take the total tensile stresses, provided that the computed tension in the concrete before the unprestressed steel is added does not exceed $0.08f'_c$.

Prestressing steel—$0.6f'_s$, or $0.8f'_{sy}$, whichever is less.

Creep, shrinkage, and elastic deformation

Decrease in prestress in steel due to creep, shrinkage, and elastic deformation shall be assumed to be as follows:

Pretensioned concrete—$6{,}000+16f_{cs}+0.04f_{st}$.

Post-tensioned concrete—$3{,}000+11f_{cs}+0.04f_{st}$.

In these criteria the efficiency of the anchorage has been assumed to be 100 percent. The designer should add to the figure given for creep and shrinkage an amount sufficient to allow for the anchorage efficiency, as determined by test.

Light-weight aggregate: An amount to be determined by tests.

Decrease in prestress due to friction

Where the prestressing steel is "draped" and wherever minor irregularities occur in the alinement of the ducts, the stress in the interior of the beam will be somewhat less than that at the jack, due to friction. This loss shall be estimated and verified in the field as given in the section on construction under the heading "Post-tensioning method (p. 5). A guide to the estimation of the loss will be found in the discussion.

[1] A notation appears on page vi.

Figure 5: 1954 Bureau of Public Roads Design Specification (D’Arcy, et. al 2003)

In 1957, the World Conference on Prestressed Concrete took place at the University of California-Berkeley. By this time, the Walnut Lane Memorial Bridge, Hampton Roads Bridge Tunnel, and Sunshine Skyway were completed along with select other prestressed concrete bridges. Without prestressed concrete, the HRBT and Sunshine Skyway would not have been possible. It was cheaper than steel in terms of cost per foot and the concrete durability allowed for minimal maintenance in the aggressive coastal environments that would have wreaked havoc

on a steel structure or caused unreasonable maintenance costs. The prestressing also allowed for longer spans than traditional reinforced concrete was capable of achieving, which minimized the number of pier foundations required.

By the late 1950s, the United States was putting their stamp on prestressed concrete. Designers were adjusting cross sections and precasters were developing standard sizes to allow for mass production. Roebling & Sons Company was paving the way with stress-relieved wire and anchoring devices with American and Wire Corporation (a division of US Steel) not far behind (Zollman 1980). The typical European cross section, shown in Figure 6, was more slender and prone to cracking whereas the American version was more "short and stubby" to help decrease cracking and improve form construction for mass production (FDOT 2015). This difference can be seen in the westbound structure of the HRBT, illustrated previously in Figure 2, where the original girders mimic the European style but the eastbound and westbound widening girders are a US style. In 1958, the ACI-ASCE Joint Committee 323 published the "Report on Prestressed Concrete" in both the ACI and PCI journals (D'Arcy, et. al 2003). This document helped incorporate prestressed concrete into the 1963 ACI-318 design code.

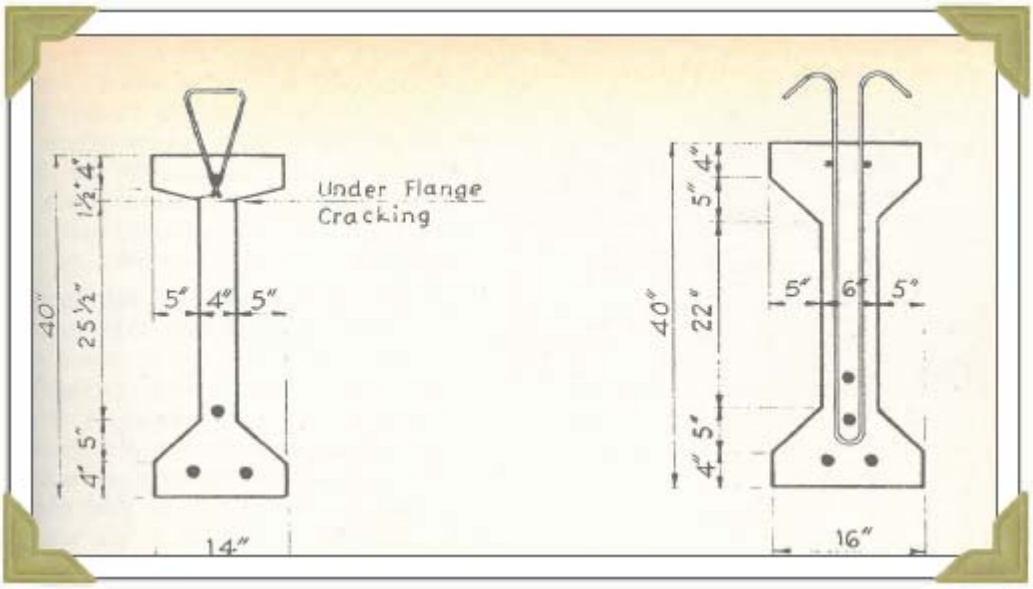

Figure 6: Cross Section Comparison [European - Left, USA – Right] (FDOT, 2015)

In June 1956, The Federal Aid Highway Act of 1956 was authorized which began construction on one of America's greatest engineering feats – the Interstate Highway System (FDOT 2015). At the same time, prestressed concrete as it was gaining traction across the nation,

especially in Florida and California. The interstate highway system caused so much demand for bridges that prestressed concrete spread around the country.

Today, the Walnut Lane Memorial Bridge still stands and is registered as a historical bridge. The Sunshine Skyway Bridge was demolished in 1980 after a massive collision with a freighter, the third of its lifetime, causing over 1200 ft of the bridge to fall into the Tampa Bay (FDOT 2015). The Hampton Roads Bridge-Tunnel remains one of the oldest American prestressed concrete structures still in existence. Due to its age, it is one of the first prestressed structures to develop durability problems because of corroding prestressing strands.

2.2 Residual Strength of Prestressed Girders

To fully understand how deterioration affects the local strength of prestressed concrete girders, the deterioration mechanism of prestressing strands must first be understood. Prestressing strands have a deterioration mechanism that is not seen in reinforcing bars because of the high stress applied. Typical reinforcing bars corrode along the outside surface causing a general "section loss" corrosion. However, prestressing strands exhibit section loss as well as pitting corrosion as shown in Figure 7 where damage indices (DI) are characterized for corroding strands. Pitting corrosion develops highly localized pits along the exposed strand. These pits cause high local strains to develop because of the angular pit shape and the high tensile stresses in the strands. As the corrosion increases, the spacing becomes smaller between adjacent pits. The stress concentrations at the pit cause microcracks to form which can propagate from pit to pit. The microcracks can also travel through the load carrying cross section, leading to abrupt, brittle failure of the strand. This process is known as stress corrosion cracking (SCC) (Ciolko, 2005). Hydrogen embrittlement, which makes the prestressing steel more brittle, is also a concern when pitting and stress corrosion cracking is present. These deterioration mechanisms can lead to abrupt and unexpected brittle fracture of the strand in highly localized areas.

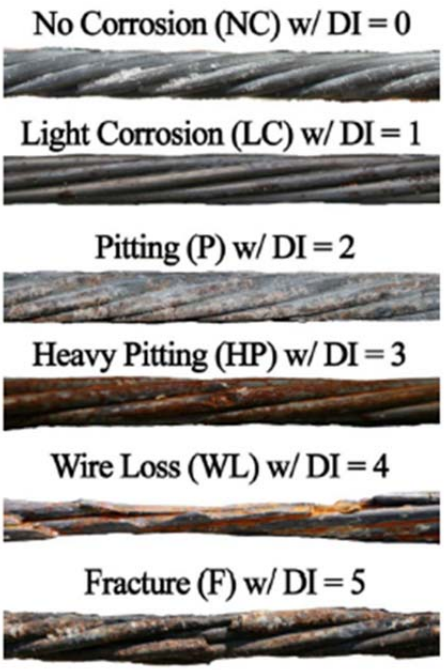

Figure 7: Typical Strand Damage Conditions (Naito, et. al, 2010)

Typical corroded reinforcing bars follow the same stress strain curve as an un-corroded rebar but the corrosion causes the bar to lose ductility and fracture at a smaller strain value. In contrast, prestressing strands do not follow the same stress strain curve when compared to an uncorroded strand. SCC and hydrogen embrittlement cause the yield strength, modulus of elasticity, ultimate stress, and ultimate strain to decrease as shown in Figure 8 (Vu, 2009). The extent to which these material properties are reduced depends on the environment and exposure time. The wires in the research performed by Vu were artificially corroded in an aggressive solution to simulate real world corrosion and pitting. The tests, which were performed over 180 days, showed the modulus of elasticity decreased 25% and the yield strength decreased 15% (Vu, 2009).

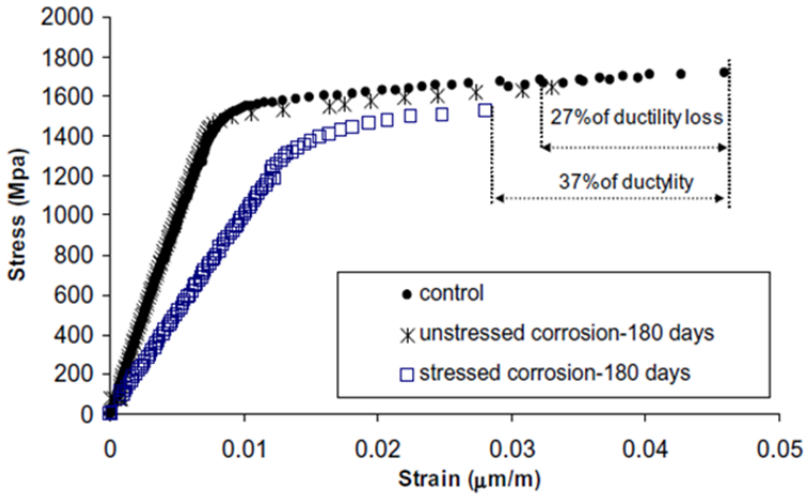

Figure 8: Effects of SCC and Hydrogen Embrittlement on Prestressing Strands (Vu, 2009)

This corrosion process is typically localized and does not change the material properties of the overall strand. However, this localized area develops weaker material properties and can be susceptible to abrupt, brittle fracture similar to a weak link in a chain. The localized corrosion is where a future failure will likely initiate as the strands at this location become more and more compromised.

Prestressing strands are typically six wires wrapped helically around a center wire. Although only the bottom portion of the strand may be exposed by the spalling, in roughly an 8 in. length, all of the helical wires make a full rotation and are exposed to a corrosive environment. The corrosion process will cause the steel to expand and ultimately can lead to a volume increase of up to 6.5 times the original strand size (Naito, 2011). This expansion causes a radial compressive force in the adjacent concrete coupled with tension perpendicular to the compression hoop. As the volume expansion continues, the tensile stress will surpass the concrete tensile resistance and lead to cracking. When multiple strands in the same row corrode, the hoop stresses will all work in a row leading to complete delamination and spalling of the concrete.

The deterioration of a prestressed girder typically progresses in an exponential fashion once the corrosion process commences. The exposure of a single strand further increases the corrosion rate and likely leads to the rupture of more strands. As each strand ruptures, additional load is required to be redistributed to the remaining strands. Each remaining strand must resist additional load at the same time it may be losing strength from the corrosion process which

causes it to rupture faster. The result is a domino effect where the deterioration rate increases with time as shown in Figure 9.

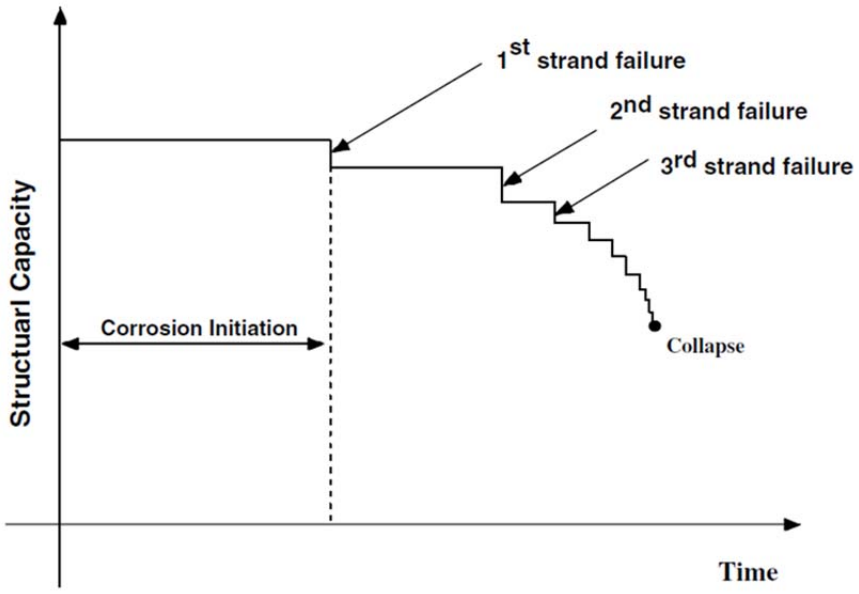

Figure 9: Lifetime Structural Capacity of a P/S Girder (Darmawan and Stewart, 2007)

The deterioration of the strands has a significant effect on the flexural strength of the girder. Typically, undamaged girders fail from concrete crushing near midspan if subjected to a destructive flexural test. With small amounts of corrosion in the strands (<10%), the ultimate load has been shown to be comparable to a sound beam (Rinaldi et. al, 2010). However the failure mechanism is more brittle because it is caused by rupture of the strands, most often in conjunction with concrete crushing. When corrosion becomes extensive, the failure mechanism can be unexpected and very brittle because it is controlled by local strand rupture. Tests have shown that artificial corrosion of 20% in all strands in a cross section can cause the flexural strength to decrease by roughly 50% of a sound beam as shown in Figure 10 (Rinaldi et. al, 2010).

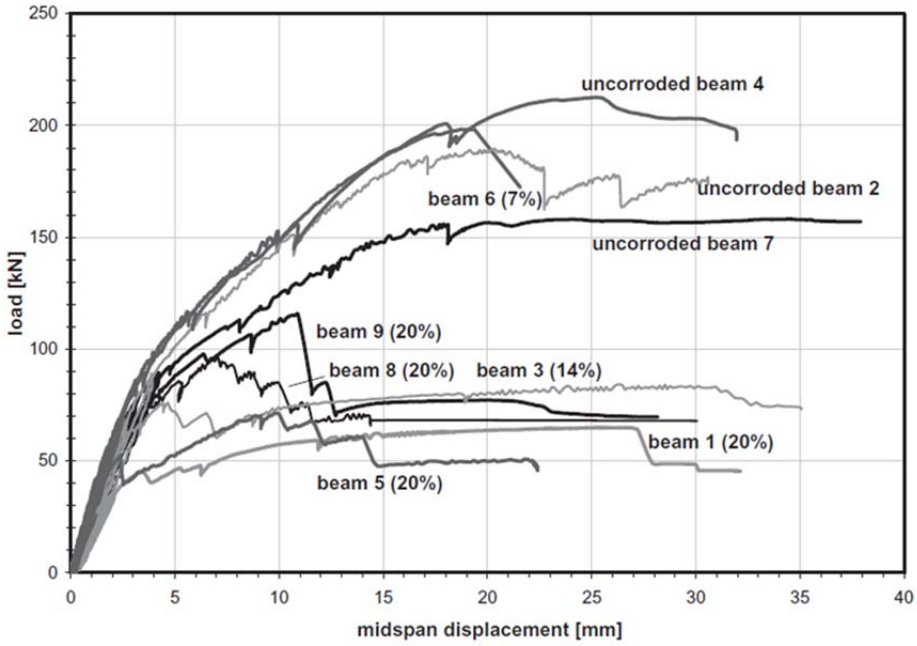

Figure 10: Effects of Strand Corrosion on Flexural Strength (Rinaldi et. al, 2010)

Similar results were seen when performing destructive testing of decommissioned prestressed concrete girders that were previously exposed to an aggressive environment for 42 years (Rogers et. al, 2012). These decommissioned girders showed extensive longitudinal cracking along with some spalling and delamination. Rogers points out that corner strands are most susceptible to corrosion since the aggressive environment is working from both surfaces so this is where deterioration typically begins and then works towards the centerline of the beam. These tests were on specimens which did not have as much deterioration as observed on some of the girders on the Hampton Roads Bridge-Tunnel.

As discussed in the previous section, prestressed beams have not been in service for a long period of time. The first bridges built with them are just now reaching the end of their service life so there are few opportunities available to test decommissioned prestressed beams. In addition, the cost of transporting large girders to testing locations for full scale destructive testing can be very expensive. Rogers worked around this by building his own load test frame out of other girders and testing directly at the bridge site. Another exception to this was the Lake View Drive Bridge in Pennsylvania. This bridge was built using adjacent box beams which are much more susceptible to prestressing corrosion due to the joints between the adjacent beams. One of the fascia beams of this bridge collapsed due to only dead load because of the extensively

corroded strands as shown in Figure 11. The tests and inspection revealed that unobservable corrosion may be up to 25% of the observed corrosion damage (Harries 2009).

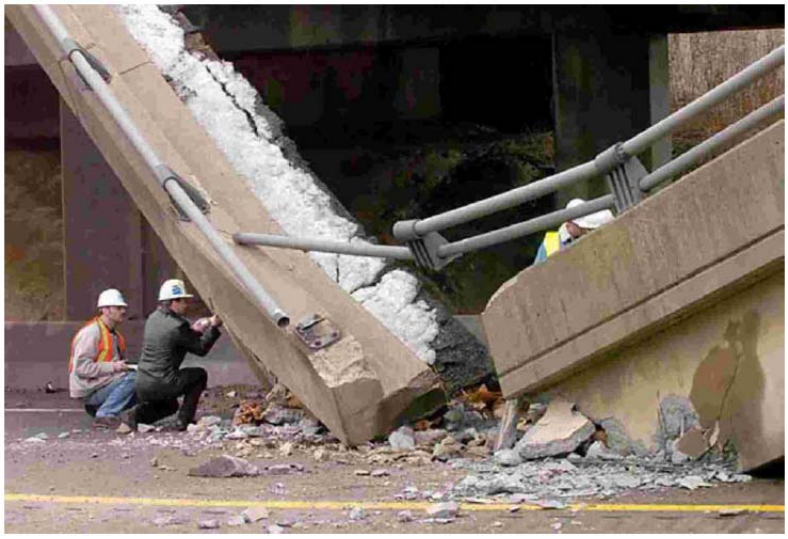

Figure 11: Collapsed Fascia Beam of the Lake View Drive Bridge (Harries 2009)

2.3 Deflection Measurement Systems

Live load tests on bridges have dated back hundreds of years including the Brooklyn Bridge when Washington Roebling used elephants to prove to the public that the bridge was reliable. Today, load tests use high accuracy equipment to measure data such as strains and displacements to understand a bridge's system performance and to calibrate and validate finite element models (FEMs). Typically, sensors are placed in contact with the bridge elements to retrieve data during the load test. Contact sensors commonly used to measure displacement include linear variable differential transformers (LVDTs) which have a piston motion of a protruding, free moving cylindrical core (Modares and Mohammadi, 2013). String potentiometers are commonly used in controlled laboratory settings for measuring displacements. Other common contact sensors include tiltmeters, accelerometers, strain gauges, and vibrating wire gauges. All of these sensors must be wired to a datalogger which sends an excitation voltage, measures a relative change in voltage or resistance, and stores the data at a predetermined frequency. The setup for these gauges and wiring can be time consuming and cumbersome especially when access is difficult or when traffic closures are needed for instrumentation. Also, long term equipment must be weather resistant to withstand environmental effects. Because of these drawbacks, field measurements of structures and destructive tests didn't become feasible until technological advancements in the late 1940s.

Coincidentally, a major field testing feat was the destructive test that Magnel performed for the Walnut Lane Memorial Bridge which used strain readings and deflection measurements at the site of the bridge. At that time, almost all equipment was kept indoors at research laboratories.

Due to the drawbacks of contact diagnostic systems, recent advancements in technology have allowed for new "non-contact" systems to be used to capture the same data. The setup typically takes less time and is more of the "point and shoot" method since these systems use satellite positioning, digital images, lasers, or interferometric radar. As the technology improves, accuracy and sampling rates are increasing and a shift towards noncontact measurement is occurring. For example, much of the surveying work performed on engineering projects is completed using some sort of global positioning system (GPS) or robotic total station (RTS). In the past, surveyors relied upon manual theodolites and dumpy levels.

Total stations are typically mounted on a tripod and used in conjunction with reflectors mounted on the object of interest. The RTS emits a narrow angle coded signal to the prismatic reflector which reflects the signal back to the RTS (Mocshas and Stiros 2014). The RTS will receive the reflected signal and internally calculate the time it took for the signal to travel and develop a distance measurement based on that time. Current total stations can sample at a frequency of 5-7 Hz and are accurate to 1/8 in. + 2ppm (Moschas and Stiros 2014). The typical reflectors have a range of 8000 ft but select top-of-the-line packages can work up to 18000 ft. The high-end packages manufactured by well-respected companies, such as Trimble or Leica, can cost around $37,000. This technology has been used recently to successfully measure dynamic deflections of electrical transmission towers due to wind loads as shown in Figure 12 where the arrows show the locations of the reflectors (Moschas and Stiros 2014). GPS systems, on the other hand, are only accurate to 1/4 in.-1/2 in. (5-10mm) and can run at a sampling frequency up to 2 Hz (Modares and Mohammadi, 2013).

Figure 12: Robotic Total Station System (Moschas and Stiros 2014)

Another noncontact measuring system, the Laser Doppler Vibrometer (LDV), was employed on the Doremus Avenue Bridge in New Jersey and the data was compared with results from contact sensors (Nassif et. al. 2004). The noncontact LDV system used laser interferometry to measure surface vibrations which is then internally modified into vibration and displacement measurements. This new system was deployed below the bridge and used to measure the girder deflections as illustrated in Figure 13.

Figure 13: LDV System (Nassif et. al 2004)

At the same time, a contact system consisting of a taut reference cable and a Linear Variable Differential Transformer (LVDT) was used to measure deflections of the same girder and the results were compared. Mounts were epoxied to the girder web above each of the

bearings and were used to anchor the cable. The cable was pulled taut between the mounts using a turnbuckle and acted as a reference point for the LVDT mounted at midspan as shown in Figure 14. The drawbacks of the LDV system included having to mount the system on a stationary tripod directly underneath the girder for measurements. The LVDT system was used for long term deflection data whereas the LDV system was short term since the equipment could not be left directly below the bridge for a long period of time.

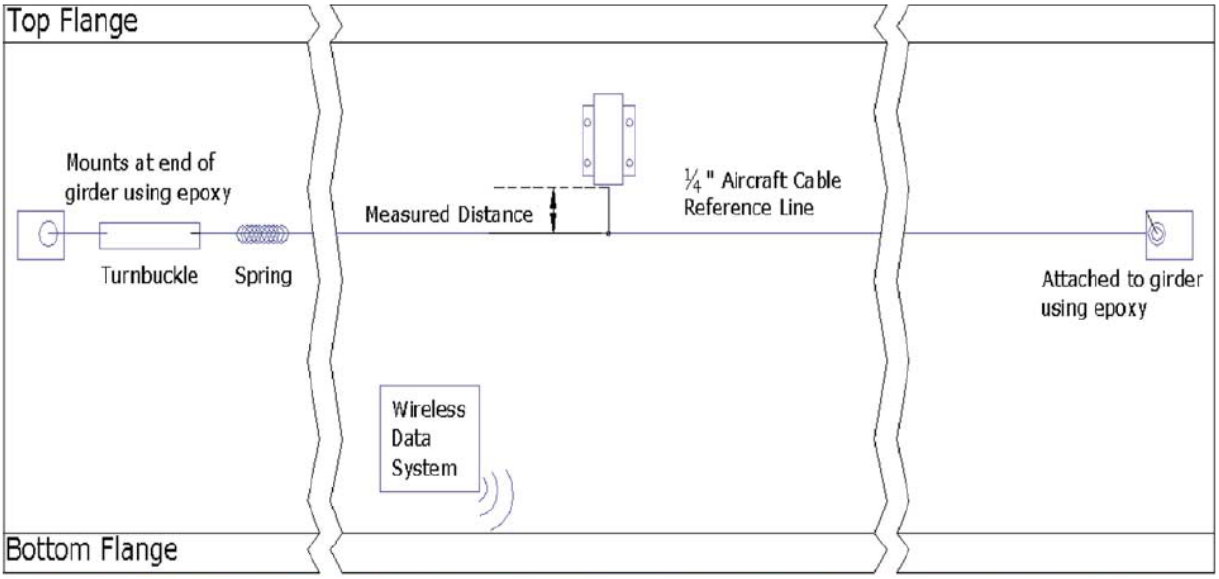

Figure 14: LVDT Contact System Setup (Nassif et. al 2004)

The wireless system results correlated extremely well to the contact system results. Since this initial test, the manufacturer of the LDV system, Polytec Incorporated, has considerably expanded its selection of LDV devices and has moved into the structural health monitoring market. Its newest technology, the Remote Sensing Vibrometer (RSV-150) has long range capabilities and is extremely accurate in terms of displacement and vibration measurements. All of this does come at a steep price which was not viable for the quantity of girders being tested at the same time for the HRBT load test.

Another emerging technology in the noncontact measurement market is digital image correlation (DIC). DIC is an optical measurement technique that is used to capture displacement data through high resolution digital photography. It emerged in engineering disciplines through mechanical engineers who used it to check tolerance limits in manufacturing components as well as analyzing stresses and strain in machined components (Peddle et. al 2011). Recent advancements in resolution and sampling frame rates of digital cameras have allowed the

technology to enter the civil engineering field for structural health monitoring applications. Typical DIC tests require a high resolution digital camera, tripod, laptop with high processing power, a calibration target, and some point of interest (POI) with a random pattern to capture. The digital images are typically captured using software and post-processed in a separate software package. One example uses Vic-Snap to capture images and Vic-2D or Vic-3D for post-processing, all of which is manufactured by Correlated Solutions Inc. (Peddle et. al 2011). Some researchers have taken the technology further and used DIC for entire elevation views of bridge girders, not just discrete target points as shown in Figure 15 (Yoneyama et. al 2007).

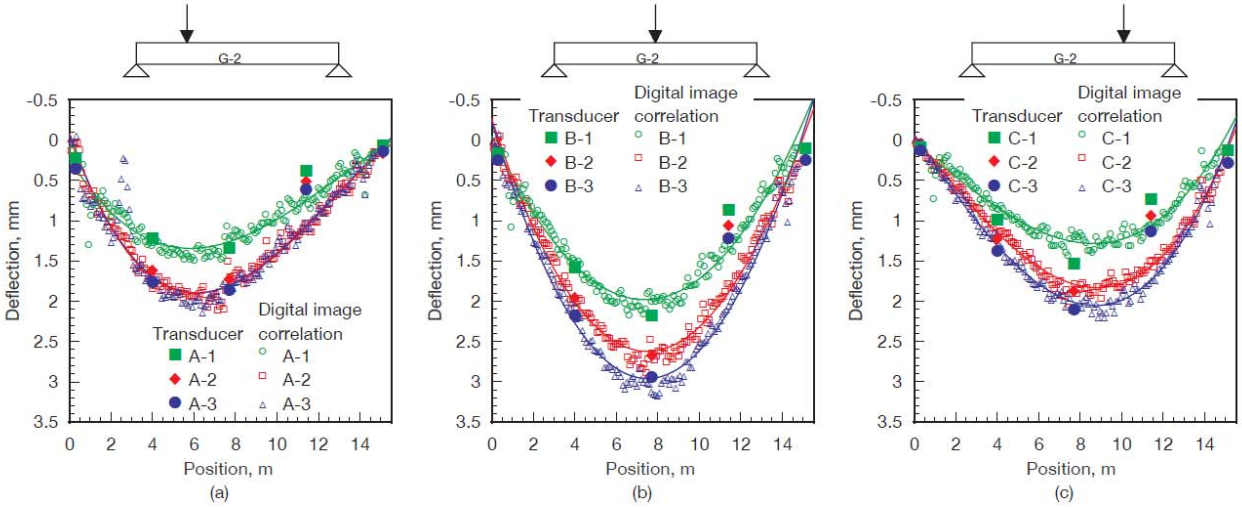

Figure 15: DIC and LVDT Comparison (Yoneyama et. al 2007)

Environmental factors can play a major role in the image capture during field tests. A large temperature change or wind gust can shift or expand the POI or tripod causing inaccurate data. Sun glare and solar positional change can also cause problems in tracking the relative displacement of each pixel throughout the field test (Feng et. al 2015). Similar to the contact devices, the accuracy of the data depends highly on calibration, which in this case, includes the camera configuration angles and distances from the POI. It also depends on the accuracy of the post-processing which must be able to identify the intensity, individuality, and location of each pixel from the first image to the last (Peddle et. al 2011).

In Peddle's research, the DIC setup was tested in the field on two bridges and compared directly with LVDT data. The results showed almost identical values with the DIC deviating from the LVDT values by about 0.001 in. (0.03 millimeters) (Peddle et. al 2011). These tests used small distances between the POI and the camera so the system was extremely accurate.

However, when greater distances are used, this accuracy is sacrificed since the image becomes dependent on the lens capabilities, like zoom and focus. One drawback between the two systems was the sampling rate; the LVDT sampled at 35 Hz and the cameras captured images at 1 Hz (Peddle et. al, 2011). Also, nighttime testing requires illumination of the structure or POI which adds setup time and equipment. It tends to decrease accuracy due to the quality of images at night (Modares and Mohammadi, 2013). Based on the literature review performed, no tests are known which combine the advantages of DIC and night vision technology, which may lead to a viable solution.

All of the above methods of displacement measurement, much of it including new non-contact technology, were not feasible for the HRBT test because of the short timeframe and tight budget. These constraints did not allow for new equipment to be purchased for the large number of girders being tested and wasn't feasible in terms of the lengthy startup time necessary to introduce new equipment and software. However, other systems discovered that used cables as reference points for contact sensors which were much more feasible in terms of timeframe and budget. A weighted stretched wire system was developed as an accurate but economical solution to measure girder deflections (Stanton, et. al 2003). The system used a pulley over one support and a fixed point (bolt) over the other bearing point to stretch a cable between as shown in Figure 16. A trolley was placed on the cable to initially cause the cable to sag due to the trolley weight. Then a weight was added on the opposite side of the pulley to tension the cable. This cable acted as a reference point for LVDTs attached to the girder at midspan to measure from. This system was proven to be accurate to 0.04-0.08 in. (1-2mm) for a 131 ft (40m) span used for long term testing of camber. Small sources of error were noted which came from temperature effects of the system and the slight friction in the pulley.

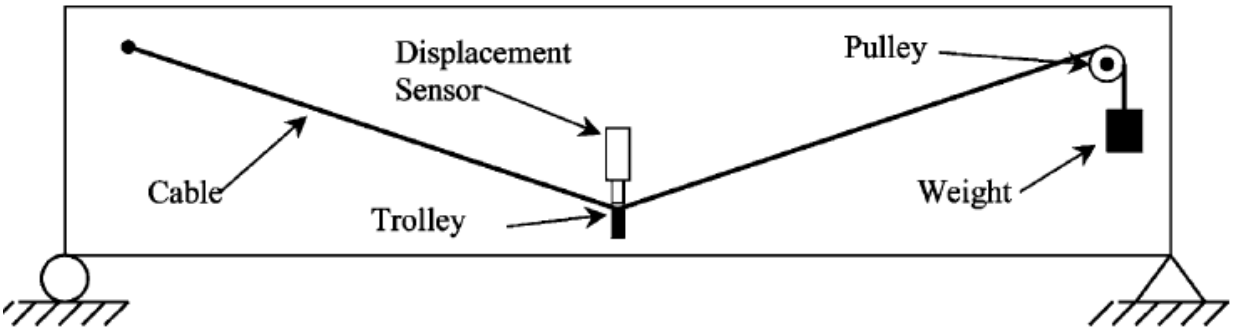

Figure 16: Weighted Stretched Wire System (Stanton, et al. 2003)

Other researchers have built upon this idea to develop a non-contact weighted stretched wire (NCWSW) system (Lan et. al 2008). The cable and pulley system was retained but the trolley was excluded so the cable was horizontal between the bolt and pulley as shown in Figure 17. A plane laser was used to illuminate a point on the cable and a video camera was used to record the bright spot on the cable. As the bridge deflected, which the camera was mounted to, the camera would move with the bridge but the cable would remain stationary. The video could be used to track the laser point on the cable and determine the deflection of the bridge. This system was implemented on a segmental cast in place box girder bridge with a main span of 360 feet. A cloth was attached to the bridge just in front of the laser so the camera area remained dark and the laser could be seen regardless of the weather or time of the day. A computer was used to post-process the video frames by finding the center of the laser point and determining the deflection measurement.

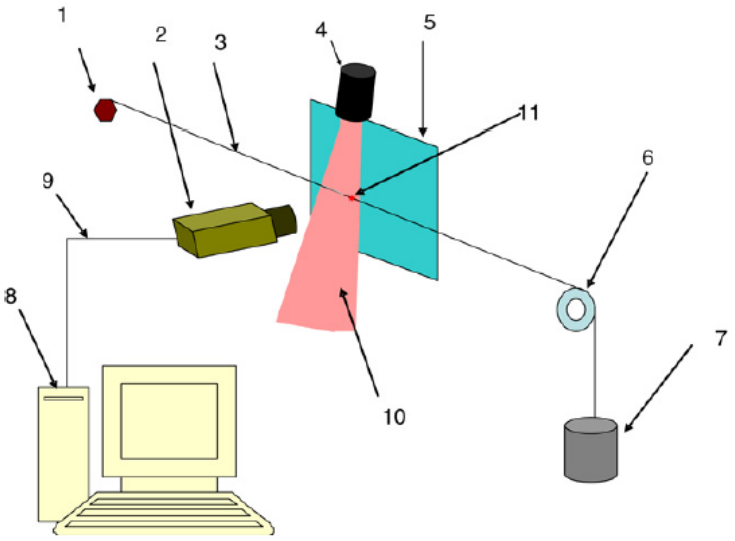

Configuration of an NCWSW system. 1. Bolt; 2. Video Camera; 3. Wire; 4. Line laser radiation; 5. Backcloth; 6. Pulley; 7. Weight; 8. Computer; 9. Data cable; 10. Line laser; 11. Bright spot on the wire.

Figure 17: NCWSW System Schematic (Lan et. al 2008)

Since the camera was not touching the wire, multiple cameras and lasers could be set up along the length of the main span for deflection readings from the same wire. One camera set up in the field is shown in Figure 18. Depending on the data desired, the frequency of the video frames can be altered. This system was employed for videos every hour over a 6 month interval to determine the deflections from temperature and creep. Prior to the implementation, the system was proven through laboratory testing with contact sensors.

Figure 18: Field Implementation of the NCWSW System (Lan et. al 2008)

In the past, live load tests have been performed at Virginia Tech where deflection measurements were desired. The measurement device used for these tests was known as a "twanger" and is shown in Figure 19. The twanger was built out of three pieces of aluminum – two rectangular with a third triangular piece. The rectangular pieces were used to sandwich the triangular piece which was facing perpendicular to the two rectangular pieces. The triangular cantilever had an eye hook on its end which was used to initially deflect the cantilever and then attached to a weight below the twanger on the ground. This deflection of the cantilever was quantified through a full bridge strain gauge circuit placed on the cantilever. This gauge was calibrated so deflections of the bridge could be recorded. As the bridge girder deflected, the entire twanger would move closer to the ground causing the cantilever to deflect less by the same amount the bridge girder moved down. Based on previous tests, the twangers were considered to be accurate to 0.001 in. depending on the amount of noise (Thornton, 2012). For the HRBT test, the weight would have to be submerged in the bay causing the tide and waves to develop considerable noise in the data compared to the deflection magnitude trying to be measured. If there was a much higher clearance between the bridge girder and the water, the twangers may have been acceptable. As the clearance grows, the movement of the wire side to side from the waves would be so little compared to the length of the wire causing small angle theory to apply. This would cause much less noise in the data and the submerged option would be feasible.

a) Twanger Subassemblage

b) Twanger Field Implementation

Figure 19: Twanger Deflection Instrument (Thornton, 2012)

2.4 Live Load Distribution Factors

Live load distribution factors are numerical measures of the percentage of load a specific girder resists within a bridge cross section. The bridge deck distributes the vehicle wheel loads to each individual girder. The live load distribution factors are used in the design and analysis of slab-girder bridges to determine the maximum load that a specific girder will experience based on the stiffness of the deck, number of design lanes, and location of wheel loads. In design, different distribution factors are calculated for shear, moment, and deflection. Since flexure was the primary concern for the deteriorated HRBT girders, the moment distribution factors were the only factors reviewed. Section 4.6.2.2 of the AASHTO Load and Resistance Factor Design (LRFD) Bridge Design Specifications includes empirical equations that have been developed for typical slab-girder bridges. These equations were developed with certain assumptions including the width of the deck remaining constant, the number of girders being greater than three, and all girders being parallel and approximately the same stiffness. In addition, the typical cross section must be included in AASHTO Table 4.6.2.2.1-1 for the equations to be applicable.

For a concrete deck composite with precast concrete girders, the equation for an interior girder with one design lane loaded from Table 4.6.2.2.2b-1 is:

$$g = 0.06 + \left(\frac{S}{14}\right)^{0.4}\left(\frac{S}{L}\right)^{0.3}\left(\frac{K_g}{12.0Lt_s{}^3}\right)^{0.1} \quad \textbf{(1)}$$

and for two or more design lanes loaded:

$$g = 0.075 + \left(\frac{S}{9.5}\right)^{0.6}\left(\frac{S}{L}\right)^{0.2}\left(\frac{K_g}{12.0Lt_s{}^3}\right)^{0.1} \quad \textbf{(2)}$$

g = live load distribution factor (number of lanes)

S = girder spacing (ft.)

L = girder length (ft.)

K_g = longitudinal stiffness parameter

t_s = deck thickness (in.)

The longitudinal stiffness parameter is calculated using AASHTO Equation 4.6.2.2.1-1:

$$K_g = n(I + Ae_g{}^2) \quad \textbf{(3)}$$

n = modular ratio = E_g/E_d

E_g = modulus of elasticity of the girder

E_d = modulus of elasticity of the deck

I = girder moment of inertia (in^4)

A = area of the girder (in^2)

e_g = distance between the center of gravity of the deck and the girder (in.)

The live load distribution factors for the exterior girders are calculated using AASHTO Table 4.6.2.2.2d-1. For two or more design lanes loaded:

$$g = e\, g_{interior} \quad \textbf{(4)}$$

where e is a modification factor:

$$e = 0.77 + \frac{d_e}{9.1} \quad \textbf{(5)}$$

d_e = horizontal distance from the exterior girder web centerline to the interior edge of the curb or traffic barrier (ft.)

To determine the single lane loaded exterior girder distribution factor, the lever rule is used. The lever rule method assumes a hinge at the adjacent girder, in this case the first interior girder, and sums the moments about the hinge to determine the reaction from the exterior girder. The leftmost wheel load is placed 2 ft from the curb/barrier and the right wheel load is spaced 6 ft from the left wheel load as shown in Figure 20. The lever rule can also be used for interior girders and multiple lanes loaded by assuming there is a hinge above each interior girder.

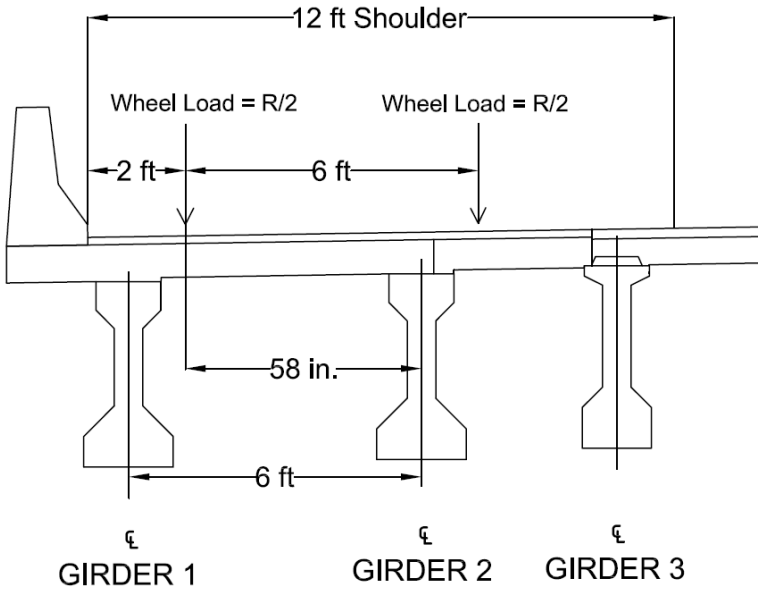

Figure 20: Lever Rule

Depending on the number of lanes loaded, a multiple presence factor is multiplied by the girder distribution factor determined from the lever rule. This factor accounts for the probability of multiple lanes loaded at the same time and are quantified in Table 1. These values are already built into the AASHTO equations and therefore are only multiplied by the lever rule distribution factor. The multiple presence factors are found in Table 3.6.1.1.2-1:

Table 1: AASHTO Multiple Presence Factors

Number of Lanes Loaded	Multiple Presence Factor, m
1	1.20
2	1.00
3	0.85
>3	0.65

The single lane is greater than 1 because the multiple presence factors were statistically calibrated to a probability of occurrence of a pair of equally loaded vehicles – each in its own design lane. It was proven that the probability of occurrence of a single vehicle that was heavier than one of the vehicles from the "pair" was the same so a higher multiple presence factor was used to account for the higher load from the single truck (AASHTO 2014).

Since the distribution factors are essentially a ratio of the amount of load that a specific girder resists, experimental load test data can be used to develop live load distribution factors. The experimental live load distribution factors can be calculated using the following equation (Barnes et. al, 2003):

$$g_{experimental} = \frac{nw_i\varepsilon_i}{\sum_{j=1}^{k}\varepsilon_j w_j} \quad \textbf{(6)}$$

n = number of lanes loaded

w_i = section modulus of the *i*th girder

ε_i = strain of the *i*th girder

k = number of girders

ε_j = strain of the *j*th girder

w_j = section modulus of the *j*th girder

Typically, the section modulus is calculated with respect to the bottom of the girder. It is included to account for the varying stiffness of the girders such as an exterior girder acting compositely with the barrier. The same equation can be used for deflection measurements instead of strain readings (Harris et. al, 2008).

CHAPTER 3 – EXPERIMENTAL PROCEDURE

3.1 Access

3.1.1 Eastbound Structure

During the first phase of testing, multiple pieces of equipment were used for access. The primary piece of equipment was a 26 ft by 78 ft spud barge that was pushed by a single engine 200 HP tug boat. The barge was mounted with winches to lift the spuds. On the bow of the barge, a Genie man-lift was used during times of low tide to reach certain girders. At high tide, the clearance was about 8 ft on a calm day with no waves. The barge had a freeboard of 3 ft so at high tide, there was a 5 ft clearance from the barge deck to the soffits of the girders. A 3 ft tidal change caused the clear height to change to a maximum of 8 ft throughout the day. Two A-frame ladders and a five foot scaffold set were brought to ensure access during low tide well as maintaining the ability to reach the top flange of the girders for select instrumentation. The tug and barge were owned and operated by Crofton Industries and are shown in Figure 21a. A VDOT supplied 14 ft C Hawk 190 boat was used to shuttle the equipment from the marina to the barge as well as for water transportation and access.

A traffic closure was implemented in the shoulder of the bridge between 10 AM and 3 PM for access during instrumentation. From the shoulder, a Moog MBI 90T platform truck was supplied by McClain & Co. and deployed in span 56. The platform was able to reach four of the seven girders, so the barge was used to complete instrumentation on the remaining girders of span 56 after span 57 instrumentation was completed. A VDOT snooper truck was also used during the setup and breakdown of the instrumentation. Both trucks are shown in Figure 21.

a) Tug Boat, Spud Barge, and Genie Lift

b) C Hawk Boat

c) Platform Truck

d) Snooper Truck

Figure 21: Eastbound Structure Access Equipment

3.1.2 Westbound Structure

Similar equipment was used for access during instrumentation and testing of the westbound structure as illustrated in Figure 22. A smaller float barge was mated with a 24 ft by 60 ft spud barge to provide a comparable work platform area as the one used during eastbound testing. The spud barge carried a 15 Ton carrydeck hydraulic boom crane (Shuttlelift 5560) to lift the spuds. The spud barge was mated to the float barge on its bow and a twin engine 1100 hp Marine Inland Tug boat on its stern. Crofton also supplied a twin outboard dive boat to work as a ferry between the barge and the marina. In addition, a larger platform Moog truck, MBI 200T, was deployed and operated by McClain & Co. which was able to access all girders from one side of the bridge. However, it was only used after load testing to remove instrumentation. Since the westbound testing occurred in the early summer months, shoulder closures were not allowed during daytime hours due to increased traffic. No snooper truck was used for the westbound instrumentation.

a) Float Barge, Spud Barge, Man Lift, Crane, Tug Boat

b) MBI 200T Platform Truck

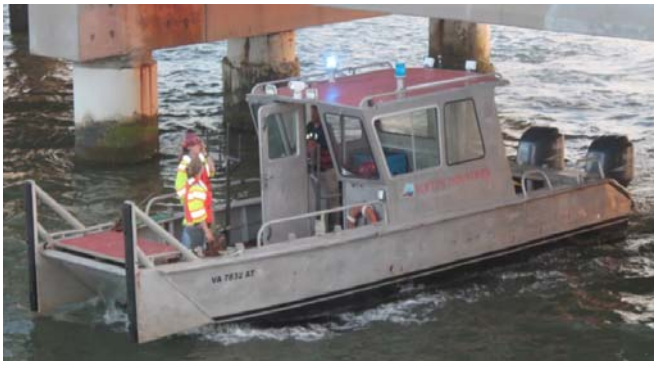

c) Crofton Dive Boat

Figure 22: Westbound Structure Access Equipment

3.2 Current Deteriorated Conditions

3.2.1 Westbound Span 31

Span 31 was designated as the "bad span" for the westbound tests. Girders 7 and 8 exhibited the most damage in their flexural region as shown in Figure 23. Girder 8 had four layers of prestressing strands exposed along the side of the bottom flange for approximately 70% of the span length. The strands showed heavy corrosion while some strands were completely severed. In Figure 23b, the orange reel is at midspan of girder 8 and the purple "8" chalk mark is 8 ft – 4 in. from the pier cap face (~L/5). Girder 7 had only three layers of strands exposed on the side of the bottom flange, but also had strands exposed on the soffit of the bottom flange (Figure 23c). The deterioration mapping diagrams from the Clark Nexsen inspection report dated June 2015 were accurate for all spans. Figures from this report of the damage mapping are presented in Appendix A.

a) Girder 7 on left, Girder 8 on right

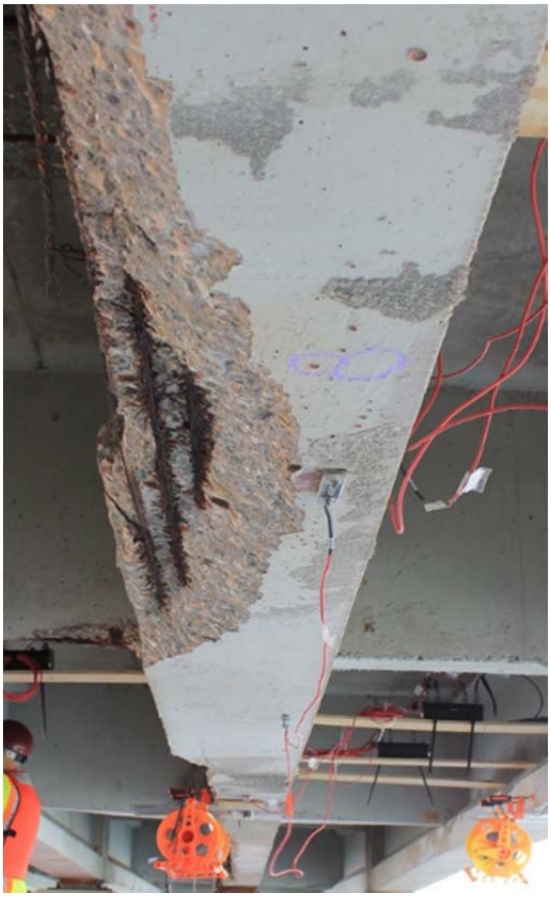

b) Girder 8 Bottom Flange Soffit

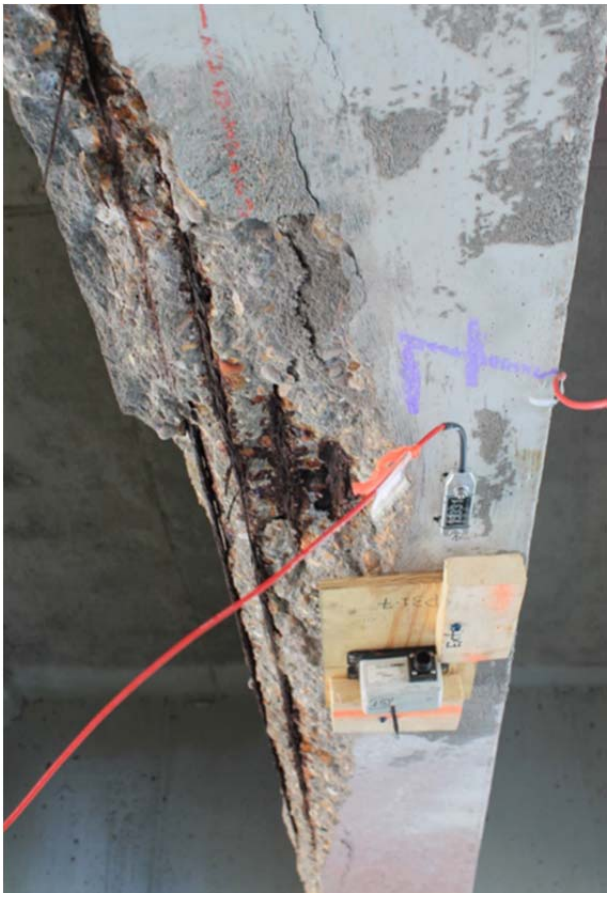

c) Girder 7 Midspan Soffit

Figure 23: Current Deterioration of Westbound Span 31

3.2.2 Westbound Span 32

Span 32, designated as the "good span" on the westbound structure, exhibited minimal damage as shown in the Nexsen report (Appendix A). This span was selected as a test span due to its apparent good condition and proximity to span 31.

3.2.3 Westbound Span 34

Span 34 was also defined as a "bad span", with damage primarily located in the shear critical region of the span. Near the bearing point, girder 4 exhibited significant damage on the bottom flange. This included heavy corrosion and a number of deteriorated strands within the primary three layers of flexural reinforcement. Figure 24 provides an illustration of this damage within the shear zone. It should also be noted that this girder had delamination and strand corrosion at midspan (see Figure 24b).

a) Girder 4 Bottom Flange at Support

b) Midspan of Girder 4 Bottom Flange

Figure 24: Current Deterioration of Westbound Span 34

3.2.4 Eastbound Span 56

The eastbound structure recently underwent rehabilitation as part of a VDOT construction contract; however, at the time of testing, no deterioration mapping was available to the project team. For span 56, mapping was performed by Virginia Tech on the day of the load test which highlighted obvious visual deterioration zones. Prior to mapping, it was known that girder 5 had severe corrosion to most of its lower layer of strands based on information provided by VDOT. Inspection mapping of this span is located in Appendix A which highlights areas of patchwork within the span. These locations were rehabilitated using shotcrete to cover spalled areas of concrete. The repairs were cosmetic only, meaning no structural repair was completed to increase member capacity. The condition of the previously exposed prestressing strands is unknown. Figure 25 shows the bottom flange of girder 5 which has been patched with shotcrete.

Figure 25: Shotcrete on Girder 5 Bottom Flange

3.2.5 Eastbound Span 57

On the first day of instrumentation, the span 57 was selected to serve as a benchmark for comparison with span 56. The criteria for selection included minimal damage and close proximity to span 56 to allow for optimization of instrumentation equipment. Span 57 was designated as the "good span" for the eastbound structure. No apparent damage on span 57 was observed beyond intermittent patching on some of the girder bottom flanges. While these patches were not documented during testing, and inspection details were not available from VDOT, examples of the conditions of the girders are shown in Figure 26.

Figure 26: Patching on Girder Bottom Flanges

3.3 Data Acquisition Equipment

The data collection focused on measuring longitudinal strain along the girder bottom flanges at midspan along with longitudinal strain distributions through the vertical girder cross-sections at select locations. Additionally, the project team measured midspan deflections as a supplemental measure of load distribution behavior. The deflection measurements presented a challenge due to the structure crossing a large body of water so the techniques employed were experimental in nature.

3.3.1 Strain Measurement System – Bridge Diagnostics Inc. (BDI) Equipment

Strain measurements were taken using the Bridge Diagnostics Incorporated (BDI) wireless Structural Testing System (STS) data acquisition system. The Virginia Tech set-up consisted of a single STS3 - Wi-Fi Mobile Base Station, 11 STS3 - Wi-Fi Nodes, 43 BDI Strain Transducers (30 – VT, 11 – Clemson, 2- BDI), and two BDI Linear Variable Displacement Transducers (LVDTs). All of the Virginia Tech owned strain transducers had been sent back to the manufacturer, BDI, roughly five months before the first HRBT load test to ensure accuracy of the sensors and the most up to date calibration file. The sensors borrowed from Clemson had been purchased within three months of the load test from the manufacturer so their calibration was accurate. The two sensors rented from BDI were calibrated prior to their shipping just two days before the first load test. All of the borrowed sensors were shipped in bubble wrap and all sensors used by VT were kept in bubble wrap to ensure their calibration.

The strain transducers were fastened to the concrete girders using a fast-set epoxy contact adhesive, Loctite 480, used in conjunction with an aerosol accelerator, Loctite 7452, shown in Figure 27.

Figure 27: Loctite Contact Adhesive and Accelerator

The strain transducers have a full wheatstone bridge concealed within a waterproof housing. They plug into the nodes which wirelessly communicate with the base station. The base station, which is essentially a Wi-Fi router, wirelessly communicates with a field laptop where the data is viewed real time and stored.

The University of Virginia set-up utilized a companion BDI sensor and data acquisition system for measuring strain and acceleration data for the live load tests. The system included a Hi Performance STS3 - Wi-Fi Mobile Base Station, 6 STS3 - Wi-Fi Nodes, 18 BDI Strain Transducers and 10 BDI accelerometers. Figure 28 provides an illustration of the various BDI system components deployed during the tests.

a) Base Station

b) Wireless Node

c) Strain Transducer

d) LVDT

e) Accelerometer

Figure 28: BDI Equipment

During the eastbound testing, the barge was anchored in Span 57 so the University of Virginia team could have access to their deflection system. This meant that the Virginia Tech

equipment in Span 56 would have to wirelessly communicate a large distance with obstacles (pier cap and diaphragms) disrupting the wireless communication. There was also a potential issue the wireless systems clashing since two base stations would be deployed and multiple nodes which could have potentially conflicting IP addresses. To ensure the testing went smoothly, the equipment was checked before the load test to ensure UVA and VT systems would not clash. It was concluded that only running one base station would minimize the wireless problems since only two spans would be tested during the eastbound test. To provide a platform for the nodes, plywood was cut to length so it could be set between the girder bottom flanges and support the nodes throughout the span.

For the westbound test, contingency plans were in place in case the surf was too rough to mobilize the barge. The weather and surf was what caused the westbound structure to be tested at a later date. Field studies were performed on the Route 114 Bridge over the New River in Radford, VA to try to place the base station on the bridge deck. It was hypothesized that the base could be placed in the traffic shoulder if an "above only" option was needed to test. During the field study, the concrete deck was too thick to allow for wireless communication with the nodes. It was concluded to place the field laptop and base station below the bridge during the next round of testing. Testing with the base station on the parapet still proved ineffective with the nodes below the bridge. A platform was built and was to be fastened to the pier cap using Tapcon concrete anchors if the "Plan B – topside access only" option was employed. The tapcon anchor system was proof tested at the VT Murray Structures Lab prior to the second round of testing by load testing one of the outriggers to a load roughly two times its design load (see Figure 29b). The platform was designed to hold the VT deflection system equipment, generator, and base station. The laptops and operator viewing the data real time would sit on the pier cap in between two girders below the end diaphragm to ensure the data acquisition went smooth. This option was never employed since the weather was pleasant during the second round of testing.

a) Instrumentation Platform

b) Proof Testing Single Outrigger

Figure 29: Instrumentation Platform Contingency Plan

During the westbound test, when Spans 31 and 32 were tested simultaneously, there were a large number of BDI sensors employed which caused all eleven VT nodes to be used. There were slight communication problems during the test since the VT base station was not rated for high performance and was being overloaded in terms of communication with all eleven nodes. This caused some of the data to not be recorded as the nodes alternated amongst each other to talk with the base station.

3.3.2 Deflection System – Cable Suspended Reference System

At the beginning of the project, a main instrument type was selected to measure the girder deflections. String potentiometers (pots) were chosen for the deflection system based on the quantity and availability of those instruments at the Murray Structures Lab. These instruments, once calibrated, were accurate to 0.001 in. To attach the pots to the girders, a piece of plywood was screwed to the base of the pot and then the plywood was clamped to the bottom of each girder at midspan as shown in Figure 30.This allowed for fast installation of the pots.

Figure 30: String Pot Setup

Each string pot was hard wired to a Campbell Scientific CR5000 datalogger to record the displacement measurements. The datalogger was kept on the barge in the UVA span so the wiring had to reach through the pier cap to the adjacent span to connect to the datalogger. Because of the long lengths of wires needed, the cable was wound onto orange reels to allow for fast installation. There were military connectors soldered onto one end of the cable which plugged into the string pot. This “quick connection” allowed for fast installation. The datalogger was connected to an additional field laptop so the deflection data could be viewed real-time during testing as shown in Figure 31. Prior to the first field test, the complete wiring configuration was set up and each string pot was calibrated using a calibrated dial gauge. This ensured the calibration factors in the CR5000 program were exact.

Figure 31: Campbell Scientific Datalogger and Wiring

The primary challenge with measuring deflections for the Bridge-Tunnel was that the tested spans were roughly one mile offshore leaving no fixed reference point to measure relative deflections. Due to the extremely tight budget and timeline of the load test, there were few options available for use. The system had to have a fast installation time but have the ability to be deployed in two spans at one time which meant a total of 18 girders instrumented at a single point in time. Preliminary calculations of the concrete girder deflections showed the system had to be accurate to ±0.002 in. Another major problem was possible noise in the data due to environmental effects. Any reference that was submerged in the water would have noise in the data from the wave action of the bay. The depth of water below these spans coupled with the typical 2ft to 3 ft waves would cause too much movement of a wire connecting to a submerged weight to accurately measure the small girder deflections. If a system was suspended, wind would become a problem. Typical winds that far offshore averaged 15-20 mph based on data from a NOAA degaussing stations near the Bridge-Tunnel.

The wires in the string pots needed to be attached to a fixed point for them to measure displacements so a suspended reference system was developed. Any deflection of the girder was thereby measured through the relative displacement of the deflecting girder with respect to the stationary reference. As for the actual reference system, proof tests of many systems were performed at the VT Murray Structures lab. The trial systems that seemed promising were set up outside the Structures Lab at similar distances between supports that were expected for the bridge test. These trial and error tests of mock setups were performed to prove their effectiveness. The systems were monitored using calibrated string pots during windy days to see if they met the noise criteria. The final eastbound system used steel cable strung between pier caps of the bridge-tunnel with a steel cable cross wire. This would essentially form an H pattern with the cross wire at midspan used to attach displacement measuring equipment. The setup is shown in Figure 32.

Figure 32: Eastbound Reference System

The longitudinal cables, running with the direction of the bridge, were attached to chokers. These chokers were made out of extra steel cable and were wrapped around the pier cap as shown in Figure 33. One end of each longitudinal cable was attached to its respective choker via a ratcheting cable winch, known as a come-along, which was used to tension the cables.

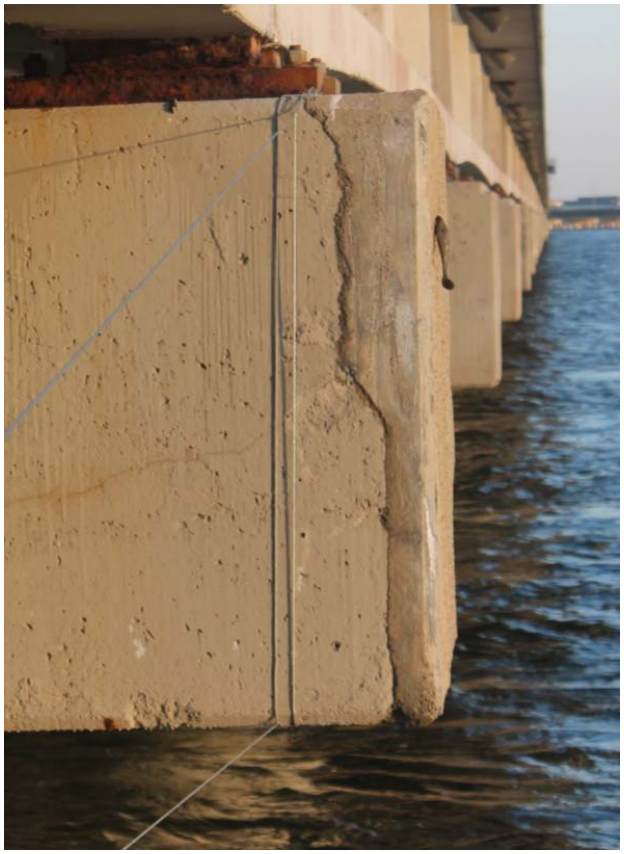

Figure 33: Chokers Wrapped Around Pier Cap

During the eastbound test, the cross wire was slightly pulled upwards due to the tension in all of the string pot wires. As the girders deflected, the cross wire would relax slightly due to its initial movement upwards. This caused "softening" of the deflection values and was the main reason why the eastbound deflection data in Span 56 was discarded. Although there was data, it was not accurate.

To rectify this problem, a new reference datum was investigated where upward movement couldn't occur. Initially, the same system was used and weight was added to the cross wire at the same locations as the string pots to counteract the tension load. To ensure no movement of the wire existed once the tension load was added, too much weight was needed at each location. It caused the longitudinal wires to be pulled inward so the exterior girder pots wouldn't be able to be attached vertically downward to the datum. Also, the magnitude of weight necessary would lead to relatively large objects that would be excited by wind vibrations. After multiple systems were investigated, a final system was constructed out of a built-up 2x4 beam and anchored within the taut cable system. Steel cables, 1/8 inch in diameter, were tensioned

above and below the beam to support it directly below midspan of the girders. The pier caps on either end of the span were again used as anchors for the cable network due to their relative fixity. To prevent downward movement, cables were strung from the top of one pier cap, below the 2x4 beam, and to the top of the pier cap on the other side (orange cables in Figure 34). To prevent upward movement, cables were strung from the bottom of a pier cap, up over top of the 2x4s, and down to the bottom of the pier cap on the other side of the span (maroon cables in Figure 34). This formed an "X" at each support location. The 2x4 beam was supported at three locations – at each end point and at its midspan. Cable chokers were again used to anchor the cables to the pier cap along with come-alongs used at each of the upper cable anchors (maroon). This synched the entire system to prevent any movement of the beam during testing. The green wires in Figure 34 represent the string pot wires extending from the pot to the suspended wood beam.

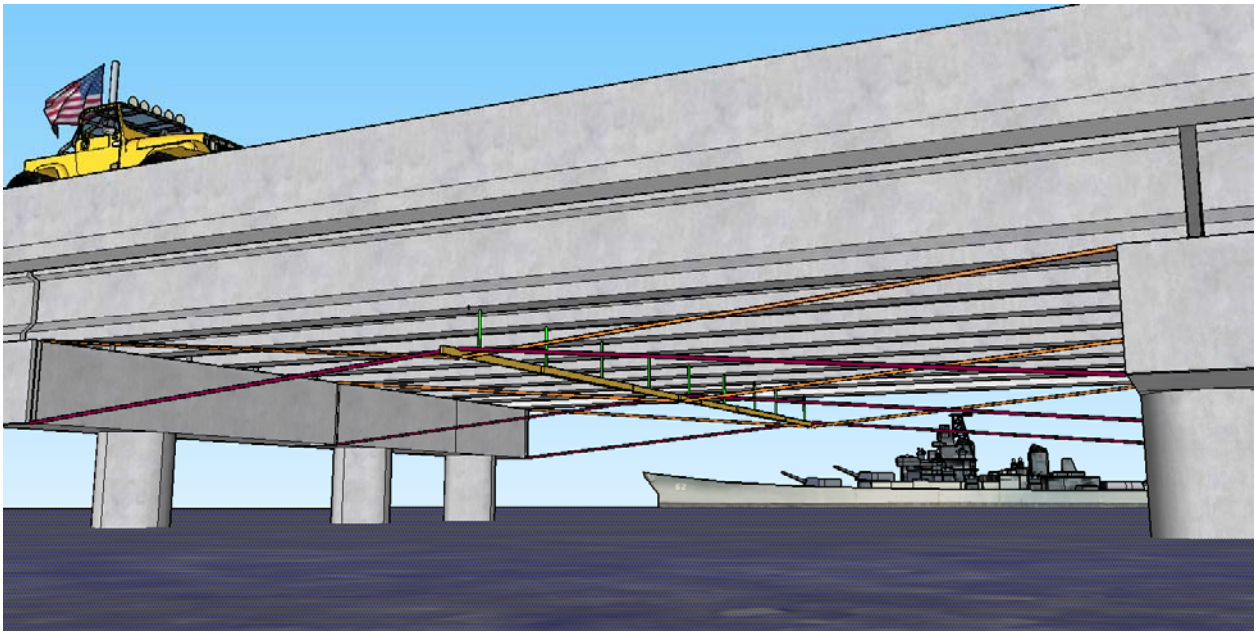

Figure 34: Cable Suspended Reference System

This system was proof tested in its expected field configuration at the Structures Lab, shown in Figure 35. The cables were strung at similar distances that would be expected during the westbound load test. Plywood strips represented the girders and had the string pots fastened

to them in the inverted position.

Figure 35: Mock Setup of the Cable Suspended System

Weights were used to deflect the plywood and a “true reading” string pot was used to measure the true deflection from the ground to the plywood as illustrated in Figure 36. The string pot on the plywood that was attached to the suspended reference proved to measure the same value. This system was left assembled during a breezy day to measure wind vibrations and the system passed the test.

Figure 36: Proving System for Final Deflection System

During the load test, there was a 20 minute time window when the barge was travelling from the marina to the Bridge-Tunnel. This time was used to build the wood beam. Two smaller beams were built out of the 2x4s and screwed together with an 18 in. lap as illustrated in Figure 37.

Figure 37: Partial Rigid Beam Assemblage

Later, when the first set of cables were strung between the pier caps, the two smaller beams were lifted onto the cables. One reached from the left cable to the middle cable. The second beam reached from the middle cable to the right cable. The two ends of the beams were butted together over the middle cable and then screwed together using 3 ft long 2x4s as lap splices which is shown in Figure 38. This assembly process essentially built two simply supported beams and spliced them together to form a single, two span continuous beam. After the beam was set into position, the cables travelling over the top of the beam to the bottom of the pier cap were lowered into position.

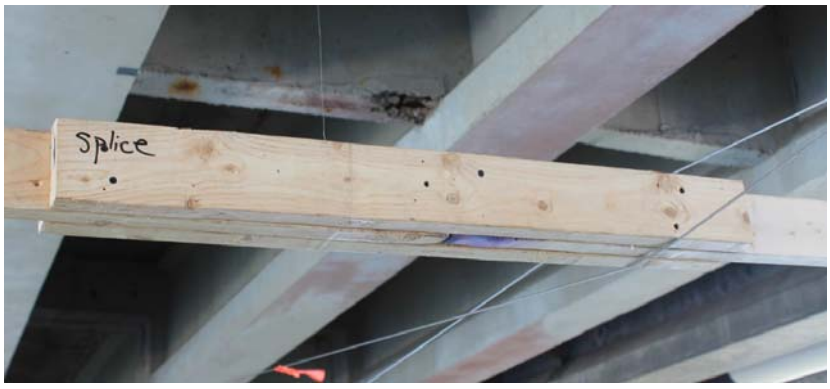

Figure 38: Rigid Beam Splice

After a quick ratcheting of the come-alongs, the system was ready for use. Plumb lines were used to locate the positions where the string pot extensions should be attached to the 2x4

beam. Wood screws were fastened into the 2x4 at these locations and then the stainless steel wire extensions from the string pot were wound around the screw to anchor it.

3.3.3 Truck Location Clicker

During testing, an LVDT connected to the BDI system was placed on the topside of the bridge. Similarly, a second LVDT was wired into the Campbell datalogger. The two LVDTs were used as "clickers" to allow team members responsible for directing the trucks to manually interface with the systems. The striking of the LVDTS would produce a peak in the data and provide a reference for the position and configuration of the trucks. Pre-defined positions along the spans were "clicked" to develop reference points in the data. Both systems were sampled at the same rate (25 Hz) so the clicker input could be used to align the strain and deflection data that was extracted from two separate data acquisition systems. This made post processing much easier since it allowed for the different truck configurations and run numbers to be synchronized during post-processing.

3.3.4 UVA Deflection System – Digital Image Correlation

As an alternative to a traditional fixed reference deflection measurement technique, the University of Virginia team utilized an emerging optical deformation technique called digital image correlation (DIC) to measure deflections during the load testing. Two dimensional DIC was used for the load test so a scaling factor was necessary to allow measurements in pixels to be converted to physical dimensions and measurements. The UVA team used a commercial 2D-DIC package (VIC 2D) from Correlated Solutions for the analyses. Due to the complex testing environment, the project team used *GoPro 3+ Silver* cameras for image acquisition and fixed size target cards to establish the scaling factor.

The cameras were compact and had a resolution up to 10MP and a video resolution up to 1080p. To accommodate the distance between camera and measurement location, the cameras were shipped to a technician in Canada to be modified to accommodate a Tamaron AF 75-300mm f/4.0-5.6 telephoto lens (Figure 39). Previous work had been completed at UVA with DIC so multiple cameras were already available and fitted to the lens and the software had already been purchased. UVA used nine cameras for their portion of the load test; one camera for each girder. UVA only needed to instrument a single span each night due to their scope of work so the number of cameras was kept to a minimum.

a) GoPro Camera

b) Modified GoPro

c) Variable Telephoto Lens

Figure 39: DIC Cameras

To test the resolution of the cameras prior to field deployment, the project team evaluated the performance in the UVA structures laboratory using a variety of lighting methods. The results of the laboratory investigation provided confidence that the technique could consistently resolve deflections on the order of ±0.005 in. under ideal conditions. It was expected that this resolution would decrease in the field due to environmental and lighting conditions.

During the load tests, cameras were mounted at the pier directly beneath each girder and aligned to acquire images of targets placed at midspan. The cameras were mounted on a rigid aluminum frame and speckled targets were taped to the girders at midspan. The targets were made in a predetermined size (6 in. x 6 in.) to provide scale and speckled with a random dot pattern for the correlation analyses. Because the testing was performed at night, each target was outfitted with a battery-powered light to illuminate the target for image acquisition. It was planned to leave the barge in the UVA span in case problems occurred with the lighting or the

cameras. A light plant was on the barge to provide supplemental light as a precautionary measure in case the battery powered lights were not sufficient.

During the live load testing, a series of image acquisition modes were used including video (30 fps) and time lapsed pictures (two images per second). Table 2 summarizes the modes used during the testing; however, it should be noted that following the testing of the eastbound spans, it was determined that the video mode yielded lower resolution images due to video compression. Therefore, for the westbound spans, only time lapsed pictures were used in the image acquisition. Although Span 32 was in the scope of Virginia Tech, it was instrumented with cameras on four of the nine girders to allow for a head-to-head comparison of the two deflection systems. Span 32 was tested the night before Span 34 so the cameras were available for use. Figure 40 illustrates the basic components and setup used for the 2D-DIC deflection measurement system deployed.

Table 2: DIC Image Acquisition Modes

Test Span	Run	Notes
Eastbound – Span 57	1	Video
	2	Time lapsed (with barge lights)
	3	Time lapsed
Westbound – Spans 32 and 34	All	Time lapsed

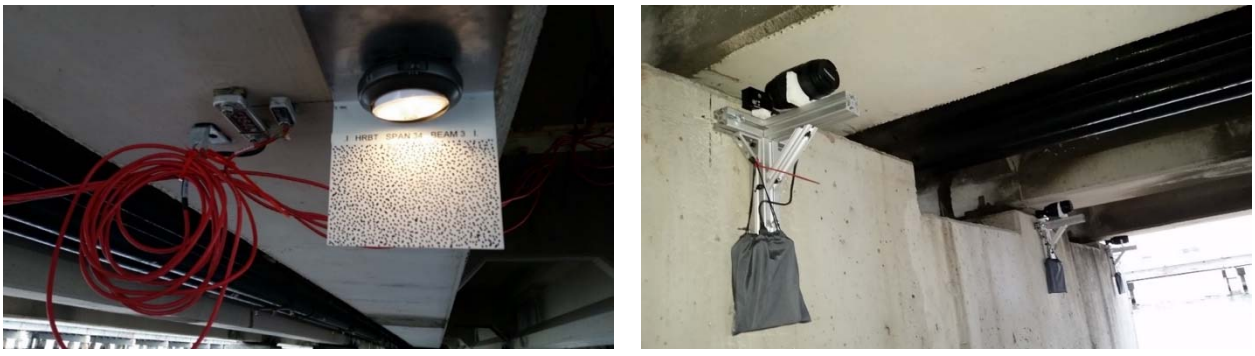

a) DIC Target Card with Local Lighting b) GoPro Camera with Bracket Mount

Figure 40: UVA Deflection System

3.4 Instrumentation Layout

The instrumentation layouts were developed in a collaborative effort between the Virginia Tech and University of Virginia project teams, with each team assuming responsibility for select spans. For the eastbound structure, Virginia Tech instrumented span 56 while the University of Virginia instrumented span 57. Similarly, for the westbound structures, Virginia Tech instrumented spans 31 and 32, while the University of Virginia instrumented span 34.

To capture strain readings, each prestressed girder had a strain transducer placed in the longitudinal direction on its soffit at midspan to measure the maximum longitudinal strain in each of the girders. On girders 7 and 8 in span 31 of the westbound structure, four additional gauges were placed along the height of the girder at midspan to provide information regarding the vertical strain distributions in the region of flexural deterioration. All five gauges on girder 8 are shown in Figure 41. A similar setup was utilized in span 32 of the westbound structure (with no observed damage) to be used as reference values for comparison. Both girders 7 and 8 were instrumented, however only three gauges were distributed over the height at each location. Additionally, girder 8 in span 31 had five strain gauges distributed along its height at approximate locations of L/5 and 9L/10. This was to obtain the strain distribution where significant shear damage was observed. Girder 8 in span 32 had three strain transducers distributed along its height at the same 9L/10 location to act as reference values. Similar instrumentation scenarios were implemented in span 34 and in both eastbound spans.

Figure 41: BDI Nodes and Strain Transducers

The following pages (Figure 42 to Figure 45) illustrate the instrumentation layout for both the eastbound (56 and 57) and westbound (31, 32, 34) spans tested.

3.4.1 Westbound Structure

3.4.1.1 Spans 31 and 32

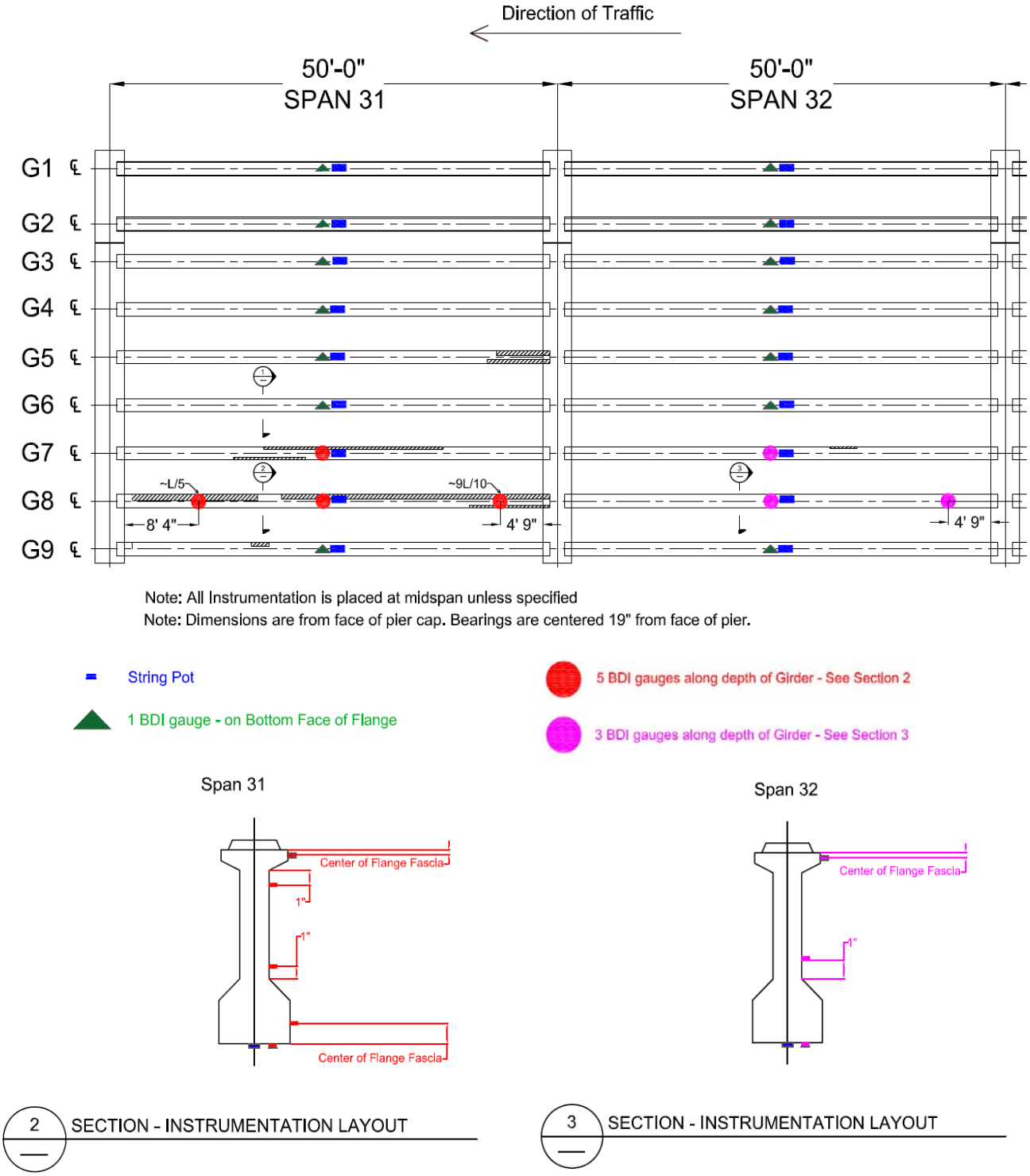

Figure 42: Spans 31 and 32 Instrumentation Plan

3.4.1.2 Span 34

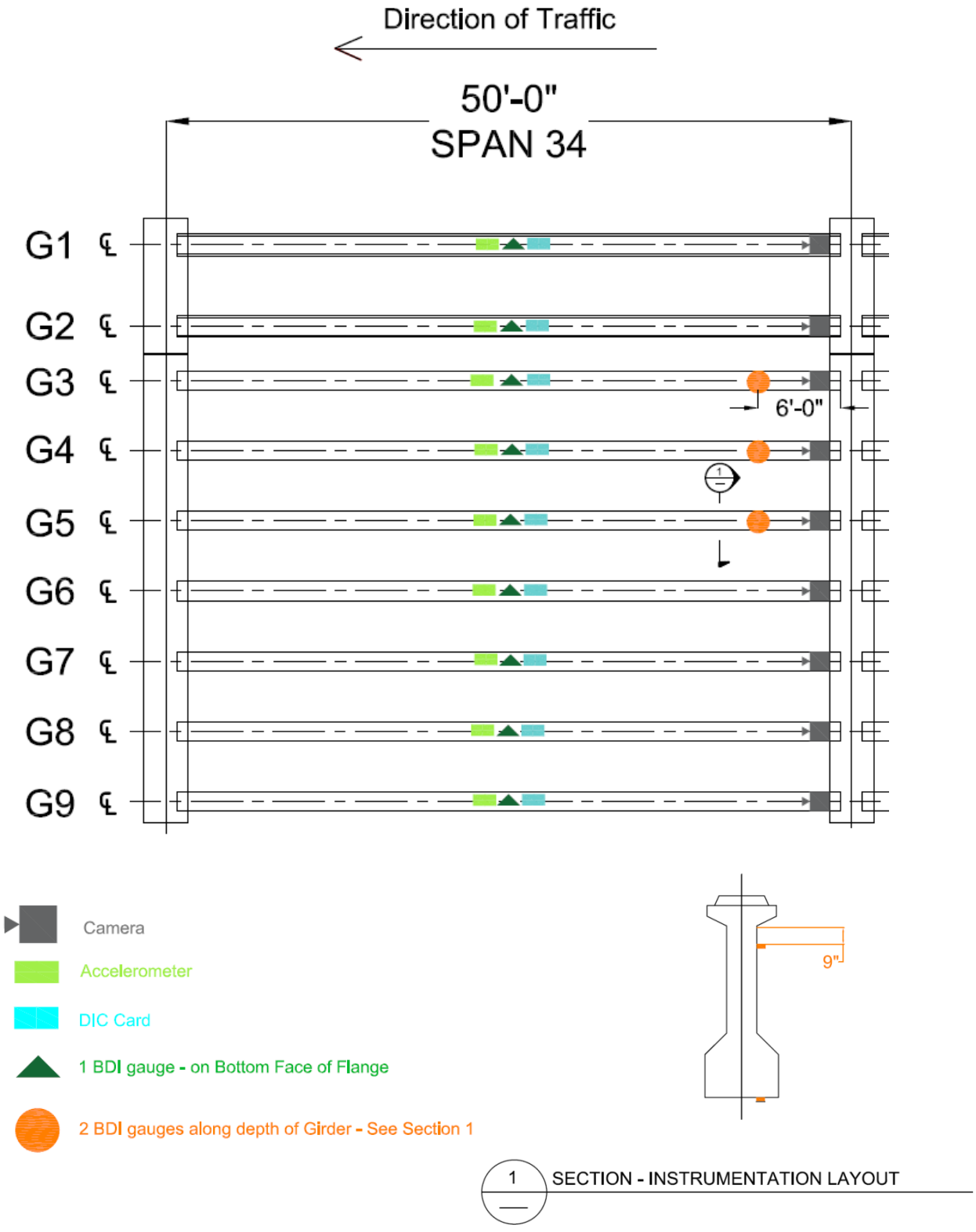

Figure 43: Span 34 Instrumentation Plan

3.4.2 Eastbound Structure

3.4.2.1 Span 56

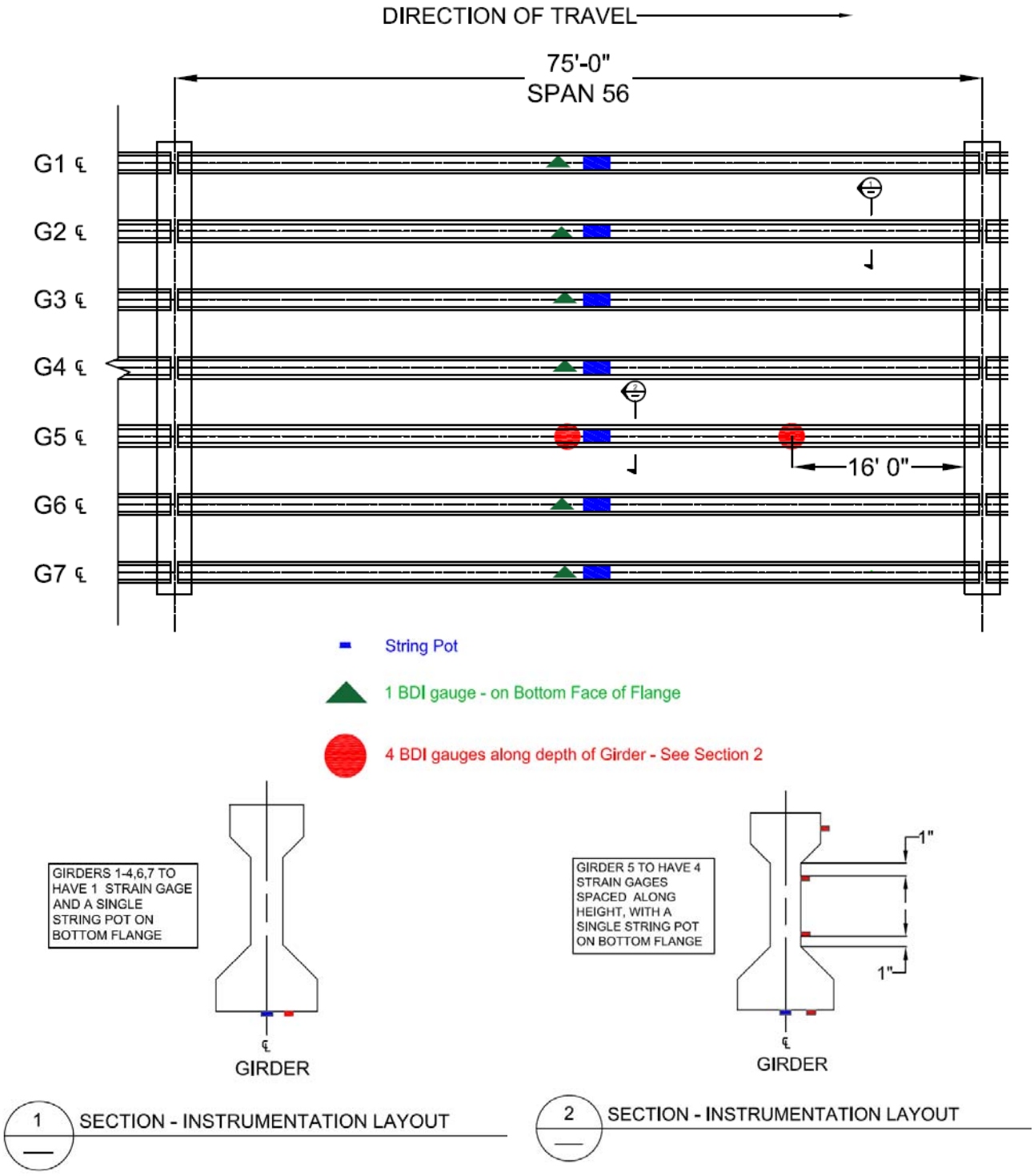

Figure 44: Span 56 Instrumentation Plan

3.4.2.2 Span 57

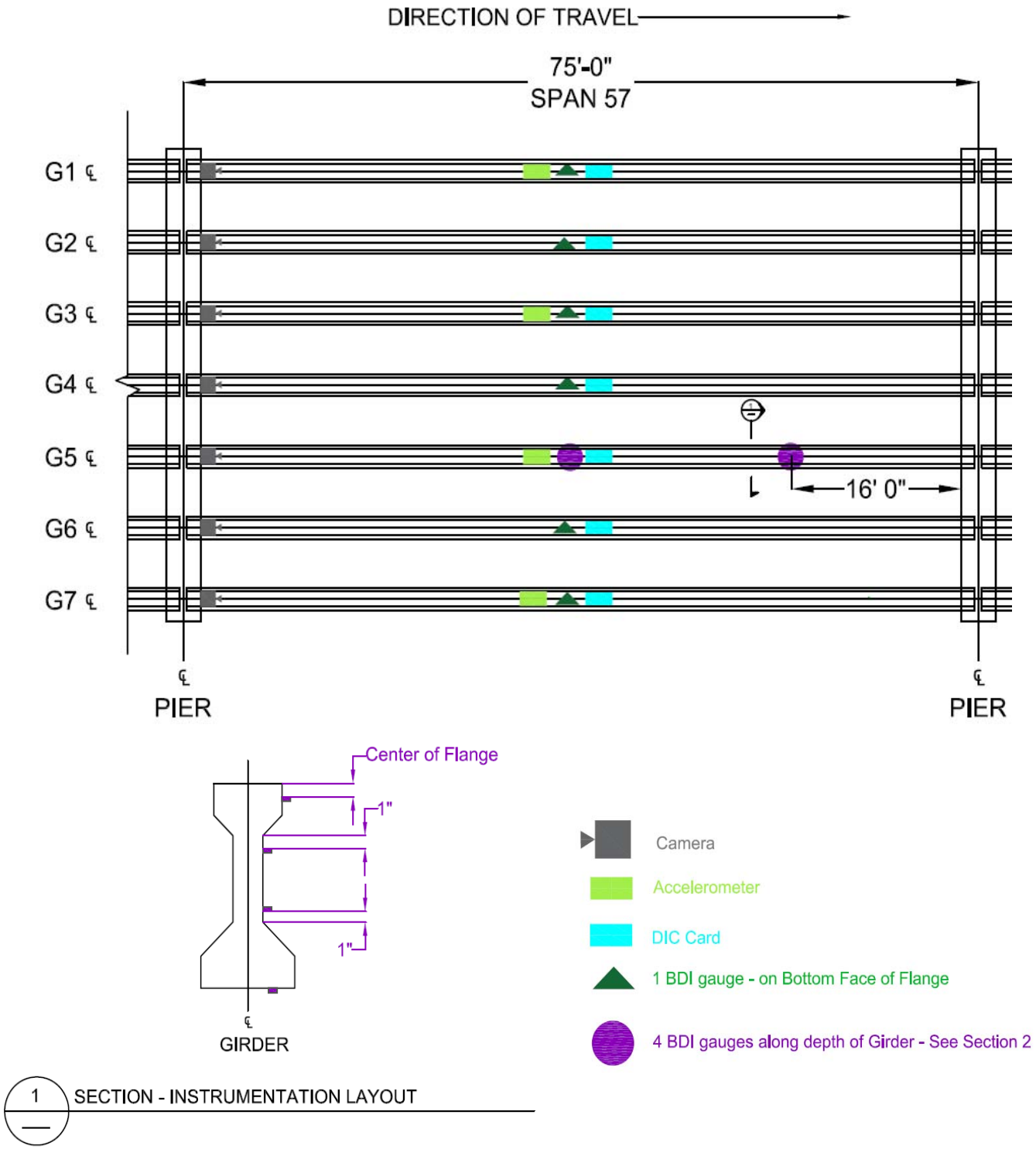

Figure 45: Span 57 Instrumentation Plan

3.4.3 Instrument Installation Time

The mobilization time from the marina to the eastbound structure was approximately one hour with the single engine 200 hp tug boat. Span 57 was instrumented in six hours, primarily from the barge with some help from the snooper. Span 56 was instrumented in all areas reachable from the smaller moog in four hours (while the barge was being used in span 57). An additional three hours were needed in the span with the barge to reach the remaining areas and troubleshoot the data acquisition systems. Even though the westbound structure was farther from the marina, the twin engine 1100 hp tug boat was able to round the artificial island and arrive at the test span in roughly 25 minutes. Span 31 took four and a half hours to instrument using only the barge. Span 32 required five and a half hours to instrument, wire the system, and troubleshoot whereas span 34 took approximately four hours.

The live load testing lasted approximately an hour and a half each night. The breakdown time for two spans from the barge, transporting back to the marina, and offloading the equipment took four hours. Using a half width Moog in one span and the barge in the other span (eastbound test night 1) decreased the time to three hours. It should be noted that the barge was much easier to work from than the Moog. Also, the two deflection systems required roughly the same amount of time to instrument.

Overall, from the time the trailer opened to load the equipment onto the barge to the time when the last piece of equipment was loaded back into the trailer after load test completion, 22 hours had elapsed. A similar time window was used for the eastbound test when the Virginia Tech and UVA teams each instrumented, tested and took down instrumentation for their respective single spans.

3.5 Truck Configurations

Six VDOT tandem dual dump trucks were filled with gravel and used as test vehicles (Figure 46). Before the load test began each night, truck dimensions were documented and portable scales were used to measure each axle load (See Appendix B). After weighing and measuring axles, the trucks were staged until intermittent traffic closures could commence at 11 PM. Once traffic was stopped at the tunnel entrance, the trucks drove to the test spans and were staged in five different configurations. Configurations 1 through 4 utilized a single truck either driving in a lane, or as close to the shoulder barrier as was physically possible. Configuration 5 used two trucks, one in each driving lane at the same time, at the same pace. Figure 47 illustrates

each of the truck configurations. All of the trucks were driven across each span at approximately 5 mph simulating a “crawl” speed so no dynamic effects were captured by the instrumentation.

Figure 46: VDOT Truck

Configuration #1

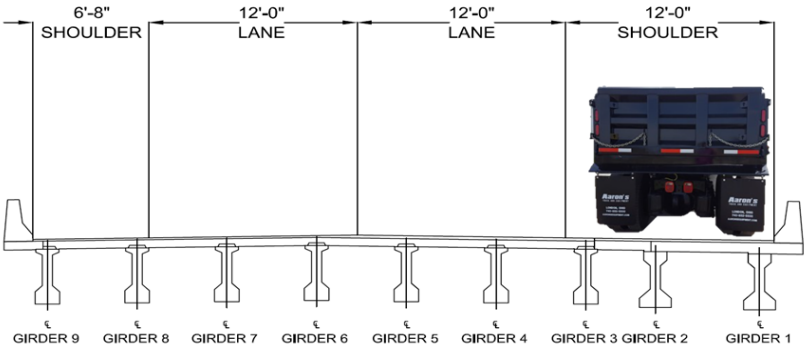

Configuration #2

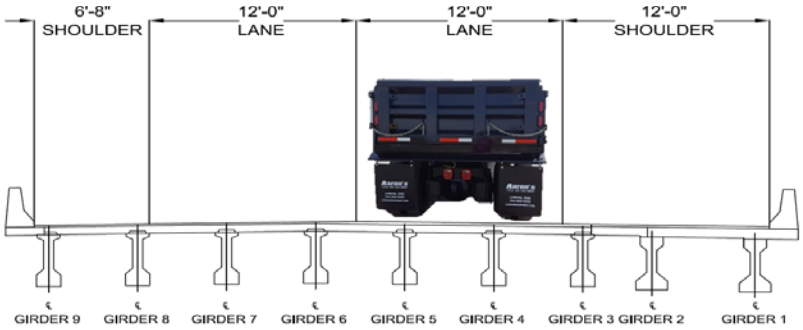

Configuration #3

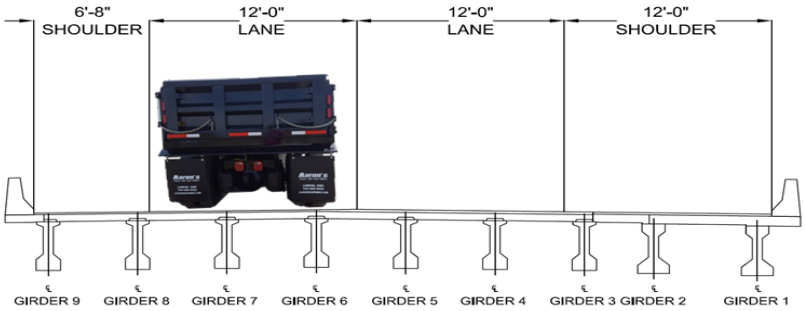

Configuration #4

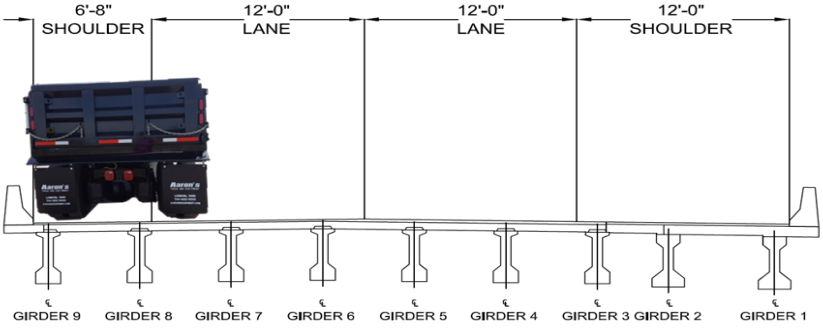

Configuration #5

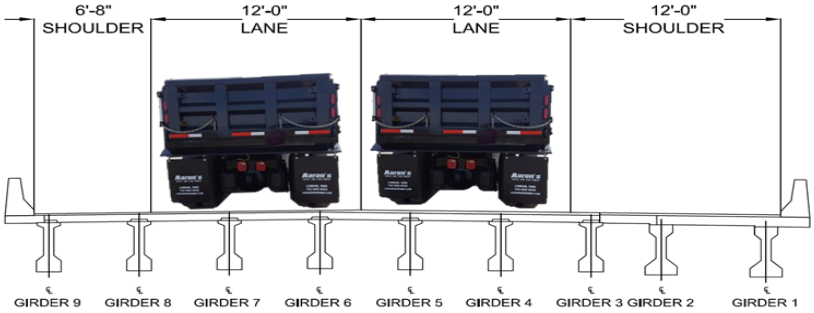

Figure 47: Truck Configurations

During the night of testing westbound spans 31 and 32, a single run of all truck configurations took five minutes. The time waiting for traffic to clear from the tunnel closure was only roughly 5 minutes leading to a total traffic stop of about ten minutes. In the second run, each truck configuration was walked forward across the test spans, reversed across the test spans, and then walked forward a second time to get three trials of data for each configuration. The total truck running time for this method was 13 minutes. Including the 5 minute delay for traffic clearing, the total bridge closure was kept to 18 minutes. The time for the trucks to make the round trip back to the staging area for the next closure averaged twenty minutes with typical midnight traffic. The same process was used for span 34 testing the following night.

Eastbound spans 56 and 57 were tested in a similar fashion but the trucks weren't reversed across the test spans. Once the trucks were staged, each configuration was walked across the test spans and kept driving. This minimized closure time to roughly ten minutes but more round trips (meaning more intermittent traffic stops) were needed.

CHAPTER 4 – LOAD TEST RESULTS AND DISCUSSION

The measurements from all live load testing were analyzed and organized into data sheets found in Appendix C. All of the data sheets follow the same format and are organized by span number and then broken up into the five truck configurations. In order to describe the results in detail, a single configuration will be discussed. The fifth truck configuration, one truck in each travel lane, was chosen as the representative example to describe the results. This configuration was run three times for each of the eastbound spans yielding three sets of data. Westbound spans 31 and 32 were tested on the same night and each truck configuration was run five different times to ensure repeatability in the data. Span 34 of the westbound structure was tested the following night and three truck runs of each configuration were performed.

4.1 Eastbound Span 56

The BDI system performed extremely well during the first round of testing, yielding a large amount of usable data. The midspan strains are plotted along the cross section for truck configuration 5 in Figure 48.

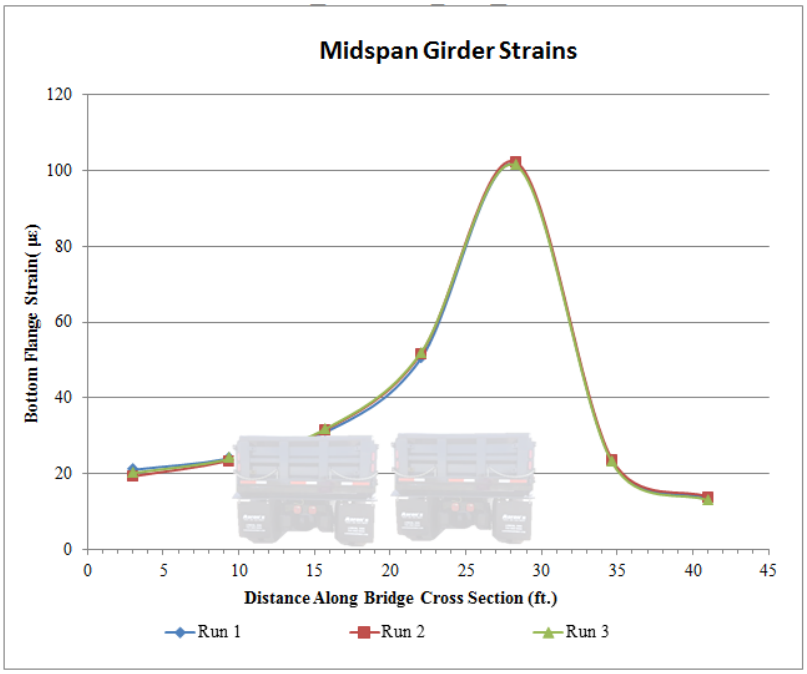

Figure 48: Eastbound Span 56 Midspan Strain Distribution

The strain values in Girder 5 were extremely elevated due to the deterioration to the girder. This was consistent through all of the truck configurations, even if the truck was on the

opposite side of the cross section. The vertical strain distribution of this girder at midspan, shown in Figure 49, illustrates this behavior.

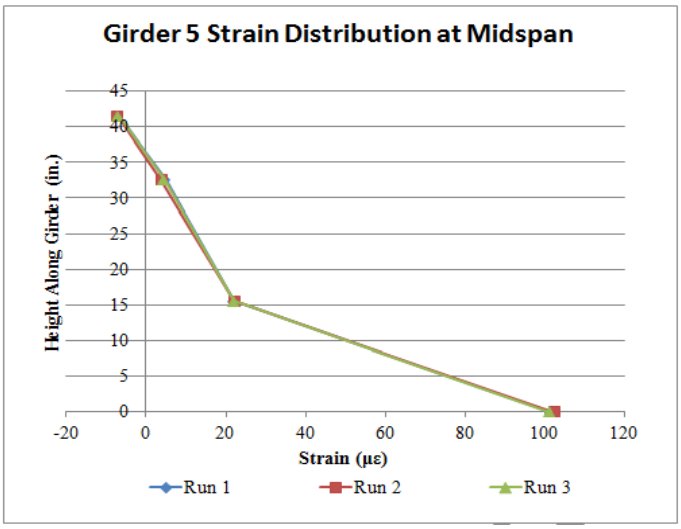

a) Vertical Strain Distribution Data

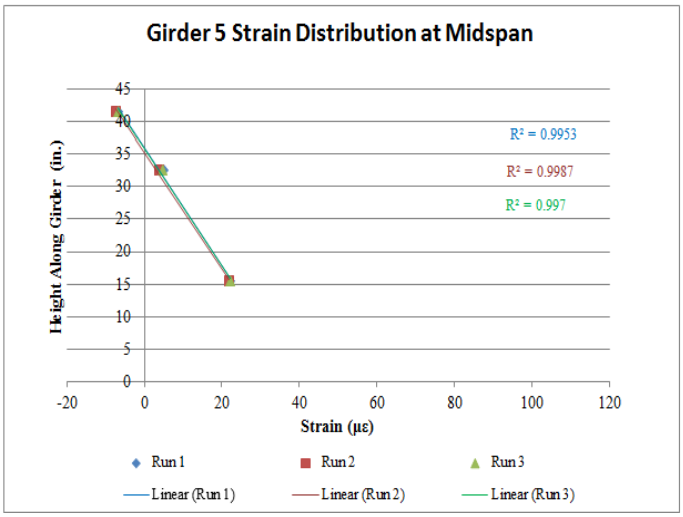

b) Linear Best Fit of Data

Figure 49: Eastbound Span 56 Midspan Vertical Strain Distribution

The strain distribution was still linear in the undamaged portion of the girder cross section. Overall, the strain distribution exhibited bilinear behavior due to the damage causing the strain distribution slope to change. Since this data was post-processed prior to the westbound test, another strain transducer was added between the bottom two transducers on the westbound girders so a better understanding of the strain distribution could be obtained during the westbound testing. The bilinear distribution was not representative of the entire girder. The

instrumentation at the 3L/4 location showed extremely linear strain distributions as shown in Figure 50. This proves that the strain distribution only changes in the locally damaged areas, not over the entire length of the girder.

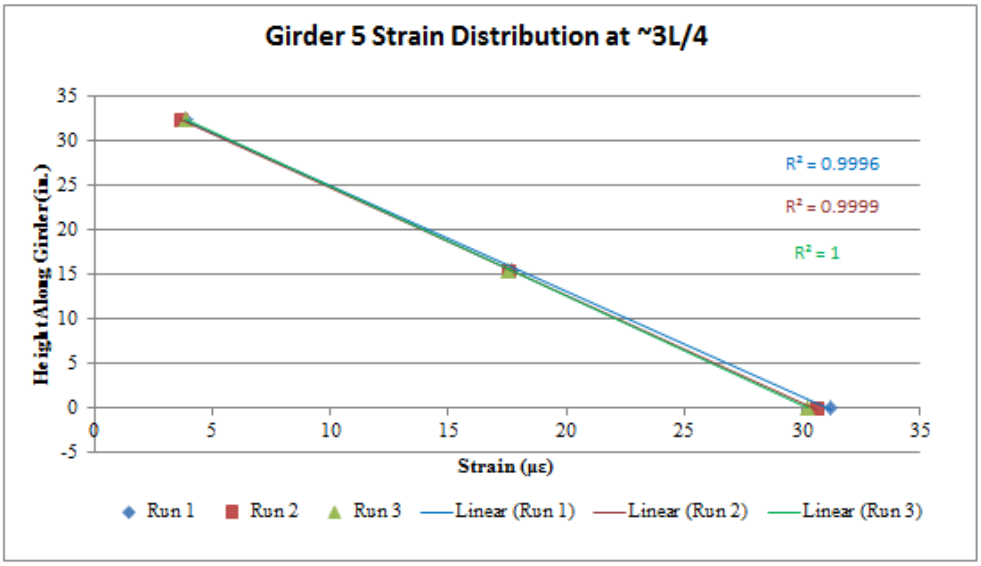

Figure 50: Eastbound Span 56 Girder 5 3L/4 Strain Distribution

Since the vertical strain distribution proved the bottom soffit strain value didn't represent the amount of load that girder 5 was resisting, the cross sectional plot was revisited. The line of best fit from the vertical distribution was used to develop an "actual" strain value on the girder soffit at midspan. This strain value was then used to adjust the cross sectional strain distribution plot, illustrated in Figure 51, which was more representative of the load distribution in the damaged span.

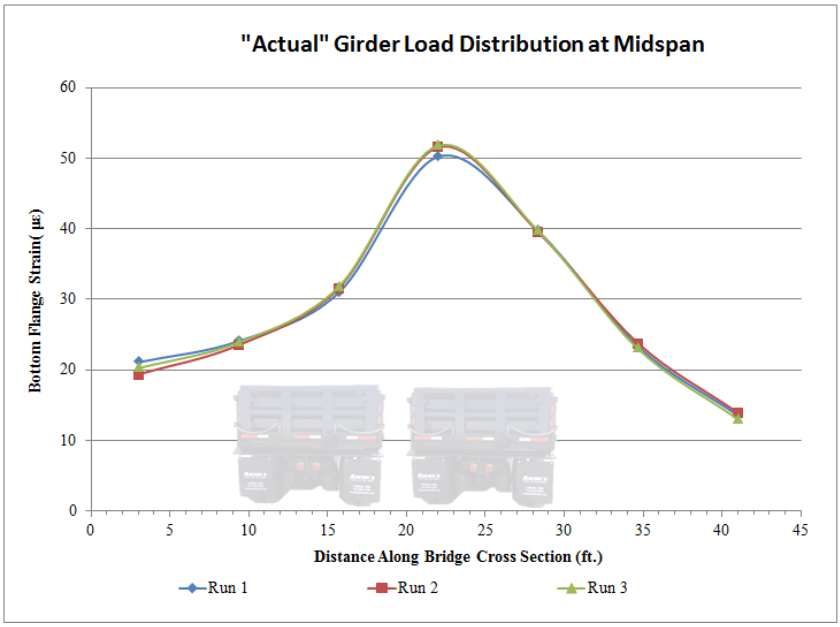

Figure 51: Eastbound Span 56 "Actual" Cross Section Strain Distribution

4.2 Eastbound Span 57

Similar to Span 56, the midspan strain results were plotted along the cross section to get an understanding of the load distribution between the girders, as shown in Figure 52. The results from the girder 2 strain transducer where higher than expected in all of the truck configurations. After this was brought to the attention of the UVA team, it was proven that this sensor was not correctly calibrated. UVA did not post-process their data until after the westbound test so this same sensor was one of the sensors used in the westbound test on span 34.

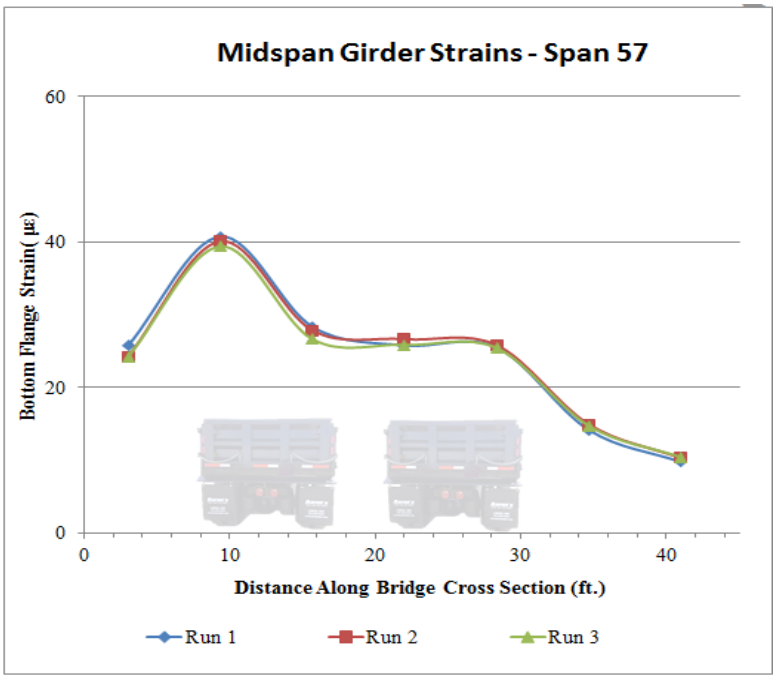

Figure 52: Westbound Span 57 Midspan Strain Distribution

The strain distribution of girder 5 was captured at midspan and 3L/4, similar to span 56. These distributions proved a linear strain distribution throughout both of the girder cross sections as shown in Figure 53. This was expected since there was no damage to this girder in span 57.

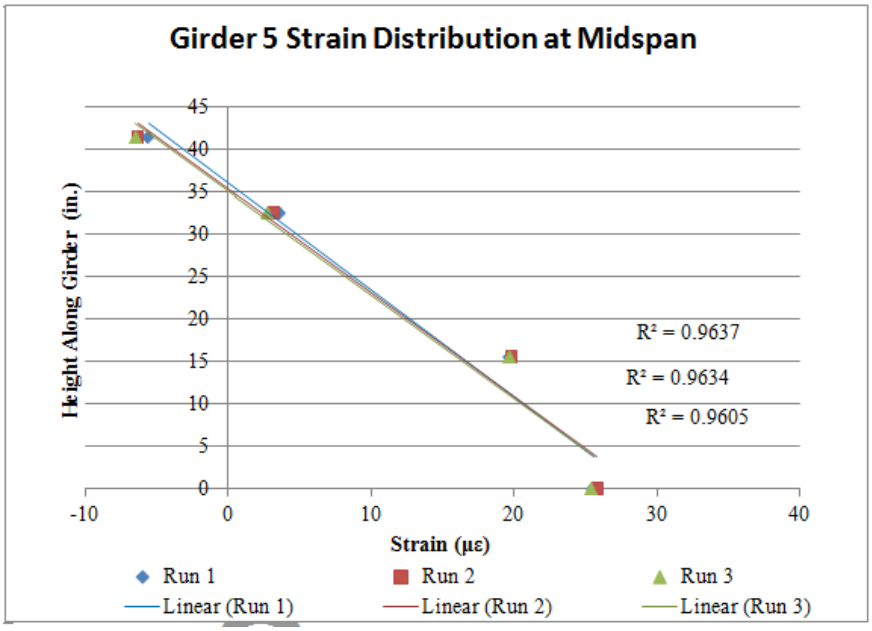

a) Girder 5 Midspan Strain Distribution Best Fit

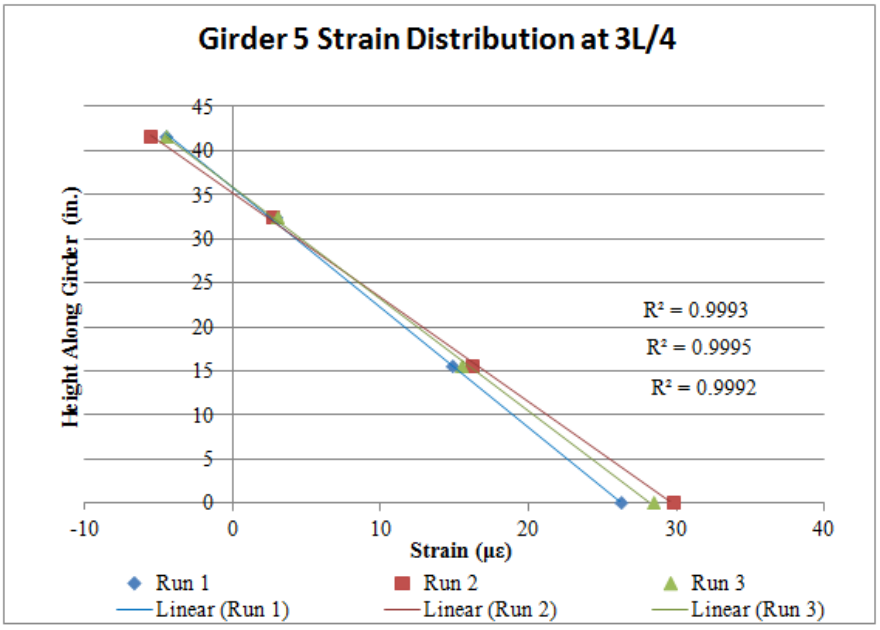

b) Girder 5 3L/4 Strain Distribution Best Fit

Figure 53: Eastbound Span 57 Strain Distributions

The camera deflection system deployed in this span worked well and was able to capture data on the girder deflections. These deflections showed a typical load distribution between girders for an undamaged span as illustrated in Figure 54. This helped prove the strain values of girder 2 were incorrect. As stated earlier, the deflection values were discarded from Span 56 so these deflections trends could not be compared to span 57 deflections. Some of the cameras

began sampling at different rates or malfunctioned and stopped working during the test which explains why some data points are missing from the figure.

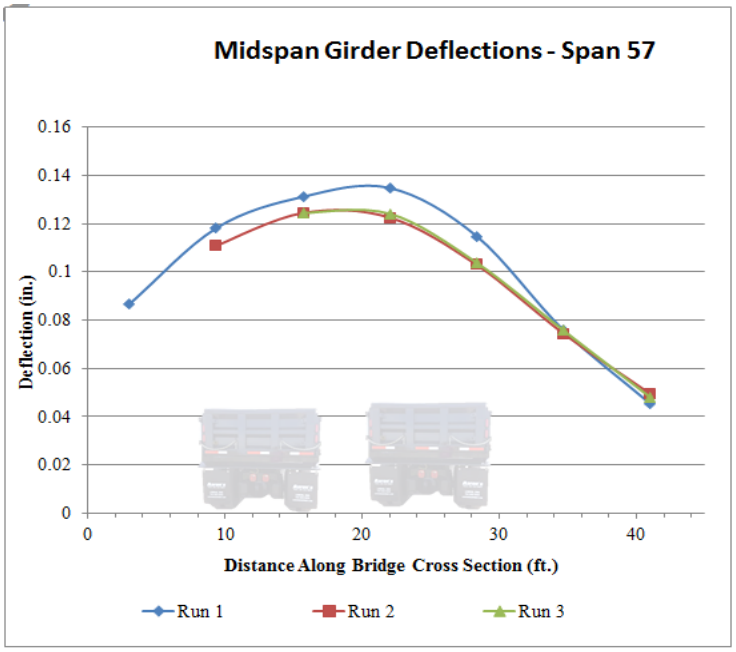

Figure 54: Eastbound Span 57 Midspan Girder Deflections

(Note: Girder 1 is on the Far Left)

4.3 Westbound Span 31

The strains in westbound span 31 resulting from truck configuration 5 (one truck in each the travel lane) are shown in Figure 55. As expected, the bottom flange soffit strains in girder 7 were relatively high because of the extensive damage. The strains (girder 6 omitted) were plotted across the width of the bridge to show a load distribution. The distribution is looking in the direction of traffic, hence the back of the trucks being seen in Figure 55, so girders are plotted 9-1 from left to right to keep the same numbering convention from VDOT inspection reports. The strain values recorded from girder 6 appeared abnormally low and did not show much variance in magnitude between different truck configurations so this data was considered faulty and was therefore omitted. The faulty data could have been from bad contact between the strain transducer and the concrete if the contact adhesive didn't fully adhere. It could also be from gauge placement. If the gauge was adjacent to a microcrack, the crack opening and closing would cause low strain values adjacent to the crack and much higher strains if the gauge bridged over the microcracks. It is also possible that the gauge was fastened to delaminated concrete/shotcrete which would cause minimal change in strain readings. Regardless, the data

was omitted as shown in Figure 55 where the trendlines are not continuous between girders 5 and 7.

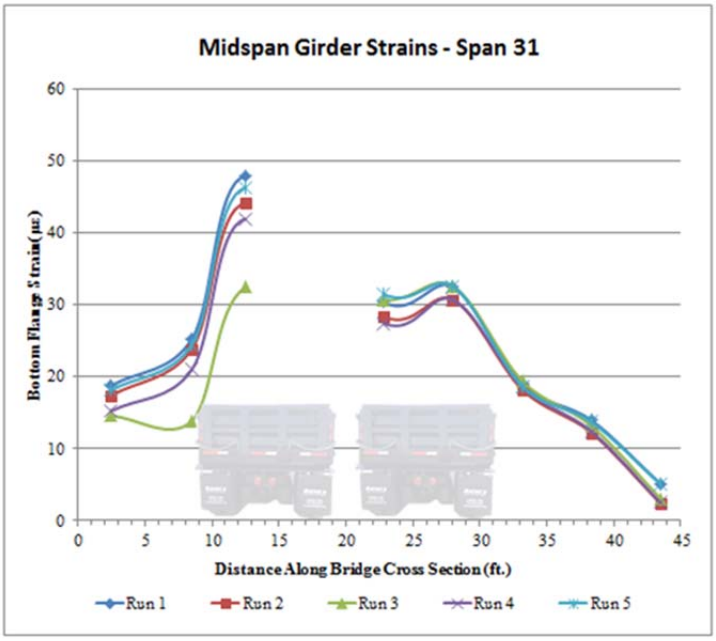

Figure 55: Span 31 Midspan Girder Strains

(Note: Girder 1 is on the Far Right)

Similarly, the midspan deflections for each of the truck configurations were plotted along the cross section, shown in Figure 56, to get a sense of load distribution. As with the strains, the plot is looking in the direction of traffic so girders are plotted 9-1 from left to right.

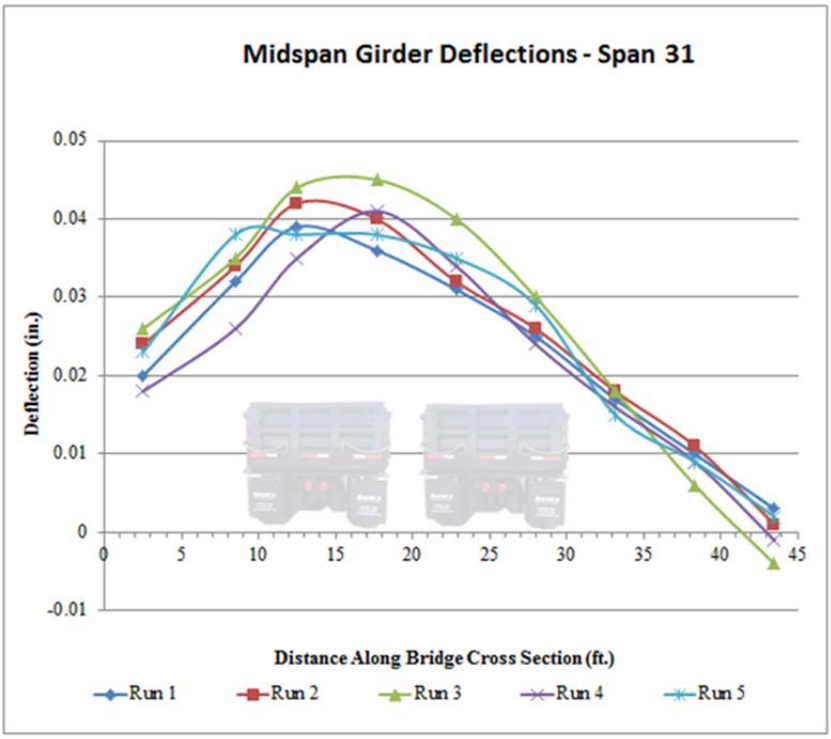

Figure 56: Span 31 Midspan Girder Deflections

(Note: Girder 1 is on the Far Right)

In contrast to the strains, no excessive magnitudes were observed in the deflections. The strains measured illustrate localized stress increases resulting from damage, but the girder deflections represent a global behavior and are not altered substantially by localized damage areas.

The vertical strain distribution data illustrates that the undamaged sections of the girders exhibited a linear strain distribution. However, the localized damaged region of the girders illustrated a nonlinear strain distribution (see Figure 57a). The strain distribution was linear above the damaged section as illustrated by the R^2 values in Figure 57b.

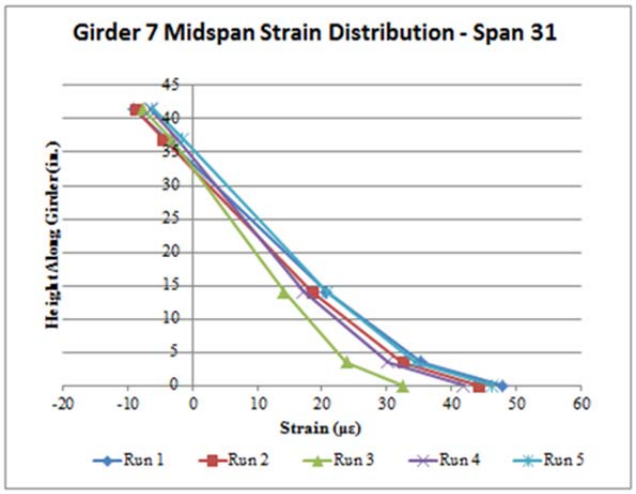

a) Strain Distribution Data

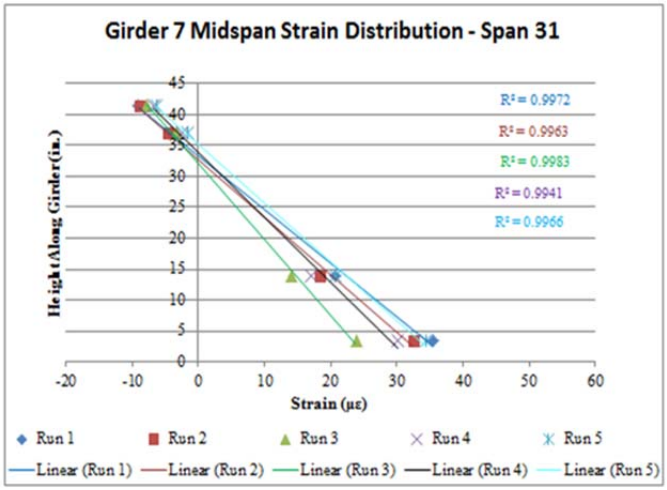

b) Linear Best Fit of Data

Figure 57: Span 31 Girder 7 Midspan Strain Distribution

The damage in girder 7 was mostly to the soffit of the bottom flange whereas girder 8 had damage near the mid-height of the bottom flange. Again, a strain increase was captured within the damage region as shown in Figure 58a. The data again illustrated that the strain distribution was linear above the damaged section with an R^2 of roughly 0.98 (see Figure 58b). The minimal amount of data in these plots is attributed to the node communication problems during the load tests. Only Run 5 was able to capture data for all of the transducers along the depth of the girder cross section. Runs 1 through 4 only captured data for the bottom two transducers which were working off a different node than the other three gauges. Overall, the data from the first four runs still correlated very well with Run 5.

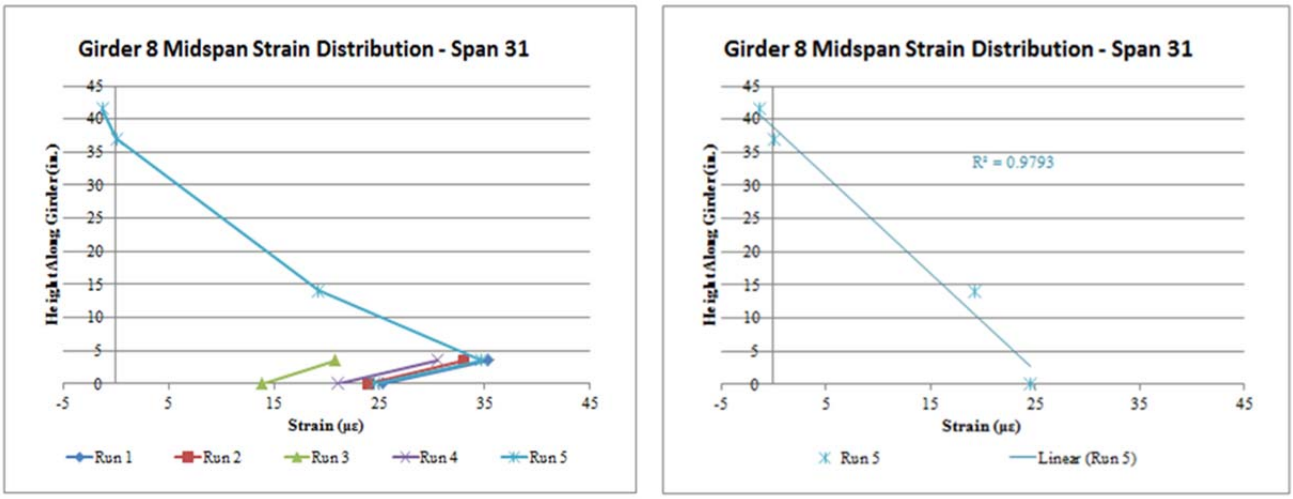

a) Strain Distribution Data b) Linear Best Fit of Data

Figure 58: Span 31 Girder 8 Midspan Strain Distribution

Data was also collected at two locations of shear damage on girder 8, L/5 and 9L/10. Both of these locations showed linear strain distributions with R^2 values of 0.98-0.99 as shown in Figure 59a and b.

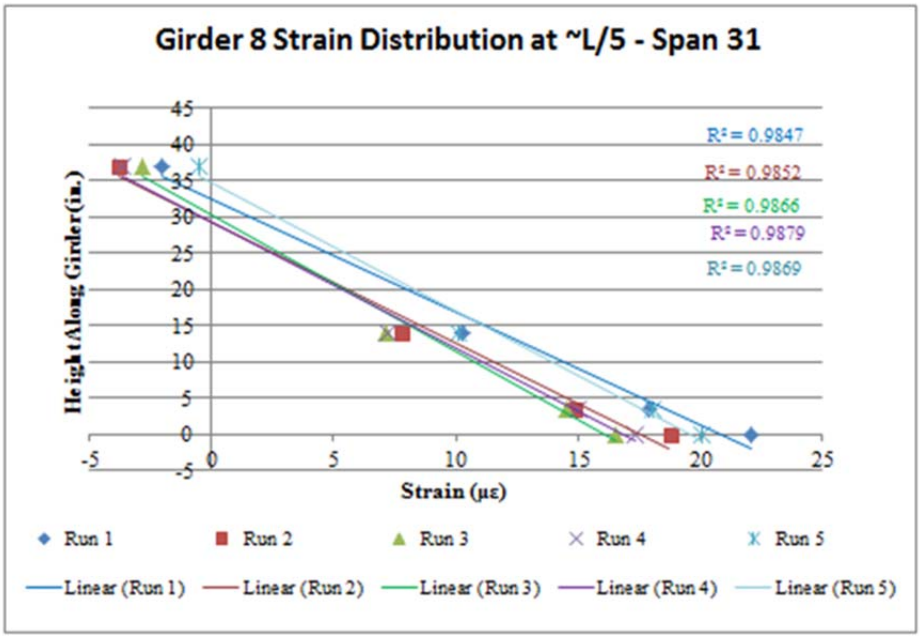

a) L/5 Linear Best Fit

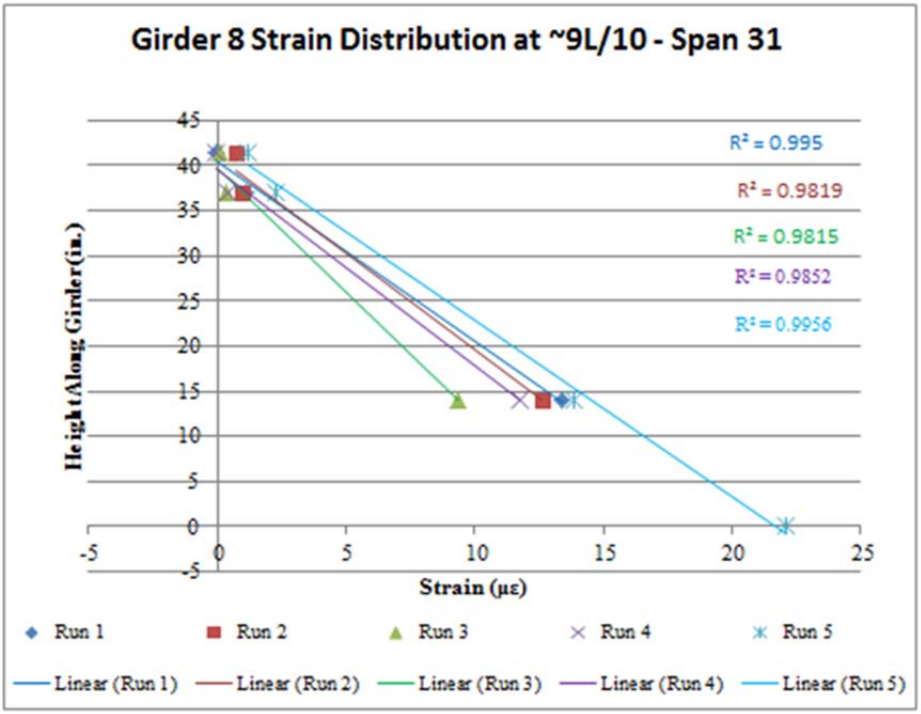

b) 9L/10 Linear Best Fit

Figure 59: Span 31 Girder 8 Shear Location Strain Distributions

4.4 Westbound Span 32

The strains and deflections on westbound span 32 were also plotted along the cross section of the bridge to illustrate the load distribution (see Figure 60a and b). There was minimal damage in this span which resulted in no spikes in strain or deflection data. Girder 7 strain magnitudes were abnormally low throughout each truck configuration so the data was omitted due to faulty instrumentation, most likely from bad contact adhesion. These values were discarded in the strain plot in Figure 60a. The deflection values in Figure 60b are from the string pot deflection system. The DIC values recorded in this span were excluded for plot clarity but are discussed later in the report.

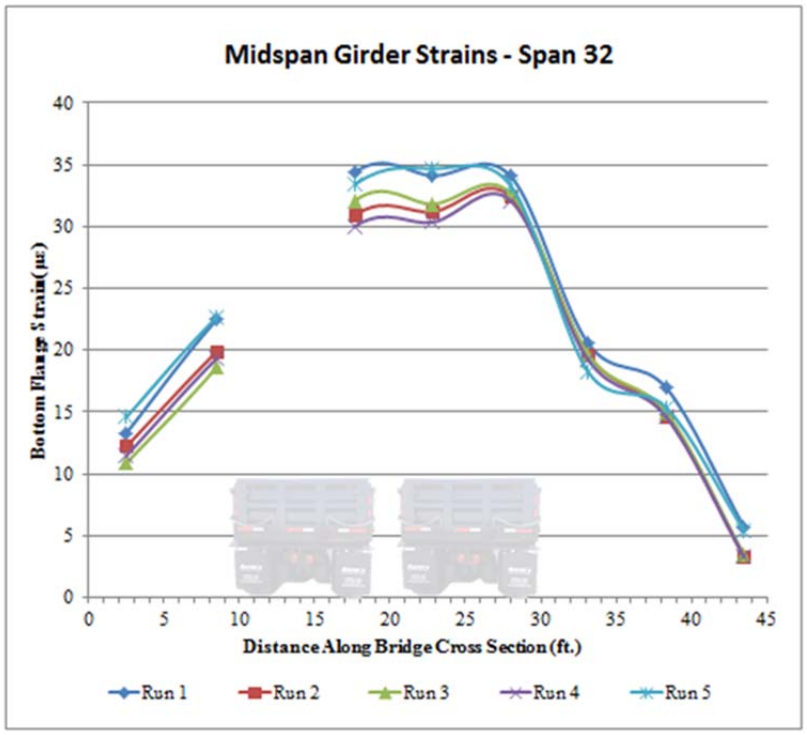

a) Span 32 Midspan Strains

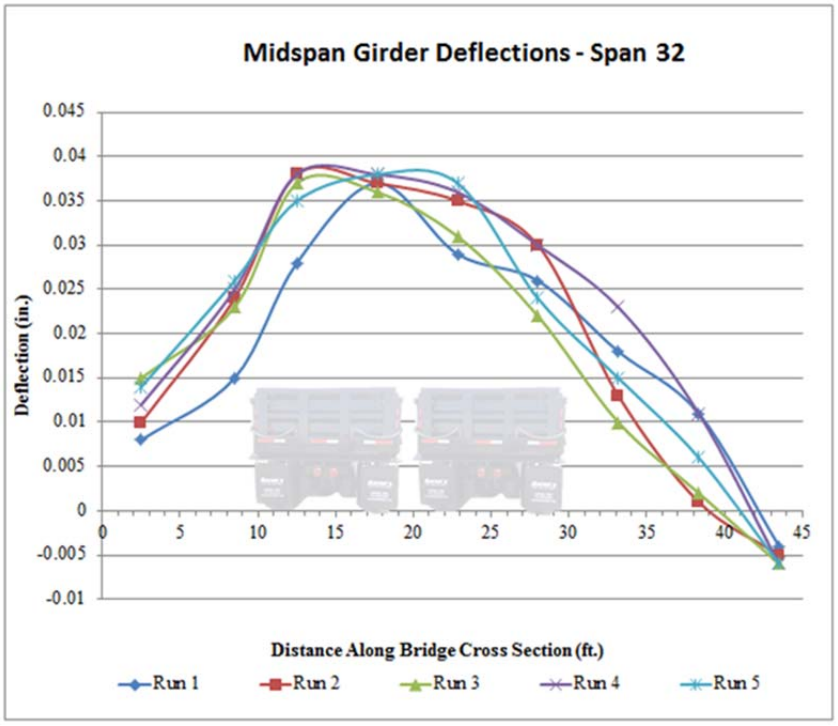

b) Span 32 Midspan Deflections

Figure 60: Span 32 Midspan Data Distributions

(Note: Girder 1 is on the Far Right)

The vertical strain distributions were plotted at midspan of girders 7 and 8 to compare with data obtained from other spans. The results show a fairly linear distribution in both girders. The bottom data point for girder 7 is the location where there wasn't enough adhesion to the concrete so the values are believed to be "softened" since they are not fully capturing the strain magnitude. Since there were only three data points along the girder height, the values were kept in the plot. The middle three runs in girder 8 showed the same softening in the soffit gauge magnitudes but the values increased in the first and final runs and became much more linear as shown in Figure 61.

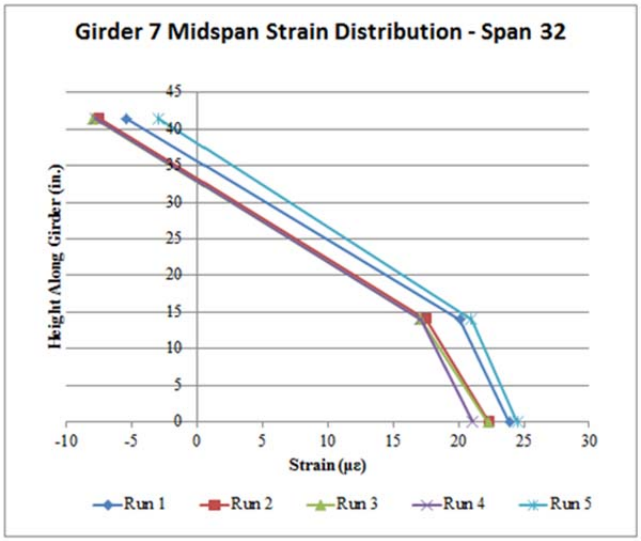

a) Girder 7 Strain Distribution

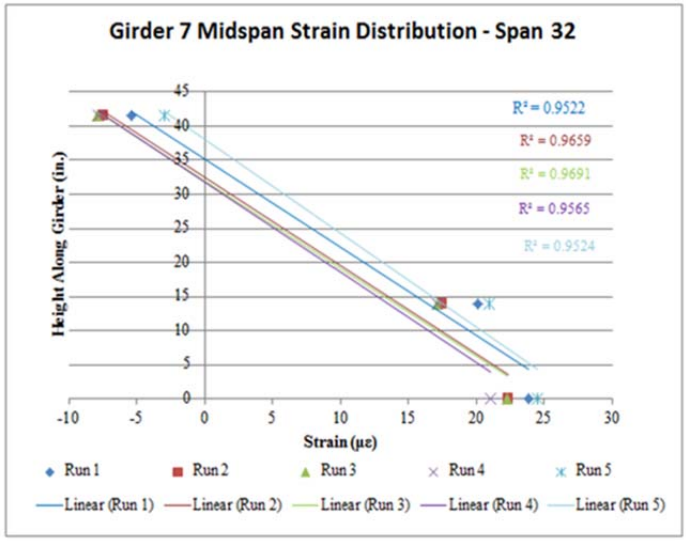

b) Girder 7 Linear Best Fit

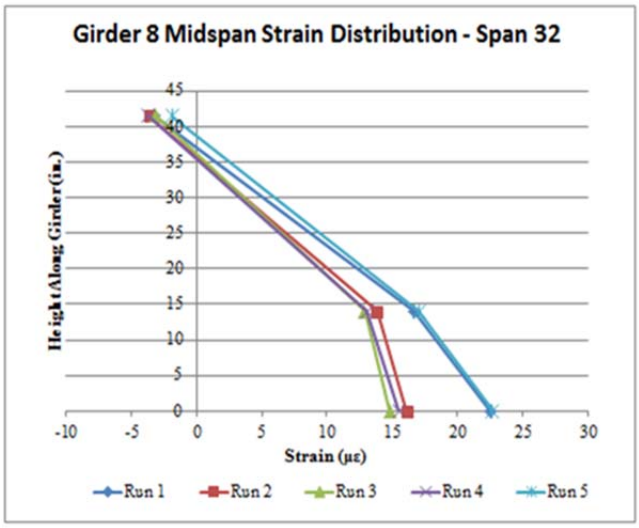

c) Girder 8 Strain Distribution

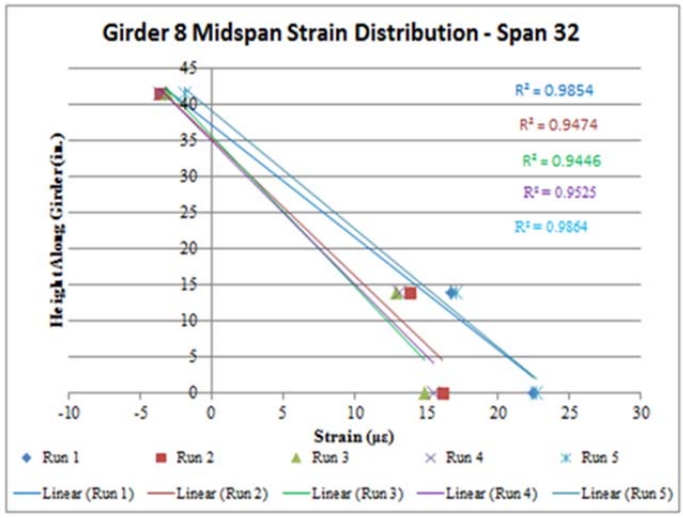

d) Girder 8 Linear Best Fit

Figure 61: Span 32 Midspan Strain Distributions

For comparison purposes with span 31, the same shear location was instrumented at ~9L/10 for span 32 (see Figure 62a). The results indicate a linear strain distribution as shown in Figure 62b.

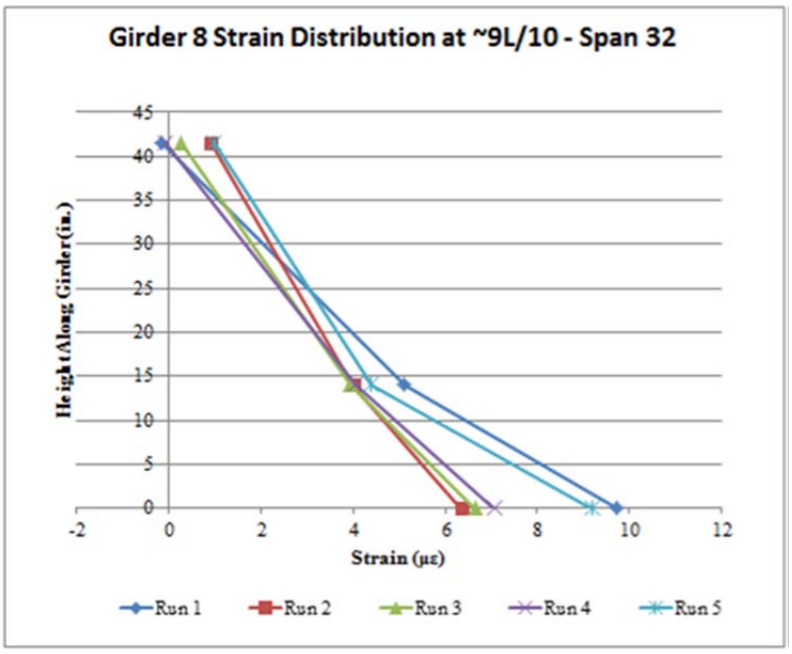

a) Vertical Strain Data

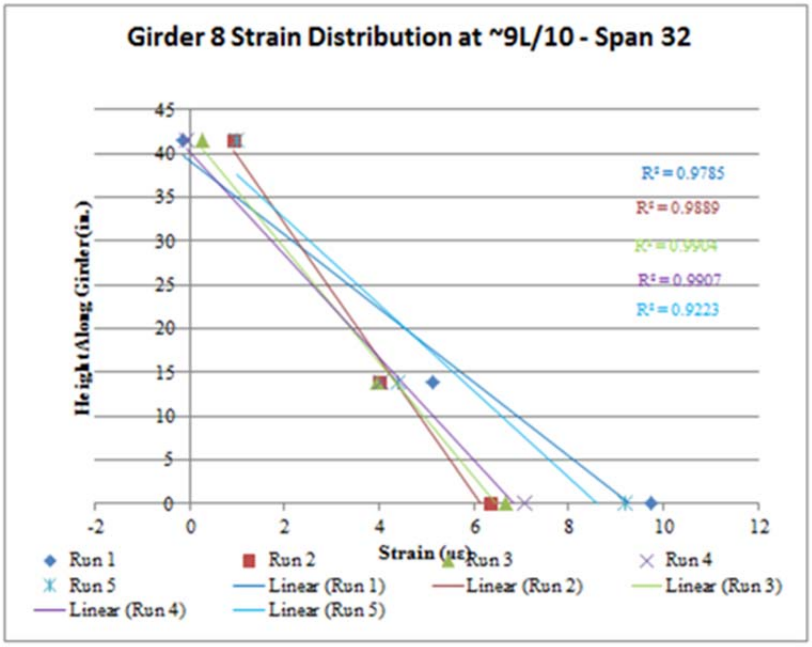

b) Linear Best Fit

Figure 62: Span 32 Girder 8 Strain Distribution

4.5 Westbound Span 34

After reviewing the data from UVA, the strain data collected in westbound span 34 was deemed to be unreliable due to inconsistencies in the level of strain relative to the expected response to loading. The measurements from these sensors were consistently low when compared to the surrounding gauges and no significant damage was noted in the region of measurement. Figure 63 illustrates the strain measurements that were deemed acceptable when compared to those measured in spans 31 and 32. It should be noted that the project team had difficulties with adhesion on at least two of the girders (G8 and G9) during installation. While the gauges were adhered, this effect could have resulted in slippage of the sensors during testing. After these inconsistencies were pointed out to the UVA team, they ran controlled laboratory tests to verify their BDI strain transducers. The controlled tests proved that at least four of their sensors were not calibrated correctly proving that the data recorded from the field test was inaccurate.

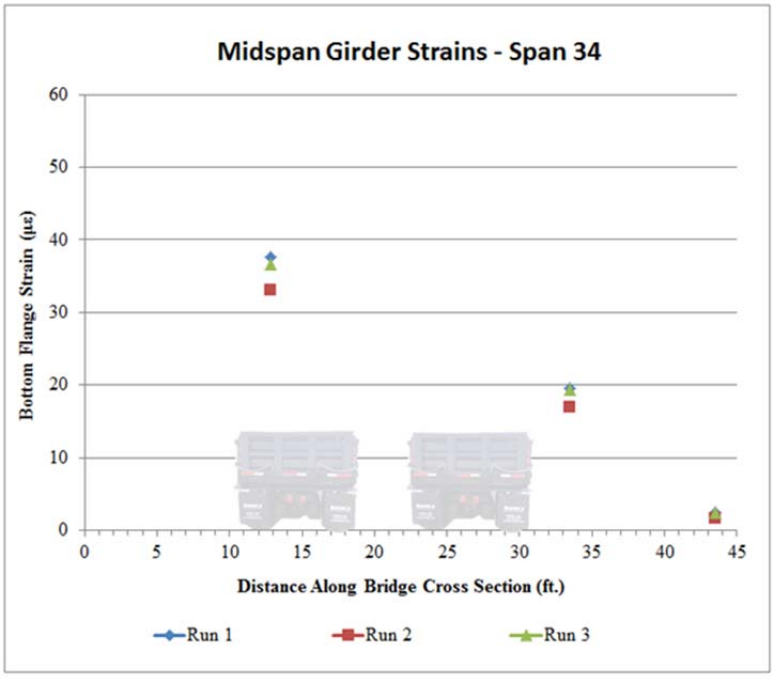

Figure 63: Span 34 Midspan Strains

(Note: Girder 1 is on the Far Right)

Deflection measurements for span 34 yielded responses that were expected for each of the loading patterns. Figure 64 illustrates the load distribution characteristics of this span for truck configuration 5, which appears to be distributed proportionally relative to the load position. This response would be expected in a span without significant damage near midspan. Recall that

girder 4 exhibited concrete cover loss on the side of the bottom flange along with a longitudinal delamination, but no broken strands at midspan. Measurements from Girder 2 were discarded because of the camera malfunctioning during the load test.

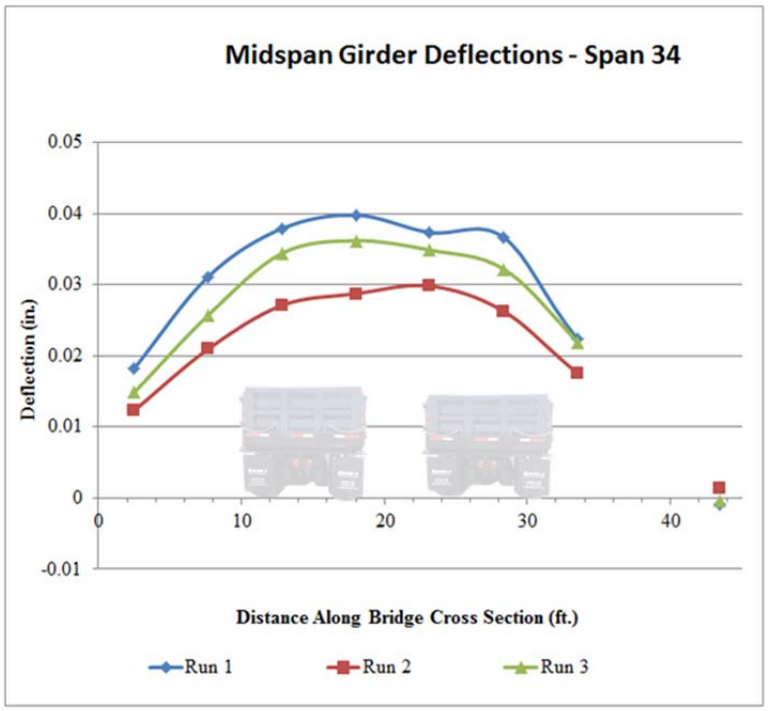

Figure 64: Span 34 Midspan Deflections

(Note: Girder 1 is on the Far Right)

For the shear region of this span with excessive deterioration (girder 4), usable data was not obtained. Only two strain transducers were placed along the height of the girder, so a linear strain distribution could not be proven.

4.6 Strain Distributions

Using the measured strain and deflection values (reported in Appendix C), comparisons were made between spans to gain a better understanding of the effects of deteriorated members on the system behavior. For each configuration, the truck made multiple passes to develop multiple runs of data. Five runs of each truck configuration were performed on the westbound spans 31 and 32. Three runs of each truck configuration were performed on the westbound span 34 and eastbound spans 56 and 57. There were slight differences between the exact transverse truck locations from run to run. To remove this discrepancy, the data for each truck configuration was averaged between all runs for each truck configuration. The average values were used in the comparison plots (see Appendix D). Figure 65 shows an example comparison plot which graphs

the average strains values in westbound spans 31, 32 and 34 for truck configuration 5. The plot keeps the same orientation as previous results by looking in the direction of traffic and girders plotted 9-1 from left to right. As previously discussed, a number of gauges yielded inconsistent measurements and are therefore not plotted, resulting in non-continuous transverse distribution lines. Similar plots were made for the other four westbound truck configurations as well as for all eastbound configurations. The plots are shown in Appendix D.

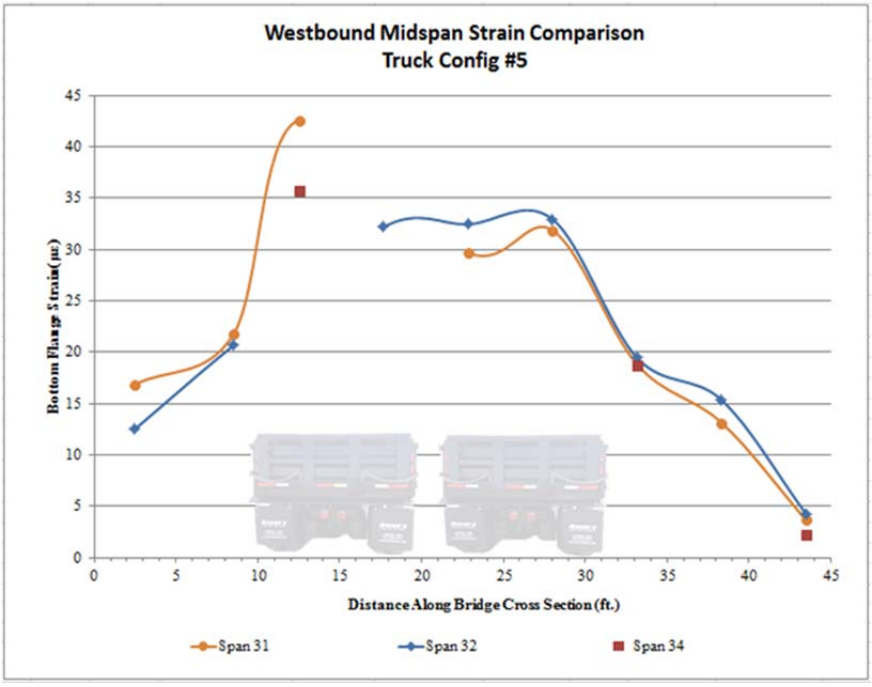

Figure 65: Westbound Midspan Strain Comparison

(Note: Girder 1 is on the Far Right)

In addition, it was observed that the damage on girder 5 of span 56 caused the neighboring girders to have higher strain readings than the undamaged span indicating they were taking on more load due to the damage in girder 5. Figure 66 shows the global load redistribution between girders because of the damage in girder 5. After comparing the spans in the eastbound structure, some of the trends did not match in the vicinity of girder 2. Nothing definitive could be concluded based on the strain values, but it is possible that the strain data on girder 2 of the eastbound span 56 were incorrect. Since nothing definitive could be concluded, the data from this gauge was kept in the data sheets and all comparison plots. Strain comparison plots for all westbound and eastbound truck configurations can be found in Appendix D.

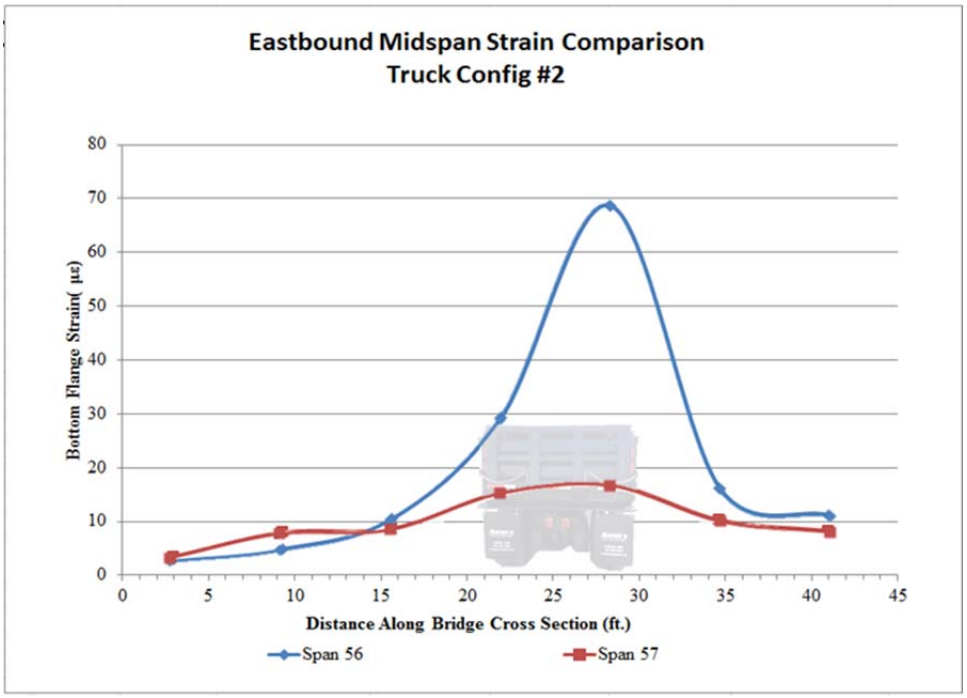

Figure 66: Eastbound Midspan Strain Comparison

(Note: Girder 1 is on the Far Left)

From the strain comparison of truck configuration 5 on the westbound structure (Figure 65), it can be seen that girder 7 in span 31 is experiencing significantly higher strains than the trend shows for the undamaged span 32. The other girders in span 31 are resisting loads similar to their undamaged counterparts in span 32. This plot can be misleading because it is solely comparing the strains on the soffits of the girder bottom flanges. While girder 7 of span 31 had damage to its soffit which caused the high strains in the concrete, the remainder of the cross section experienced normal strains. This is illustrated in Figure 67 which compares the cross-sectional strain distribution from girder 7 of span 31 to girder 7 of span 32. Similar behavior was seen in the comparison of girder 8 in spans 31 and 32. The undamaged portions of the deteriorated girder in span 31 closely mimicked the strain values of the undamaged girder in span 32 as shown in Figure 68.

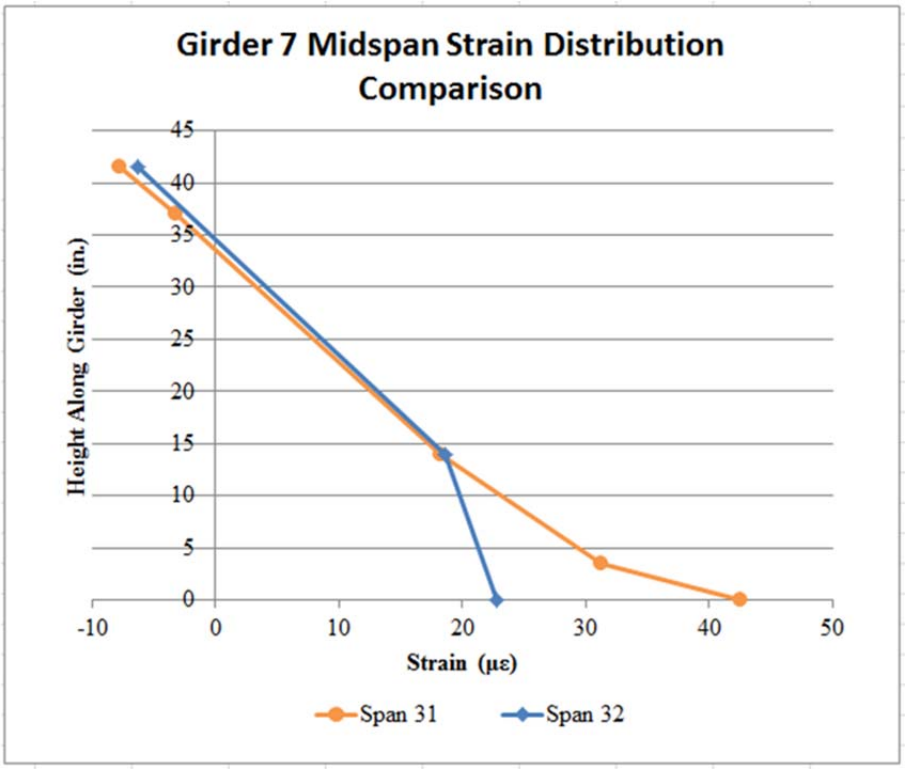

Figure 67: Westbound Girder 7 Midspan Strain Distribution

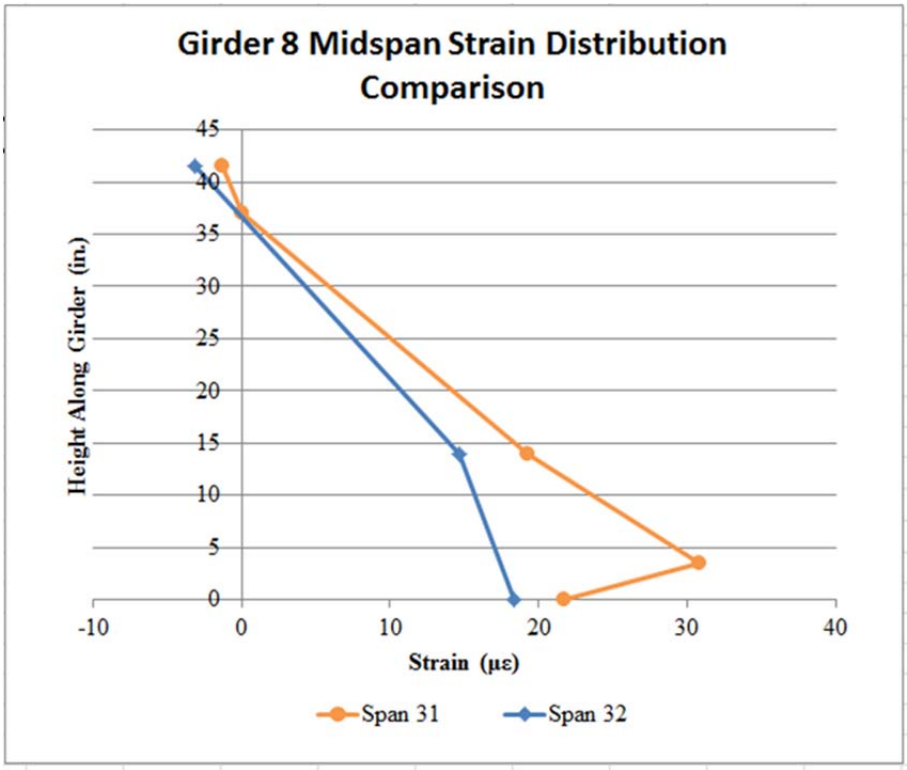

Figure 68: Westbound Girder 8 Midspan Strain Distribution Comparison

Similar results were seen in girder 5 of eastbound span 56 where there was a significant increase in strain readings at the bottom of the girder where the entire bottom layer of strands was heavily corroded. Figure 69 shows the undamaged portions of the girders experiencing extremely similar strain magnitudes.

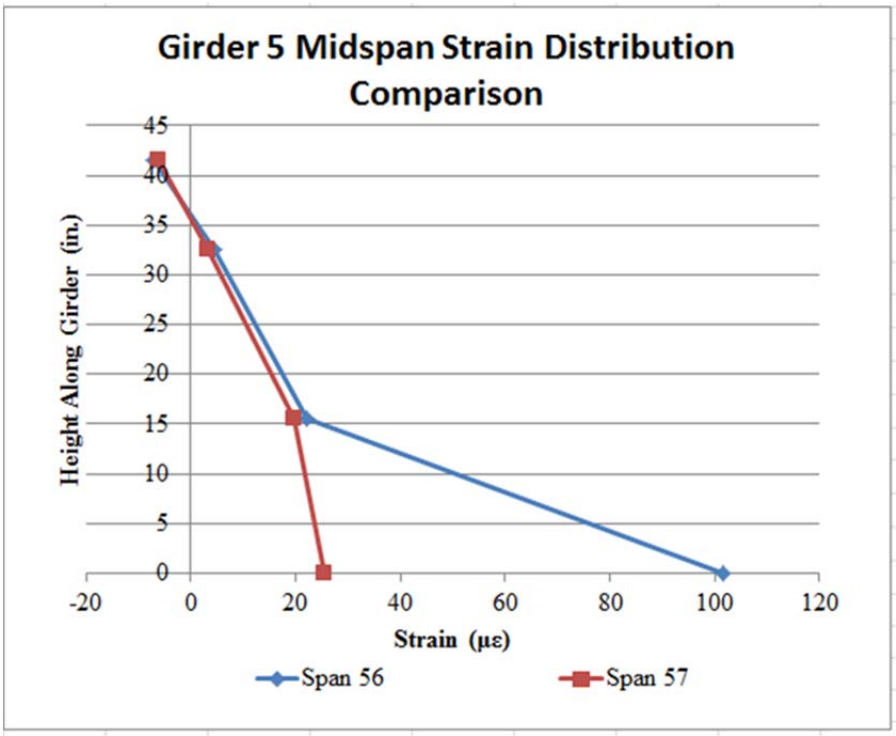

Figure 69: Eastbound Vertical Strain Distribution Comparison

There are two hypotheses that have been developed to explain this behavior. The first theory is that the strain transducer was instrumented with the gage length spanning over a microcrack in the concrete. As the girders were loaded, the crack would open which would be measured by the gage since the crack movement would be recorded as an elongation of the gage length.

The second hypothesis explains the strain increase using stress redistribution within the damaged bottom flange. For example, in girder 7 of westbound span 31, only a portion of the flange was damaged. It has already been proven that no load shedding occurred between adjacent girders so the damaged girder would have to carry a full load through its damaged and undamaged cross sections. More specifically, the tensile stress being carried by the bottom flange would have to transition from a full width flange to a smaller width flange. The smaller flange would represent the portion of the flange that was not deteriorated within the damaged cross section. This is illustrated in Figure 70. Since the same stress would have to pass through

the damaged cross section as the undamaged cross section, a stress concentration would be formed since there is less area to carry the same load. It is possible that the strain transducer was capturing this stress redistribution which would explain the elevated strain values in the test results.

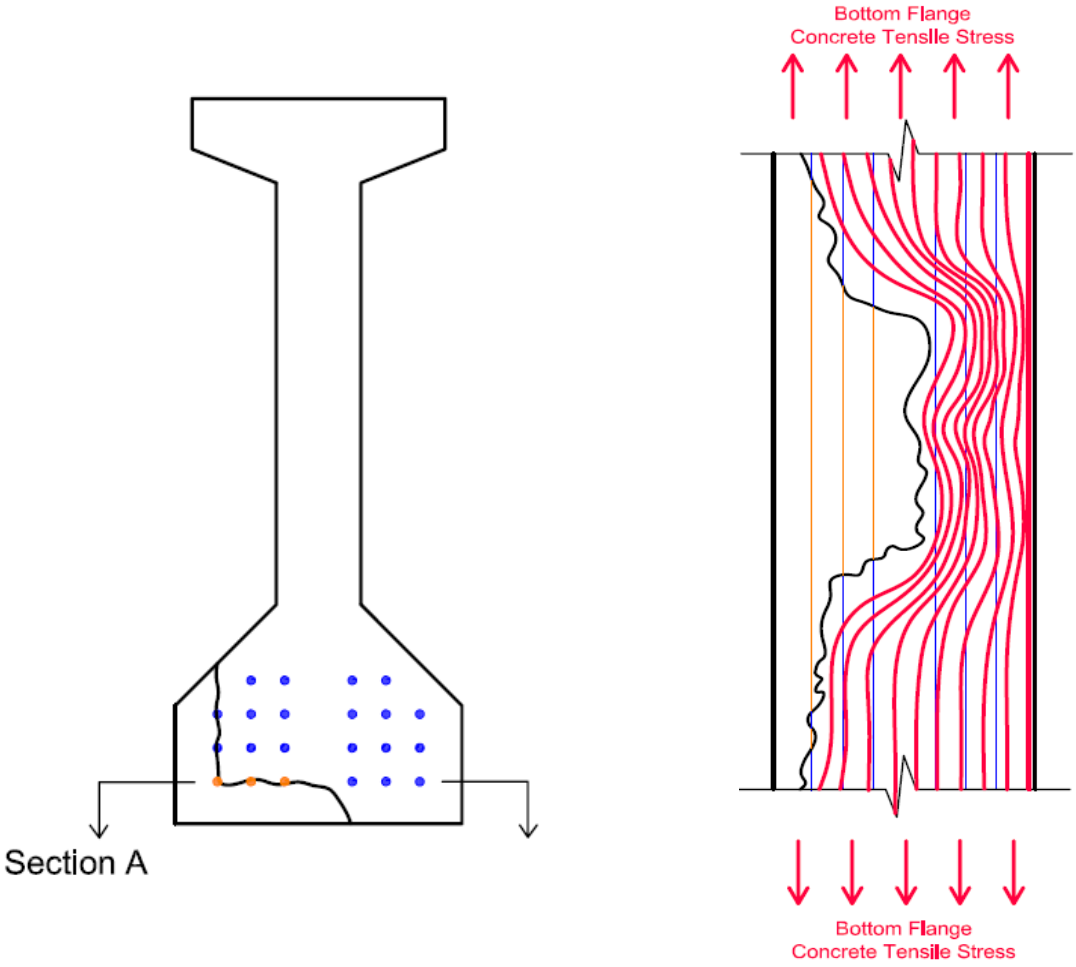

Westbound Span 31 Girder 7 Midspan Cross Section

Section A

Figure 70: Damaged Cross Section Stress Redistribution

Further investigation was performed to try to prove one of the theories. Expected strains were calculated for the undamaged girders from the exact truck loads and dimensions used in the load tests. The results for truck configuration 5 of westbound span 31 girder 7 and eastbound span 56 girder 5 are shown in Appendix E. The strain live load distribution factors, discussed later in Chapter 5, were used to determine the load being resisted by the girder being analyzed. A portion of the calculations included calculating the cracking moment of the transformed

composite girder. The purpose of this calculation was to determine if the moment calculated from the trucks was causing the section to transition from linear elastic to cracked elastic. The cracking moments were calculating assuming an undamaged cross section. Based on the results shown in Table 3, the damaged girders were not experiencing moment anywhere near their respective cracking moments even though the cracking moment would reduce slightly due to the damage. Even through the damaged girders weren't behaving as a cracked elastic section, it is still possible that there were microcracks in the damaged regions. The microcracks could be effects of the extensive concrete spalling. For this reason, neither hypothesis could be proven correct.

Table 3: Cracking Moment Investigation of Damaged Girders

Approach Structure	Truck Configuration	Girder of Interest	Truck Moment (M_{truck})	Cracking Moment (M_{cr})
Westbound	Configuration #5	Girder 7	161 k-ft	362 k-ft
Eastbound	Configuration #5	Girder 5	300 k-ft	512 k-ft

The theoretical strain values calculated were approximately double the measured experimental strain values for both the eastbound and westbound scenarios. There are several possible reasons for the expected strains to be higher than those recorded. It was assumed in the calculations that the girder was simply supported. In reality, there was restraint at the supports because of the corroded bearings and because of the continuous concrete deck. These two restrains would induce negative moments at the supports and lower the positive moments at midspan, effectively reducing the midspan strains. Also, there was no information about the girder concrete to determine a modulus of elasticity value other than the specified concrete compressive strength. A conservative equation was used in the calculations to estimate the modulus but this could be underestimating the actual value which would raise the expected strain values. An overestimate was also seen in the deflection magnitudes. Preliminary calculations were performed to determine the amount of accuracy needed in the deflection measurement system. Under the two truck configuration, maximum deflections were expected to be around 0.09 in. During the test, however, the maximum deflection was only 0.042 in, again about half of the expected value.

Comparisons are illustrated in Figure 71. The plots compare the actual experimental data, a line of best fit representing a linear strain distribution based on the experimental data, and the theoretical strain distribution. Even though the strain magnitudes were not similar, the elastic neutral axis for both girders was within 1 in. of the experimental values.

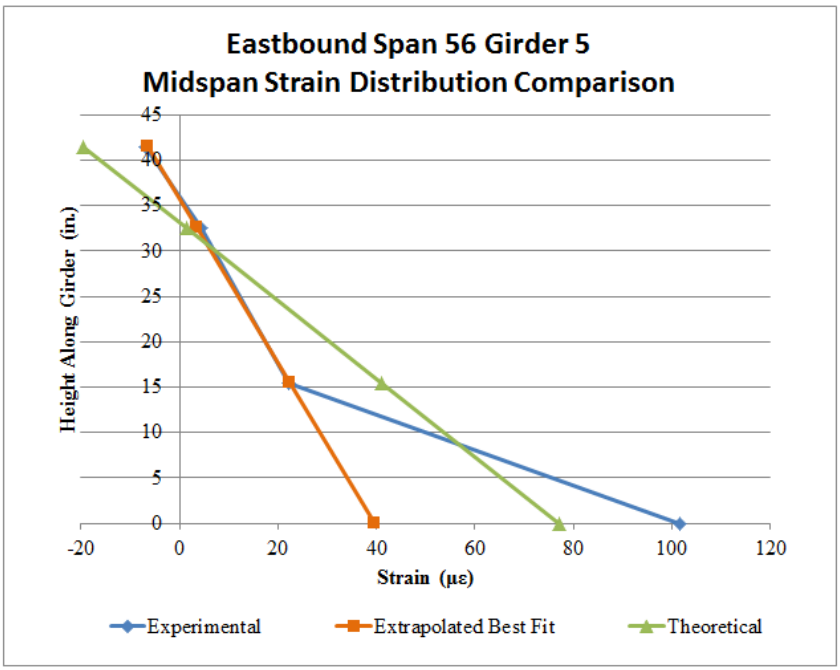

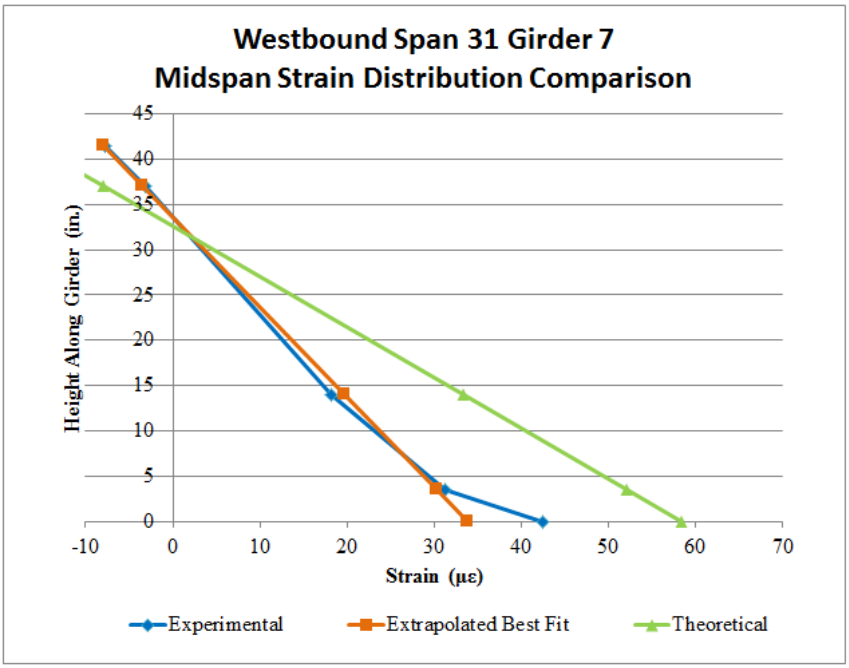

Figure 71: Theoretical Strain Distribution Comparisons

4.7 Deflection Distribution

An alternative comparison can be seen by analyzing the girder deflections. A similar approach was taken to compare deflections by averaging all of the runs for each truck configuration together and overlaying the data from each of the spans tested. Figure 72 shows the deflections from each westbound span overlaid for truck configuration 5. Plots for the other four truck configurations can be found in Appendix D.

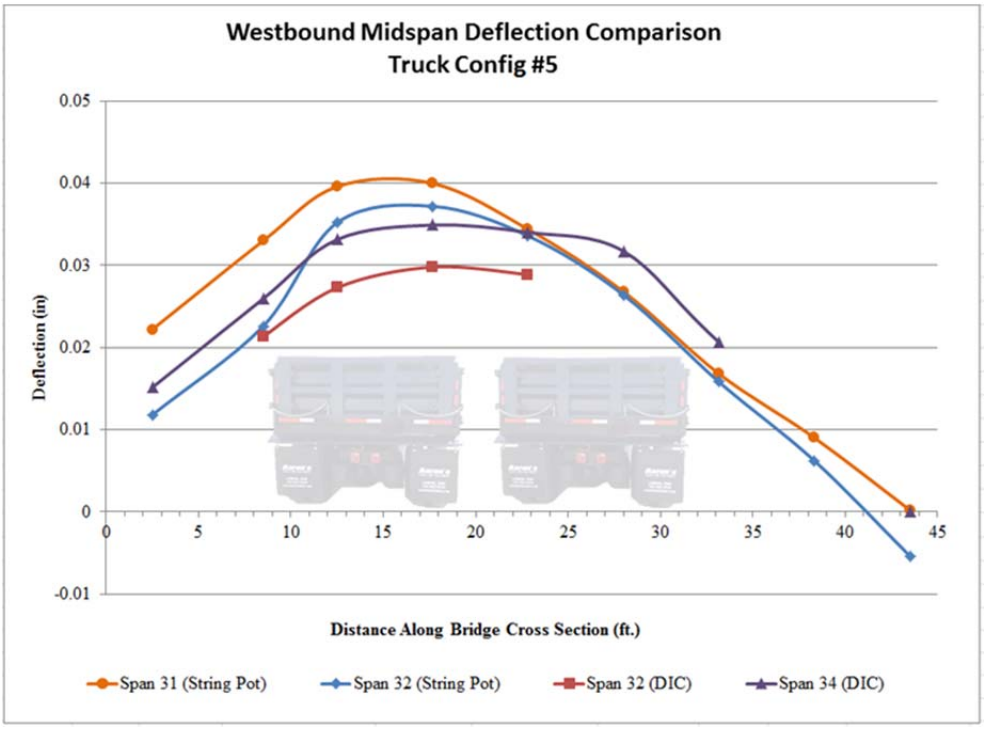

Figure 72: Westbound Deflection Comparison

(Note: Girder 1 is on the Far Right)

Each westbound span had similar deflection of the girders. The only discrepancies were the slightly larger deflections in girders 6-9 in span 31. Based on the results, local damage, even if substantial, did not greatly affect the deflection magnitude of the individual girders. Deflections indicate a more global response and are a function of both the overall stiffness of the girders as well as the load resisted by each member. As previously discussed, the damage caused local areas of strain increases and load redistribution between neighboring strands and concrete. However those local irregularities are not exhibited on the same member where the cross-section is not damaged.

Both the deflection values and strain values can be used to develop live load distribution factors. Because of the localized strain increases resulting from the damage, the factors will be

different depending on which data is used. The average strains and deflections for each girder were graphed with strains on the left axis and deflections on the right axis to illustrate how the load distribution across the cross section compares between the two measurement types. Figure 73 shows the comparison for truck configuration 5 for the westbound structure. Comparisons for the other configurations can be found in Appendix D. The inconsistent strain measurements were once again excluded from these comparison plots.

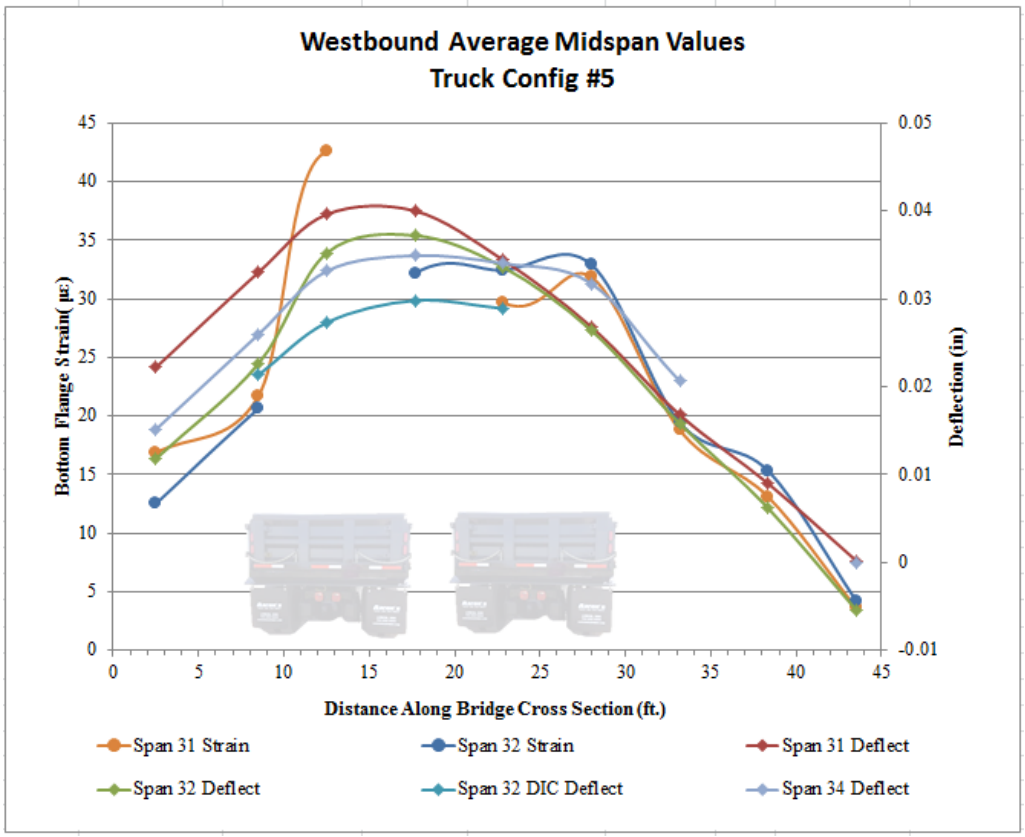

Figure 73: Westbound Midspan Comparisons

(Note: Girder 1 is on Far Right)

A large portion of girder 7 in span 31 was deteriorated with exposed and corroded strands including several severed strands. To quantify this in terms of deflection, a comparison was made between girder moments of inertia with and without damage. The short term composite gross moment of inertia was calculated for the original westbound girders using as-built plans. The short term cross section moment of inertia combined the concrete deck and precast girder using the modular ratio, n, of the differing concrete strengths. Similarly, the short term transformed composite moment of inertia was calculated with the strand layout in the as-built plans. Again, a modular ratio was used to convert the prestressing steel area into an equivalent

concrete area. Finally, four strands were neglected in the bottom layer of strands and two strands in the next three layers to represent 100% damage to the exterior-most strands. The results are shown in Table 4.

Table 4: Moment of Inertia Comparison

Cross Section	Moment of Inertia (in^4)
Undamaged Gross Composite Girder	222,250
Undamaged Transformed Composite Girder	271,950
Damaged Transformed Composite Girder	265,210

Using the moment of inertia values given in Table 4, accounting for the damage decreases the moment of inertia by only 2%. This change would affect the deflection since it depends on the moment of inertia. Because the girders were initially very stiff, and the reduction in moment of inertia was minimal, the change in deflection resulting from the damage was difficult to measure. In addition, the 2% reduction in moment of inertia was conservative since the damage in the strands was in a localized region. Those strands that had section loss still had some capacity remaining, and those strands that were severed were able to redevelop in sound concrete away from the damaged section. It has been shown by other research that severed strands will redevelop in the AASHTO recommended $60d_b$ length and that adjacent strands pick up the redistributed force from the severed strand (Kasan and Harries, 2011). Overall, the deterioration and corrosion results in a localized strength problem, but does not result in excessive deflections.

4.8 Analysis Recommendations

The measured strains and deflections reported in Appendix C may be used to benchmark analytical models of the bridge during the load rating process. It is recommended to neglect all strength of strands in areas which are exposed and exhibit heavy corrosion (Naito et. al, 2010). Where a strand is exposed for only a portion of the span and then continues into a sound cross section later in the span, it is conservative to neglect the strand for the entire span length. However, to more closely represent in-field conditions, the cross-section may be assumed to be undamaged after a distance of 60 d_b from where the cross-section is no longer damaged. For example, in span 34 of the westbound structure there is extensive damage near the support. The

exposed and damaged strands should be neglected in the damage area, but the AASHTO recommended 60 d_b may be used as a "redevelopment length" once the strand enters sound concrete. After that length, it can be assumed the strand is at full strength as long as no further damage is observed.

Some girders exhibited damage over their entire length, such as girder 5 in eastbound span 56. In cases such as this, it is recommended to neglect all prestressing strands in the lowest layer due to extensive spalling of the concrete. Engineering judgement should be used for prestressing strands that are not yet exposed in the damaged regions. For example, on girders 7 and 8 in span 31, the concrete showed signs of longitudinal cracking suggesting that the strands that are currently still enveloped in concrete are undergoing corrosion to an unknown extent. It is recommended to use a minimum of 25% reduction in cross sectional area for these strands showing signs of longitudinal cracking and neighboring damaged areas (Naito et. al, 2010). If the above recommendations are implemented, Figure 74 indicates the strand layout that should be used when calculating the flexural strength of the damaged girders in the load rating. In addition, the Lehigh ATLSS report has a load rating example for an adjacent box girder bridge with corroded strands that may be helpful during the load rating process of the HRBT damaged spans.

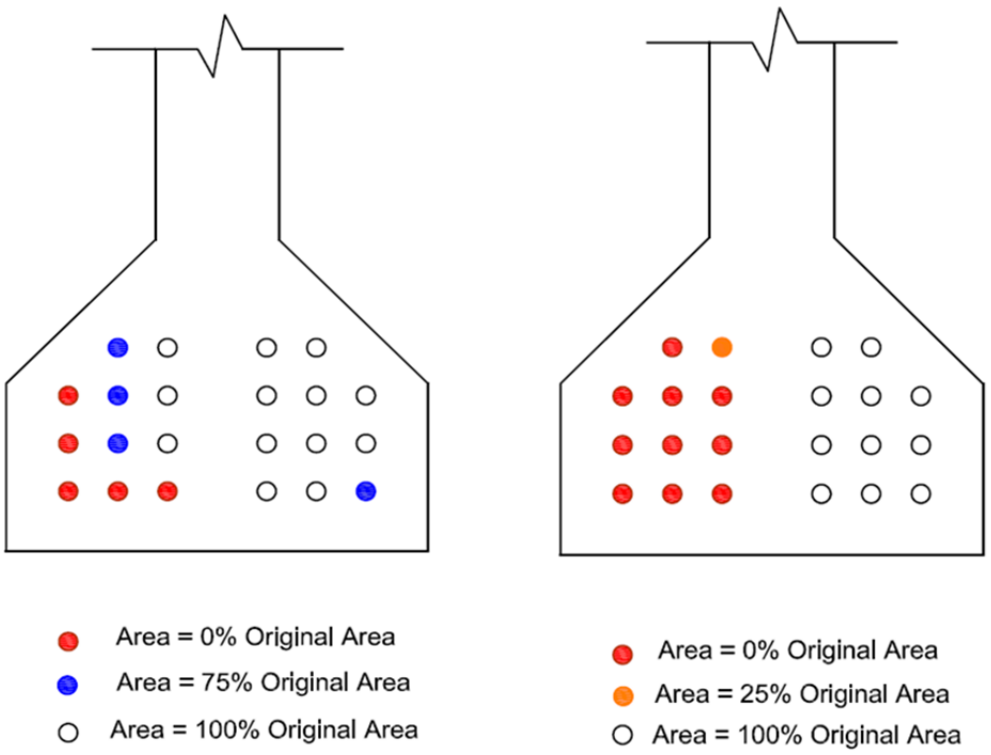

a) Span 31 Girder 7 Midspan b) Span 31 Girder 8 Midspan

Figure 74: Midspan Girder Strand Deterioration

CHAPTER 5 – LIVE LOAD DISTRIBUTION FACTORS

Three methods were used to determine the live load distribution factors for the Bridge-Tunnel approaches. Two of the methods were experimental since they were based on either the strain data or the deflection data. The third method used the AASHTO design equations. Having three sets of distribution factors allowed for comparisons between the actual load distributions found through experimental data and those calculated with design equations.

5.1 Experimental Live Load Distribution Factors

The midspan strain readings along the bottom soffits of the girders were used to develop the first set of live load distribution factors. Some of the girders tested had damage to their midspan location as discussed in Chapter 4.This deterioration caused a spike in strain readings, indicating a stress concentration, at the localized damage regions of the girders. After review, these strain readings did not represent the load distribution factors because they did not accurately describe the load being resisted by the girder. Instead, the strain values in the undamaged sections at the same girder location were used to develop a line of best fit for the strain distribution. This line of best fit is illustrated as an orange line in Figure 75. Point A represents an extrapolated strain value within the damaged area of the cross section that accurately describes the load being resisted by the girder. This value used to determine the live load distribution factors instead of the actual bottom soffit strain reading, point B.

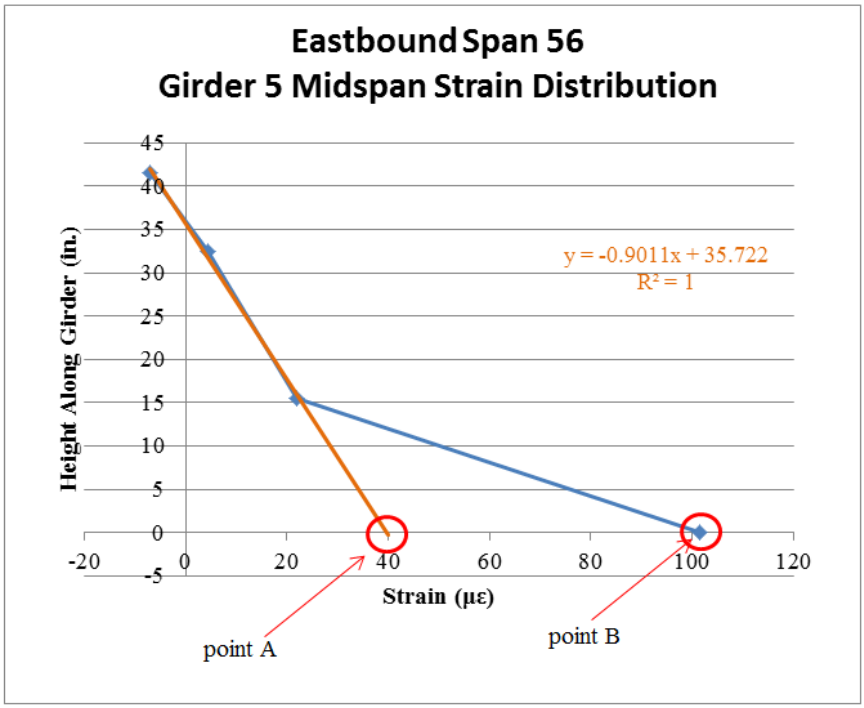

Figure 75: Strain Data Used in Live Load Distribution Factor Formulation

Once all of the applicable strain values were determined, experimental live load distribution factors were calculated using the Barnes equation:

$$g_{experimental} = \frac{nw_i\varepsilon_i}{\sum_{j=1}^{k}\varepsilon_j w_j} \quad (7)$$

n = number of lanes loaded

w_i = section modulus of the ith girder

ε_i = strain of the ith girder

k = number of girders

ε_j = strain of the jth girder

w_j = section modulus of the jth girder

In this equation, the damaged girder cross sections are accounted for by using a reduced moment of inertia in the section modulus calculations. The recommendations described in Section 4.8 were used to calculate the damaged cross sectional properties. All of the section moduli were calculated with respect to the bottom soffit of the girders since this was the location of the strain transducer whose data was used in the calculations. Using the above equation, distribution factors were calculated for each girder in EB span 56, EB span 57, WB span 31 and WB span 32. These calculations were completed for each of the truck configurations performed

during the live load test. Configurations one through four yielded single lane live load distribution factors and configuration five generated two-lane live load distribution factors. To determine the controlling live load distribution factors, the data from various combinations of single lane truck configurations were added together to develop experimental live load distribution factors for all possible two-lane configurations. Superposition was used because the data indicated that the girders were still behaving elastically under the applied test loads. Additionally, the single left lane and single right lane values were added together and results were extremely close to the values obtained from truck configuration five which included one truck in each travel lane. After all single lane and two lane factors were developed, the maximum value was chosen as the controlling case for each girder.

The same approach was used to develop live load distribution factors from the measured deflection values. The same section modulus values were used in these calculations as the strain equations.

5.2 AASHTO Live Load Distribution Factors and Comparisons

The final set of distribution factors used the AASHTO equations previously described in Chapter 2. The interior girders were based on the empirical equations. The exterior girders were based on the maximum distribution factor produced from either the empirical equation or the lever rule. All calculations are organized in Appendix E.

The empirical equations are based on assumptions previously outlined in Chapter 2 which did not hold true for the Bridge-Tunnel cross sections. The damage caused decreased moment of inertia and stiffness values in some girders so it was unclear if it could be assumed that all of the girders were of approximately equal stiffness. The eastbound spans had a typical cross section with equal sized girders and equal spacing. The only possible irregularity was the damage to girder four which may have caused a slight decrease in stiffness. The westbound spans posed more of a problem because of its widened cross section. The two girders in the cross section that were added during the widening project were larger than the original girders so their stiffnesses were not equal to the original girders. Also, the widened girders were spaced differently than the original girders. There was also an irregular spacing at the transition between the widened girders and original cross section. The dimensional spacing and size irregularities are shown in Figure 76.

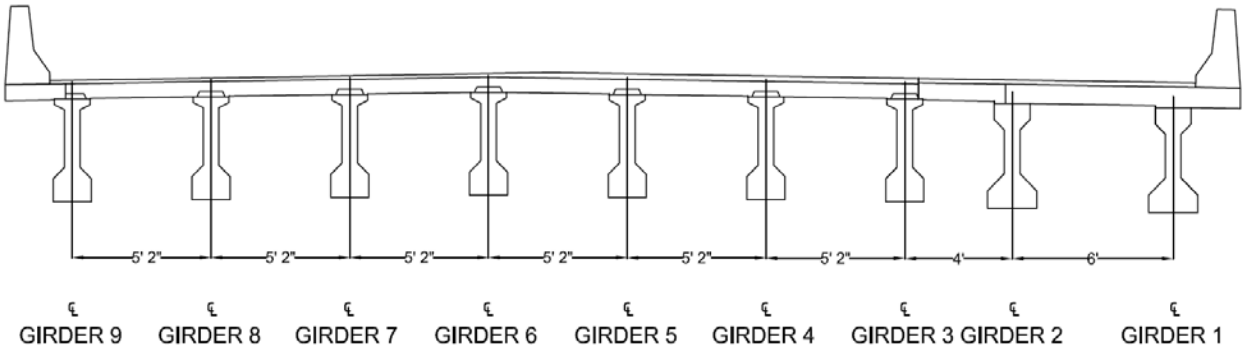

Figure 76: Westbound Cross Section Girder Spacing

Because of these irregularities, it was unclear if the AASHTO equation would yield appropriate live load distribution factors to be used in the load rating. Comparisons were made between the AASHTO design distribution factors and the experimental distribution factors to determine how applicable the AASHTO values were and if they were conservative or unconservative. The westbound comparison is shown below in Figure 77.

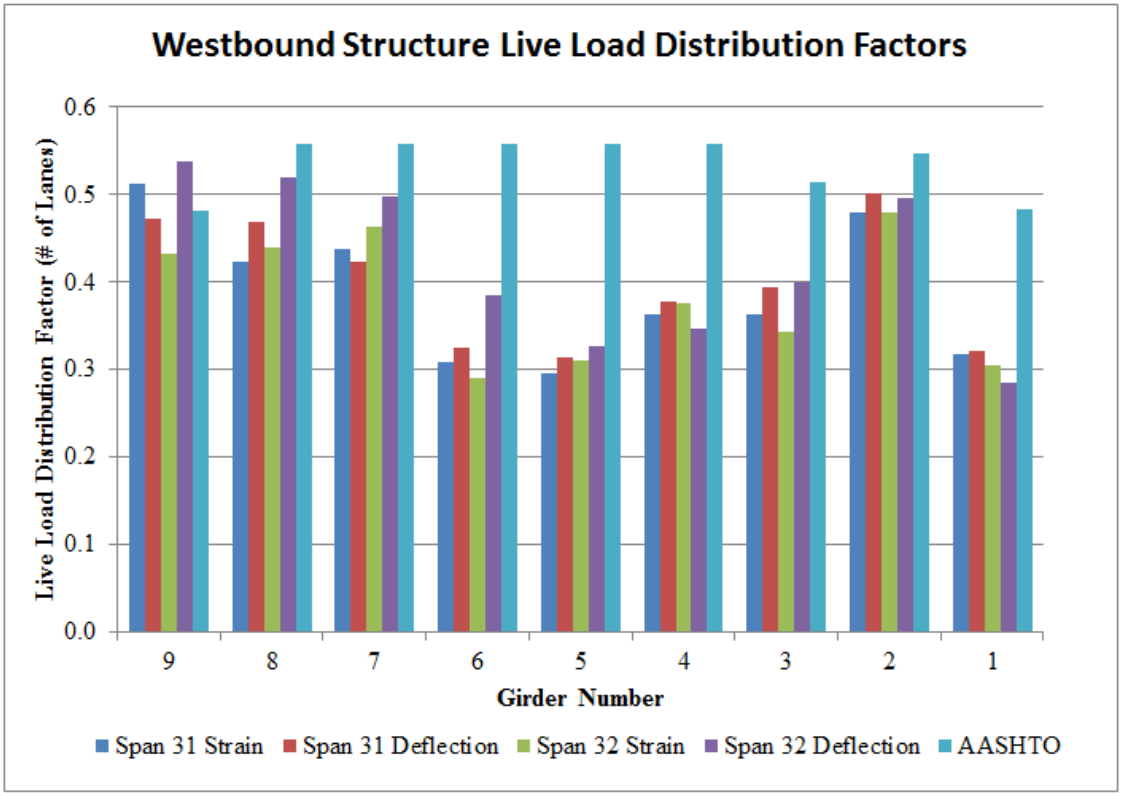

Figure 77: Westbound Live Load Distribution Factor Comparison

The experimental live load distribution factors were extremely similar to one another regardless of span or data type (strain or deflection). Overall, the AASHTO equations were conservative, especially for the interior girders.

The experimental results showed that girders seven through nine had much higher distribution factors than the rest of the cross section. When trying to determine the controlling distribution factors, the results from two individual truck configurations were added together to determine the effects of a two-lane loaded configuration as stated previously. For girders 7-9, truck configurations three (left lane) and four (left shoulder) were combined to develop the largest load to be resisted. The problem with using superposition in these two configurations is that the double truck configuration isn't actually possible with the given bridge cross section. The shoulder is only 6 ft-8 in. wide so a truck cannot fit in solely the shoulder without having its passenger side wheels travelling in the left lane. This is shown schematically in Figure 78. If following the AASHTO LRFD Specifications, this cross section would only be designed for three "live load" lanes due to its width. This is addressed in Section 3.6.1.1.1 which states, "The number of design lanes should be determined by taking the integer part of w/12, where w is the clear roadway width in feet between curbs and/or barriers" (AASHTO 2014). In this situation, the clear width is 42 ft- 8 in. which, when divided by 12, yields 3.55 so only three design lanes should be included in the design. To truly determine the live load distribution factors for these girders with two lanes loaded, two trucks would have to be driven side by side over the span. One truck would have to be 2 ft from the barrier (truck configuration #4) and the second one would be adjacent to the first truck. It would look similar to Figure 78 but the second truck would have to move to the right by four feet. This would reduce the load on girders 7-9 and increase the load on the remaining girders in the cross section. This would effectively lower the live load distribution factors for girders 7-9 from those values shown in Figure 77.

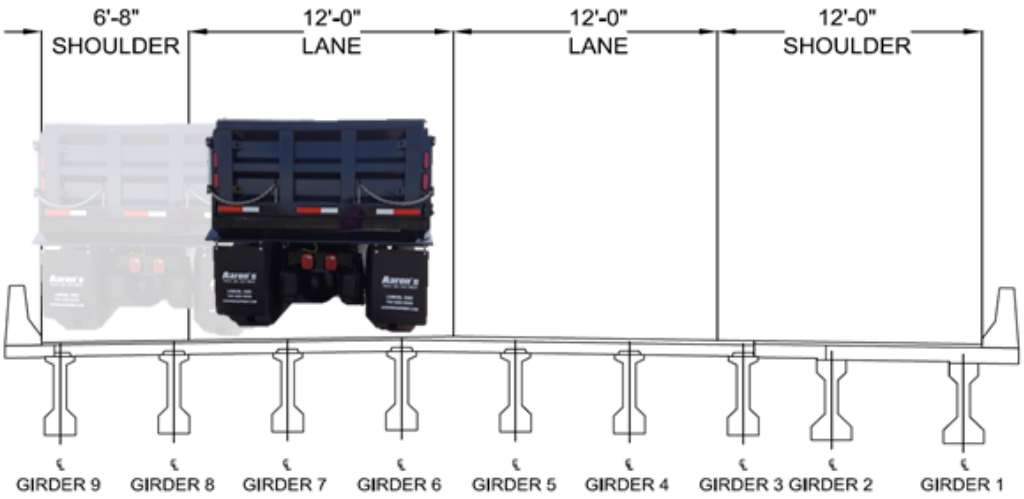

Figure 78: Westbound Truck Configuration Discrepancy

The current experimental distribution factors for girders 7-9 show an "overload condition" of the girders because of the superimposing the effects of both trucks. Even with this overload condition, the experimental factors were still very close to or less than the factors derived from AASHTO. This shows that the design equations are conservative. The underlying motivation of this bridge test was to determine if the live load distribution factor could be reduced for the damaged girders in westbound span 31. Even with the overload condition shown in the comparison, a reduction would be permitted. For both of the damaged members, girders 7 and 8, the AASHTO equations quantify the load distribution as 0.56 lanes. The average of the experimental distribution factors produces 0.455 lanes for girder 7 and 0.463 lanes for girder 8. By taking out the overload effects, it estimated that the live load distribution factors would be reduced to 0.38-0.4 lanes for each of the damaged girders. However, since the scenario was not possible, the exact values are not currently known. This reduction from the design values of 0.56 lanes would most likely allow the girders pass to the load rating. It is known that there is reduced flexural strength in these girders so reducing the load being resisted through these new live load distribution factors may be enough to prove the girders still have enough capacity.

One location where the AASHTO equations were accurate was for girder 2. This girder had close spacing with its neighboring girders and one of the adjacent girders was one of the original girders which had a smaller cross section. Since it is larger than the original girder, and has a small spacing, it is much stiffer. This causes it to attract more load, and therefore, has a

higher live load distribution factor. This is captured by the experimental data and matches closely to the AASHTO value.

A similar procedure was completed for the eastbound spans and the results are shown in Figure 79. Again, there is an overload condition for girders 1 and 2 because of the width of the bridge deck. The clear spacing is 40 ft so it should only be designed for three travel lanes.

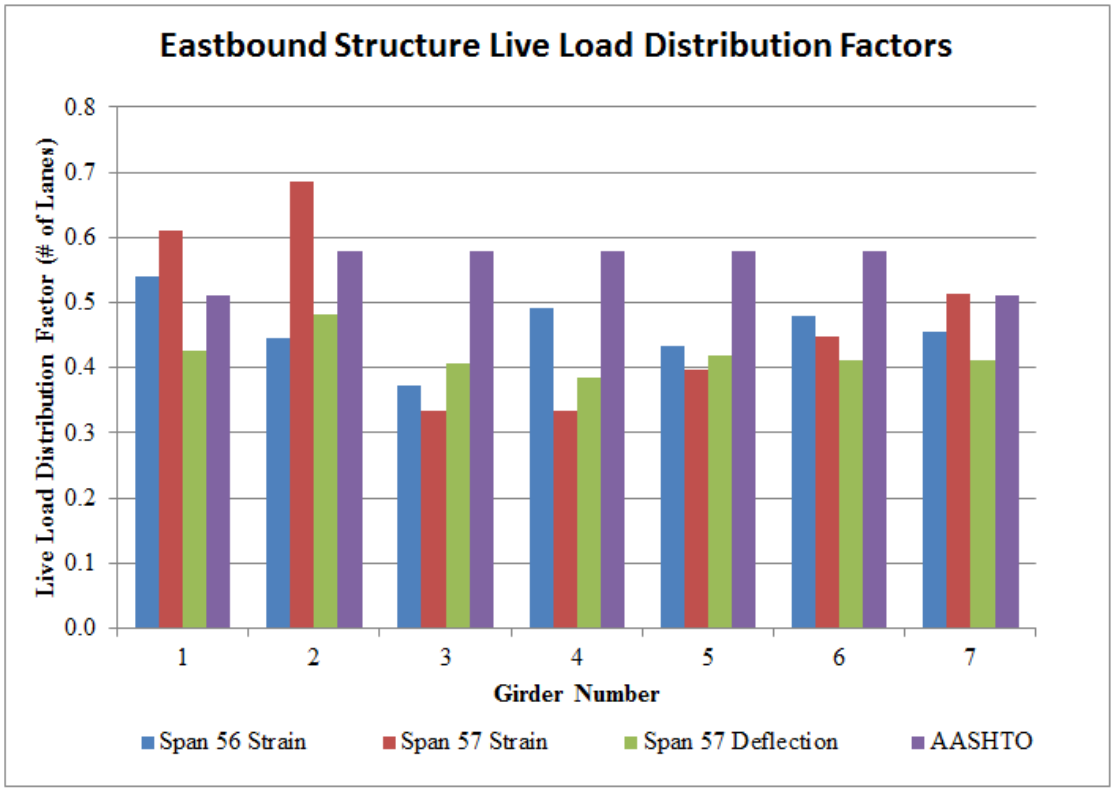

Figure 79: Eastbound Live Load Distribution Comparison

Similar to the westbound structure, the AASHTO live load distribution factors are conservative compared to the experimental results. In eastbound span 56, girder 4 showed extensive damage to its bottom flange. Based on the comparison, it is feasible to lower the live load distribution factor from the AASHTO value of 0.58 to the maximum experimental value of 0.48. This would reduce the load resisted by the damaged girder in the load rating and may help it pass the rating.

CHAPTER 6 – COMPARISON OF DEFLECTION SYSTEMS

The two deflection systems used in this load test had the common goal of measuring extremely small deflections on a structure located a mile offshore, but they were very different in their approach. The cables suspended reference (CSR) system was a low cost, practical, hard wired system whereas the digital image correlation (DIC) system was a high cost wireless alternative using emerging technology. Each system possessed strengths and weaknesses.

6.1 Cable Suspended Reference System

The CSR system was developed to maintain an extremely low budget so the materials used were readily available at a local hardware store. The expensive equipment used in the system, more specifically the datalogger and string potentiometers, were already owned as part of the structural engineering laboratory so there was no additional cost. Much of the work for this system was performed prior to the load test. This included cutting the lumber and steel cables to length as well as making the steel chokers. The 4-wire electrical cable was pre-cut to length and wound on the spooling reels for easy deployment in the field. The military connectors were soldered to the end of the electrical cables and tested to ensure good connections were made. The program for the datalogger was written and tested for bugs before going into the field. The string pots were calibrated with a dial gauge and their necessary calibration factors were added to the datalogger program. The pots were also attached to their plywood bases so they could easily be clamped to the girders once the barge was under the test span.

The time and manpower for field setup for the CSR system was mainly concentrated on installing the steel suspension cables and the hard-wiring of the string potentiometers. The string potentiometers were quick to install and the 2x4 beam was simple to implement once the cables were in the correct position. One disadvantage with this system was the loss of access because of the steel cables. It was possible to use a ladder from the barge to access any problematic equipment after the cables were strung but it was not possible to use any overhead equipment like the Moog platform or the snooper.

On the night when two spans were tested, this system was implemented in both spans. One span had longer electrical cable lengths because the datalogger was left on the barge in the opposite span. The system was reliable so once the equipment was working properly, it was possible to move on to the next span and never have to re-enter the original span.

During the actual load test, the LVDTs allowed for manual interfacing with the datalogger. This capability combined with the timestamp in the data allowed for extremely easy post-processing of the deflection data. It did not matter how many truck configurations were performed or if the trucks were driving forwards and backwards multiple times. It was all captured through the manual click code established and the clicks were easily located in the post-processed data because of their high peaks. These clicks also allowed for easy meshing with the strain data so the truck location, deflection data values, and strain data values were known for every timestamp throughout the test.

The string pots were calibrated in the program to display units of inches not millivolts. So, during the load test, a real time table of values and plot was shown on the laptop screen which represented the actual deflections of the girders. The real time software also included flags which were used to "zero" the data prior to each truck configuration. This ensured no false offsets were retained in the data. This also allowed the data collection to be paused as the trucks made their 20 minute round trip repositioning themselves for the following run. After the load test was completed, the data was stored on the laptop and quickly saved to a flash drive so multiple copies existed.

The capabilities of this system could be expanded compared to what was utilized in the load test. The sampling frequency could be changed to a faster rate to capture fast moving trucks and dynamic effects. The entire system was hard-wired so the datalogger could be connected to a power source for long-term monitoring.

The system was not perfect as it did have some drawbacks. The setup and breakdown time were equal for this system because each spool of electrical cable has to be wound up and all of the suspended steel cable had to be dismantled. Also, there was much more equipment needed for this setup compared to a noncontact system.

6.2 Digital Image Correlation System

The cameras and lenses used were fairly common and could easily be purchased online. The camera to lens connection was not an easy task so the equipment was shipped to a manufacturer specializing in these modifications. Most of the preparation work included purchasing and gathering equipment because of the high end technology being implemented. Aside from the technology, the brackets were built by UVA and the DIC cards were speckled prior to the load test. Most of the work with the DIC system was in the post-processing stage so

once the equipment was on hand, instrumentation was feasible. During the load test, the DIC system required a large amount of time for drilling into the pier cap to hang the support brackets. There was also quite a bit of time tied up in focusing the cameras. In comparison, both systems took roughly the same time to install.

During the load test, there was no manual interface with the cameras to mark the truck configurations or the location of the truck within the span. Other projects using DIC have used signs flashed in front of the DIC card so they could be captured by the camera to mark the beginning of a certain truck configuration. Because no interface was present, the post processing was much more difficult since there were no reference points as to which truck configuration the photos belonged to.

Another drawback was the sampling rate. The string pots were set to sample at 25 Hz whereas the cameras were only capable of running at 2 Hz. Some of the cameras "acted up" and changed to a 1 Hz frequency midway through the load test. There were also some instances where cameras would shut off and not take any photos for a small period of time. As for accuracy, the cameras were proven to be accurate to 0.005 in. whereas the string pots were accurate to 0.001 in. The cameras were also run off of an external battery pack to there was only a finite amount of time the instrumentation could be used.

Prior to the load test, an area of concern was the night-time testing and how the cameras would capture the speckled pattern. The LED lights above the DIC card worked very well. Regardless, the barge was left in the DIC span in case supplemental lighting was needed or if camera problems occurred as the system seemed less reliable than the CSR system.

During the breakdown, the cameras and DIC cards can be taken down very quickly. Most of the installation time was spent with drilling and focusing which didn't have to be replicated during the tear down.

As the camera technology increases, faster sampling rates will be achievable. There is also research being performed where the photos are used to determine surface strains of structural members. The future is bright for the noncontact system and its shortcomings will get resolved.

6.3 System Comparisons

One of the main differences between the systems is the initial cost. A comparison was performed between the two systems assuming a single 75 ft span was going to be tested with

nine girders in the bridge cross section. The pay items and costs are shown in Table 5 for the CSR system.

Table 5: Cost Estimate for Cable Suspended Reference System

Item	Quantity	Unit Cost, $	Total Cost, $
String Potentiometers	9	400	3600
½ in. Plywood	1	15	15
2 ft Bar Clamp	22	15	330
Military Connectors	9	21	189
4 Wire Electrical Cable	500 LF	1.10	550
CR5000 Datalogger	1	4000	4000
Plastic Reels	9	3.90	35.10
1/8 in. Steel Cable	500 LF	0.266	133
D Rings	36	0.66	23.76
Comealongs	3	27	81
2 in. x4 in. x 8 ft -8 in Lumber	9	3.02	27.18
1-1/4 in. Wood Screws	1 LB Box	6.47	6.47
24 Gauge Galvanized Wire	1 Roll	2.98	2.98
Cordless Screw Gun	1	260	260
Solder	1	3.97	3.97
Solder Gun	1	50	50
TOTAL COST			$9,300

Although the price seems high, the expensive items are typically readily available in a structural engineering laboratory and will not have to be purchased for the project. By excluding the string potentiometers and datalogger, the price decreases to just $1700. If two spans were tested at one time, more equipment would be needed and the price would double. The same cost estimate was performed in Table 6 for the DIC System.

Table 6: Cost Estimate for DIC System

Item	Quantity	Unit Cost, $	Total Cost, $
Go Pro Camera	9	275	2475
Tamaron Telephoto Lens	9	145	1305
Camera-Lens Modification	9	220	1980
Lens Adapter	9	10	90
External Battery Pack	9	20	180
Aluminum Bracket	9	25	225
Hammer Drill	1	100	100
Expansion Bolts	27	0.54	14.58
LED Lighting	9	3	27
DIC Card	9	1	9
Go Pro Remote	1	40	40
VIC2D Post-Processing Software	1	7500	7500
TOTAL COST			$13,950

To compare effectiveness of the two systems, a table was developed outlining strengths and weaknesses of each. As shown in Table 7, the CRS system proved to be the better fit for the project. As the DIC technology improves, there will likely be a movement away from hard-wired systems. There are currently other projects where the DIC is currently the better option. This includes the Yoneyama project described in Chapter 2 which gathered deflection points along the entire elevation view of an exterior bridge girder, not just at discrete points.

Table 7: Head to Head Comparison of Deflection Systems

	CSR System	DIC System
Cost	X	
Sampling Rate	X	
Amount of Supplemental Equipment		X
Accuracy	X	
Real Time Monitoring/View of Deflection Values	X	
Timestamp/Ability to Mesh With Strain Data	X	
No Access Restrictions After Implementation		X
Ability to Easily Set Up From Aerial Equipment		X
Ability to Save/Backup Data Quickly In Field	X	
Fast Tear Down Time		X
Long Term Monitoring Capability	X	

6.4 Data Comparison

In westbound Span 32, four cameras from the DIC system were installed even though the span was completely instrumented with the CSR system. This was purposely done to compare the deflection values head to head. The results were very promising and the magnitudes were extremely similar as illustrated in Figure 80. The DIC magnitudes consistently tended to be lower than the CSR system. This could be attributed to slight calibration differences, but is most likely due to the sampling rate. The CSR system was taking measurements 25 times per second whereas the DIC system was sampling twice per second. It is possible that the DIC system was not sampling fast enough to capture the absolute peak. Regardless of this slight discrepancy, the offset was evident in every data point, regardless of which system was “correct”. So, the relative displacement of the girders with respect to each other was still accurate and could be used to develop live load distribution factors. Overall, both systems were able to capture the slight deflections of the girders. Both systems are viable options for future testing.

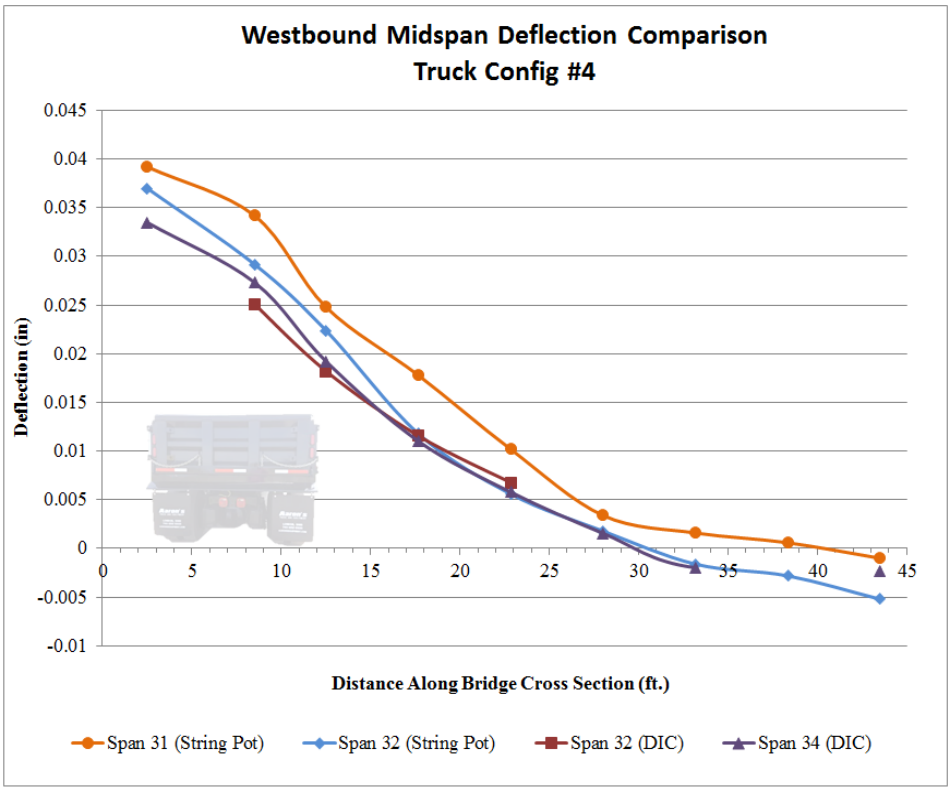

a) Westbound Configuration #4 Deflection Comparison

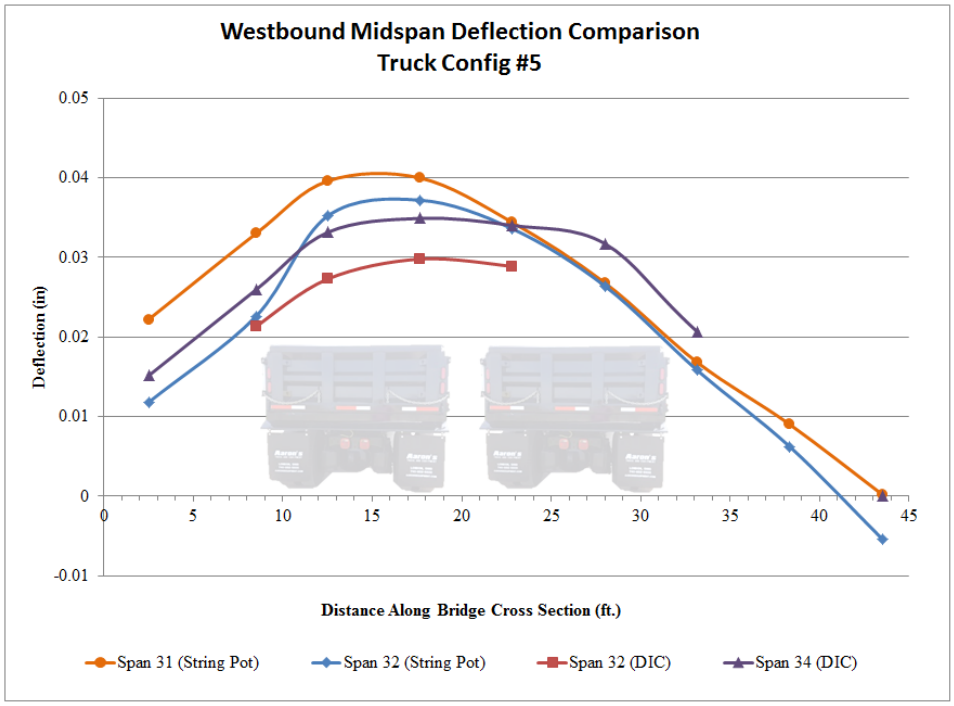

b) Westbound Configuration #5 Deflection Comparison

Figure 80: Deflection System Data Comparison

CHAPTER 7 – CONCLUSION AND RECOMMENDATIONS

7.1 Conclusion

A successful live load test was completed for selected spans of the Hampton Roads Bridge-Tunnel. The purpose of the load test was to aid in the load rating process of the approach structures. The current deterioration conditions were causing portions of the structure to fail the necessary load ratings, meaning load posting may have to be employed. Westbound spans 31 (flexural damage), 32 (good condition), and 34(shear damage) were tested along with eastbound spans 56 (flexural damage), and 57(good condition). The strain and deflection data recovered from the test were used to make recommendations for the load rating. Significant findings and observations made during the live load testing include:

- A localized increase in strain readings within damaged areas. This increase could be from stress redistribution from damaged prestressing strands to neighboring strands and the surrounding concrete. This would push the concrete into the cracked elastic stage. It could also be from strain instrumentation bridging microcracks and capturing the opening and closing of the crack.
- Damaged cross sections exhibit linear strain distributions in the undamaged portions and nonlinear strain distribution in the damaged portion of the cross section.
- Strain distribution comparisons proved the damaged girders are not shedding load to adjacent girders.
- Both strain and deflection measurements were successful and are useful in determining live load distribution factors.
- Deflection measurements did not capture excessive magnitudes due to damaged girders. The deterioration of the girders is a localized strength problem, not a deflection problem since deflections depend more on the global properties of the girder.
- The live load distribution factors determined through empirical AASHTO equations were conservative. The factors can be reduced for damaged girders based on the experimental live load distribution factors. This will decrease the load being resisted by the damaged girders and will help the girders to pass the necessary ratings.
- Both deflection systems were successful and captured similar magnitude data when compared head to head.

7.2 Recommendations

7.2.1 Live Load Test

The live load test was a success but improvements could definitely be made. Access in the bay was much easier from the barge than with either the Moog platform or the snooper truck from the roadway. Water access also limits the amount of lane closure time during instrument installation. Since the barge is more useful, it is better to test in the late spring or summer when the bay will not be as rough. The waves depend on the wind speed, but more importantly, the wind direction. Large waves will be a detriment to the barge because of possible bending of the spuds. If a small tug boat is used, it is also possible that the steel cables connecting the tug to the barge could snap.

Based on the development of the live load distribution factors, it is recommended to run more truck configurations. If a sixth truck configuration was performed, the overload condition would have been evident in the experimental live load distribution factors. The sixth configuration would include a truck as close to the barrier as possible and a second truck adjacent to the first. The cross section of the bridge should be observed carefully prior to the load test to pick the number and location of the truck configurations.

It is definitely recommended to only test and instrument one span per day. Typically this means instrumenting during the day, testing at night, and then removing instrumentation the same night. Two spans can be accomplished in one day, as it was for both the westbound and eastbound tests, but it makes load testing much more difficult. Problems arise with the BDI system since wireless communication will have to be constant between spans where diaphragms and pier caps can pose problems. It also leads to much more wiring being needed for wired systems since the datalogger will only be in one span. The major drawbacks are the doubled amount of instrumentation necessary and the lack of access in one span since the barge will only be spudded in one of the two test spans.

A final recommendation is to check as many measurements prior to the actual test. The best option would be a visit to the test site prior to the load test. Do not rely on any information given by the local Department of Transportation (DOT) such as barge dimensions, water depth measurements, clearance heights, equipment capabilities, and equipment sizes. Most of this information will govern the schedule and plan put in place to complete the load test. It will also help in choosing the correct equipment. It is highly recommended to take the measurements

firsthand and talk to the marine contractor to ensure the reliability of the information. It also pays to have multiple contingency plans in case equipment breaks down or the weather does not cooperate.

7.2.2 Hampton Roads Bridge-Tunnel

In terms of the future of the Hampton Roads Bridge-Tunnel girders, there is a good chance that they will not fail in the near future because of the redundancy in the bridge cross section. The high number of girders in the cross section and the large number of strands in each girder allow for redistribution of loads which will prevent catastrophic collapse. With that being said, there is substantial damage to some of the girders that is hindering its structural performance and their ability to pass load ratings. When the next load rating occurs in ten years or so, the deterioration will only be worse and there is a better chance that some spans will not pass for all required truck loads. If the girders are left in the current condition to continually deteriorate, it is possible for a girder collapse similar to the Lake View Drive Bridge.

In terms of maintenance, the shotcrete is an adequate short term solution to keep the strands from being directly exposed to the harsh weather. Over time though, the corrosion will continue and the shotcrete will spall off so it is essentially “band-aid and lipstick” for the girders. The strands covered in shotcrete are already compromised and will only get worse with time. A structural retrofit would be needed to regain the lost strength from the damage. There are construction companies that specialize in the retrofit and repair of prestressed concrete bridges such as Freysinnet USA. Retrofit techniques include cathodic protection, electrochemical treatment, carbon fiber wrapping and external post-tensioning. The external post-tensioning typically is not exposed to the environment because the external strands will have some sort of protective sheathing similar to stay cables.

Inspections will play a key role in maintaining an up to date picture on the deterioration. Instead of the abiding by federal laws and performing an inspection every two years, it recommended to perform an inspection every year. It would be best to inspect the bridge during the winter or at the start of spring season. This is because the winter months will have rough surf conditions which will cause frequent salt spray on the girders. Also, these are the coldest months which will cause the strands to be more brittle and have a higher tendency to rupture. For the better conditioned spans, the faster the deterioration is discovered, the easier and cheaper it is to repair.

For future bridges in the area or replacements done to existing bridges, it is recommended to use larger concrete covers in the realm of three inches. The corner strands are typically the first to corrode since they are closest to two exposed faces of the flange so thicker covers on the sides of the flange would also be beneficial. It is also recommended to use a penetrating sealer on new construction. Clear penetrating sealers like SikaGard 740W, ACT ATS-100, or Evonik Protectosil are effective. The best option is a two part barrier – a penetrating sealer primer combined with a paint top coat is extremely durable and aesthetically pleasing. Products like Simpson Strong Tie FX-460, Sikagard 550W with 740W primer, or Klaas Coatings Si-Rex03 are all good options. Most of the named products are water-based so using them over the bay shouldn't pose any environmental concerns.

7.3 Future Research

Since the Hampton Roads Bridge-Tunnel is one of the oldest prestressed concrete structures in the United States, it is one of the first to show signs of significant deterioration. The younger prestressed structures will soon begin showing similar degradation mechanisms. The research performed is at the forefront of residual strength of prestressed concrete girders and will help pave the way for the residual strength research to come. There has been no documented information on live load testing of this type of damaged in-service bridge. Future research possibilities include full scale testing of decommissioned bridge girders as well as structural repair and retrofitting techniques. There is also opportunity on the microscopic level to further understand the corrosion mechanisms of the strands and material testing. All of this type of research can also be accompanied with a modelling approach, such as finite element models of the decommissioned girders and repair methods.

The means and methods used in the load testing are also at the tip of the spear in terms of originality. The digital image correlation system is in its infancy, but has a lot of promise because of its non-contact capabilities. It will likely become the most popular deflection measurement system in the years to come. The cable suspended reference system was developed specifically for this test so it provides a new tool for a low cost system to measure deflections in difficult access areas. This research has proven the capabilities of both systems, especially in a head-to-head comparison. This proven track record allows for future live load tests on bridges in difficult access areas. Examples include high profile structures similar to the HRBT such as the Chesapeake Bay Bridge-Tunnel and the James River Bridge. Both of these are extremely long

structures over water and are located in harsh environments. Again, modelling can accompany these live load tests by modelling an entire span in a three dimensional model. Once calibrated to the field data, the model will provide many more data points of the structure instead of solely relying upon the small number of data points received from the load test instrumentation. Overall, there are multiple avenues of future research pertaining to the residual strength of prestressed concrete structures.

REFERENCES

AASHTO (2011). Manual for bridge evaluation, 2nd Ed. American Association of State Highway and Transportation Officials. Washington, DC.

AASHTO (2014). LRFD bridge design specifications, 7th Ed. American Association of State Highway and Transportation Officials. Washington, DC.

ASCE (2013). "*2013 Report Card for America's Infrastructure*". American Society of Civil Engineers. http://www.infrastructurereportcard.org/a/#p/bridges/conditions-and-capacity

Barnes R., Stallings J., Porter P. (2003). Live-load response of Alabama's high-performance concrete bridge. *Transportation Research Board: Journal of the Transportation Research Board No. 1845 Paper No. 03-4319*, pp. 115-124.

Billington D.P. (2004). Historical perspective on prestressed concrete. *PCI Journal 49 (1),* pp. 14-30.

Chajes M., Shenton III H. (2005). Using diagnostic load tests for accurate load rating of typical bridges. *ASCE Structures Congress 2005*.

Ciolko, A. (2005). Corrosion and prestressed concrete bridges. *Proceedings of the 2005 Structures Congress and the 2005 Forensic Engineering Symposium,* pp. 157-168.

Clark Nexsen. (June 2015). Hampton roads bridge tunnel south approach inspection report, Virginia Beach, VA.

D'Arcy T., Nasser G., Ghosh S.K (2003). Building code provisions for precast/prestressed concrete: a brief history. *PCI Journal, 48 (6),* pp. 116-124.

Darmawan M., Stewart M. (2007). Spatial time-dependent reliability analysis of corroding pretensioned prestressed concrete bridge girders. *Structural Safety, 29 (1)*, pp. 16-31.

FDOT (2015). War is over: research expansion. *Florida Department of Transportation Research Showcase.* Fall 2015.

Feng M., Fukuda Y., Feng D., Mizuta M. (2015). Nontarget vision sensor for remote measurement of bridge dynamic response. *Journal of Bridge Engineering, 20(12)*, 04015023.

Gasparini D. (2006). The prestressing of structures: a historical review. *Proceedings of the Second International Congress on Construction History.* Volume 2 pp. 1221-1232.

Harries K. (2009). Structural testing of prestressed concrete girders from the Lake View Drive Bridge. *Journal of Bridge Engineering, 14 (2)*, pp. 78-92.

Harris D., Cousins T., Murray T., Sotelino E. (2008). Field investigation of a sandwich plate system bridge deck. *Journal of Performance of Constructed Facilities, 22 (5)*, pp. 305-315.

Kasan J., Harries K. (2011). Redevelopment of prestressing force in severed prestressed strands. *Journal of Bridge Engineering, 16 (3)*, pp. 431-437.

Lan Z., Yang X., Chen W., Zhou J., Zhou Z., Huang Z., Zhang B. (2008). Study on non-contact weighted-stretched-wire system for measuring bridge deflections and its effect factors. *Engineering Structures, 30(9)*, pp. 2413-2419.

Modares M., Mohammadi J. (2013). Sensors used in structural health monitoring. *Health Assessment of Engineered Structures- Bridges, Buildings, and Other Infrastructure.* World Scientific, Hackensack, NJ.

Moschas F., Stiros S. (2014). High accuracy measurement of deflections of an electricity transmission line tower. *Engineering Structures, 80*, pp. 418-425.

Naito C., Jones L., Hodgson I. (2010). Inspection methods & techniques to determine non-visible corrosion of prestressing strands in concrete bridge components: Task 3 – forensic evaluation and rating methodology. *ATLSS Report No. 09-10*.

Naito C., Jones L., Hodgson I. (2011). Development of flexural strength rating procedures for adjacent prestressed concrete box girder bridges. *Journal of Bridge Engineering, 16 (5),* pp. 662-670.

Naito C., Warncke J. (2008). Inspection methods & techniques to determine non-visible corrosion of prestressing strands in concrete bridge components: Task 1 – literature review. *ATLSS Report No. 08-06*.

Nassif H., Gindy M., Davis J. (2005). Comparison of laser doppler vibrometer with contact sensors for monitoring bridge deflection and vibration. *NDT & E International, 38(3),* pp. 213-218.

Nurnberger U. (2002). Corrosion induced failure mechanisms of prestressing steel. *Materials and Corrosion, 53 (8)*, pp. 591-601.

Peddle J., Goudreau A., Carlson E., Santini-Bell, E. (2011). Bridge displacement measurement through digital image correlation. *Bridge Structures, 7(4),* pp. 165-173.

Rinaldi Z., Imperatore S., Valente C., Pardi L. (2010). Experimental evaluation of the structural behaviour of corroded prestressed concrete beams. P*roceedings of the 6th International Conference on Concrete under Severe Conditions, CONSEC'10, v 1,* pp. 429-436.

Rogers R.A., Wotherspoon L., Scott A., Ingham J.M. (2012). Residual strength assessment and destructive testing of decommissioned concrete bridge beams with corroded pretensioned reinforcement. *PCI Journal, 57 (3)*, pp. 100-118.

Stanton J. F., Eberhard M. O., Barr P. J. (2003). A weighted-stretched-wire system for monitoring deflections. *Engineering Structures, 25(3),* pp. 347-357.

Tanaka Y., Shimomura T., Yamaguchi T. (2014). Experimental and numerical study on the residual strength of deteriorated prestressed concrete bridge beams affected by chloride attack. *20th AIAA/CEAS Aeroacoustics Conference, 2014, 20th AIAA/CEAS Aeroacoustics Conference*, pp. 621-626.

Thornton, N. (2012). Live load testing of Appalachia, VA concrete arch bridges for load rating recommendation. *Master's Thesis*. Virginia Polytechnic Institute and State University, Blacksburg, VA.

Vu N., Castel A., Francois, R. (2009). Effect of stress corrosion cracking on stress strain response of steel wires used in prestressed concrete beams. *Corrosion Science 51 (2009)*, pp. 1453-1459.

Yoneyama S. (2007). Bridge deflection measurement using digital image correlation. *Experimental Techniques, 31(1),* pp. 34-40.

Zollman C. (1978). Part 1- Magnel's impact on the advent of prestressed concrete. *PCI Journal 23 (3),* pp. 22-48.

Zollman C. (1980). Part 9- the end of the "beginnings". *PCI Journal, 25 (1),* pp. 124-145.

APPENDIX A

DETERIORATION MAPPING OF TEST SPANS

APPENDIX A-1

INSPECTION MAPPING FROM CLARK NEXSEN INSPECTION REPORT

(JUNE 2015)

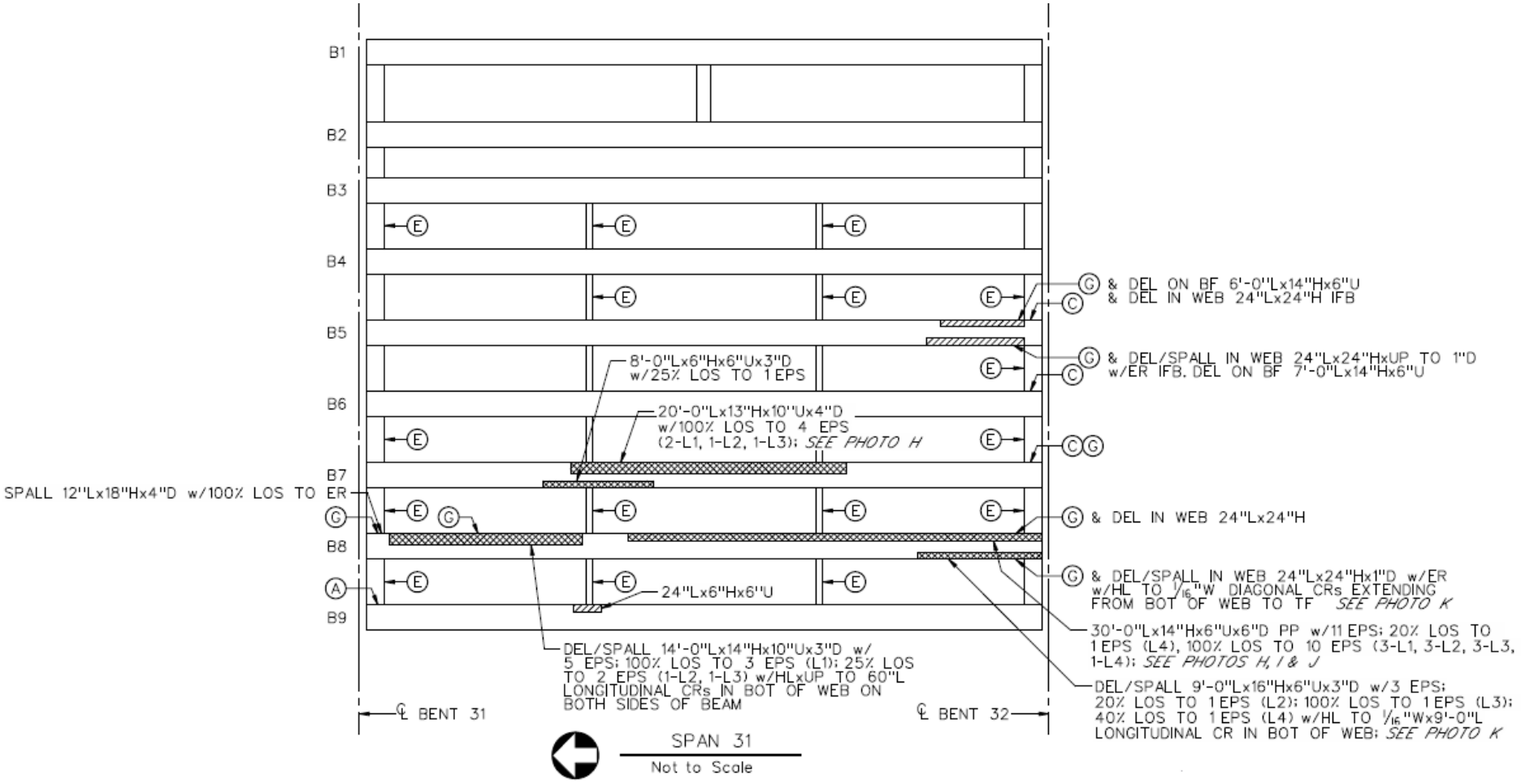
B1
B2
B3
B4
B5
B6
B7
B8
B9
SPALL 12"Lx18"Hx4"D w/100% LOS TO ER
8'-0"Lx6"Hx6"Ux3"D w/25% LOS TO 1 EPS
20'-0"Lx13"Hx10"Ux4"D w/100% LOS TO 4 EPS (2-L1, 1-L2, 1-L3); SEE PHOTO H
24"Lx6"Hx6"U
DEL/SPALL 14'-0"Lx14"Hx10"Ux3"D w/ 5 EPS; 100% LOS TO 3 EPS (L1); 25% LOS TO 2 EPS (1-L2, 1-L3) w/HLxUP TO 60"L LONGITUDINAL CRs IN BOT OF WEB ON BOTH SIDES OF BEAM
& DEL ON BF 6'-0"Lx14"Hx6"U & DEL IN WEB 24"Lx24"H IFB
& DEL/SPALL IN WEB 24"Lx24"HxUP TO 1"D w/ER IFB. DEL ON BF 7'-0"Lx14"Hx6"U
& DEL IN WEB 24"Lx24"H
& DEL/SPALL IN WEB 24"Lx24"Hx1"D w/ER w/HL TO 1/16"W DIAGONAL CRs EXTENDING FROM BOT OF WEB TO TF SEE PHOTO K
30'-0"Lx14"Hx6"Ux6"D PP w/11 EPS; 20% LOS TO 1 EPS (L4), 100% LOS TO 10 EPS (3-L1, 3-L2, 3-L3, 1-L4); SEE PHOTOS H, I & J
DEL/SPALL 9'-0"Lx16"Hx6"Ux3"D w/3 EPS; 20% LOS TO 1 EPS (L2); 100% LOS TO 1 EPS (L3); 40% LOS TO 1 EPS (L4) w/HL TO 1/16"Wx9'-0"L LONGITUDINAL CR IN BOT OF WEB; SEE PHOTO K
℄ BENT 31
℄ BENT 32
SPAN 31
Not to Scale

PHOTO H
(BEAMS 7 & 8, SPAN 31)

PHOTO I
(BEAM 8, SPAN 31)

PHOTO J
(BEAM 8, SPAN 31)

PHOTO K
(BEAM 8, SPAN 31)

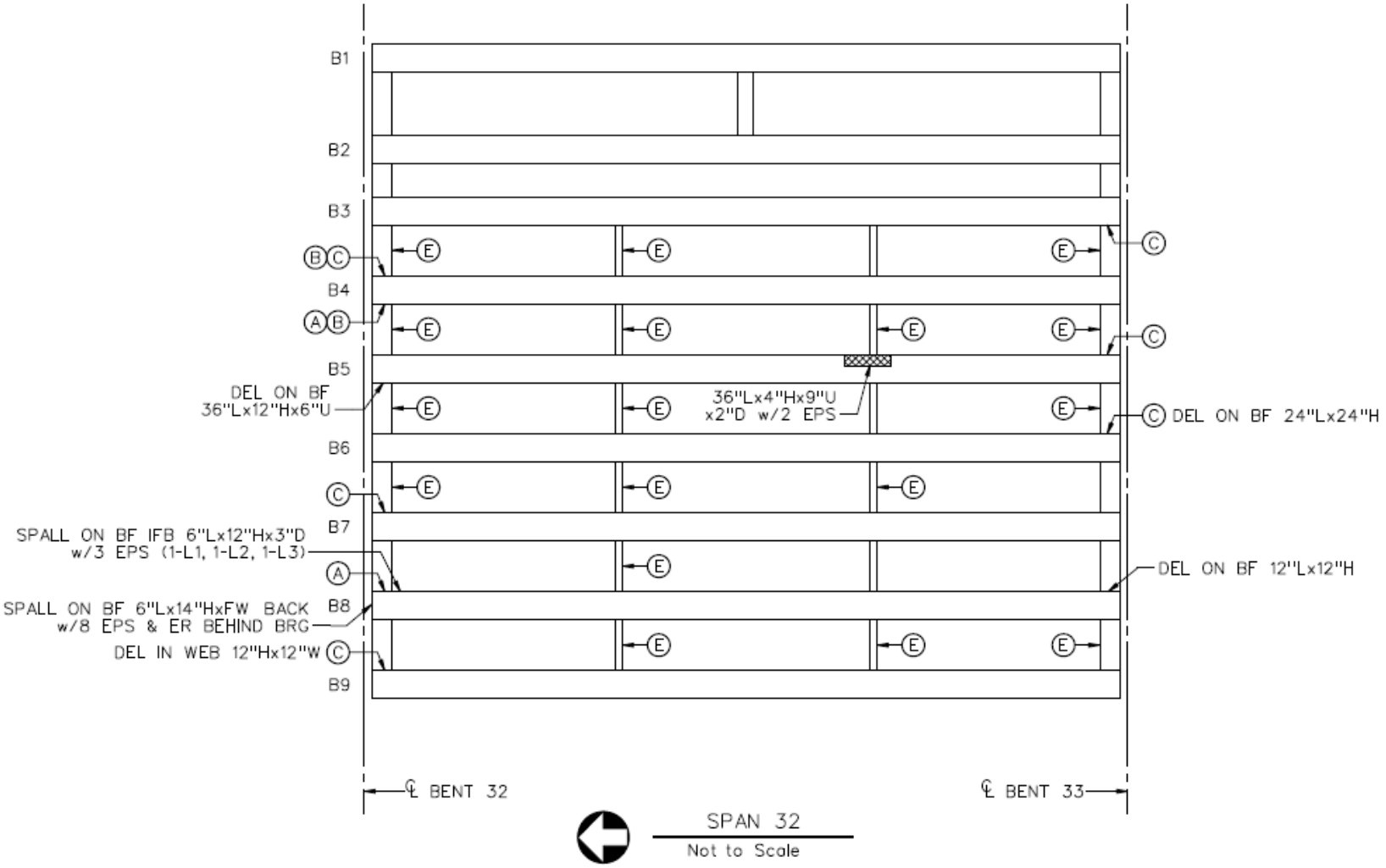

SPAN 32

Not to Scale

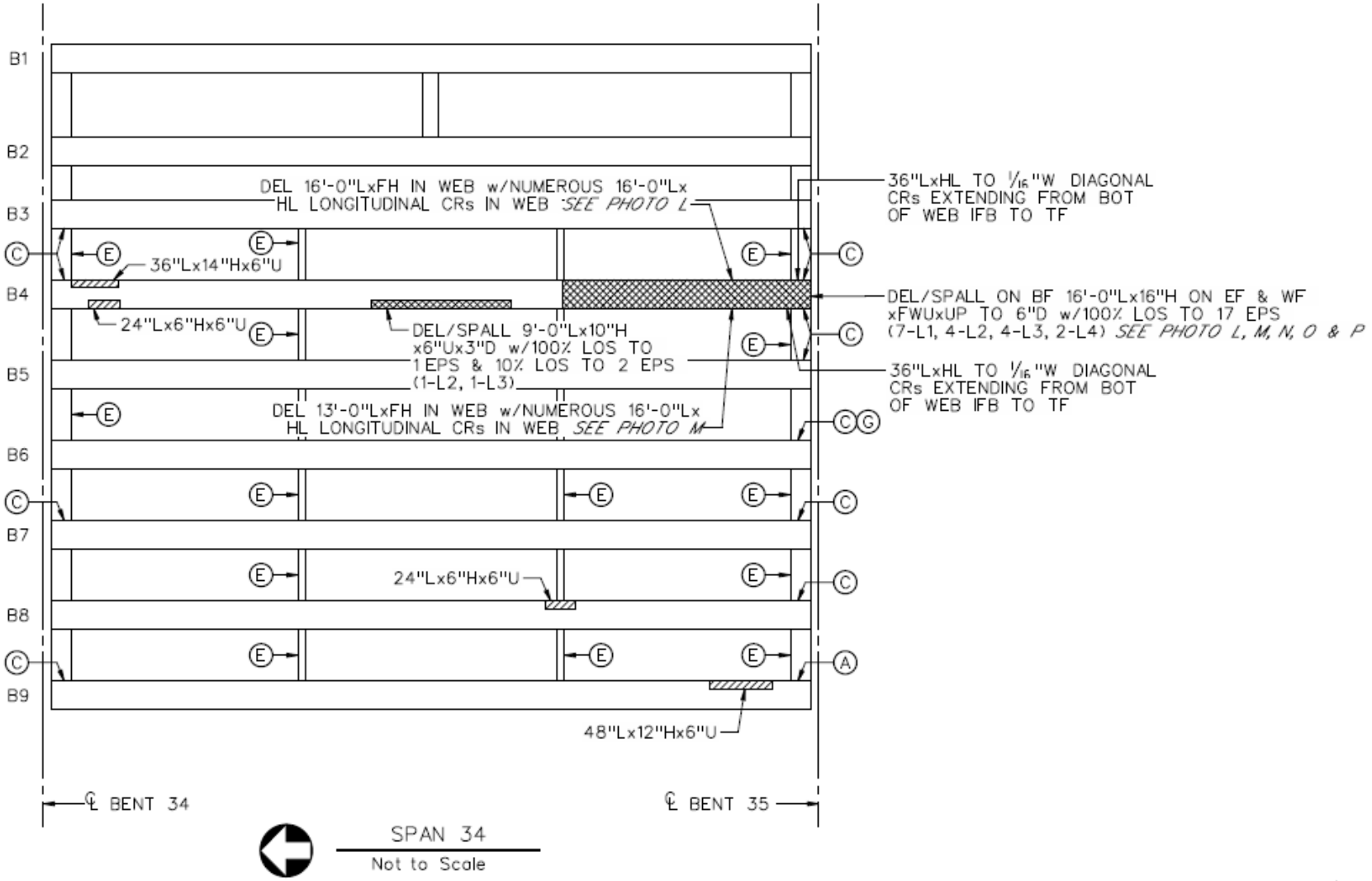
B1
B2
B3
B4
B5
B6
B7
B8
B9
DEL 16'-0"LxFH IN WEB w/NUMEROUS 16'-0"Lx HL LONGITUDINAL CRs IN WEB SEE PHOTO L
36"LxHL TO 1/16"W DIAGONAL CRs EXTENDING FROM BOT OF WEB IFB TO TF
36"Lx14"Hx6"U
24"Lx6"Hx6"U
DEL/SPALL 9'-0"Lx10"H x6"Ux3"D w/100% LOS TO 1 EPS & 10% LOS TO 2 EPS (1-L2, 1-L3)
DEL/SPALL ON BF 16'-0"Lx16"H ON EF & WF xFWUxUP TO 6"D w/100% LOS TO 17 EPS (7-L1, 4-L2, 4-L3, 2-L4) SEE PHOTO L, M, N, O & P
36"LxHL TO 1/16"W DIAGONAL CRs EXTENDING FROM BOT OF WEB IFB TO TF
DEL 13'-0"LxFH IN WEB w/NUMEROUS 16'-0"Lx HL LONGITUDINAL CRs IN WEB SEE PHOTO M
24"Lx6"Hx6"U
48"Lx12"Hx6"U
℄ BENT 34
℄ BENT 35
SPAN 34
Not to Scale

PHOTO L
(BEAM 4, SPAN 34)

PHOTO M
(BEAM 4, SPAN 34)

PHOTO N
(BEAM 4, SPAN 34)

PHOTO O
(BEAM 4, SPAN 34)

PHOTO P
(BEAM 4, SPAN 34)

APPENDIX A-2

INSPECTION MAPPING PERFORMED BY VIRGINIA TECH

(APRIL 2016)

DIRECTION OF TRAVEL

ALL BEARINGS CORRODING

75'-0"
SPAN 56

TO NORTH

G1 ℄
G2 ℄
G3 ℄
G4 ℄
G5 ℄
G6 ℄
G7 ℄

PATCHWORK ON BOT. FLANGE & WEB
48"
24"
24"
8"
PATCHWORK WITH SMALL CORROSION STAIN BOT. FLANGE
CORROSION STAINING BOT. OF DECK
108"
24"
SPALL IN BOT. FLANGE
96"
"HOLLOW" SOUNDING IN PATCHWORK
60"
36"
DELAMINATION WITH SMALL CRACKING
36"
60"
48"
54"
SPALL IN WEB WITH EXPOSED & CORRODING REBAR
DIAPHRAGM PATCHWORK
12ft DELAMINATION OF PATCHWORK FROM U/S OF DECK
CORROSION STAINING AT THIS LOCATION
108"
24"
SMALL CRACK & DELAMINATION IN BOT. FLANGE
84"
36"
36"

℄ PIER

℄ PIER

DENOTES PATCHWORK ON BOTTOM FLANGE

A — PLAN - EB DEFECT MAPPING

No.	Revision	By	Chk	Appd	Date
1					

Original Scale (11"x17") **AS SHOWN**

Design			
Drawn			
Dsg Verifier			
Drg Check			

* Refer to Revision 1 for Original Signature

Virginia Tech 1872 Invent the Future

Subject: Hampton Roads Bridge Tunnel

Title: EB SPAN 56 DEFECT MAP

Discipline: Structural

Drawing No.

Rev. 121

APPENDIX B

TRUCK DIMENSIONS AND WEIGHTS

APPENDIX B-1:

EASTBOUND TRUCKS

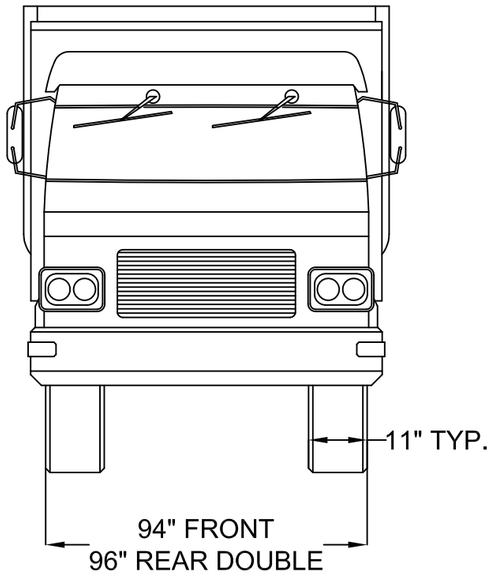

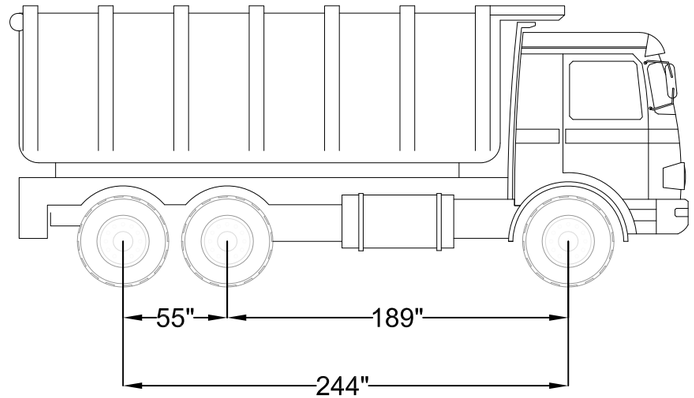

A — TRUCK DIMENSIONS
N.T.S

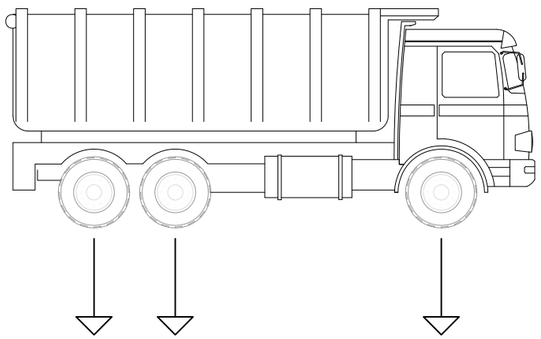

TOTAL WEIGHT:
46180 lb

DRIVER SIDE:	8000 lb	7780 lb	7400 lb
PASSENGER SIDE:	7500 lb	7840 lb	7660 lb

A — TRUCK AXLE WEIGHTS
N.T.S

EB TRUCK CONFIGURATION 1
RIGHT SHOULDER
TRUCK NO. R14156

No.	Revision	By	Chk	Appd	Date
1					

Original Scale (11"x17") **AS SHOWN**

Design			
Drawn			
Dsg Verifier			
Drg Check			

* Refer to Revision 1 for Original Signature

VirginiaTech
Invent the Future

Subject: Hampton Roads Bridge Tunnel

Title: EB-TC1-R14156

Discipline: Structural

Drawing No.:

Rev.: 124

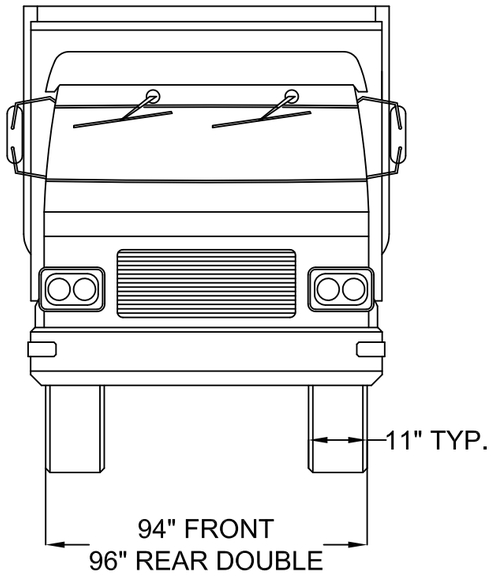

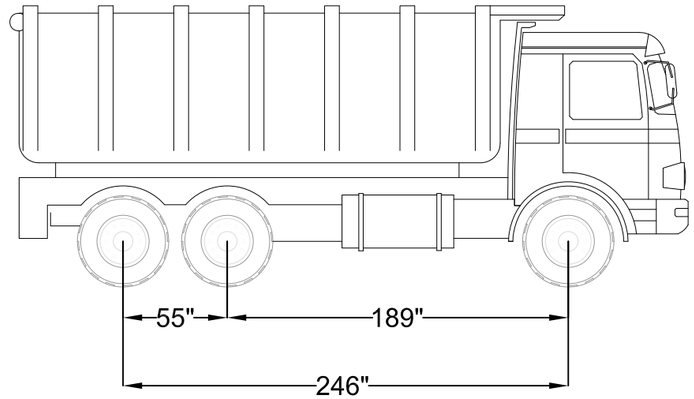

A — TRUCK DIMENSIONS
N.T.S

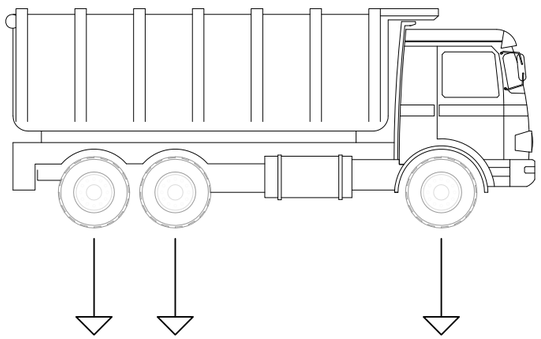

TOTAL WEIGHT:
50760 lb

DRIVER SIDE:	9600 lb	9320 lb	7980 lb
PASSENGER SIDE:	8220 lb	8000 lb	7640 lb

A — TRUCK AXLE WEIGHTS
N.T.S

EB TRUCK CONFIGURATION 2
RIGHT LANE
TRUCK NO. R14155

No.	Revision	By	Chk	Appd	Date
1					

Original Scale (11"x17") **AS SHOWN**

Design | Drawn | Dsg Verifier | Drg Check

* Refer to Revision 1 for Original Signature

VirginiaTech — Invent the Future

Subject: Hampton Roads Bridge Tunnel

Title: EB-TC2-R14155

Discipline: Structural

Drawing No.

Rev.

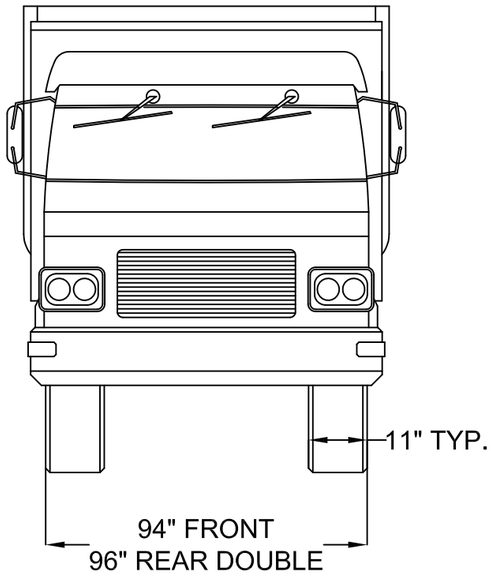

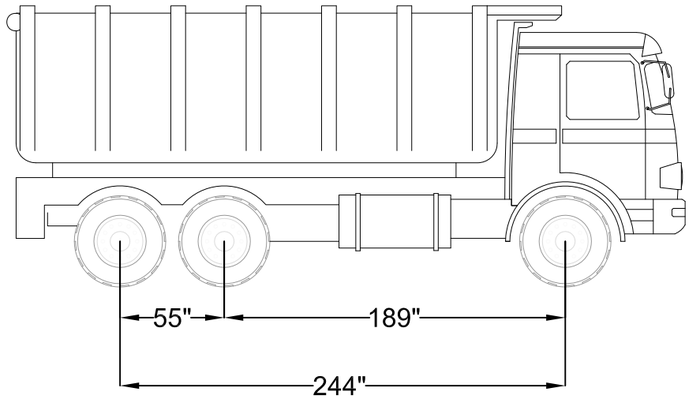

A — TRUCK DIMENSIONS
N.T.S

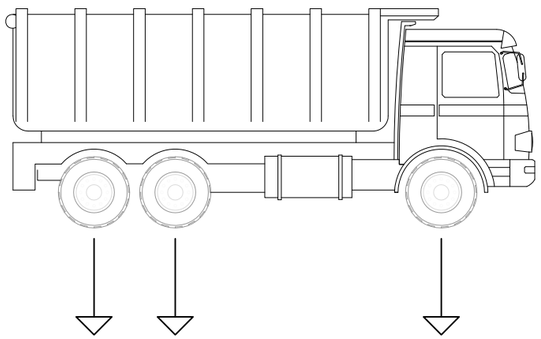

TOTAL WEIGHT:
53020 lb

EB TRUCK CONFIGURATION 3
LEFT LANE
TRUCK NO. R14149

	9280 lb	8960 lb	8200 lb
DRIVER SIDE:			
PASSENGER SIDE:	9520 lb	9260 lb	7800 lb

A — TRUCK AXLE WEIGHTS
N.T.S

No.	Revision	By	Chk	Appd	Date
1					

Original Scale (11"x17") **AS SHOWN**

Design			
Drawn			
Dsg Verifier			
Drg Check			

* Refer to Revision 1 for Original Signature

VirginiaTech
Invent the Future

Subject: Hampton Roads Bridge Tunnel

Title: EB-TC3-R14149

Discipline: Structural

Drawing No.

Rev. 126

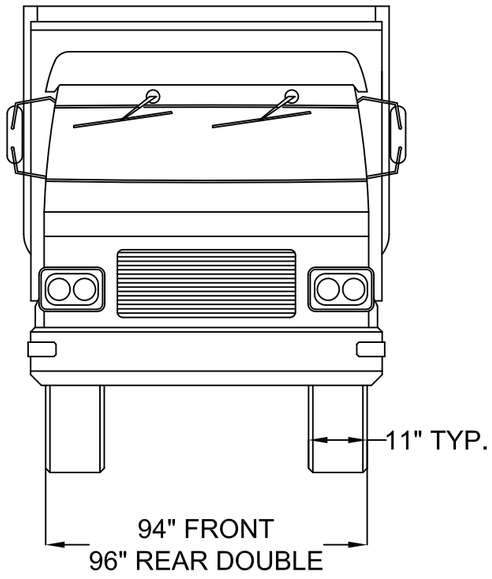

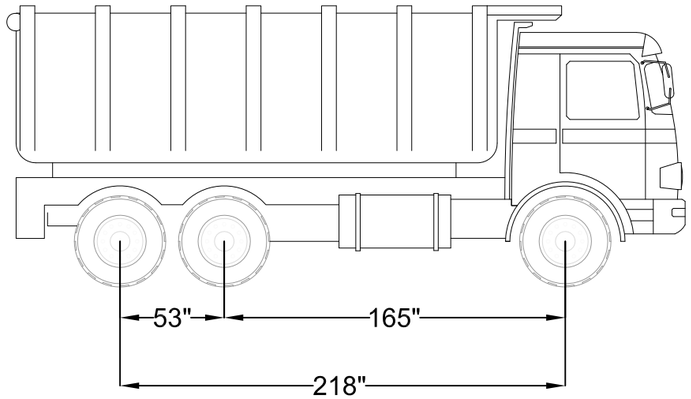

A — TRUCK DIMENSIONS
N.T.S

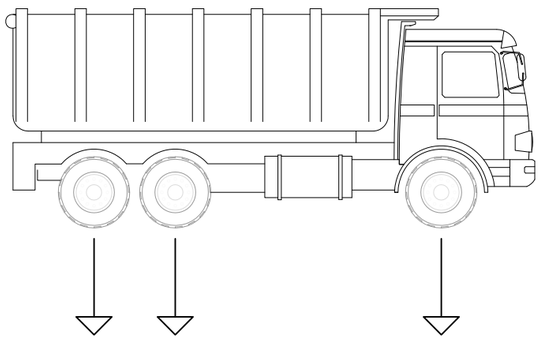

TOTAL WEIGHT:
52900 lb

DRIVER SIDE:	8760 lb	8540 lb	8260 lb
PASSENGER SIDE:	9600 lb	9620 lb	8120 lb

A — TRUCK AXLE WEIGHTS
N.T.S

EB TRUCK CONFIGURATION 4
LEFT SHOULDER
TRUCK NO. R09174

No.	Revision	By	Chk	Appd	Date
1					

Original Scale (11"x17") **AS SHOWN**

Design			
Drawn			
Dsg Verifier			
Drg Check			

* Refer to Revision 1 for Original Signature

VirginiaTech 1872 Invent the Future

Subject: Hampton Roads Bridge Tunnel

Title: EB-TC4-R09174

Discipline: Structural

Drawing No.:

Rev.: 127

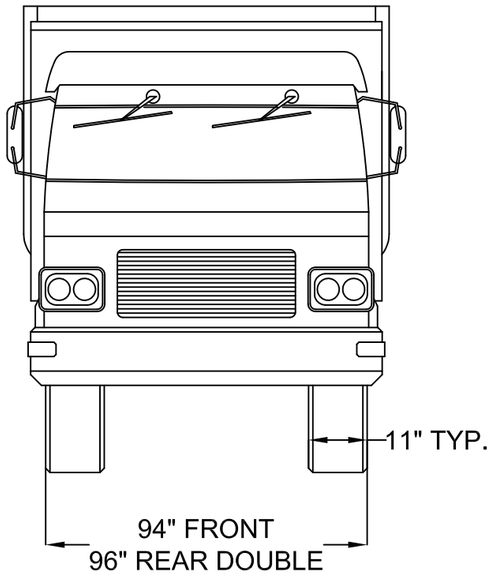

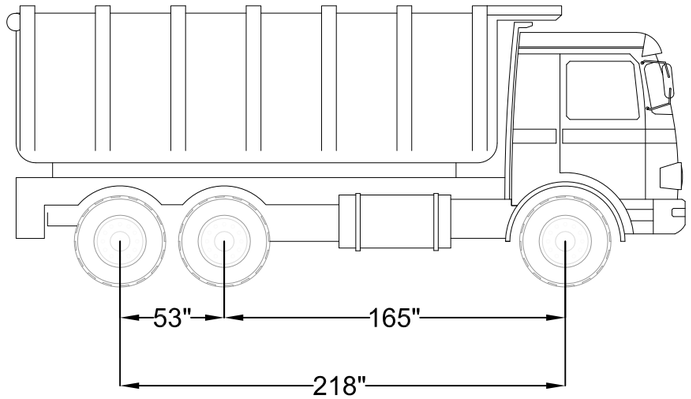

A — TRUCK DIMENSIONS
N.T.S

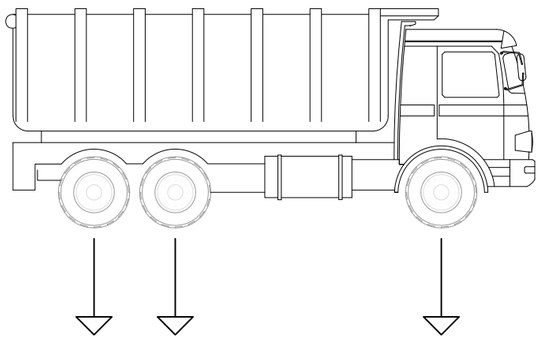

TOTAL WEIGHT:
56060 lb

DRIVER SIDE:	9820 lb	9700 lb	7980 lb
PASSENGER SIDE:	10160 lb	9940 lb	8460 lb

A — TRUCK AXLE WEIGHTS
N.T.S

EB TRUCK CONFIGURATION 5
TWO TRUCKS - LEFT LANE TRUCK
TRUCK NO. R09363

No.	Revision	By	Chk	Appd	Date
1					

Original Scale (11"x17") **AS SHOWN**

Design			
Drawn			
Dsg Verifier			
Drg Check			

* Refer to Revision 1 for Original Signature

VirginiaTech
Invent the Future

Subject: Hampton Roads Bridge Tunnel

Title: EB-TC5-LL-R09363

Discipline: Structural

Drawing No.

Rev. 128

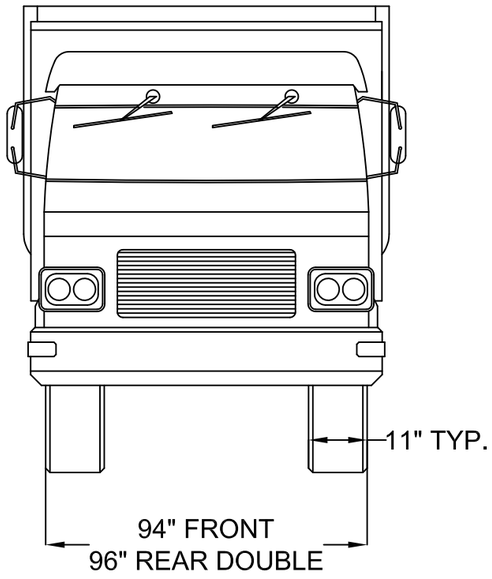

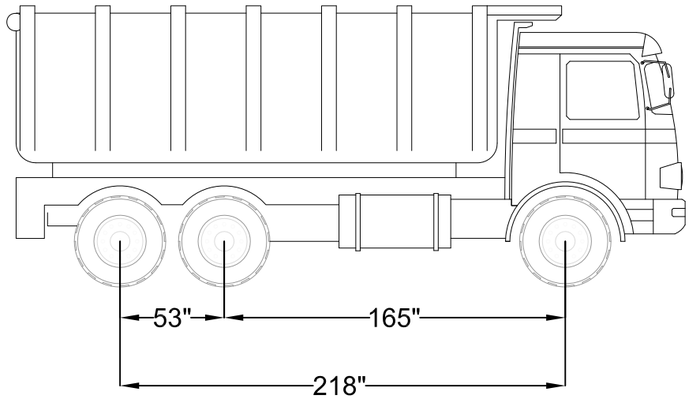

A — TRUCK DIMENSIONS
N.T.S

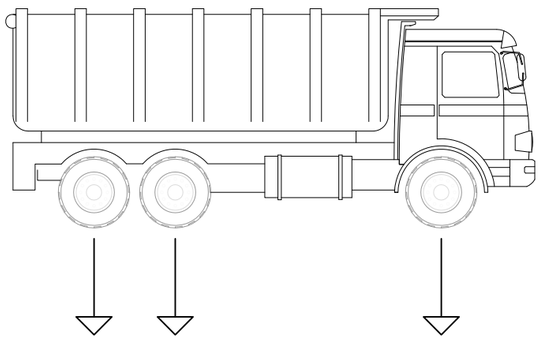

TOTAL WEIGHT:
55760 lb

EB TRUCK CONFIGURATION 5
TWO TRUCKS - RIGHT LANE TRUCK
TRUCK NO. R07382

	9880 lb	9280 lb	8060 lb
DRIVER SIDE:	9880 lb	9280 lb	8060 lb
PASSENGER SIDE:	10460 lb	10340 lb	7740 lb

A — TRUCK AXLE WEIGHTS
N.T.S

No.	Revision	By	Chk	Appd	Date
1					

Original Scale (11"x17") AS SHOWN

Design | Drawn | Dsg Verifier | Drg Check

* Refer to Revision 1 for Original Signature

VirginiaTech 1872 Invent the Future

Subject: Hampton Roads Bridge Tunnel

Title: EB-TC5-RL-R07382

Discipline: Structural

Drawing No.

Rev. 129

APPENDIX B-2:

WESTBOUND TRUCKS

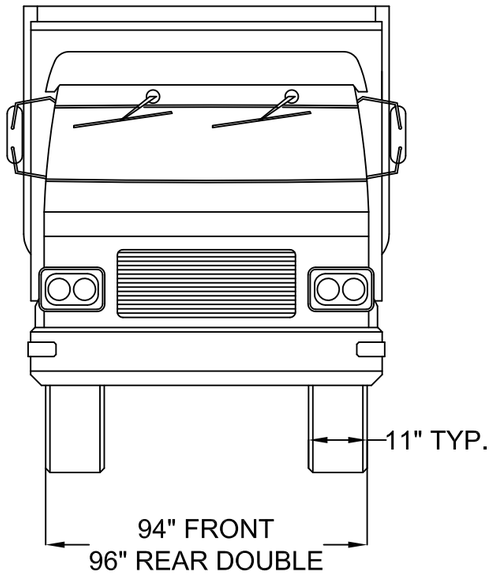

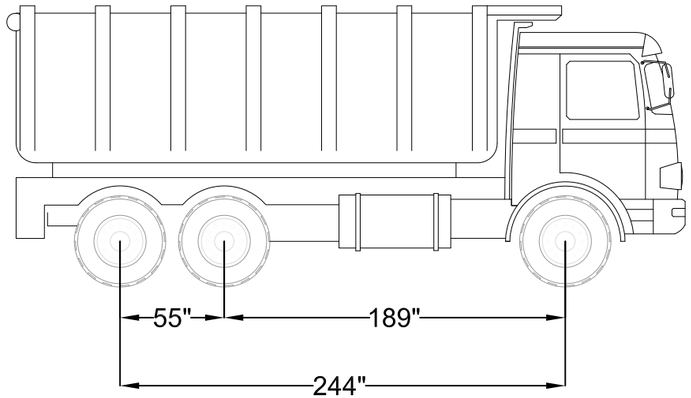

A — TRUCK DIMENSIONS
N.T.S

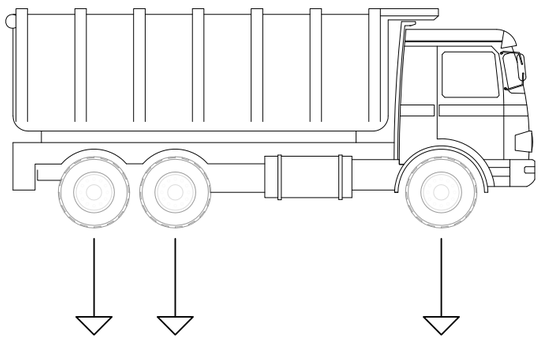

TOTAL WEIGHT:
55740 lb

WB TRUCK CONFIGURATION 1
RIGHT SHOULDER
TRUCK NO. R14156

		10200 lb	10400 lb	8260 lb
DRIVER SIDE:				
PASSENGER SIDE:		9460 lb	9840 lb	7580 lb

A — TRUCK AXLE WEIGHTS
N.T.S

No.	Revision	By	Chk	Appd	Date
1					

Original Scale (11"x17") **AS SHOWN**

Design | Drawn | Dsg Verifier | Drg Check

* Refer to Revision 1 for Original Signature

VirginiaTech
Invent the Future

Subject: Hampton Roads Bridge Tunnel

Title: WB-TC1-R14156

Discipline: Structural

Drawing No.

Rev. 131

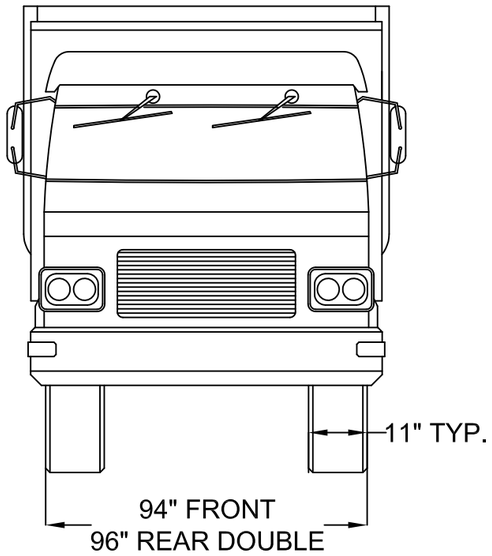

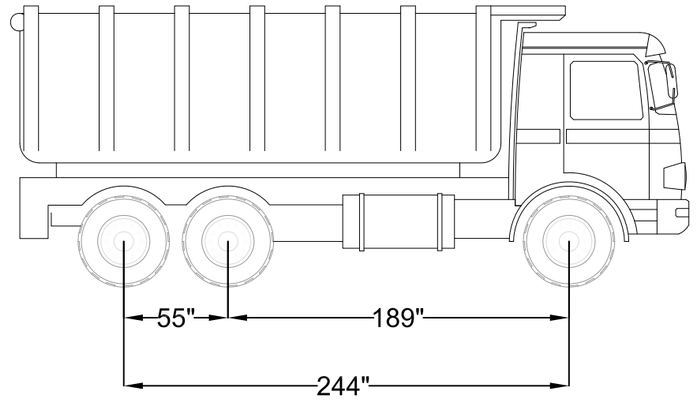

A — TRUCK DIMENSIONS
N.T.S

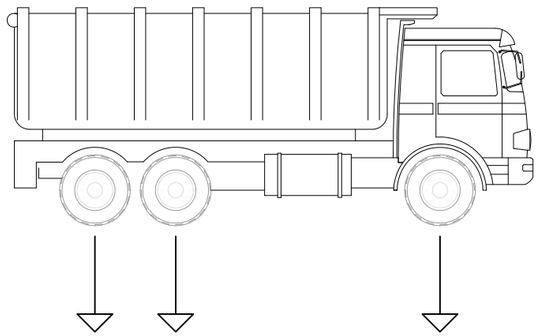

TOTAL WEIGHT:
54600 lb

WB TRUCK CONFIGURATION 2
RIGHT LANE
TRUCK NO. R14155

	9920 lb	9980 lb	7960 lb
DRIVER SIDE:			
PASSENGER SIDE:	9640 lb	9800 lb	7300 lb

A — TRUCK AXLE WEIGHTS
N.T.S

No.	Revision	By	Chk	Appd	Date
1					

Original Scale (11"x17") **AS SHOWN**

Design | Drawn | Dsg Verifier | Drg Check

* Refer to Revision 1 for Original Signature

VirginiaTech 1872 Invent the Future

Subject: Hampton Roads Bridge Tunnel

Title: WB-TC2-R14155

Discipline: Structural

Drawing No.

Rev. 132

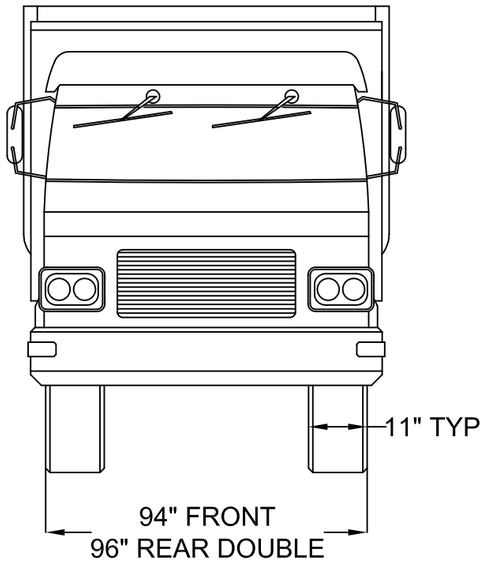

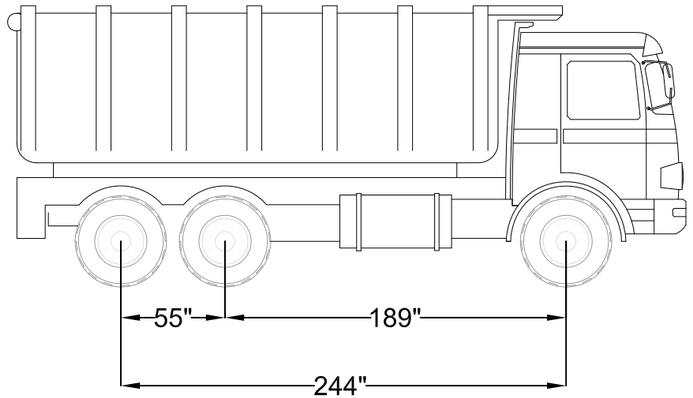

A — TRUCK DIMENSIONS
N.T.S

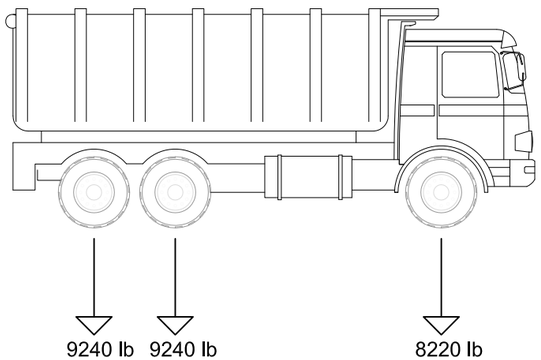

TOTAL WEIGHT:
52840 lb

DRIVER SIDE:	9240 lb	9240 lb	8220 lb
PASSENGER SIDE:	8920 lb	9380 lb	7840 lb

A — TRUCK AXLE WEIGHTS
N.T.S

WB TRUCK CONFIGURATION 3
LEFT LANE
TRUCK NO. R14149

No.	Revision	By	Chk	Appd	Date
1					

Original Scale (11"x17") **AS SHOWN**

Design			
Drawn			
Dsg Verifier			
Drg Check			

* Refer to Revision 1 for Original Signature

VirginiaTech
Invent the Future

Subject: Hampton Roads Bridge Tunnel

Title: WB-TC3-R14149

Discipline: Structural

Drawing No.:

Rev.: 133

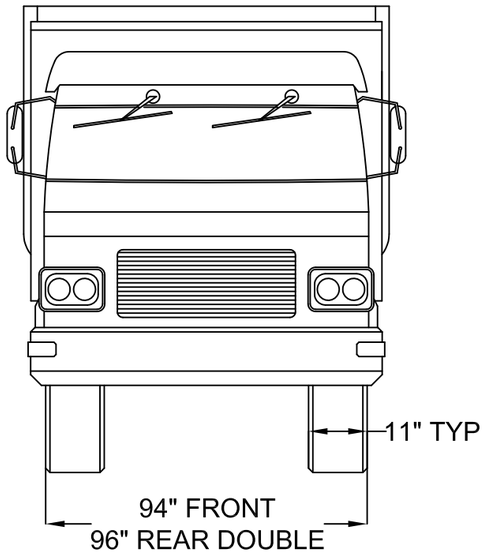

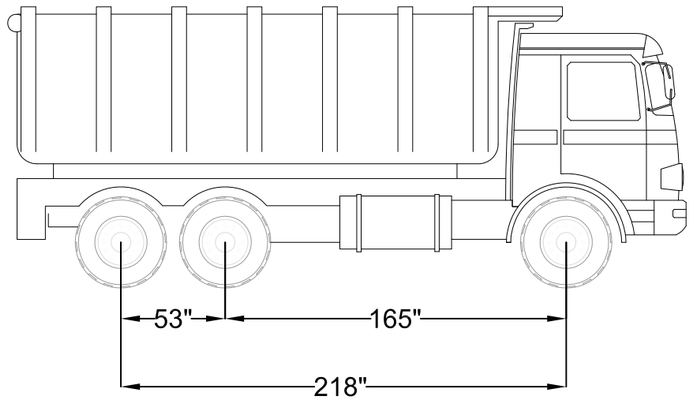

A — TRUCK DIMENSIONS
N.T.S

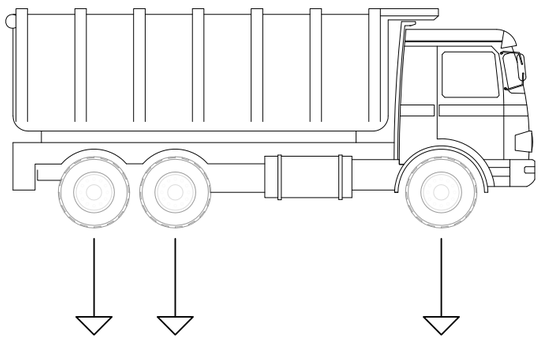

TOTAL WEIGHT:
54000 lb

DRIVER SIDE:	8960 lb	9420 lb	8920 lb
PASSENGER SIDE:	8860 lb	9060 lb	8780 lb

A — TRUCK AXLE WEIGHTS
N.T.S

WB TRUCK CONFIGURATION 4
LEFT SHOULDER
TRUCK NO. R09174

No.	Revision	By	Chk	Appd	Date
1					

Original Scale (11"x17") **AS SHOWN**

Design			
Drawn			
Dsg Verifier			
Drg Check			

* Refer to Revision 1 for Original Signature

VirginiaTech
Invent the Future

Subject: Hampton Roads Bridge Tunnel

Title: WB-TC4-R09174

Discipline: Structural

Drawing No.:

Rev.: 134

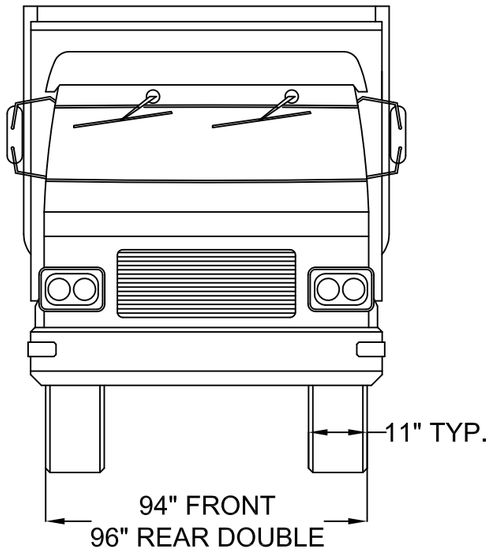

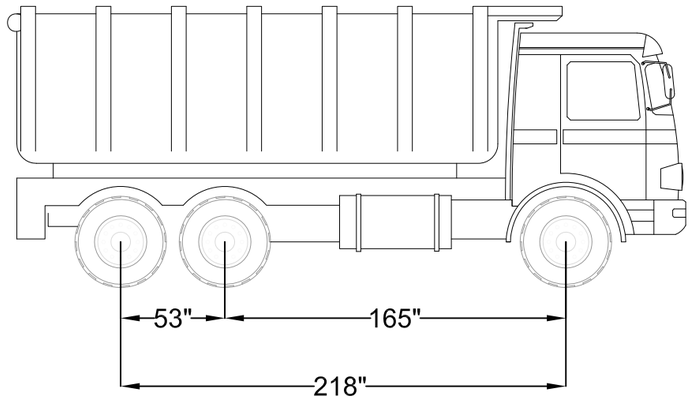

A — TRUCK DIMENSIONS
N.T.S

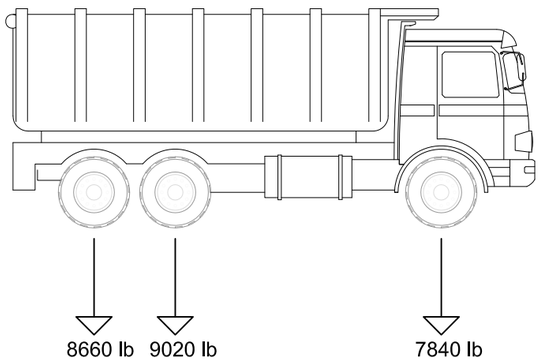

TOTAL WEIGHT:
52200 lb

DRIVER SIDE:	8660 lb	9020 lb		7840 lb
PASSENGER SIDE:	9560 lb	9880 lb		7240 lb

A — TRUCK AXLE WEIGHTS
N.T.S

WB TRUCK CONFIGURATION 5
TWO TRUCKS - LEFT LANE TRUCK
TRUCK NO. R07382

No.	Revision	By	Chk	Appd	Date
1					

Original Scale (11"x17") **AS SHOWN**

Design | Drawn | Dsg Verifier | Drg Check

* Refer to Revision 1 for Original Signature

VirginiaTech 1872 Invent the Future

Subject: Hampton Roads Bridge Tunnel

Title: WB-TC5 LL-R07382

Discipline: Structural

Drawing No.

Rev. 135

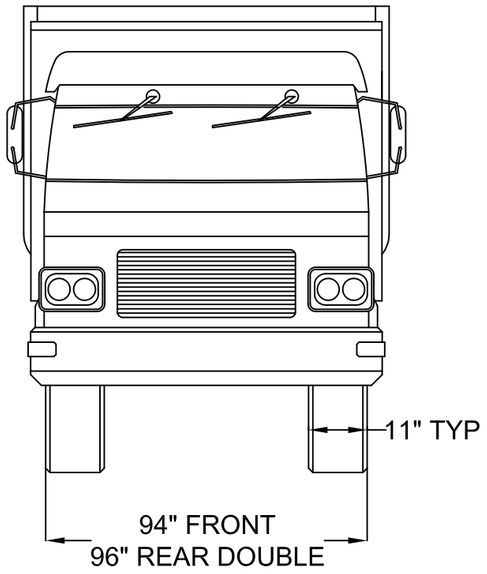

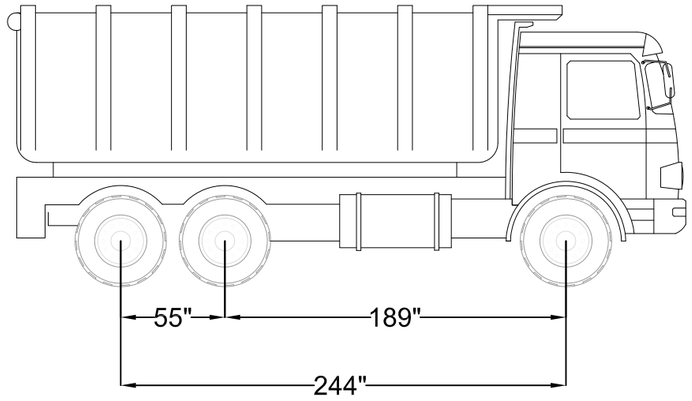

A — TRUCK DIMENSIONS
N.T.S

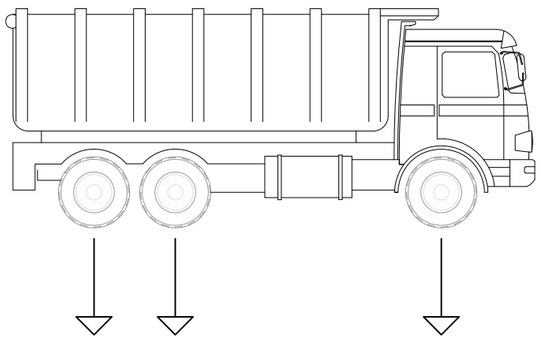

TOTAL WEIGHT:
51760 lb

DRIVER SIDE:	9740 lb	10060 lb	7360 lb
PASSENGER SIDE:	8820 lb	9340 lb	6440 lb

A — TRUCK AXLE WEIGHTS
N.T.S

WB TRUCK CONFIGURATION 5
TWO TRUCKS - RIGHT LANE TRUCK
TRUCK NO. R12067

No.	Revision	By	Chk	Appd	Date
1					

Original Scale (11"x17") **AS SHOWN**

Design | Drawn | Dsg Verifier | Drg Check

* Refer to Revision 1 for Original Signature

VirginiaTech 1872 Invent the Future

Subject: Hampton Roads Bridge Tunnel

Title: WB-TC5 RL-R12067

Discipline: Structural

Drawing No.

Rev. 136

APPENDIX C

SUMMARY DATA SHEETS

APPENDIX C-1:

EASTBOUND SPAN 56

Live Load Testing Results HRBT EASTBOUND STRUCTURE SPAN 56 For Hampton Roads Bridge Tunnel	VirginiaTech Invent the Future	Made	JJR	Date	5/26/2016	Job Number	449462
		Checked	EAE	Date	5/31/2016	Connection	
		Backchk'd	JJR	Date	5/31/2016	Sheet No.	1

Truck Configuration 1

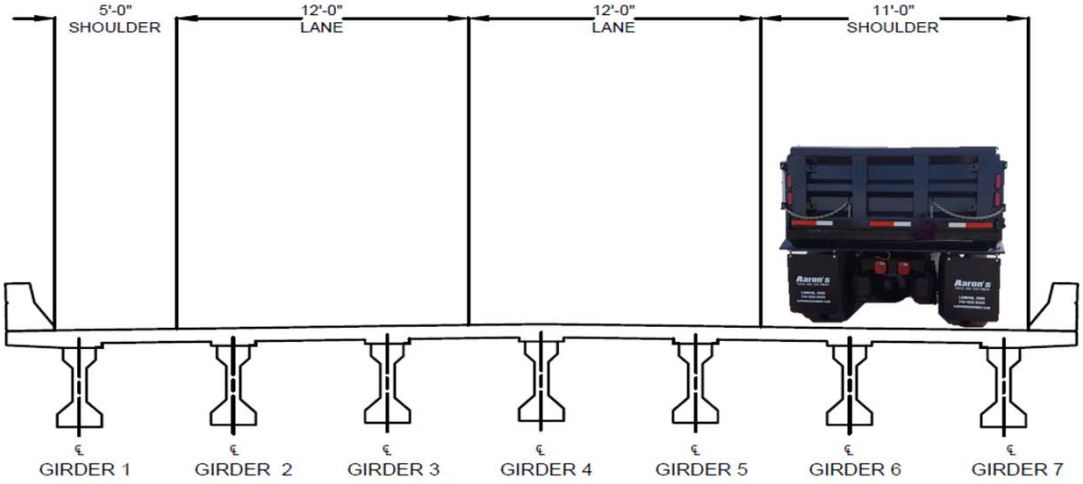

1. Midspan Measurements

		Girder 1	Girder 2	Girder 3	Girder 4	Girder 5	Girder 6	Girder 7
Run 1	Bottom Face of Flange Strain (με) :	-0.89	1.35	4.04	11.55	49.86	31.32	32.66
	*Deflection (in.) :	N/A	N/A	N/A	N/A	N/A	N/A	N/A
Run 2	Bottom Face of Flange Strain (με) :	-0.66	1.30	3.67	10.79	46.08	30.83	34.40
	*Deflection (in.) :	N/A	N/A	N/A	N/A	N/A	N/A	N/A
Run 3	Bottom Face of Flange Strain (με) :	-0.75	1.46	3.73	10.72	47.27	29.62	31.54
	*Deflection (in.) :	N/A	N/A	N/A	N/A	N/A	N/A	N/A

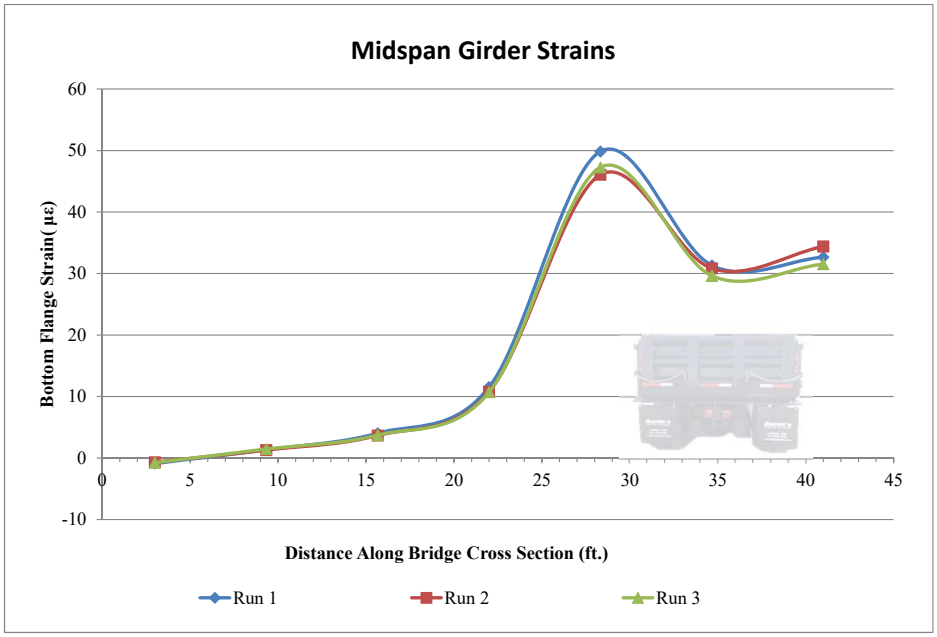

* The deflection values were discarded due to faulty deflection system setup. The cross wire movement prevented the string pots from collecting the full deflection values and leading to softened and inaccurate magnitudes.

NOTES:

1. Girders are numbered from the east in accordance with original bridge plans
2. Span 56 is the small craft navigation span as seen in the contract drawings
3. Girder 5 has considerable damage as shown in Inspection Report
4. Deflection Values not useful - see report

REFERENCES:

1. As - Built Contract Drawings T-3 (224-03) dated December 1977
2. VDOT July 2014 Special Inspection Report for EB South Approach Bridge

Truck Configuration 1 Continued

2. Girder 5 Strain Distribution at Midspan

	Strain Transducer Readings (με)			
Location	Run 1	Run 2	Run 3	Height (in.)
midheight of top flange	-4.94	-5.08	-5.58	41.5
1" below top of CT web	0.73	0.50	-0.14	32.5
1" above bottom of CT web	8.95	8.73	8.16	15.5
Bot. Face of Flange	49.86	46.08	47.27	0

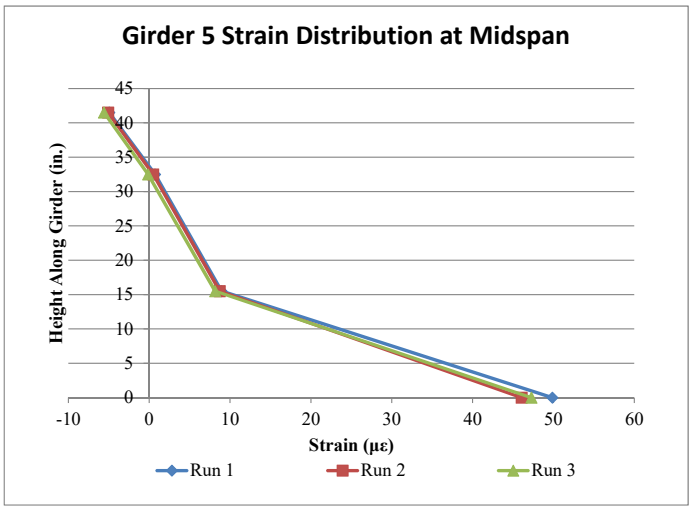

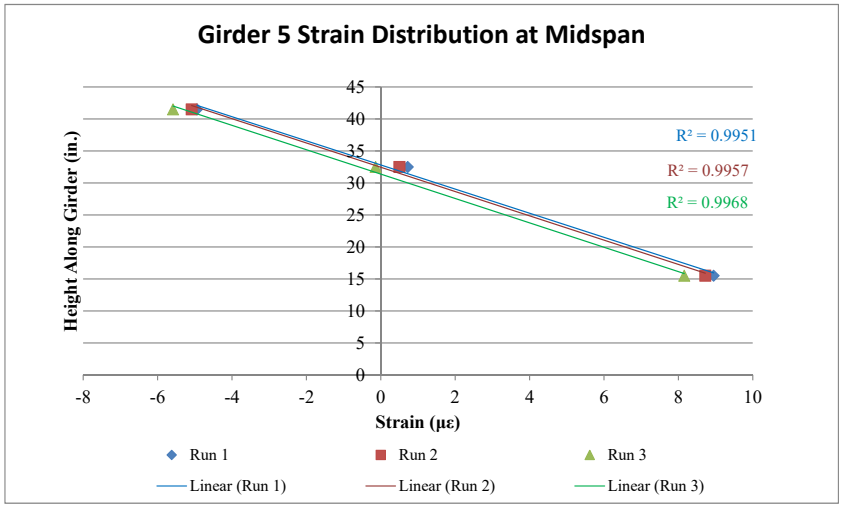

Based on the observed data, there is a bilinear strain distribution caused by the damage to the bottom of the girder flange. The concrete is experiencing much higher strains than it would for an undamaged section. Due to the lack of sound P/S strands, the concrete is forced to carry higher strains.

3. Girder 5 Strain Distribution at ~3L/4

	Strain Transducer Readings (με)			
Location	Run 1	Run 2	Run 3	Height (in.)
**midheight of top flange	-0.33	-0.17	0.04	41.5
1" below top of CT web	0.66	0.21	-0.05	32.5
1" above bottom of CT web	7.38	7.11	6.39	15.5
Bot. Face of Flange	14.20	13.61	13.17	0

** Based on the observed data, it is evident that the top flange strain transducer was not adhered to the flange fully. This lead to faulty values.

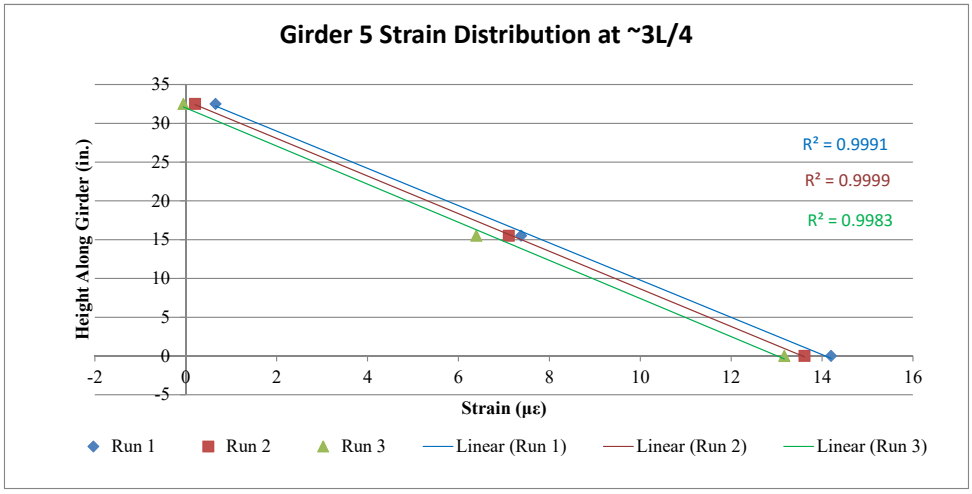

NOTES:

1. Girders are numbered from the east in accordance with original bridge plans
2. Span 56 is the small craft navigation span as seen in the contract drawings
3. Girder 5 has considerable damage as shown in Inspection Report

REFERENCES:

1. As - Built Contract Drawings T-3 (224-03) dated December 1977
2. VDOT July 2014 Special Inspection Report for EB South Approach Bridge

Truck Configuration 1 Continued

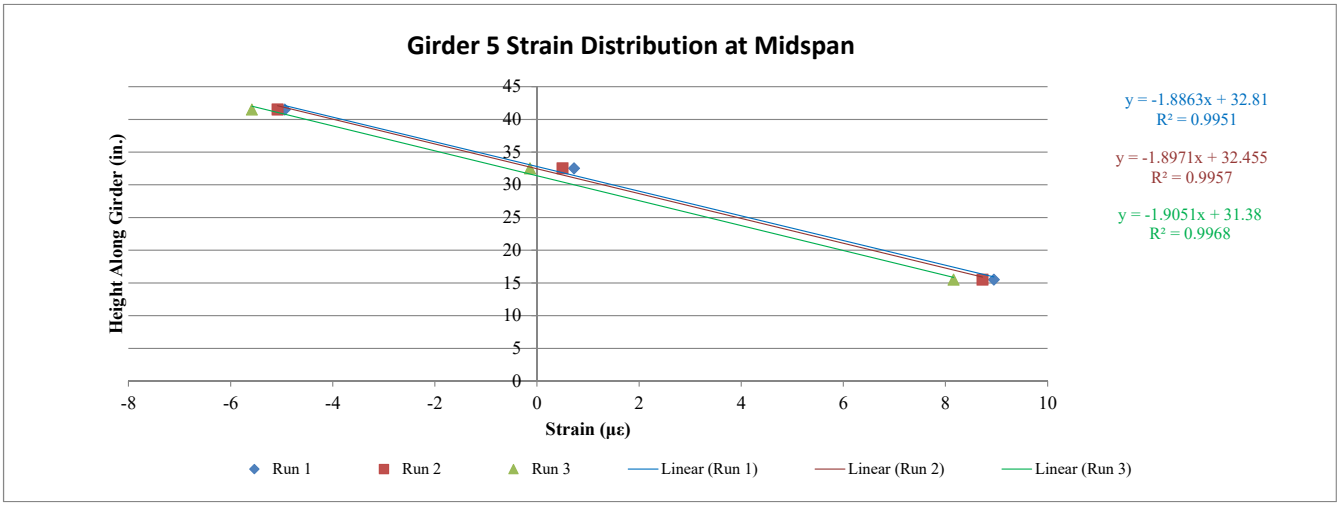

Determine Strain at Bottom Face of Flange Based on Line of Best Fit:

y (height) ***	m	x (strain)	b
0	-1.8863	17.394	32.81
0	-1.8971	17.108	32.455
0	-1.9051	16.472	31.38

*** the "y" height of zero corresponds to the height of the bottom face of the girder flange based on the axis configuration. The undamaged strains at this location are found using the line of best fit equation for a linear strain distribution through the entire height of the girder.

Undamaged Strain Values:

	Girder 1	Girder 2	Girder 3	Girder 4	Girder 5	Girder 6	Girder 7
Run 1	-0.89	1.35	4.04	11.55	17.39	31.32	32.66
Run 2	-0.66	1.30	3.67	10.79	17.11	30.83	34.40
Run 3	-0.75	1.46	3.73	10.72	16.47	29.62	31.54

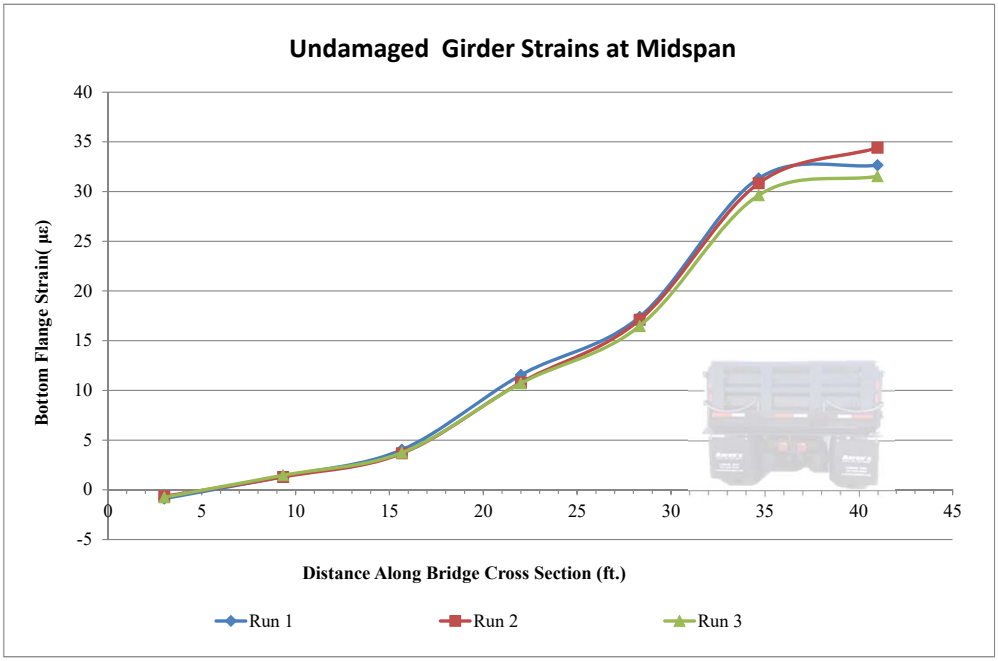

NOTES:

1. Girders are numbered from the east in accordance with original bridge plans
2. Span 56 is the small craft navigation span as seen in the contract drawings
3. Girder 5 has considerable damage as shown in Inspection Report

REFERENCES:

1. As - Built Contract Drawings T-3 (224-03) dated December 1977
2. VDOT July 2014 Special Inspection Report for EB South Approach Bridge

Live Load Testing Results	VirginiaTech Invent the Future	Made	JJR	Date	5/26/2016	Job Number	449462
HRBT EASTBOUND STRUCTURE SPAN 56		Checked	EAE	Date	5/31/2016	Connection	
For Hampton Roads Bridge Tunnel		Backchk'd	JJR	Date	5/31/2016	Sheet No.	1

Truck Configuration 2

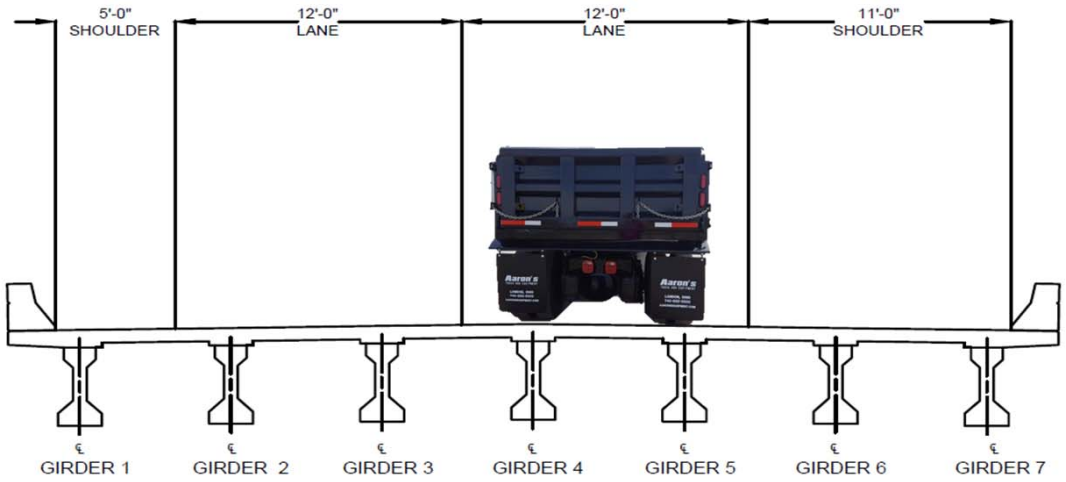

1. Midspan Measurements

		Girder 1	Girder 2	Girder 3	Girder 4	Girder 5	Girder 6	Girder 7
Run 1	Bottom Face of Flange Strain (με) :	2.75	4.49	10.30	29.06	68.19	16.33	11.40
	*Deflection (in.) :	N/A	N/A	N/A	N/A	N/A	N/A	N/A
Run 2	Bottom Face of Flange Strain (με) :	2.99	5.06	10.36	29.55	69.55	16.32	11.62
	*Deflection (in.) :	N/A	N/A	N/A	N/A	N/A	N/A	N/A
Run 3	Bottom Face of Flange Strain (με) :	3.18	5.34	10.90	29.30	68.28	16.15	10.78
	*Deflection (in.) :	N/A	N/A	N/A	N/A	N/A	N/A	N/A

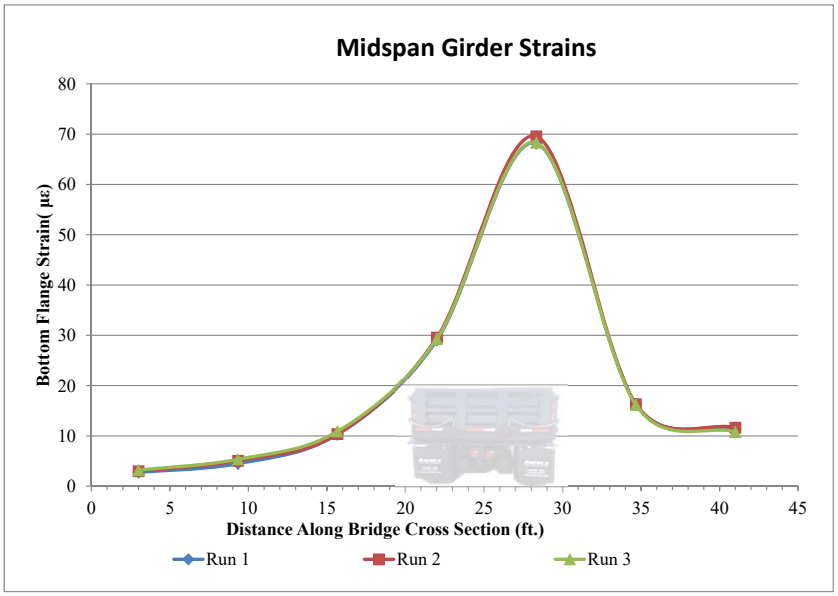

* The deflection values were discarded due to faulty deflection system setup. The cross wire movement prevented the string pots from collecting the full deflection values and leading to softened and inaccurate magnitudes.

NOTES:

1. Girders are numbered from the east in accordance with original bridge plans
2. Span 56 is the small craft navigation span as seen in the contract drawings
3. Girder 5 has considerable damage as shown in Inspection Report
4. Deflection Values not useable - see report

REFERENCES:

1. As - Built Contract Drawings T-3 (224-03) dated December 1977
2. VDOT July 2014 Special Inspection Report for EB South Approach Bridge

Truck Configuration 2 Continued

2. Girder 5 Strain Distribution at Midspan

	Strain Transducer Readings (με)			
Location	Run 1	Run 2	Run 3	Height (in.)
midheight of top flange	-4.73	-4.35	-4.24	41.5
1" below top of CT web	3.49	3.97	3.72	32.5
1" above bottom of CT web	14.78	15.37	15.02	15.5
Bot. Face of Flange	68.19	69.55	68.28	0

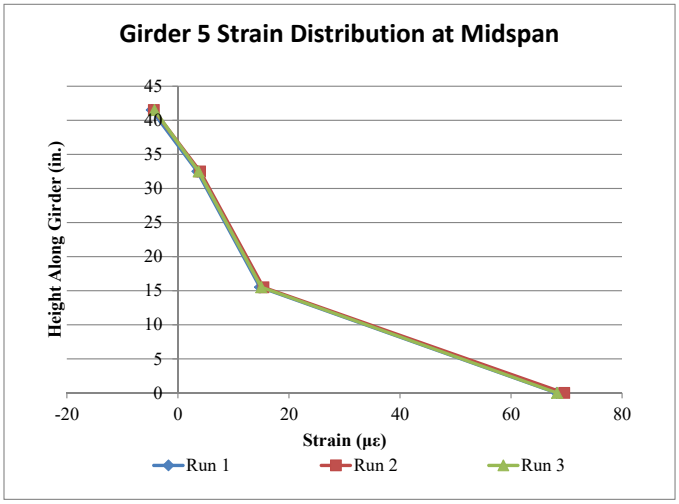

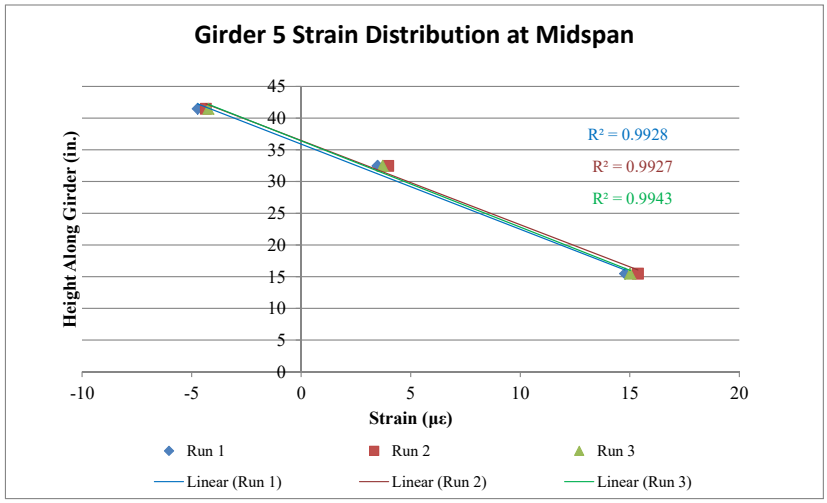

Based on the observed data, there is a bilinear strain distribution caused by the damage to the bottom of the girder flange. The concrete is experiencing much higher strains than it would for an undamaged section. Due to the lack of sound P/S strands, the concrete is forced to carry higher strains.

3. Girder 5 Strain Distribution at ~3L/4

	Strain Transducer Readings (με)			
Location	Run 1	Run 2	Run 3	Height (in.)
**midheight of top flange	-0.03	0.04	-0.01	41.5
1" below top of CT web	2.74	2.65	2.75	32.5
1" above bottom of CT web	11.89	12.00	12.13	15.5
Bot. Face of Flange	20.96	20.60	20.76	0

** Based on the observed data, it is evident that the top flange strain transducer was not adhered to the flange fully. This lead to faulty values.

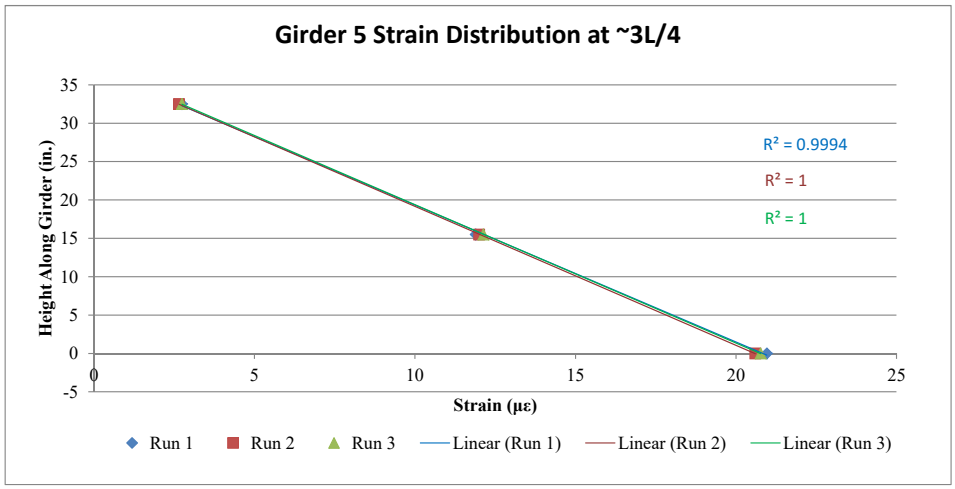

NOTES:

1. Girders are numbered from the east in accordance with original bridge plans
2. Span 56 is the small craft navigation span as seen in the contract drawings
3. Girder 5 has considerable damage as shown in Inspection Report

REFERENCES:

1. As - Built Contract Drawings T-3 (224-03) dated December 1977
2. VDOT July 2014 Special Inspection Report for EB South Approach Bridge

Truck Configuration 2 Continued

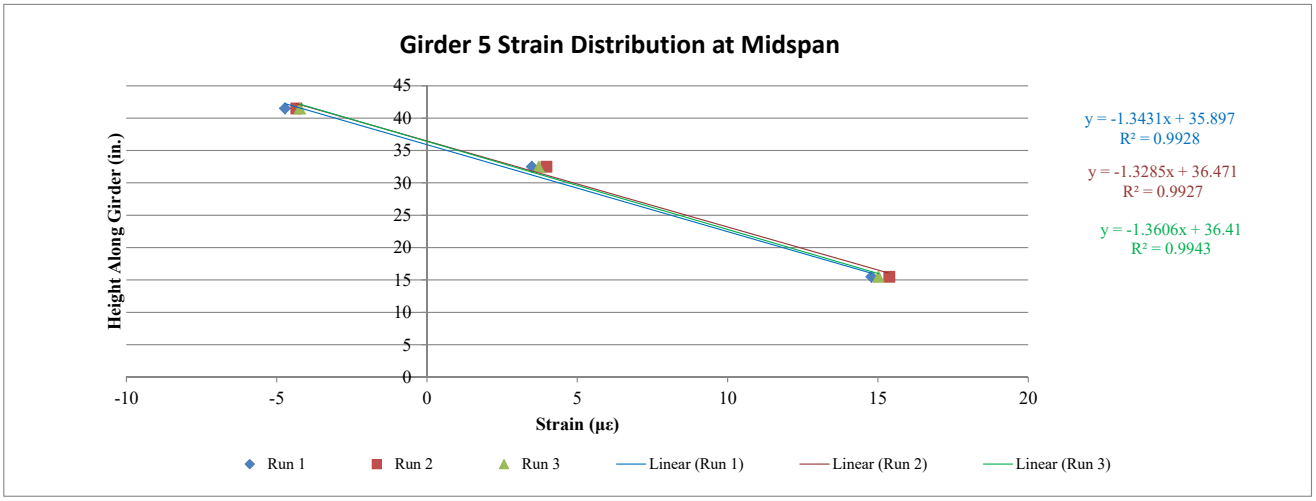

Determine Strain at Bottom Face of Flange Based on Line of Best Fit:

y (height) ***	m	x (strain)	b
0	-1.3431	26.727	35.897
0	-1.3285	27.453	36.471
0	-1.3606	26.760	36.41

*** the "y" height of zero corresponds to the height of the bottom face of the girder flange based on the axis configuration. The undamaged strains at this location are found using the line of best fit equation for a linear strain distribution through the entire height of the girder.

Undamaged Strain Values:

	Girder 1	Girder 2	Girder 3	Girder 4	Girder 5	Girder 6	Girder 7
Run 1	2.75	4.49	10.30	29.06	26.73	16.33	11.40
Run 2	2.99	5.06	10.36	29.55	27.45	16.32	11.62
Run 3	3.18	5.34	10.90	29.30	26.76	16.15	10.78

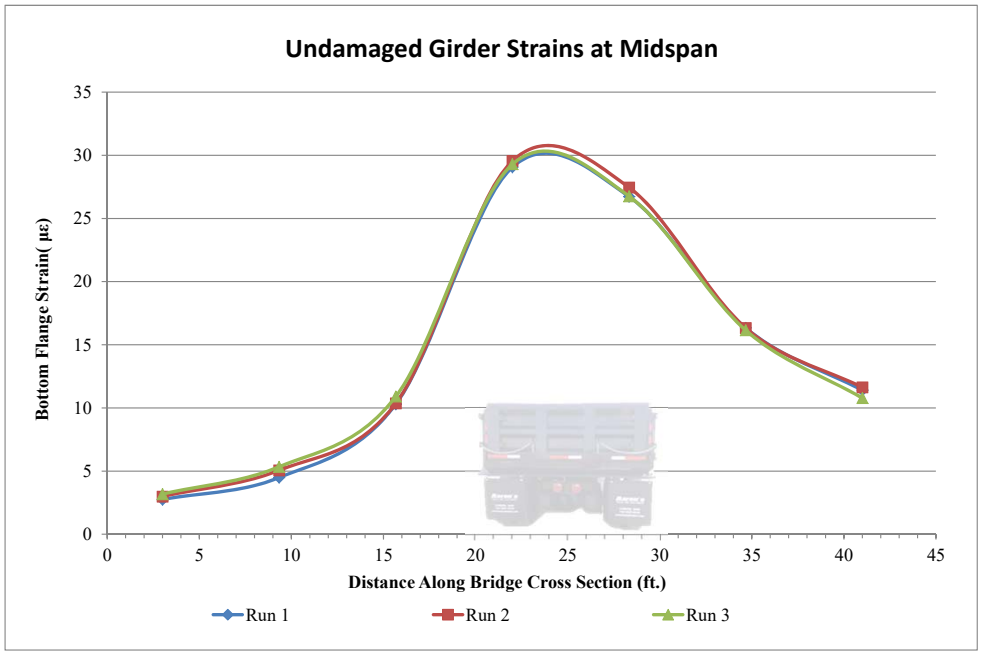

NOTES:

1. Girders are numbered from the east in accordance with original bridge plans
2. Span 56 is the small craft navigation span as seen in the contract drawings
3. Girder 5 has considerable damage as shown in Inspection Report

REFERENCES:

1. As - Built Contract Drawings T-3 (224-03) dated December 1977
2. VDOT July 2014 Special Inspection Report for EB South Approach Bridge

Live Load Testing Results	VirginiaTech Invent the Future	Made	JJR	Date	5/26/2016	Job Number	449462
HRBT EASTBOUND STRUCTURE SPAN 56		Checked	EAE	Date	5/31/2016	Connection	
For Hampton Roads Bridge Tunnel		Backchk'd	JJR	Date	5/3102016	Sheet No.	1

Truck Configuration 3

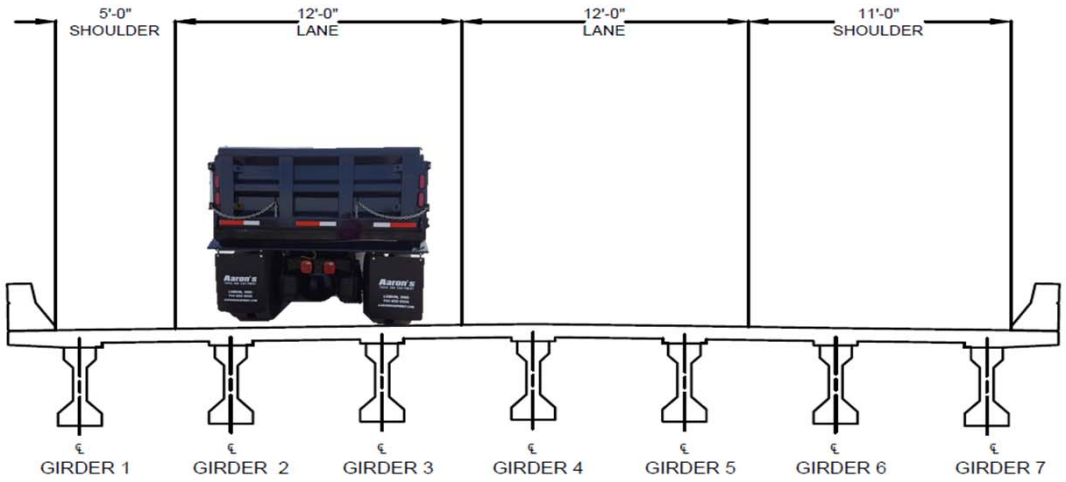

1. Midspan Measurements

		Girder 1	Girder 2	Girder 3	Girder 4	Girder 5	Girder 6	Girder 7
Run 1	Bottom Face of Flange Strain (με) :	13.58	15.42	17.37	16.34	21.85	5.71	2.03
	*Deflection (in.) :	N/A	N/A	N/A	N/A	N/A	N/A	N/A
Run 2	Bottom Face of Flange Strain (με) :	14.23	16.19	17.93	16.68	22.75	5.70	2.02
	*Deflection (in.) :	N/A	N/A	N/A	N/A	N/A	N/A	N/A
Run 3	Bottom Face of Flange Strain (με) :	14.28	15.91	17.58	16.29	21.81	5.27	2.06
	*Deflection (in.) :	N/A	N/A	N/A	N/A	N/A	N/A	N/A

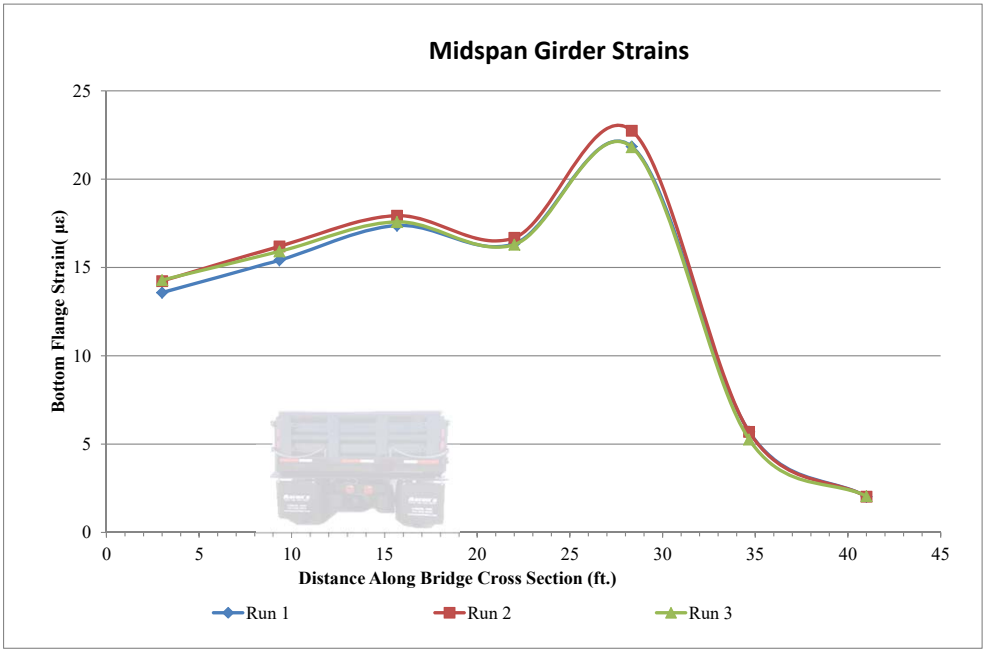

* The deflection values were discarded due to faulty deflection system setup. The cross wire movement prevented the string pots from collecting the full deflection values and leading to softened and inaccurate magnitudes.

NOTES:

1. Girders are numbered from the east in accordance with original bridge plans
2. Span 56 is the small craft navigation span as seen in the contract drawings
3. Girder 5 has considerable damage as shown in Inspection Report
4. Deflection Values not usable - see report

REFERENCES:

1. As - Built Contract Drawings T-3 (224-03) dated December 1977
2. VDOT July 2014 Special Inspection Report for EB South Approach Bridge

Truck Configuration 3 Continued

2. Girder 5 Strain Distribution at Midspan

	Strain Transducer Readings (με)			
Location	Run 1	Run 2	Run 3	Height (in.)
midheight of top flange	-2.17	-2.71	-2.19	41.5
1" below top of CT web	0.47	0.23	0.34	32.5
1" above bottom of CT web	5.06	5.02	4.94	15.5
Bot. Face of Flange	21.85	22.75	21.81	0

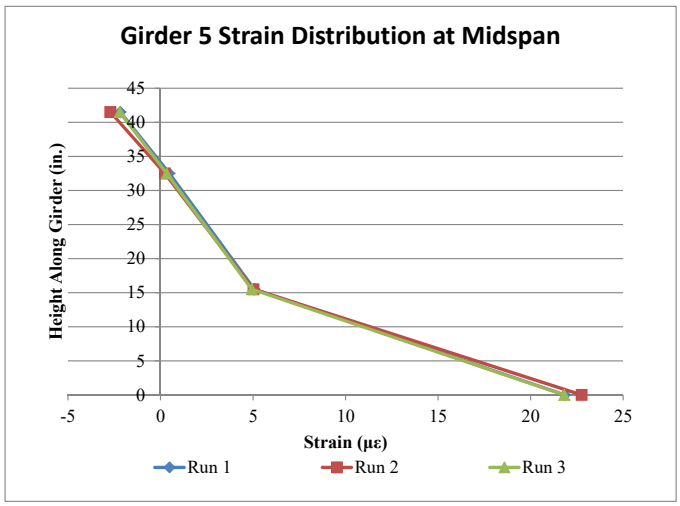

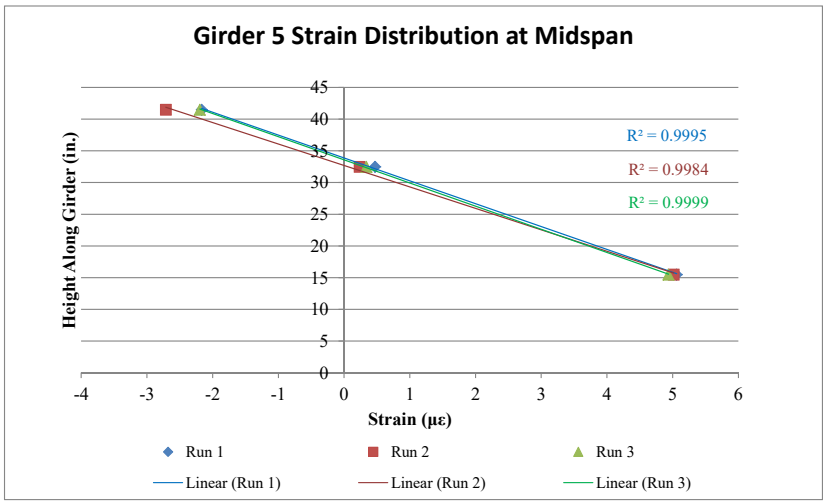

Based on the observed data, there is a bilinear strain distribution caused by the damage to the bottom of the girder flange. The concrete is experiencing much higher strains than it would for an undamaged section. Due to the lack of sound P/S strands, the concrete is forced to carry higher strains.

3. Girder 5 Strain Distribution at ~3L/4

	Strain Transducer Readings (με)			
Location	Run 1	Run 2	Run 3	Height (in.)
**midheight of top flange	-0.01	0.00	-0.04	41.5
1" below top of CT web	0.33	0.45	0.14	32.5
1" above bottom of CT web	4.42	4.38	4.09	15.5
Bot. Face of Flange	7.63	7.86	7.47	0

** Based on the observed data, it is evident that the top flange strain transducer was not adhered to the flange fully. This lead to faulty values.

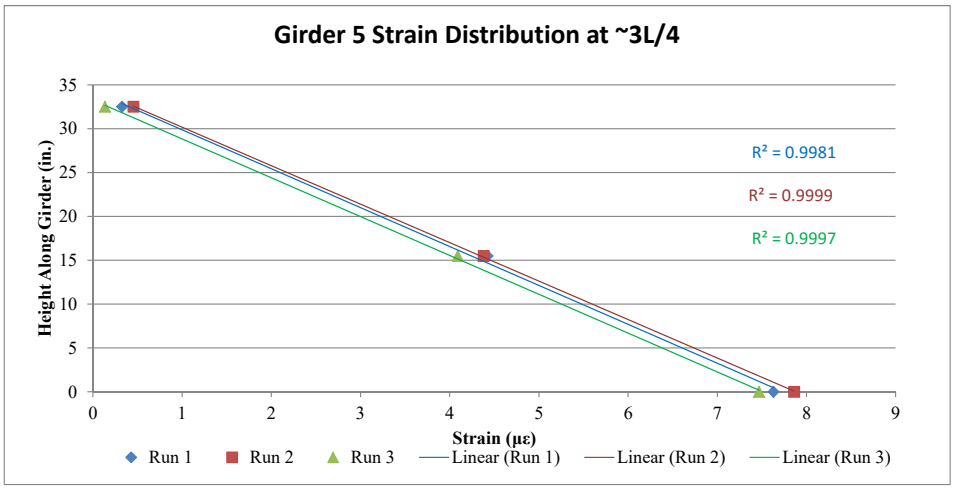

NOTES:

1. Girders are numbered from the east in accordance with original bridge plans
2. Span 56 is the small craft navigation span as seen in the contract drawings
3. Girder 5 has considerable damage as shown in Inspection Report

REFERENCES:

1. As - Built Contract Drawings T-3 (224-03) dated December 1977
2. VDOT July 2014 Special Inspection Report for EB South Approach Bridge

Truck Configuration 3 Continued

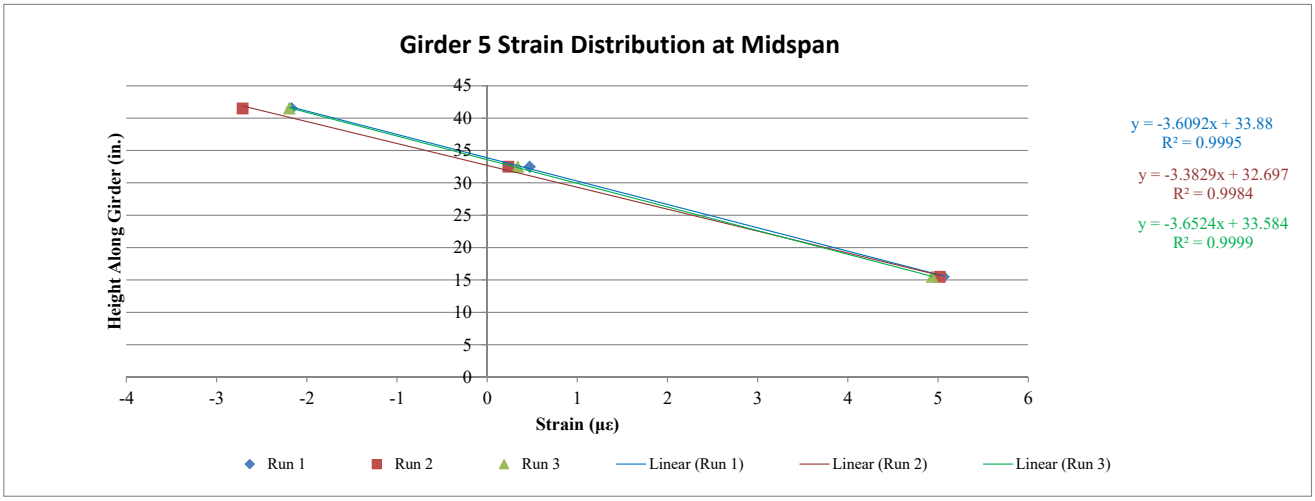

Determine Strain at Bottom Face of Flange Based on Line of Best Fit:

y (height) ***	m	x (strain)	b
0	-3.6092	9.3871	33.88
0	-3.3829	9.6654	32.697
0	-3.6524	9.1950	33.584

*** the "y" height of zero corresponds to the height of the bottom face of the girder flange based on the axis configuration. The undamaged strains at this location are found using the line of best fit equation for a linear strain distribution through the entire height of the girder.

Undamaged Strain Values:

	Girder 1	Girder 2	Girder 3	Girder 4	Girder 5	Girder 6	Girder 7
Run 1	13.58	15.42	17.37	16.34	9.39	5.71	2.03
Run 2	14.23	16.19	17.93	16.68	9.67	5.70	2.02
Run 3	14.28	15.91	17.58	16.29	9.20	5.27	2.06

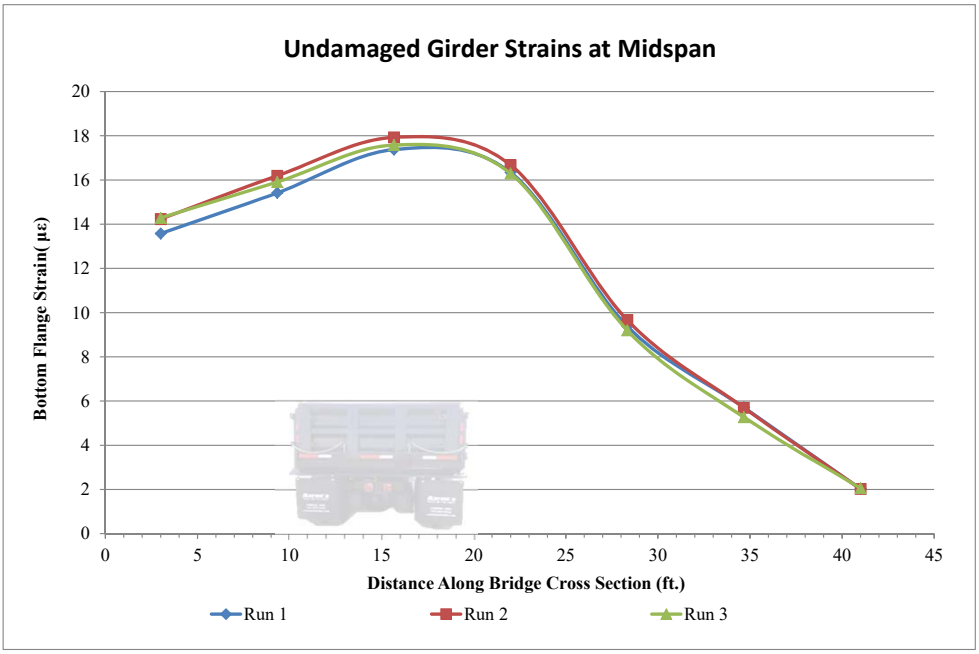

NOTES:

1. Girders are numbered from the east in accordance with original bridge plans
2. Span 56 is the small craft navigation span as seen in the contract drawings
3. Girder 5 has considerable damage as shown in Inspection Report

REFERENCES:

1. As - Built Contract Drawings T-3 (224-03) dated December 1977
2. VDOT July 2014 Special Inspection Report for EB South Approach Bridge

Live Load Testing Results	VirginiaTech Invent the Future	Made	JJR	Date	5/26/2016	Job Number	449462
HRBT EASTBOUND STRUCTURE SPAN 56		Checked	EAE	Date	5/31/2016	Connection	
For Hampton Roads Bridge Tunnel		Backchk'd	JJR	Date	5/31/2016	Sheet No.	1

Truck Configuration 4

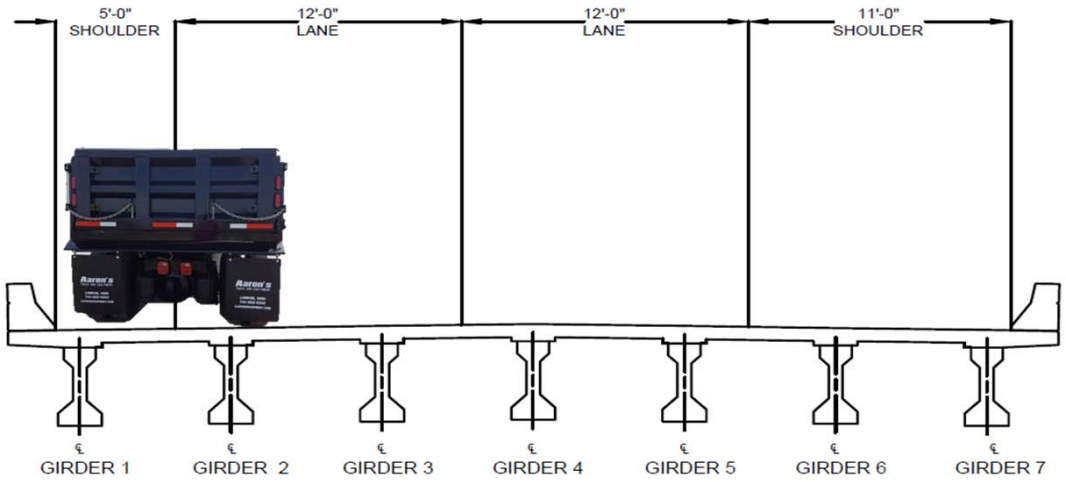

1. Midspan Measurements

		Girder 1	Girder 2	Girder 3	Girder 4	Girder 5	Girder 6	Girder 7
Run 1	Bottom Face of Flange Strain (με) :	27.01	18.30	11.36	10.21	11.19	1.74	0.61
	*Deflection (in.) :	N/A	N/A	N/A	N/A	N/A	N/A	N/A
Run 2	Bottom Face of Flange Strain (με) :	28.99	18.90	11.32	9.79	10.06	1.18	0.27
	*Deflection (in.) :	N/A	N/A	N/A	N/A	N/A	N/A	N/A
Run 3	Bottom Face of Flange Strain (με) :	26.52	18.82	12.10	10.68	12.51	2.38	0.60
	*Deflection (in.) :	N/A	N/A	N/A	N/A	N/A	N/A	N/A

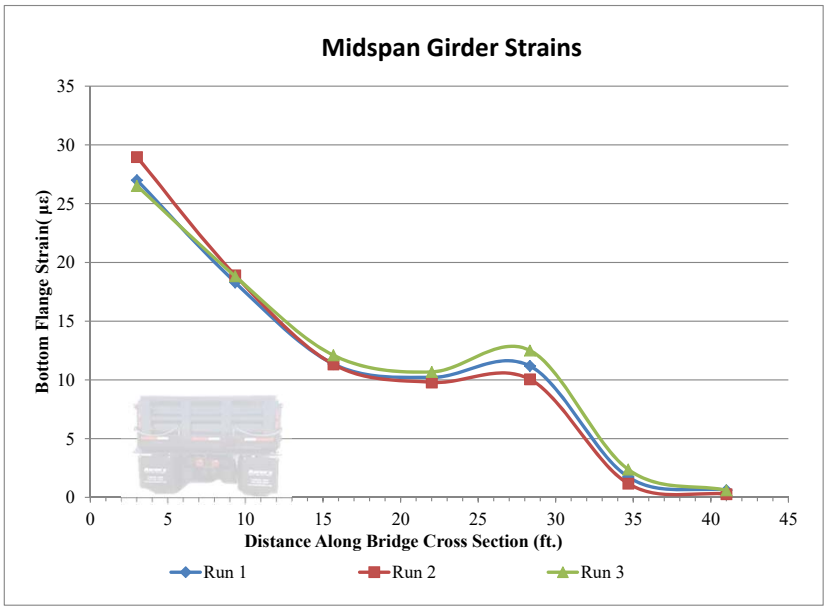

* The deflection values were discarded due to faulty deflection system setup. The cross wire movement prevented the string pots from collecting the full deflection values and leading to softened and inaccurate magnitudes.

NOTES:

1. Girders are numbered from the east in accordance with original bridge plans
2. Span 56 is the small craft navigation span as seen in the contract drawings
3. Girder 5 has considerable damage as shown in Inspection Report
4. Deflection Values were not usable - see report

REFERENCES:

1. As - Built Contract Drawings T-3 (224-03) dated December 1977
2. VDOT July 2014 Special Inspection Report for EB South Approach Bridge

Truck Configuration 4 Continued

2. Girder 5 Strain Distribution at Midspan

	Strain Transducer Readings (με)			
Location	Run 1	Run 2	Run 3	Height (in.)
midheight of top flange	-2.13	-2.10	-2.04	41.5
1" below top of CT web	-0.31	-0.48	-0.45	32.5
1" above bottom of CT web	2.38	1.95	2.54	15.5
Bot. Face of Flange	11.19	10.06	12.51	0

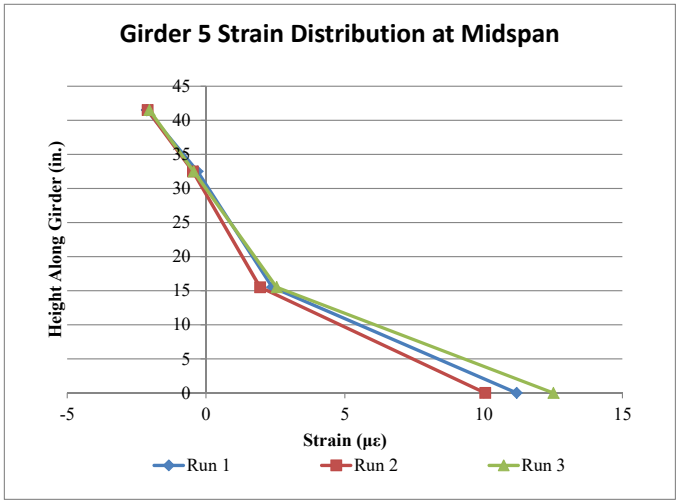

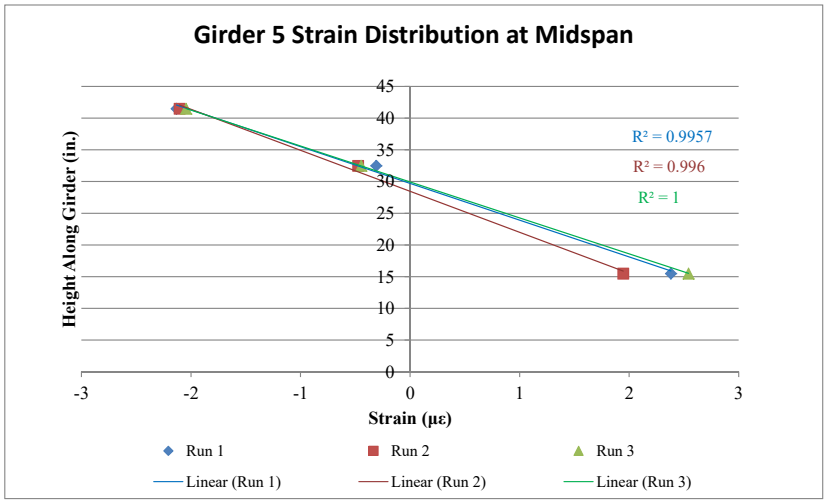

Based on the observed data, there is a bilinear strain distribution caused by the damage to the bottom of the girder flange. The concrete is experiencing much higher strains than it would for an undamaged section. Due to the lack of sound P/S strands, the concrete is forced to carry higher strains.

3. Girder 5 Strain Distribution at ~3L/4

	Strain Transducer Readings (με)			
Location	Run 1	Run 2	Run 3	Height (in.)
**midheight of top flange	-0.05	-0.06	0.02	41.5
1" below top of CT web	-0.43	-0.22	-0.11	32.5
1" above bottom of CT web	1.97	1.87	2.06	15.5
Bot. Face of Flange	4.16	3.66	4.33	0

** Based on the observed data, it is evident that the top flange strain transducer was not adhered to the flange fully. This lead to faulty values.

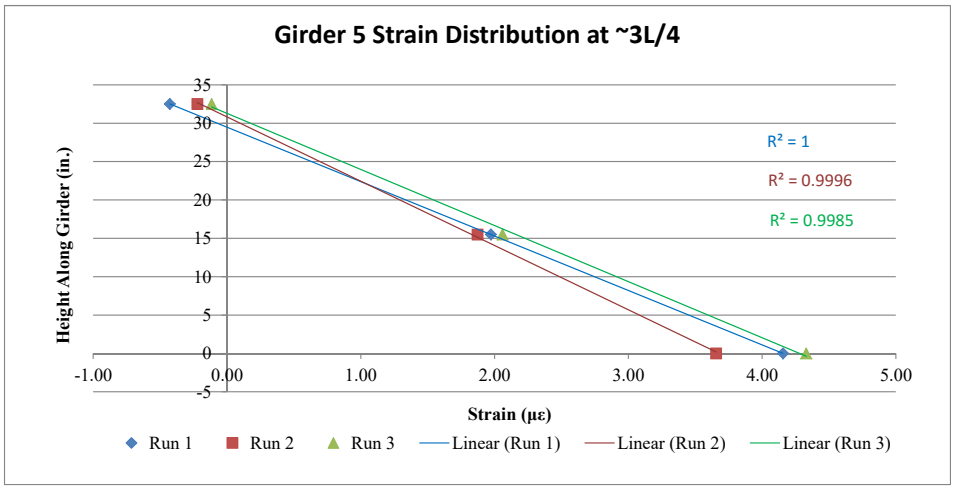

NOTES:

1. Girders are numbered from the east in accordance with original bridge plans
2. Span 56 is the small craft navigation span as seen in the contract drawings
3. Girder 5 has considerable damage as shown in Inspection Report

REFERENCES:

1. As - Built Contract Drawings T-3 (224-03) dated December 1977
2. VDOT July 2014 Special Inspection Report for EB South Approach Bridge

Truck Configuration 4 Continued

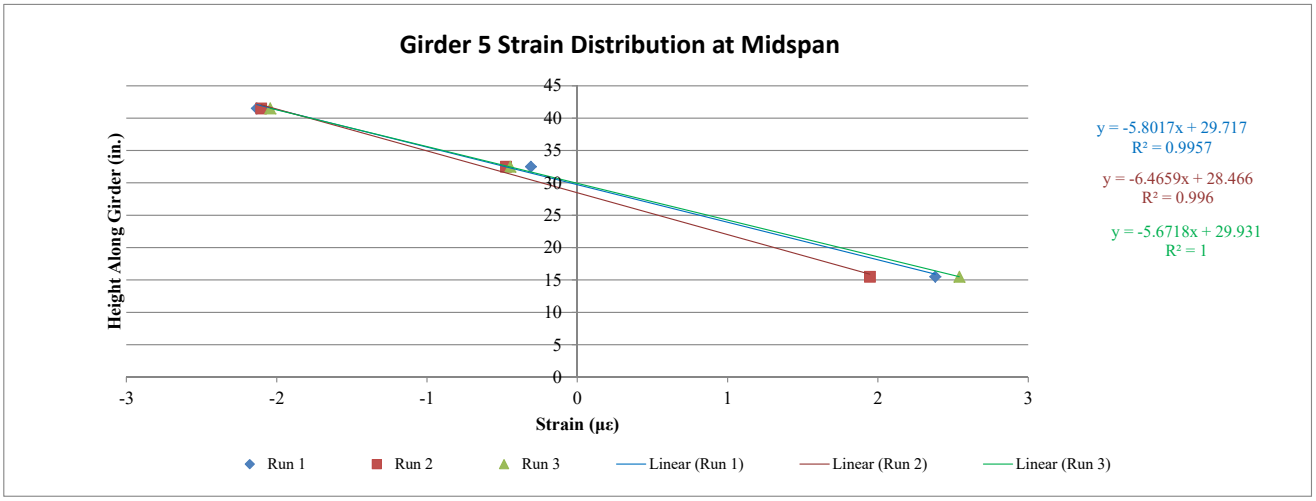

Determine Strain at Bottom Face of Flange Based on Line of Best Fit:

y (height) ***	m	x (strain)	b
0	-5.8017	5.122	29.717
0	-6.4659	4.402	28.466
0	-5.6718	5.277	29.931

*** the "y" height of zero corresponds to the height of the bottom face of the girder flange based on the axis configuration. The undamaged strains at this location are found using the line of best fit equation for a linear strain distribution through the entire height of the girder.

Undamaged Strain Values:

	Girder 1	Girder 2	Girder 3	Girder 4	Girder 5	Girder 6	Girder 7
Run 1	27.01	18.30	11.36	10.21	5.12	1.74	0.61
Run 2	28.99	18.90	11.32	9.79	4.40	1.18	0.27
Run 3	26.52	18.82	12.10	10.68	5.28	2.38	0.60

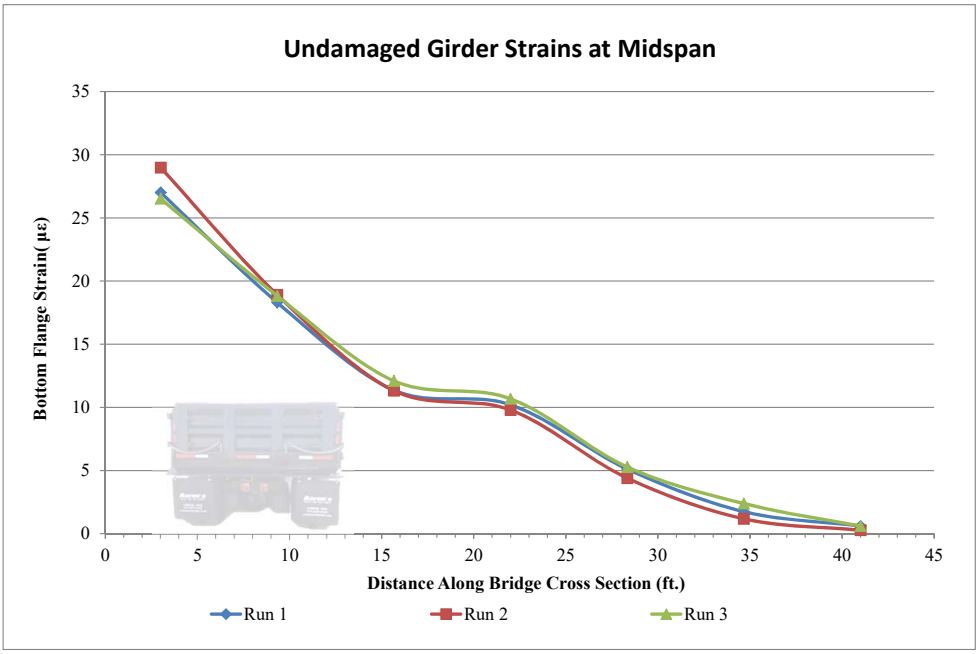

NOTES:

1. Girders are numbered from the east in accordance with original bridge plans
2. Span 56 is the small craft navigation span as seen in the contract drawings
3. Girder 5 has considerable damage as shown in Inspection Report

REFERENCES:

1. As - Built Contract Drawings T-3 (224-03) dated December 1977
2. VDOT July 2014 Special Inspection Report for EB South Approach Bridge

Live Load Testing Results	VirginiaTech Invent the Future	Made	JJR	Date	5/26/2016	Job Number	449462
HRBT EASTBOUND STRUCTURE SPAN 56		Checked	EAE	Date	5/31/2016	Connection	
For Hampton Roads Bridge Tunnel		Backchk'd	JJR	Date	5/31/2016	Sheet No.	1

Truck Configuration 5

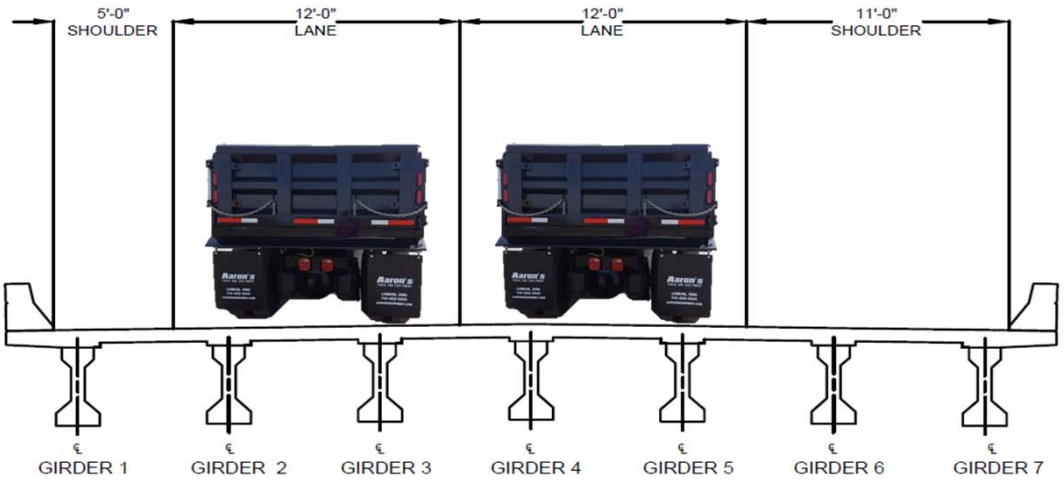

1. Midspan Measurements

		Girder 1	Girder 2	Girder 3	Girder 4	Girder 5	Girder 6	Girder 7
Run 1	Bottom Face of Flange Strain (με) :	21.09	24.06	30.89	50.23	101.51	23.32	13.57
	*Deflection (in.) :	N/A	N/A	N/A	N/A	N/A	N/A	N/A
Run 2	Bottom Face of Flange Strain (με) :	19.37	23.51	31.52	51.56	102.19	23.77	13.93
	*Deflection (in.) :	N/A	N/A	N/A	N/A	N/A	N/A	N/A
Run 3	Bottom Face of Flange Strain (με) :	20.25	23.90	31.72	51.77	101.24	23.01	13.01
	*Deflection (in.) :	N/A	N/A	N/A	N/A	N/A	N/A	N/A

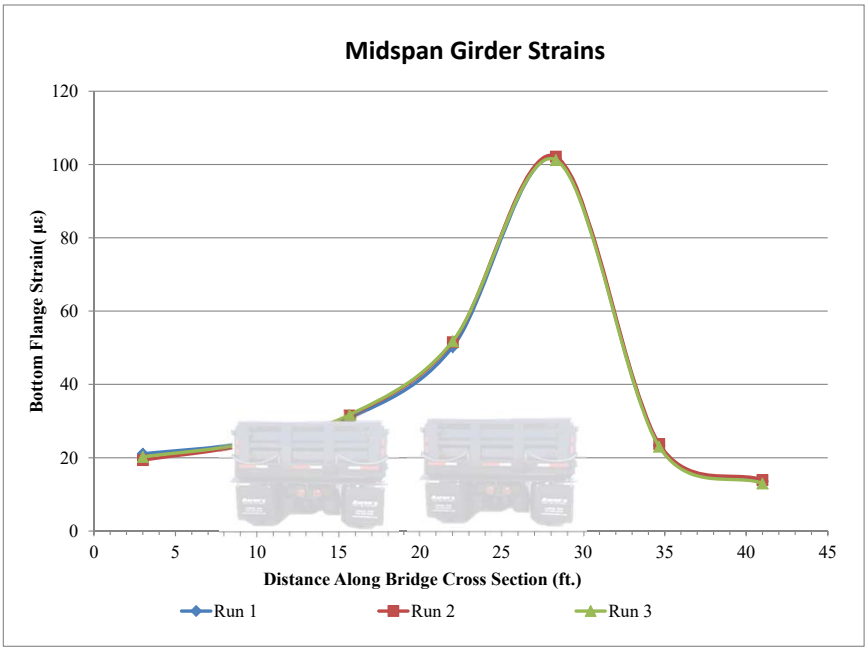

* The deflection values were discarded due to faulty deflection system setup. The cross wire movement prevented the string pots from collecting the full deflection values and leading to softened and inaccurate magnitudes.

NOTES:

1. Girders are numbered from the east in accordance with original bridge plans
2. Span 56 is the small craft navigation span as seen in the contract drawings
3. Girder 5 has considerable damage as shown in Inspection Report
4. Deflection Values were not useful - see report

REFERENCES:

1. As - Built Contract Drawings T-3 (224-03) dated December 1977
2. VDOT July 2014 Special Inspection Report for EB South Approach Bridge

Truck Configuration 5 Continued

2. Girder 5 Strain Distribution at Midspan

	Strain Transducer Readings (με)			
Location	Run 1	Run 2	Run 3	Height (in.)
midheight of top flange	-6.78	-7.23	-6.85	41.5
1" below top of CT web	4.98	3.83	4.60	32.5
1" above bottom of CT web	22.13	21.99	22.15	15.5
Bot. Face of Flange	101.51	102.19	101.24	0

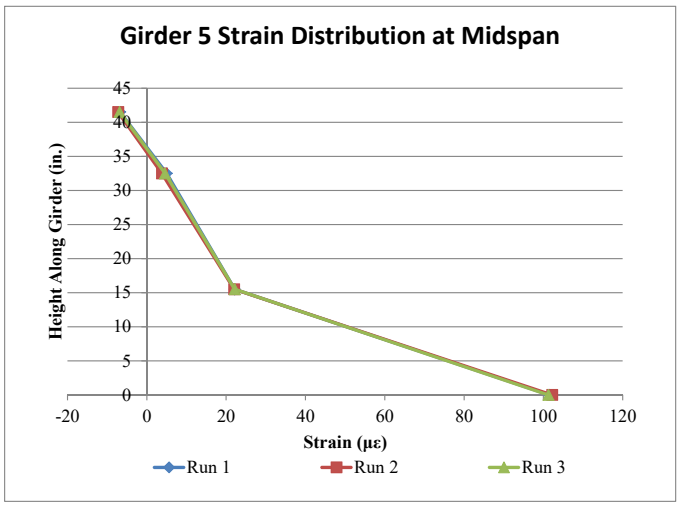

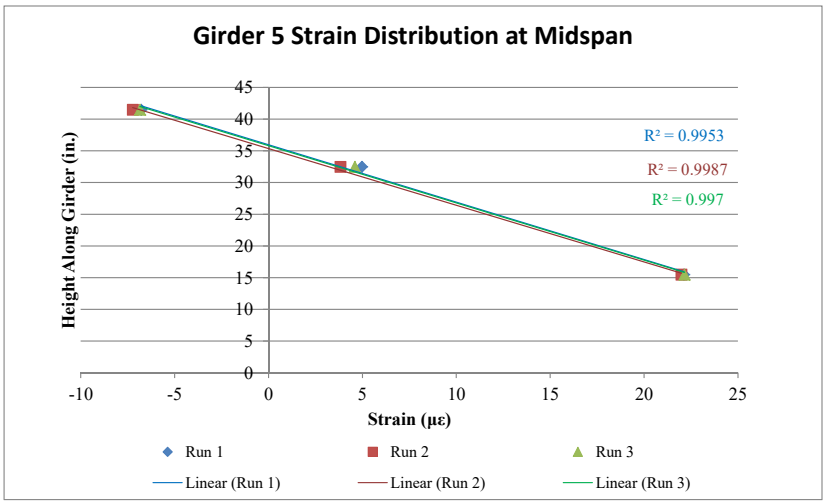

Based on the observed data, there is a bilinear strain distribution caused by the damage to the bottom of the girder flange. The concrete is experiencing much higher strains than it would for an undamaged section. Due to the lack of sound P/S strands, the concrete is forced to carry higher strains.

3. Girder 5 Strain Distribution at ~3L/4

	Strain Transducer Readings (με)			
Location	Run 1	Run 2	Run 3	Height (in.)
**midheight of top flange	-0.01	-0.03	0.01	41.5
1" below top of CT web	3.88	3.66	3.87	32.5
1" above bottom of CT web	17.67	17.55	17.55	15.5
Bot. Face of Flange	31.18	30.61	30.21	0

** Based on the observed data, it is evident that the top flange strain transducer was not adhered to the flange fully. This lead to faulty values.

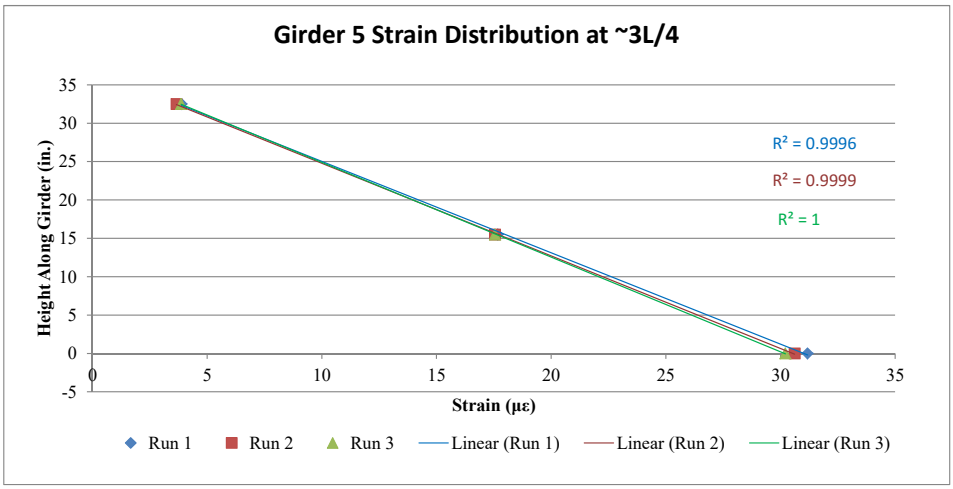

NOTES:

1. Girders are numbered from the east in accordance with original bridge plans
2. Span 56 is the small craft navigation span as seen in the contract drawings
3. Girder 5 has considerable damage as shown in Inspection Report

REFERENCES:

1. As - Built Contract Drawings T-3 (224-03) dated December 1977
2. VDOT July 2014 Special Inspection Report for EB South Approach Bridge

Truck Configuration 5 Continued

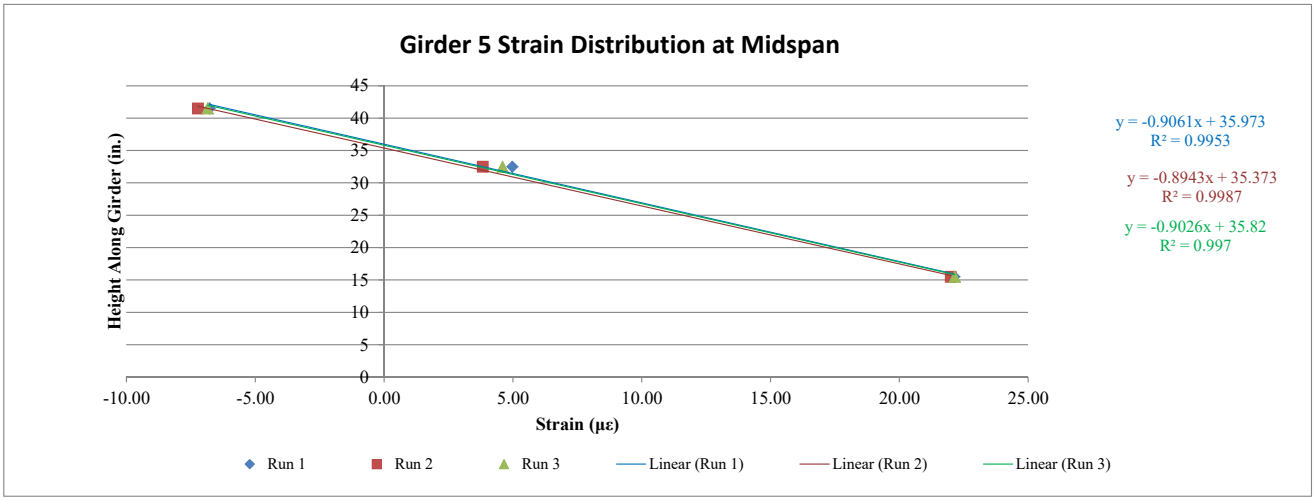

Determine Strain at Bottom Face of Flange Based on Line of Best Fit:

y (height) ***	m	x (strain)	b
0	-0.9061	39.701	35.973
0	-0.8943	39.554	35.373
0	-0.9026	39.685	35.82

*** the "y" height of zero corresponds to the height of the bottom face of the girder flange based on the axis configuration. The undamaged strains at this location are found using the line of best fit equation for a linear strain distribution through the entire height of the girder.

Undamaged Strain Values at Bottom Face of Flange:

	Girder 1	Girder 2	Girder 3	Girder 4	Girder 5	Girder 6	Girder 7
Run 1	21.09	24.06	30.89	50.23	39.70	23.32	13.57
Run 2	19.37	23.51	31.52	51.56	39.55	23.77	13.93
Run 3	20.25	23.90	31.72	51.77	39.69	23.01	13.01

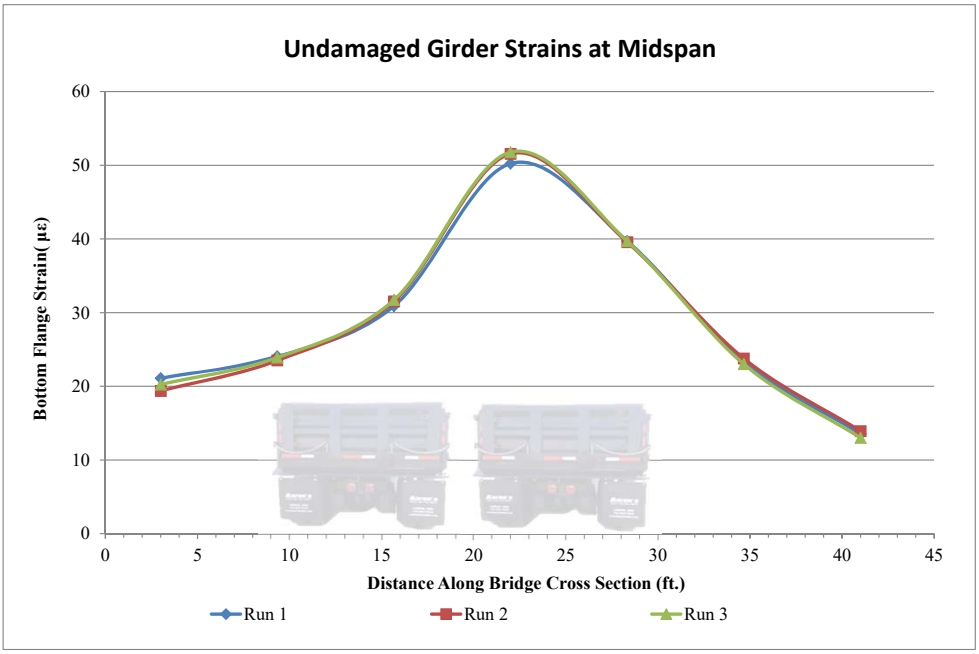

NOTES:

1. Girders are numbered from the east in accordance with original bridge plans
2. Span 56 is the small craft navigation span as seen in the contract drawings
3. Girder 5 has considerable damage as shown in Inspection Report

REFERENCES:

1. As - Built Contract Drawings T-3 (224-03) dated December 1977
2. VDOT July 2014 Special Inspection Report for EB South Approach Bridge

APPENDIX C-2:

EASTBOUND SPAN 57

Live Load Testing Results HRBT EASTBOUND STRUCTURE SPAN 57 For Hampton Roads Bridge Tunnel		Made AB	Date 7/30/2016	Job Number XXXXX
		Checked	Date	Connection
		Backchk'd	Date	Sheet No. 1

Truck Configuration 1

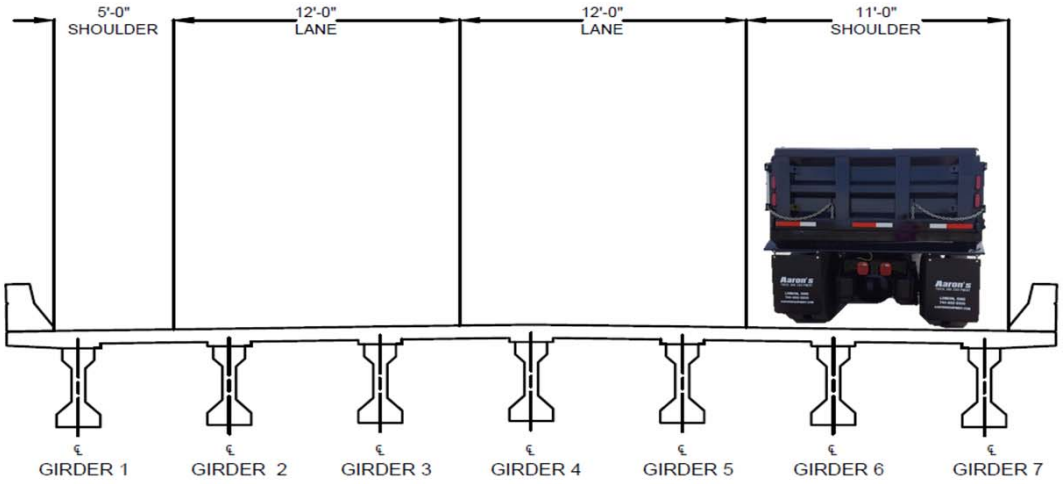

1. Midspan Measurements

		Girder 1	Girder 2	Girder 3	Girder 4	Girder 5	Girder 6	Girder 7
Run 1	Bottom Face of Flange Strain (με) :	-0.21	2.12	2.96	5.44	10.47	19.94	26.49
	Deflection (in.) :	0.01	-0.01	-0.02	-0.04	-0.05	-0.06	-0.07
Run 2	Bottom Face of Flange Strain (με) :	-0.73	1.53	2.85	5.50	10.66	19.65	25.26
	Deflection (in.) :	-	-0.02	-0.03	-0.04	-0.05	-0.07	-0.08
Run 3	Bottom Face of Flange Strain (με) :	-0.95	1.23	2.73	5.20	10.25	19.74	26.18
	Deflection (in.) :	-	-0.01	-0.02	-0.04	-0.05	-0.07	-0.08

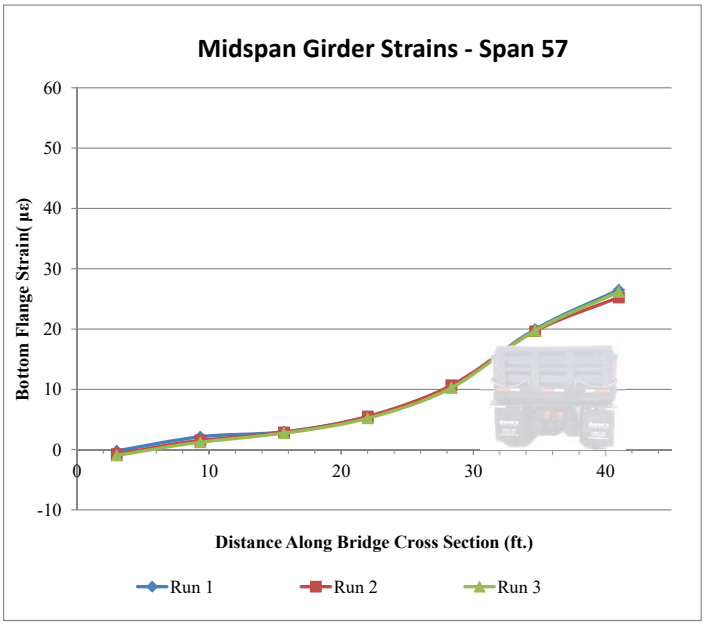

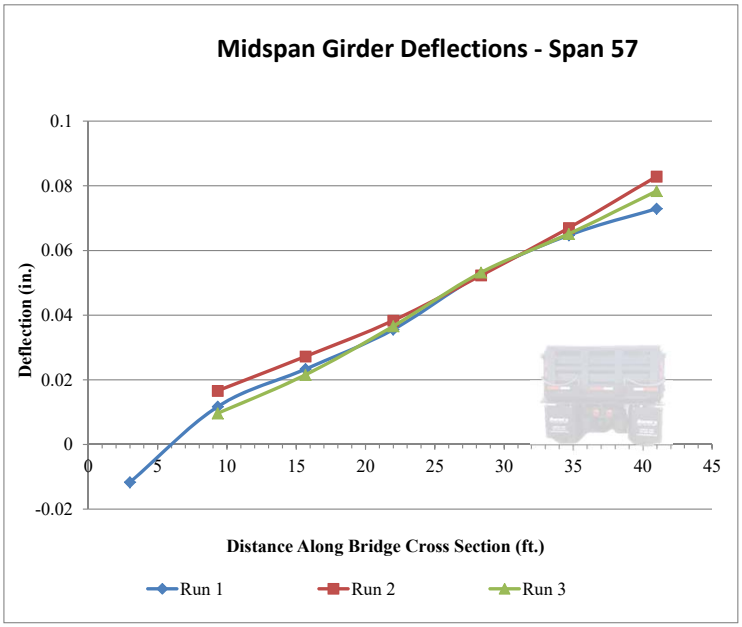

Note: The midspan deflection of Girder 1 was not captured for Runs 2 and 3 due to low quality (excessively dark) images aquired during testing.

NOTES:

1. Girders are numbered from the east in accordance with original bridge plans.
2. Deflection values were measured using the digital image correlation method.

REFERENCES:

1. As - Built Contract Drawings T-3 (224-03) dated December 1977
2. VDOT July 2014 Special Inspection Report for EB South Approach Bridge

Truck Configuration 1 Continued

2. Girder 5 Strain Distribution at Midspan

	Strain Transducer Readings (με)			
Location	Run 1	Run 2	Run 3	Height (in.)
midheight of top flange	-3.30	-3.45	-3.57	41.5
1" below top of CT web	0.77	0.34	0.23	32.5
1" above bottom of CT web	7.43	7.22	6.63	15.5
Bot. Face of Flange	10.47	10.66	10.25	0

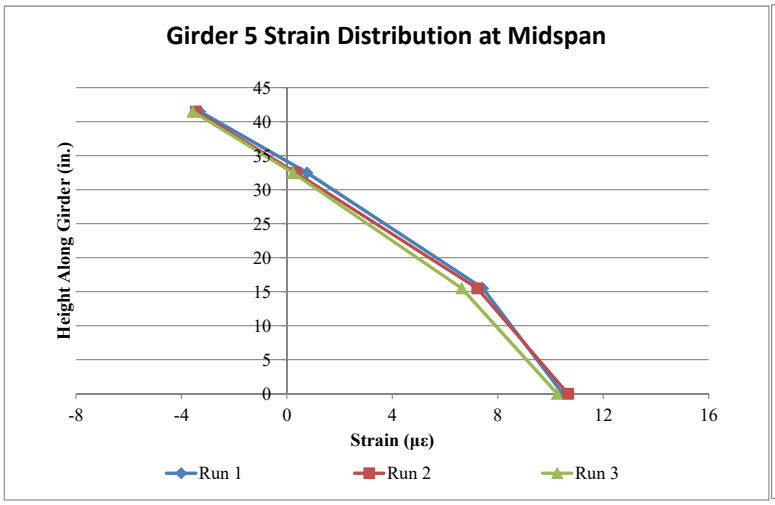

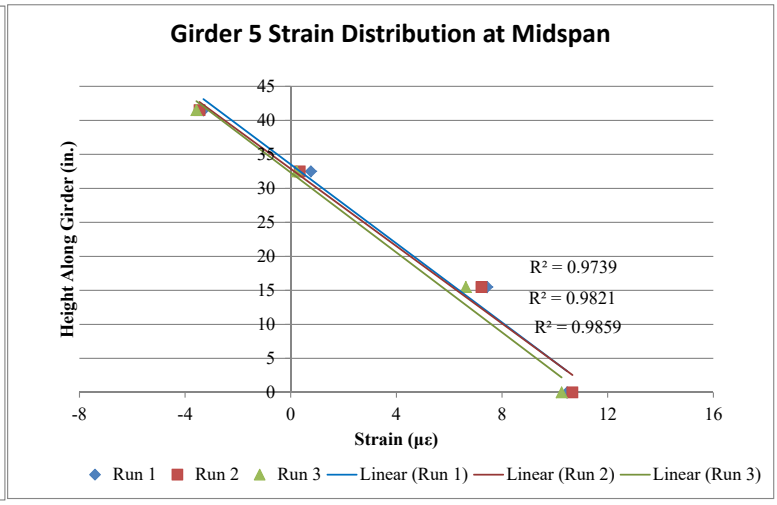

3. Girder 5 Strain Distribution at ~3L/4

	Strain Transducer Readings (με)			
Location	Run 1	Run 2	Run 3	Height (in.)
midheight of top flange	-3.05	-3.68	-3.82	41.5
1" below top of CT web	0.89	-0.23	-0.13	32.5
1" above bottom of CT web	6.02	5.64	5.25	15.5
Bot. Face of Flange	12.76	12.44	11.54	0

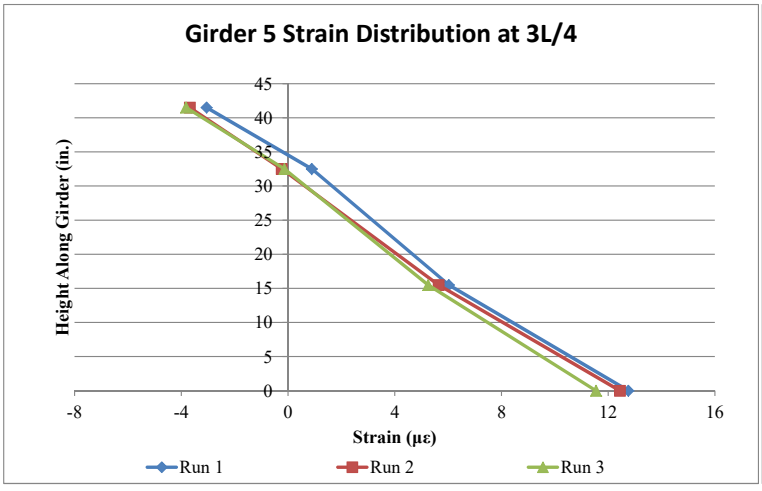

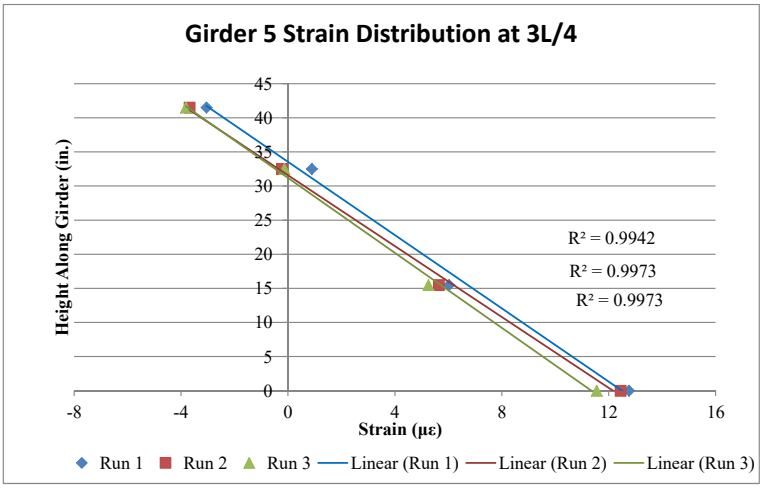

NOTES:

1. Girders are numbered from the east in accordance with original bridge plans.
2. Deflection values were measured using the digital image correlation method.

REFERENCES:

1. As - Built Contract Drawings T-3 (224-03) dated December 1977
2. VDOT July 2014 Special Inspection Report for EB South Approach Bridge

Live Load Testing Results HRBT EASTBOUND STRUCTURE SPAN 57 For Hampton Roads Bridge Tunnel	UNIVERSITY of VIRGINIA SCHOOL OF ENGINEERING	Made AB	Date 7/30/2016	Job Number XXXXX
		Checked	Date	Connection
		Backchk'd	Date	Sheet No. 1

Truck Configuration 2

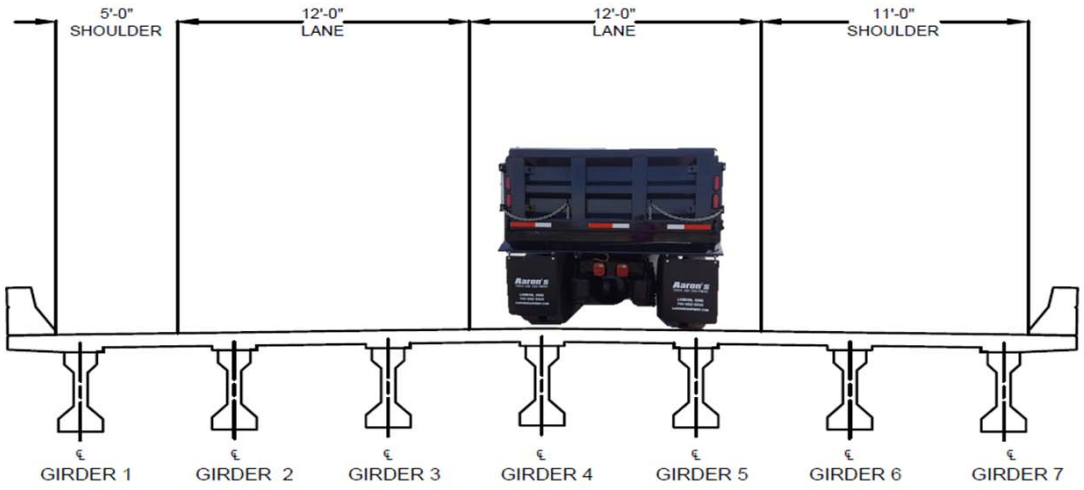

1. Midspan Measurements

		Girder 1	* Girder 2	Girder 3	Girder 4	Girder 5	Girder 6	Girder 7
Run 1	Bottom Face of Flange Strain (με) :	3.18	7.70	8.22	14.94	17.06	10.76	8.67
	Deflection (in.) :	-	-0.03	-0.04	-0.06	-0.06	-0.04	-0.03
Run 2	Bottom Face of Flange Strain (με) :	3.51	7.88	8.67	15.71	16.83	10.03	8.12
	Deflection (in.) :	-	-0.03	-0.05	-0.06	-0.06	-0.05	-0.03
Run 3	Bottom Face of Flange Strain (με) :	3.95	8.54	9.29	15.70	16.86	10.15	8.17
	Deflection (in.) :	-	-	-0.05	-0.06	-0.06	-0.04	-0.03

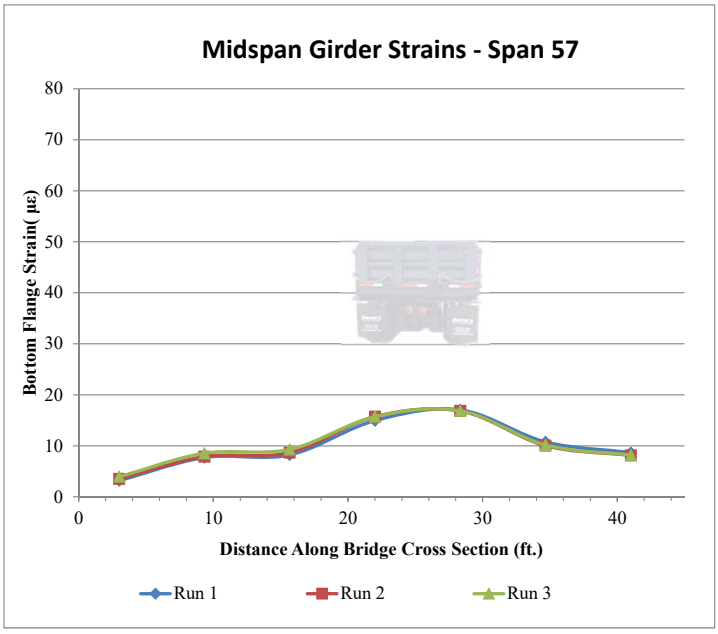

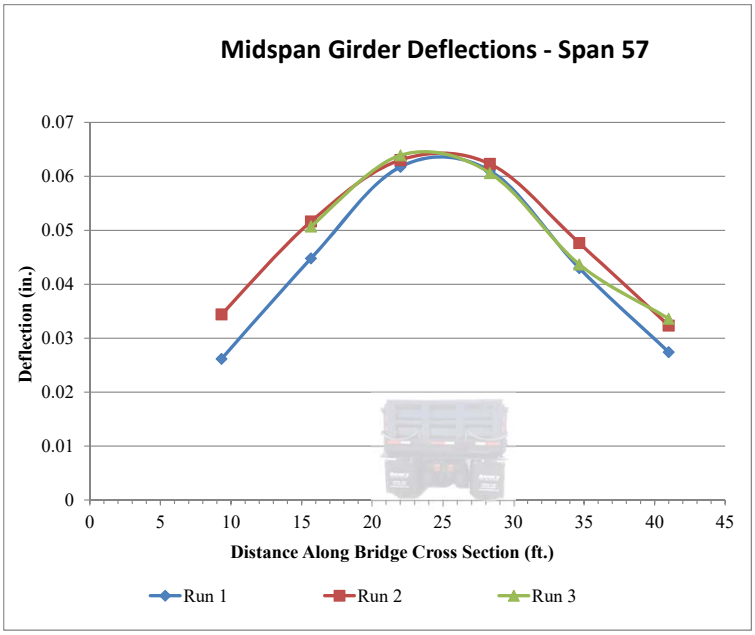

Note: No signs of obvious damage were present in Girder 2, but the peak response (or response not decreasing at a proportional rate for this load case) may be indicative of potential damage that is not observable.

Note: The midspan deflection of Girder 1 was not captured in any of the Runs (1-3) and for Girder 2 in Run 3 due to low quality (excessively dark) images aquired during testing.

NOTES:

1. Girders are numbered from the east in accordance with original bridge plans
2. Deflection values were measured using the digital image correlation method.

REFERENCES:

1. As - Built Contract Drawings T-3 (224-03) dated December 1977
2. VDOT July 2014 Special Inspection Report for EB South Approach Bridge

Truck Configuration 2 Continued

2. Girder 5 Strain Distribution at Midspan

	Strain Transducer Readings (με)			
Location	Run 1	Run 2	Run 3	Height (in.)
midheight of top flange	-4.28	-4.12	-3.78	41.5
1" below top of CT web	1.90	1.78	2.27	32.5
1" above bottom of CT web	13.00	12.94	13.05	15.5
Bot. Face of Flange	17.06	16.83	16.86	0

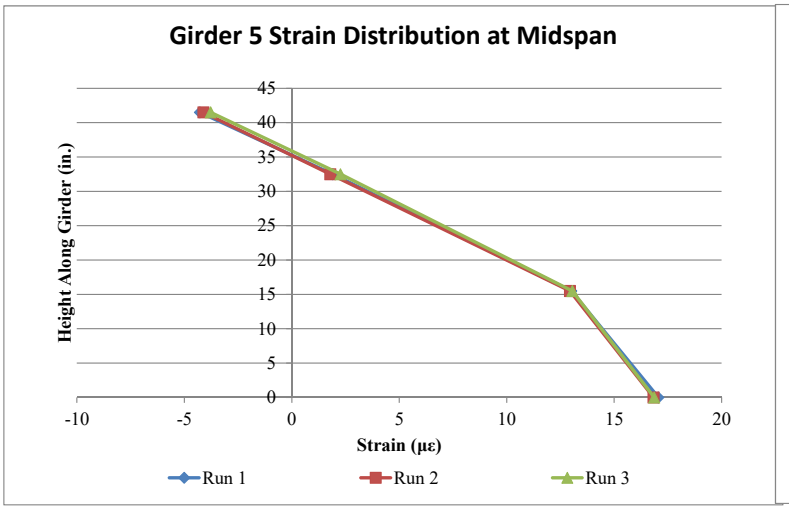

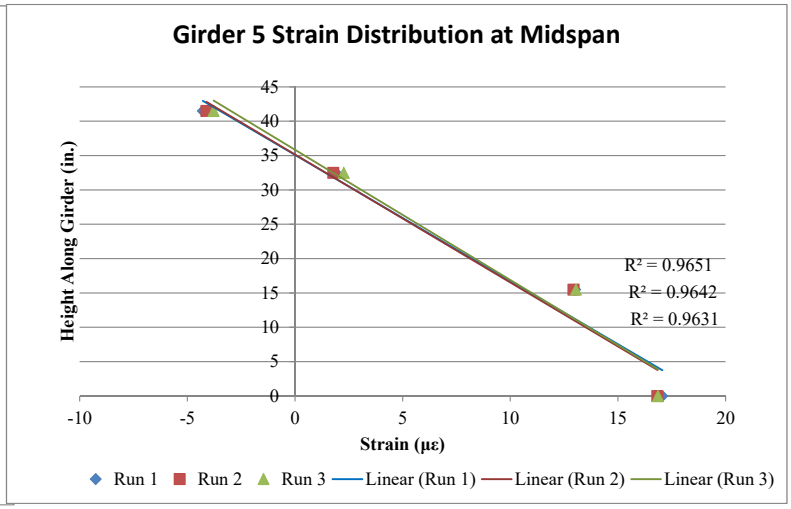

3. Girder 5 Strain Distribution at ~3L/4

	Strain Transducer Readings (με)			
Location	Run 1	Run 2	Run 3	Height (in.)
midheight of top flange	-3.80	-3.30	-2.57	41.5
1" below top of CT web	1.68	2.06	3.01	32.5
1" above bottom of CT web	10.22	10.54	11.07	15.5
Bot. Face of Flange	19.68	18.97	18.86	0

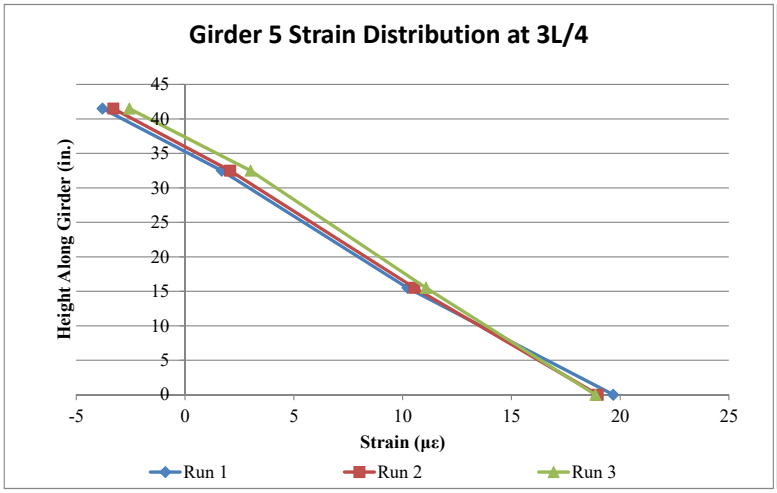

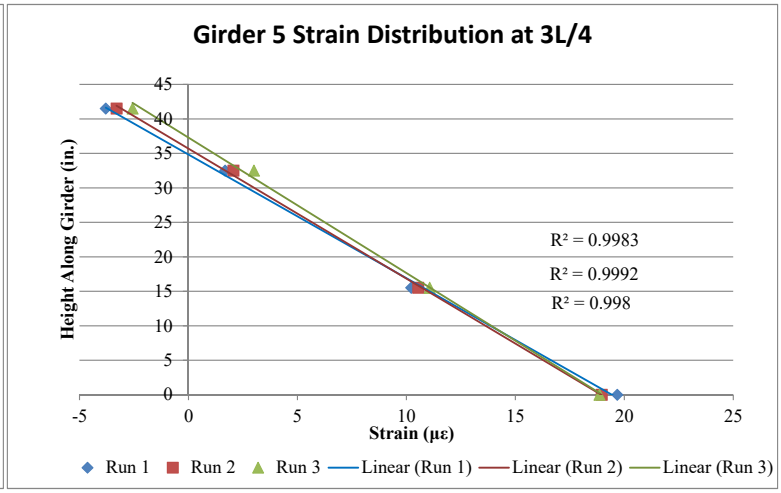

NOTES:

1. Girders are numbered from the east in accordance with original bridge plans
2. Deflection values were measured using the digital image correlation method.

REFERENCES:

1. As - Built Contract Drawings T-3 (224-03) dated December 1977
2. VDOT July 2014 Special Inspection Report for EB South Approach Bridge

Live Load Testing Results HRBT EASTBOUND STRUCTURE SPAN 57 For Hampton Roads Bridge Tunnel	UNIVERSITY of VIRGINIA SCHOOL OF ENGINEERING	Made AB	Date 7/30/2016	Job Number XXXXX
		Checked	Date	Connection
		Backchk'd	Date	Sheet No. 1

Truck Configuration 3

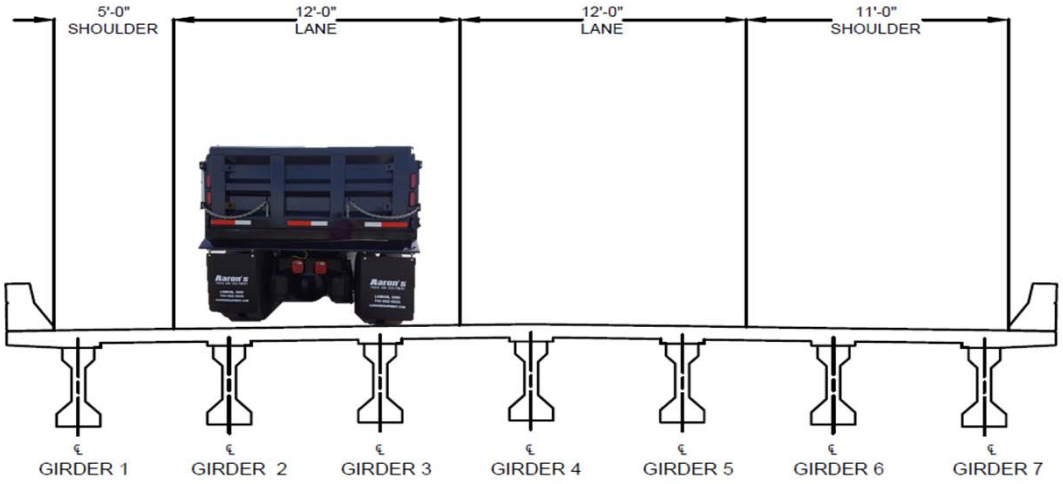

1. Midspan Measurements

		Girder 1	Girder 2	Girder 3	Girder 4	Girder 5	Girder 6	Girder 7
Run 1	Bottom Face of Flange Strain (με) :	16.38	25.79	16.79	9.89	6.33	3.53	1.57
	Deflection (in.) :	-0.05	-0.07	-0.07	-0.06	-0.04	-0.03	-0.01
Run 2	Bottom Face of Flange Strain (με) :	17.73	26.51	16.43	8.87	5.62	3.23	1.07
	Deflection (in.) :	-	-0.07	-0.06	-0.05	-0.03	-0.02	-0.01
Run 3	Bottom Face of Flange Strain (με) :	17.24	26.76	16.48	9.40	6.21	3.54	1.23
	Deflection (in.) :	-	-	-0.06	-0.05	-0.04	-0.03	-0.02

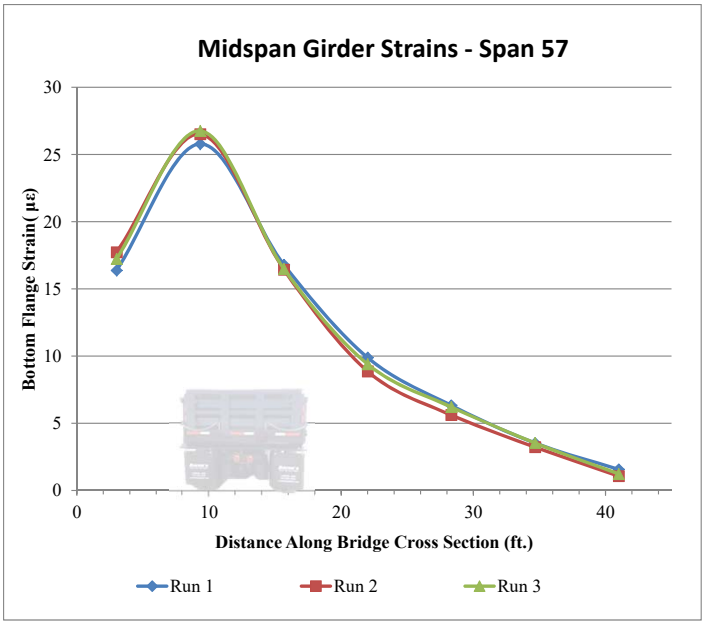

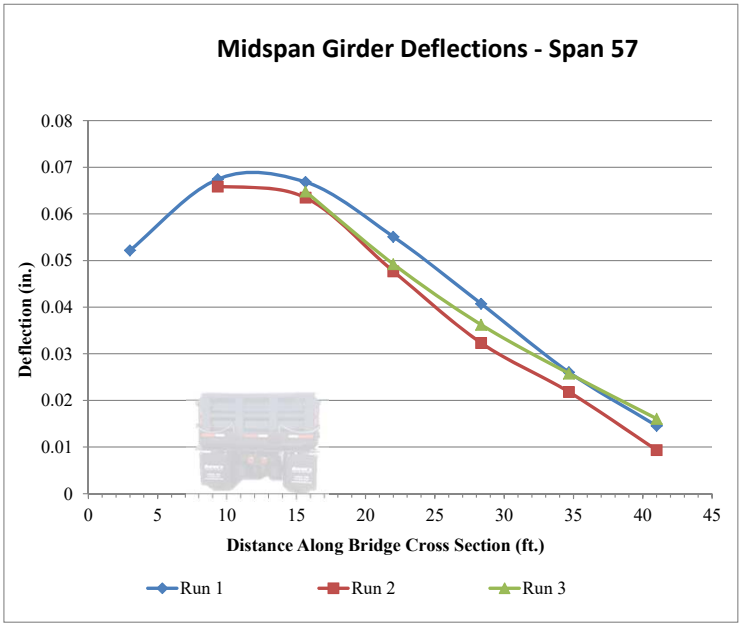

Note: No signs of obvious damage were present in Girder 2, but the peak response may be indicative of potential damage that is not observable.

Note: The midspan deflection of Girder 1 was not captured in any of the Runs (1-3) and for Girder 2 in Run 3 due to low quality (excessively dark) images aquired during testing.

NOTES:

1. Girders are numbered from the east in accordance with original bridge plans
2. Deflection values were measured using the digital image correlation method.

REFERENCES:

1. As - Built Contract Drawings T-3 (224-03) dated December 1977
2. VDOT July 2014 Special Inspection Report for EB South Approach Bridge

Truck Configuration 3 Continued

2. Girder 5 Strain Distribution at Midspan

	Strain Transducer Readings (με)			
Location	Run 1	Run 2	Run 3	Height (in.)
midheight of top flange	-1.57	-1.80	-1.78	41.5
1" below top of CT web	0.74	0.36	0.57	32.5
1" above bottom of CT web	5.44	4.39	4.81	15.5
* Bot. Face of Flange	6.33	5.62	6.21	0

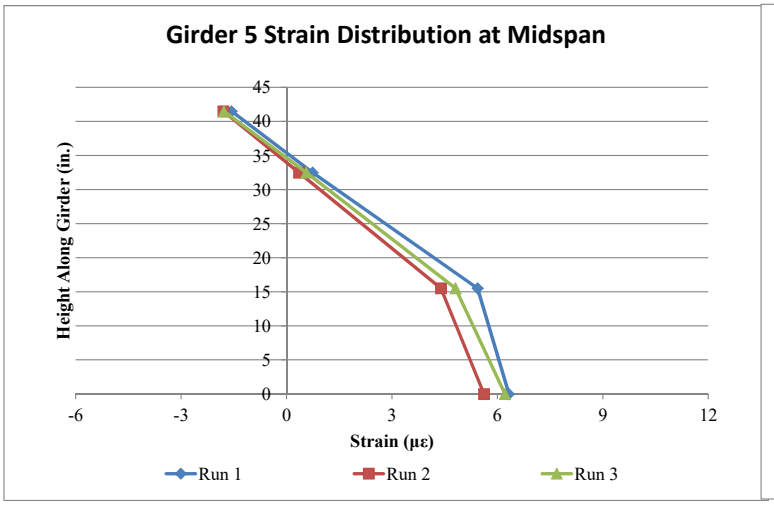

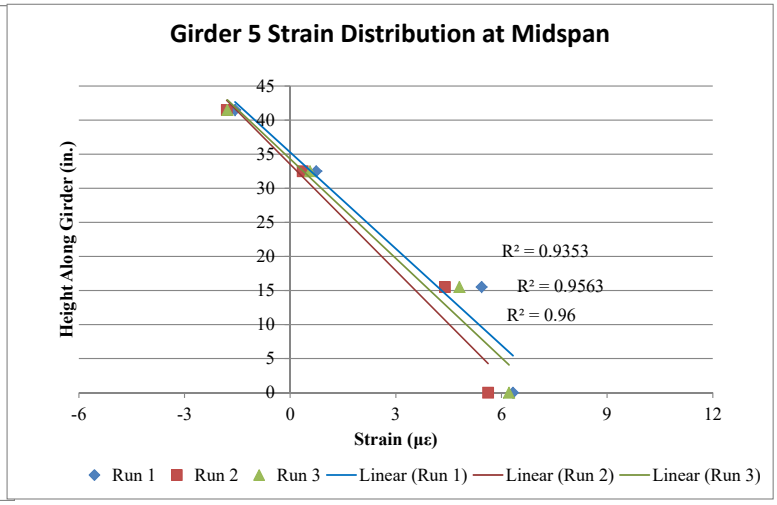

* Based on the observed data, there is not a linear strain distribution at the low level of strains.The concrete is experiencing lower strains , and strands are forced to carry more strains.

3. Girder 5 Strain Distribution at ~3L/4

	Strain Transducer Readings (με)			
Location	Run 1	Run 2	Run 3	Height (in.)
midheight of top flange	-1.83	-1.95	-1.80	41.5
1" below top of CT web	0.38	0.01	0.42	32.5
1" above bottom of CT web	4.44	3.76	4.32	15.5
Bot. Face of Flange	8.03	7.02	7.94	0

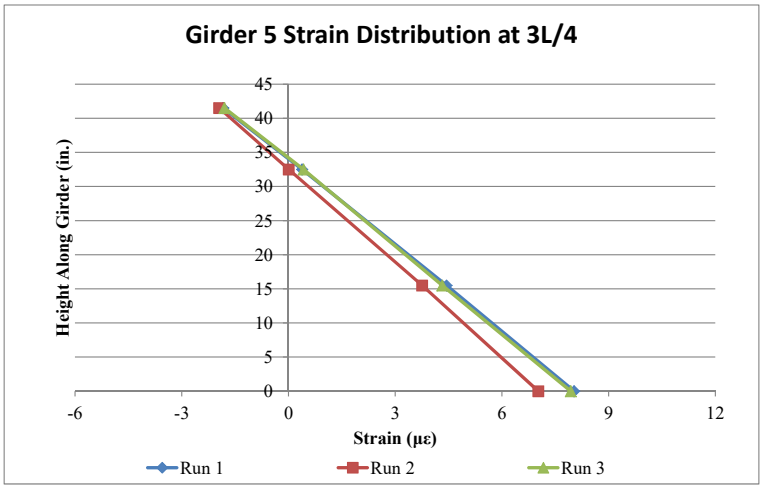

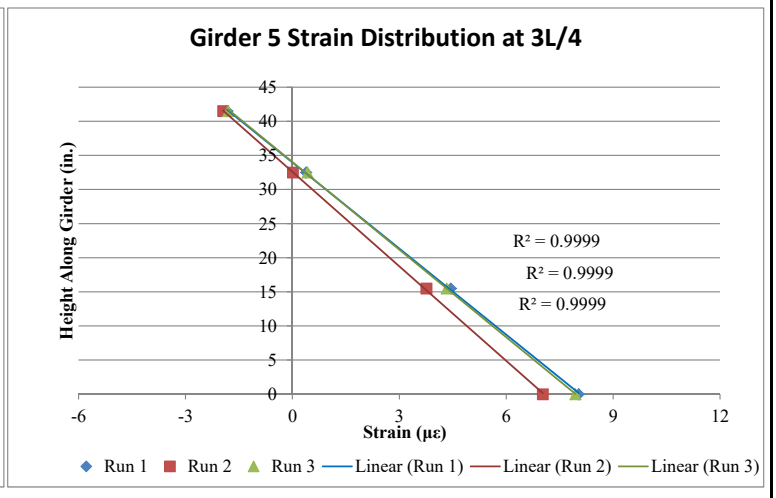

NOTES:

1. Girders are numbered from the east in accordance with original bridge plans
2. Deflection values were measured using the digital image correlation method.

REFERENCES:

1. As - Built Contract Drawings T-3 (224-03) dated December 1977
2. VDOT July 2014 Special Inspection Report for EB South Approach Bridge

Live Load Testing Results HRBT EASTBOUND STRUCTURE SPAN 57 For Hampton Roads Bridge Tunnel	UNIVERSITY of VIRGINIA SCHOOL OF ENGINEERING	Made AB	Date 7/30/2016	Job Number XXXXX
		Checked	Date	Connection
		Backchk'd	Date	Sheet No. 1

Truck Configuration 4

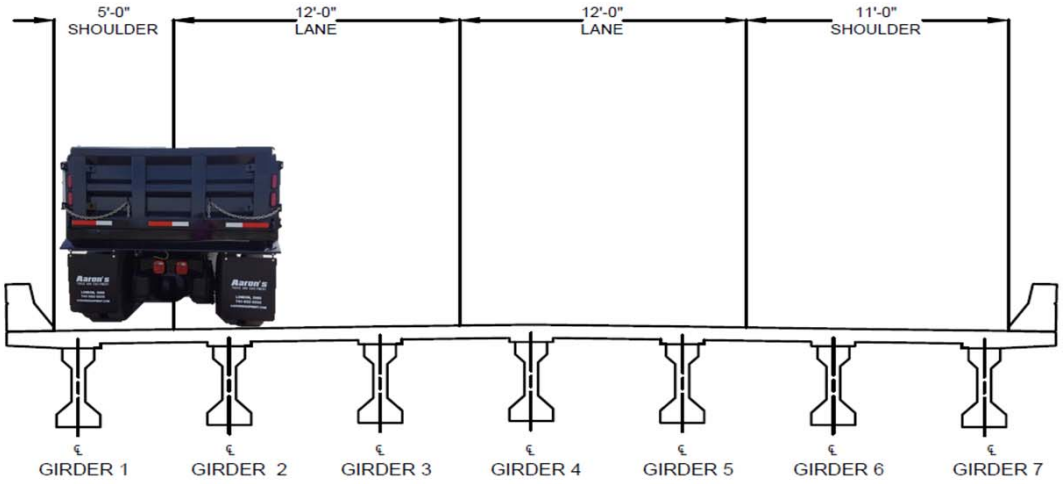

1. Midspan Measurements

		Girder 1	Girder 2	Girder 3	Girder 4	Girder 5	Girder 6	Girder 7
Run 1	Bottom Face of Flange Strain (με) :	34.02	30.22	10.44	5.83	3.03	1.30	-0.40
	Deflection (in.) :	-0.07	-0.07	-0.05	-0.04	-0.02	-0.01	0.00
Run 2	Bottom Face of Flange Strain (με) :	33.06	29.27	10.29	5.95	3.39	1.32	-0.52
	Deflection (in.) :	-	-0.07	-0.05	-0.03	-0.02	-0.01	0.00
Run 3	Bottom Face of Flange Strain (με) :	32.10	29.73	10.85	5.96	2.92	1.35	-0.38
	Deflection (in.) :	-	-	-0.05	-0.04	-0.03	-0.01	-0.01

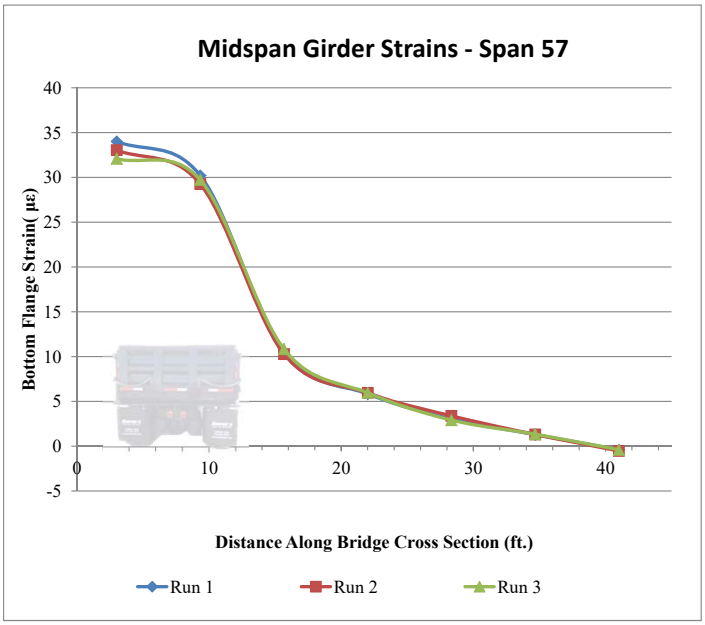

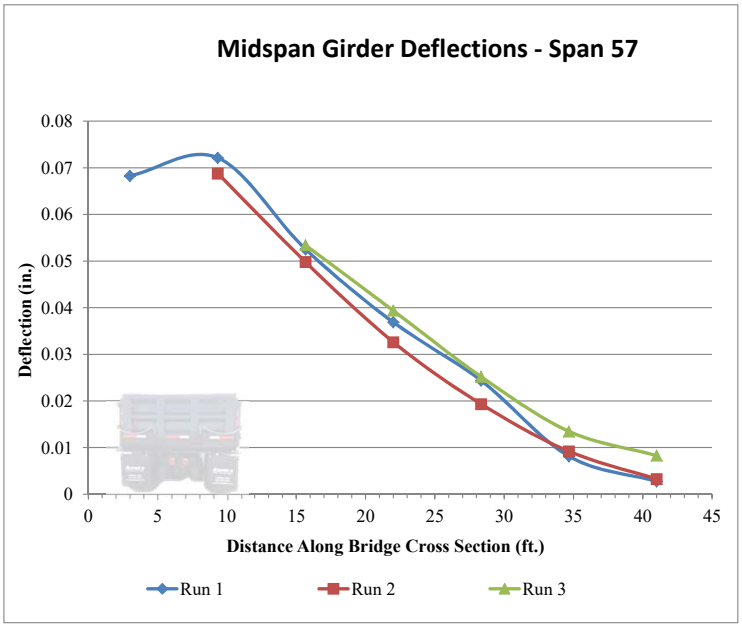

Note: No signs of obvious damage were present in Girder 2, but the peak response (or response not decreasing at a proportional rate for this load case) may be indicative of potential damage that is not observable.

Note: The midspan deflection of Girder 1 was not captured in any of the Runs (1-3) and for Girder 2 in Run 3 due to low quality (excessively dark) images aquired during testing.

NOTES:

1. Girders are numbered from the east in accordance with original bridge plans
2. Deflection values were measured using the digital image correlation method.

REFERENCES:

1. As - Built Contract Drawings T-3 (224-03) dated December 1977
2. VDOT July 2014 Special Inspection Report for EB South Approach Bridge

Truck Configuration 4 Continued

2. Girder 5 Strain Distribution at Midspan

	Strain Transducer Readings (με)			
Location	Run 1	Run 2	Run 3	Height (in.)
midheight of top flange	-1.09	-1.11	-1.47	41.5
1" below top of CT web	0.16	-0.02	-0.17	32.5
1" above bottom of CT web	2.41	2.36	2.41	15.5
* Bot. Face of Flange	3.03	3.39	2.92	0

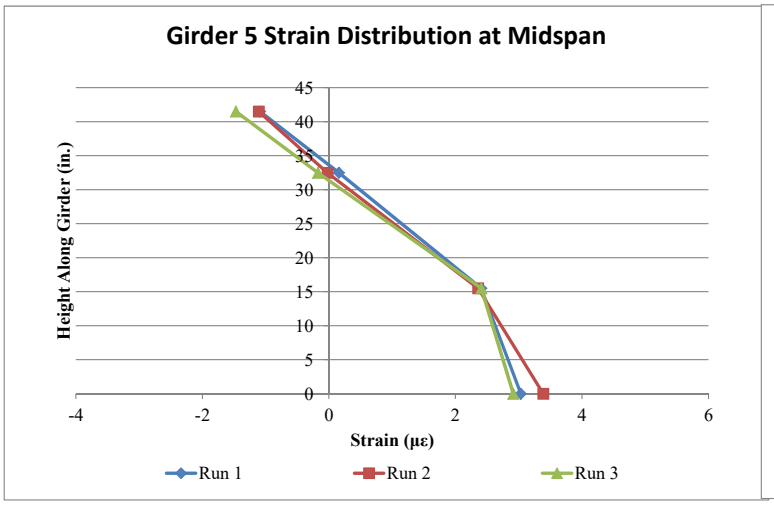

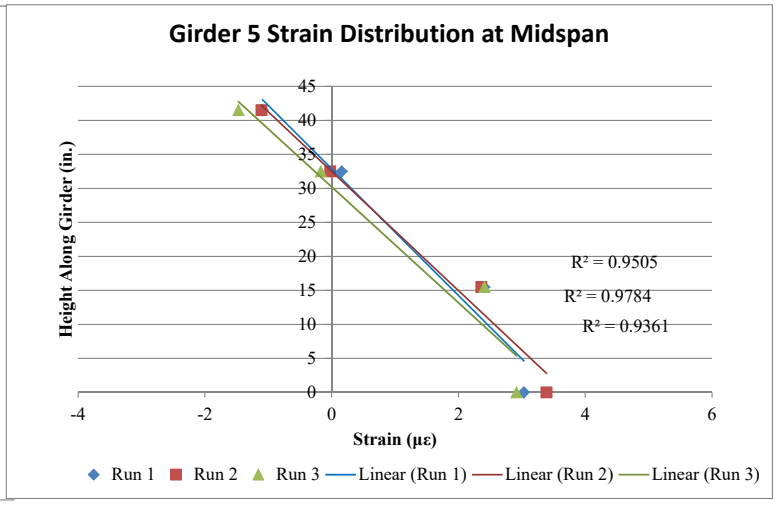

* Based on the observed data, there is not a linear strain distribution at the low level of strains.The concrete is experiencing lower strains , and strands are forced to carry more strains.

3. Girder 5 Strain Distribution at ~3L/4

	Strain Transducer Readings (με)			
Location	Run 1	Run 2	Run 3	Height (in.)
midheight of top flange	-1.57	-1.60	-1.59	41.5
1" below top of CT web	-0.18	-0.31	-0.25	32.5
1" above bottom of CT web	2.17	2.20	2.29	15.5
Bot. Face of Flange	4.03	4.05	3.88	0

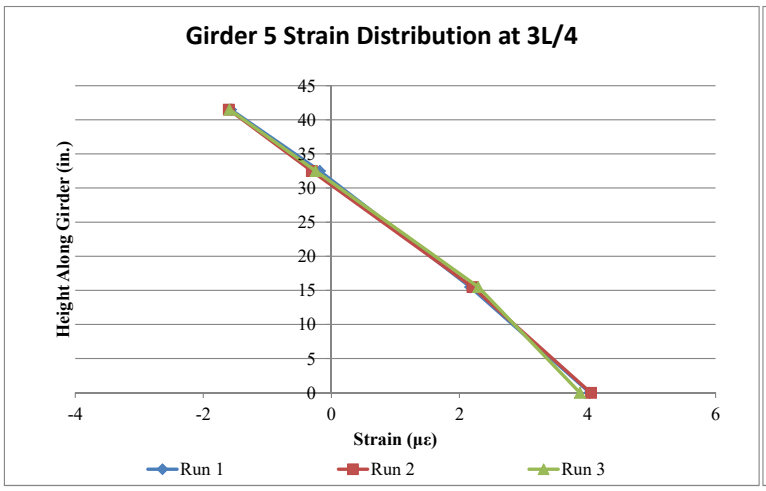

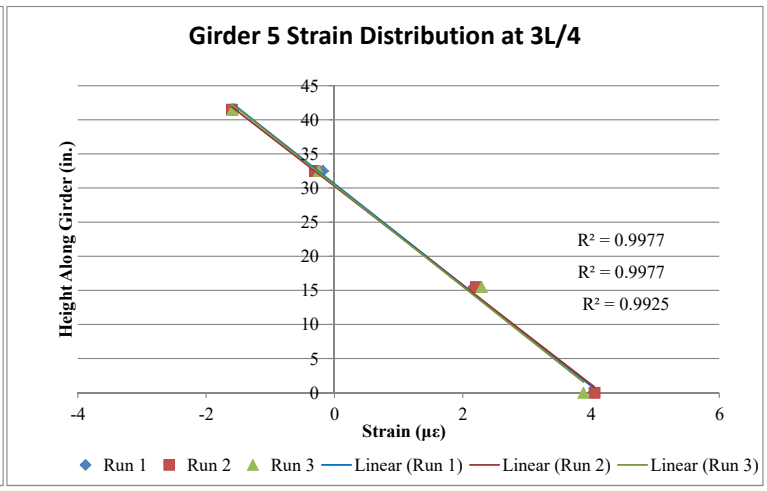

NOTES:

1. Girders are numbered from the east in accordance with original bridge plans
2. Deflection values were measured using the digital image correlation method.

REFERENCES:

1. As - Built Contract Drawings T-3 (224-03) dated December 1977
2. VDOT July 2014 Special Inspection Report for EB South Approach Bridge

Live Load Testing Results HRBT EASTBOUND STRUCTURE SPAN 57 For Hampton Roads Bridge Tunnel	UNIVERSITY of VIRGINIA SCHOOL OF ENGINEERING	Made AB	Date 7/30/2016	Job Number XXXXX
		Checked	Date	Connection
		Backchk'd	Date	Sheet No. 1

Truck Configuration 5

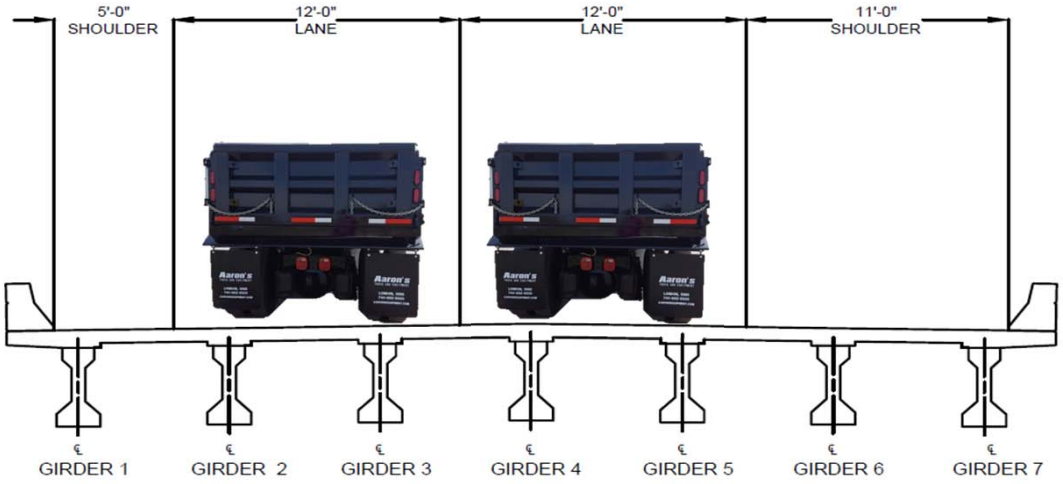

1. Midspan Measurements

		Girder 1	* Girder 2	Girder 3	Girder 4	Girder 5	Girder 6	Girder 7
Run 1	Bottom Face of Flange Strain (με) :	25.77	40.76	28.38	25.81	25.54	14.19	9.79
	Deflection (in.) :	-0.09	-0.12	-0.13	-0.13	-0.11	-0.08	-0.05
Run 2	Bottom Face of Flange Strain (με) :	24.27	40.11	27.88	26.68	25.85	14.97	10.34
	Deflection (in.) :	-	-0.11	-0.12	-0.12	-0.10	-0.07	-0.05
Run 3	Bottom Face of Flange Strain (με) :	24.27	39.42	26.67	25.90	25.46	14.76	10.46
	Deflection (in.) :	-	-	-0.12	-0.12	-0.10	-0.08	-0.05

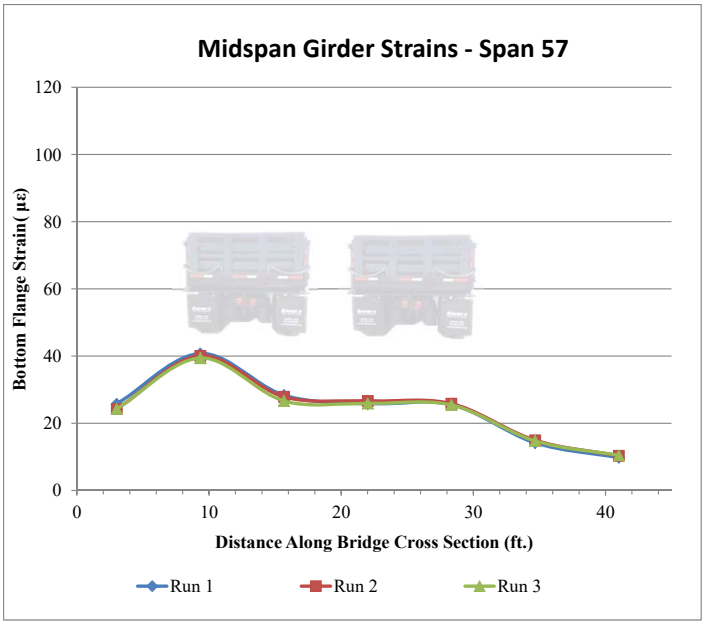

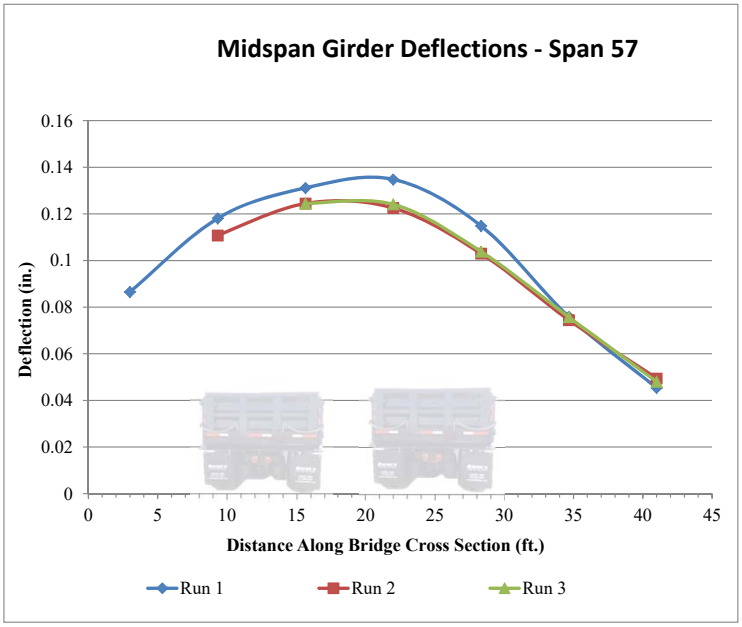

Note: No signs of obvious damage were present in Girder 2, but the peak response may be indicative of potential damage that is not observable.

Note: The midspan deflection of Girder 1 was not captured in any of the Runs (1-3) and for Girder 2 in Run 3 due to low quality (excessively dark) images aquired during testing.

NOTES:

1. Girders are numbered from the east in accordance with original bridge plans
2. Deflection values were measured using the digital image correlation method.

REFERENCES:

1. As - Built Contract Drawings T-3 (224-03) dated December 1977
2. VDOT July 2014 Special Inspection Report for EB South Approach Bridge

Truck Configuration 5 Continued

2. Girder 5 Strain Distribution at Midspan

	Strain Transducer Readings (με)			
Location	Run 1	Run 2	Run 3	Height (in.)
midheight of top flange	-5.53	-6.32	-6.45	41.5
1" below top of CT web	3.71	3.22	2.87	32.5
1" above bottom of CT web	19.71	19.85	19.81	15.5
Bot. Face of Flange	25.54	25.85	25.46	0

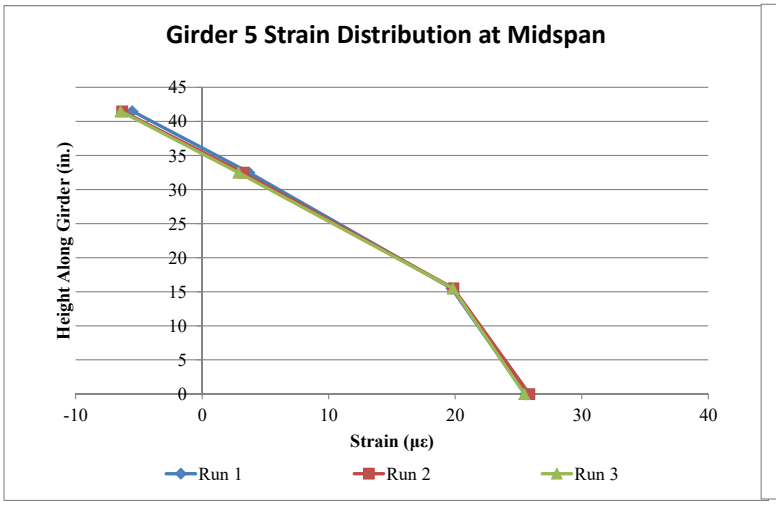

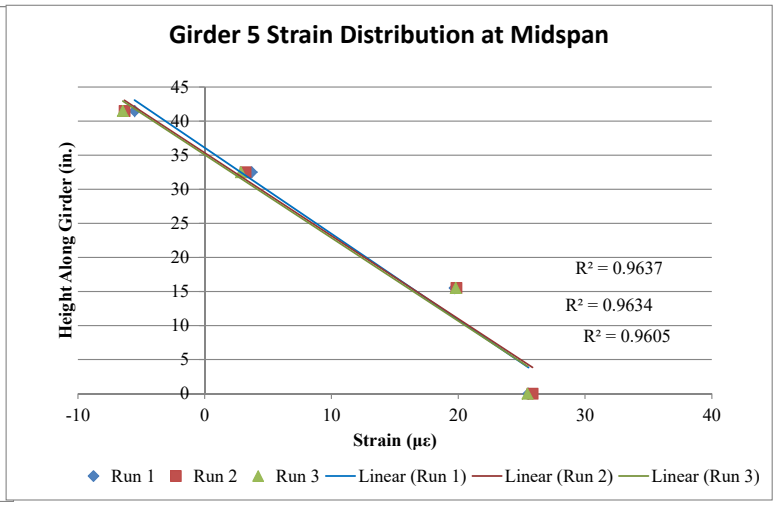

3. Girder 5 Strain Distribution at ~3L/4

	Strain Transducer Readings (με)			
Location	Run 1	Run 2	Run 3	Height (in.)
midheight of top flange	-4.47	-5.52	-4.50	41.5
1" below top of CT web	2.95	2.71	3.02	32.5
1" above bottom of CT web	14.83	16.27	15.46	15.5
Bot. Face of Flange	26.30	29.86	28.44	0

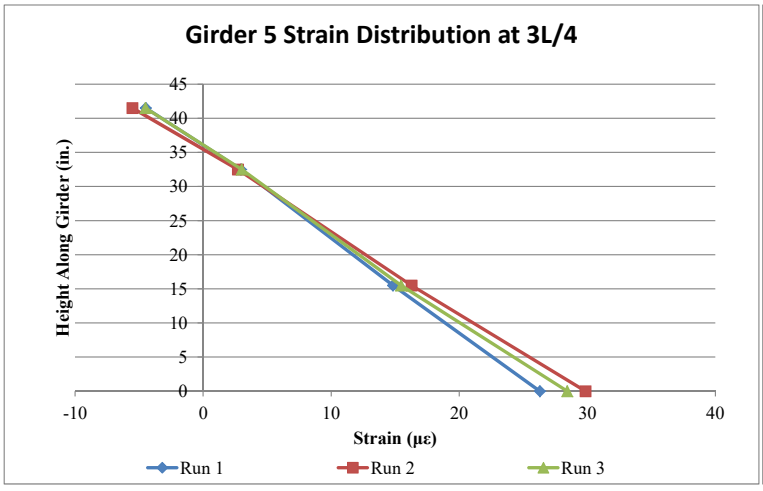

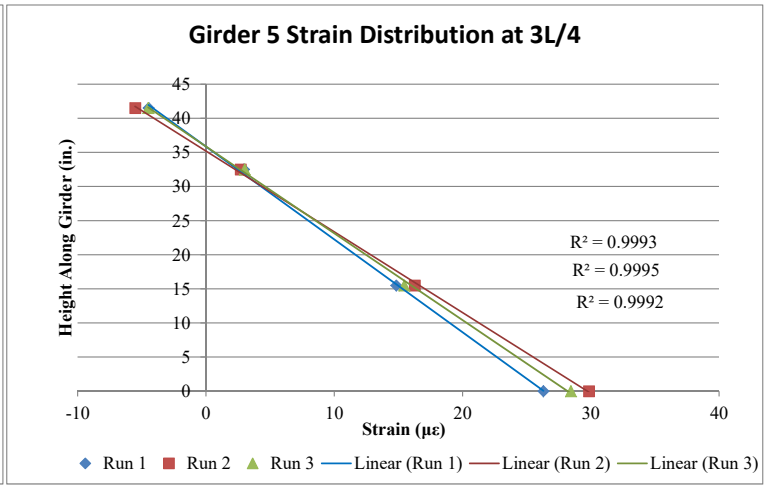

NOTES:

1. Girders are numbered from the east in accordance with original bridge plans
2. Deflection values were measured using the digital image correlation method.

REFERENCES:

1. As - Built Contract Drawings T-3 (224-03) dated December 1977
2. VDOT July 2014 Special Inspection Report for EB South Approach Bridge

APPENDIX C-3:

WESTBOUND SPAN 31

Live Load Testing Results HRBT WESTBOUND STRUCTURE SPAN 31 For Hampton Roads Bridge Tunnel	VirginiaTech Invent the Future	Made JJR	Date 7/11/2016	Job Number 449462
		Checked EAE	Date 7/21/2016	Connection
		Backchk'd JJR	Date 7/22/2016	Sheet No. 1

Truck Configuration 1

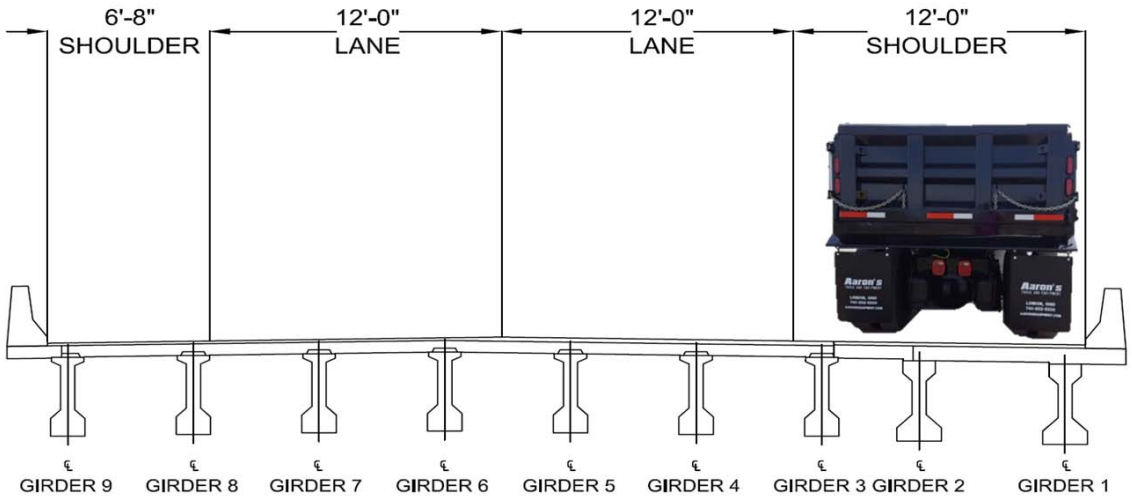

1. Midspan Measurements - Span 31

		Girder 9	Girder 8	Girder 7	Girder 6*	Girder 5	Girder 4	Girder 3	Girder 2	Girder 1
Run 1	Bottom Face of Flange Strain (με) :	-1.06	-0.46	0.97	0.89	5.64	11.24	20.10	23.00	17.33
	Deflection (in.) :	-0.004	-0.002	0	0.003	0.008	0.014	0.017	0.021	0.015
Run 2	Bottom Face of Flange Strain (με) :	-1.29	-0.41	0.72	0.79	4.91	9.97	18.89	23.05	19.02
	Deflection (in.) :	-0.004	-0.005	-0.002	0.001	0.002	0.007	0.011	0.013	0.011
Run 3	Bottom Face of Flange Strain (με) :	-1.15	-0.32	0.57	0.79	4.66	9.67	17.93	22.93	20.15
	Deflection (in.) :	-0.004	-0.002	-0.002	0.001	0.004	0.009	0.012	0.016	0.012
Run 4	Bottom Face of Flange Strain (με) :	-1.14	-0.55	0.44	0.72	4.74	9.94	18.72	23.26	19.09
	Deflection (in.) :	-0.007	-0.005	-0.001	0.002	0.003	0.004	0.008	0.011	0.007
Run 5	Bottom Face of Flange Strain (με) :	-1.10	-0.27	0.85	0.73	4.87	9.86	18.38	23.01	19.67
	Deflection (in.) :	-0.003	-0.001	0	0.001	0.004	0.007	0.011	0.013	0.012

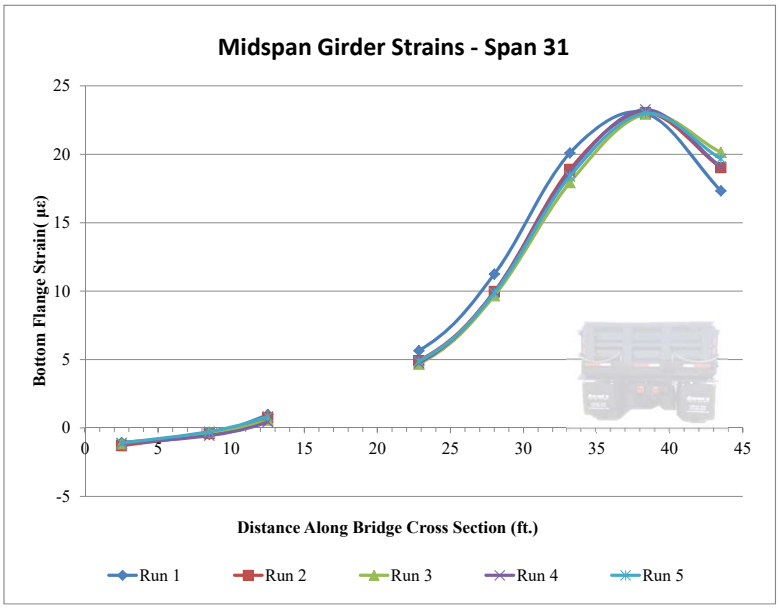

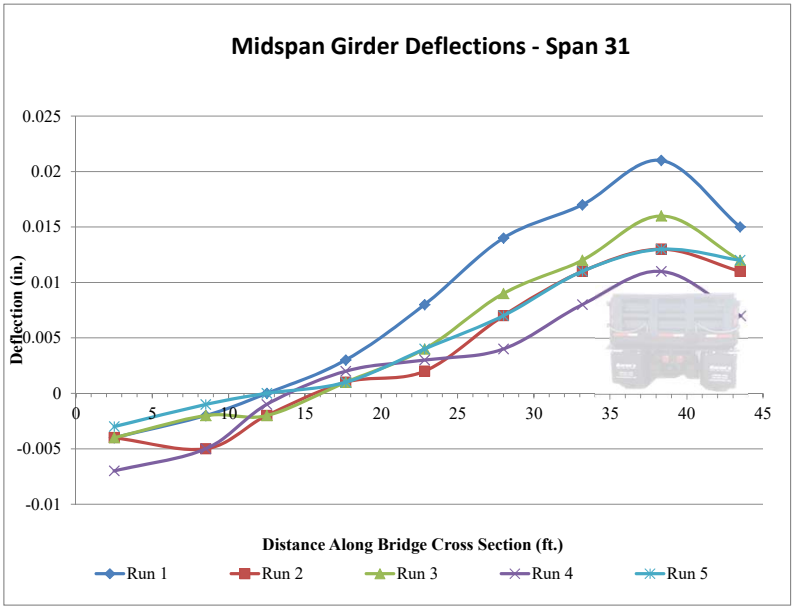

* The contact adhesive didn't hold on the strain transducer of the bottom flange of Girder 6. Values above are shown in red. They are not included in the strain distribution plot above.

NOTES:

1. Girders are numbered from the east in accordance with widened bridge plans
2. Spans are numbered starting at the South Island and end at Willoughby Spit
3. Traffic flows from Willoughby Spit to the South Island on the WB Structure
4. Girders 7 and 8 have considerable damage as shown in the Inspection Mapping
5. Deflection values are given assuming downwards is (+) and upwards is (-)

REFERENCES:

1. Contract Drawings 171-20G dated July 17, 1995 (South Approach Bridge WBL Widening)
2. VDOT Inspection Report and Damage Mapping Details - WB Structure Dated June 2015

Live Load Testing Results HRBT WESTBOUND STRUCTURE SPAN 31 For Hampton Roads Bridge Tunnel	VirginiaTech Invent the Future	Made JJR	Date 7/11/2016	Job Number 449462
		Checked EAE	Date 7/21/2016	Connection
		Backchk'd JJR	Date 7/22/2016	Sheet No. 1

Truck Configuration 2

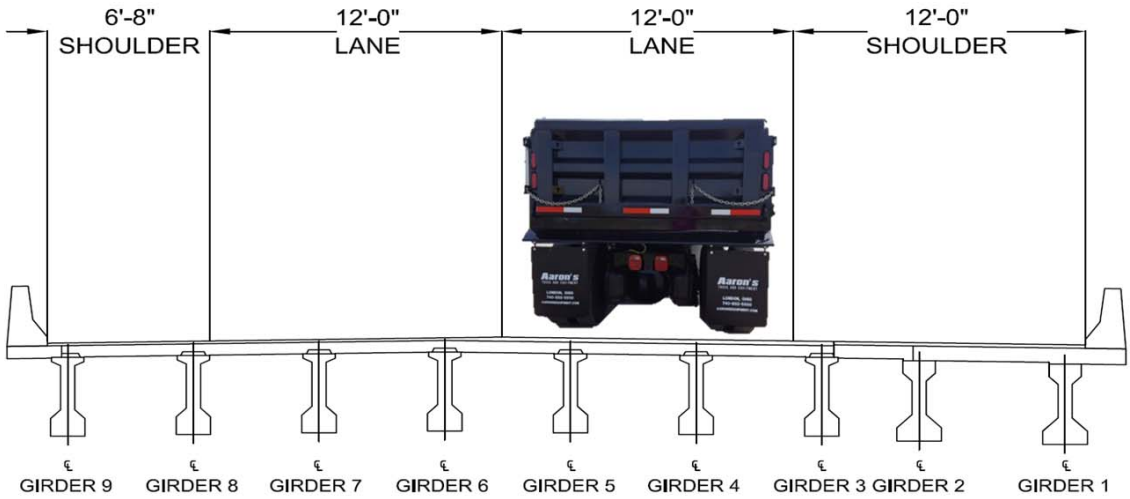

1. Midspan Measurements - Span 31

		Girder 9	Girder 8	Girder 7	Girder 6*	Girder 5	Girder 4	Girder 3	Girder 2	Girder 1
Run 1	Bottom Face of Flange Strain (με) :	0.64	2.49	8.58	4.26	21.37	27.10	16.72	12.04	3.78
	Deflection (in.) :	0	0.004	0.009	0.012	0.023	0.025	0.02	0.016	0.005
Run 2	Bottom Face of Flange Strain (με) :	0.34	2.08	6.84	3.53	19.25	26.74	18.19	12.35	3.19
	Deflection (in.) :	-0.001	0.005	0.006	0.007	0.013	0.018	0.016	0.008	0.001
Run 3	Bottom Face of Flange Strain (με) :	0.25	2.26	7.52	4.19	20.24	26.90	17.31	12.11	3.23
	Deflection (in.) :	0	0.004	0.011	0.012	0.016	0.018	0.013	0.005	0.001
Run 4	Bottom Face of Flange Strain (με) :	0.68	2.32	7.78	3.59	20.10	27.13	17.08	12.11	3.40
	Deflection (in.) :	-0.002	0.003	0.006	0.009	0.016	0.017	0.012	0.006	0.002
Run 5	Bottom Face of Flange Strain (με) :	0.70	2.45	7.48	3.77	20.04	26.47	17.33	11.83	3.31
	Deflection (in.) :	0.003	0.006	0.007	0.016	0.021	0.021	0.017	0.009	0.001

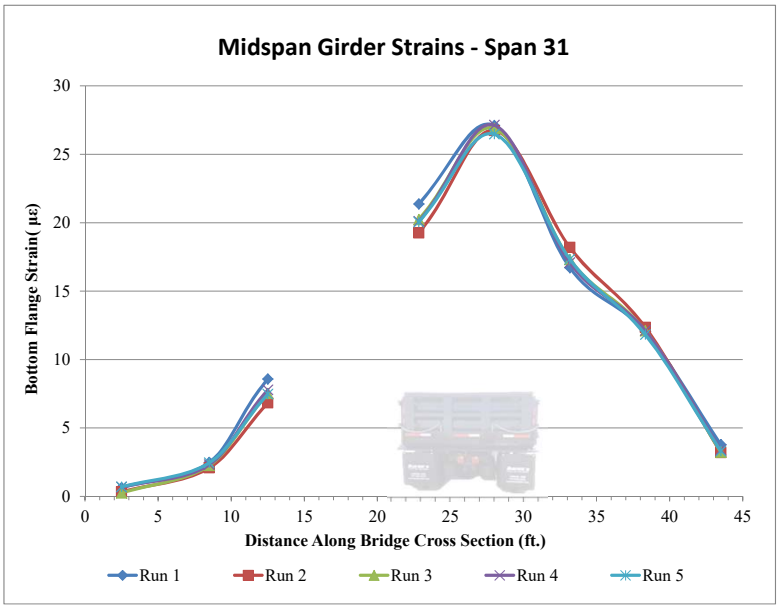

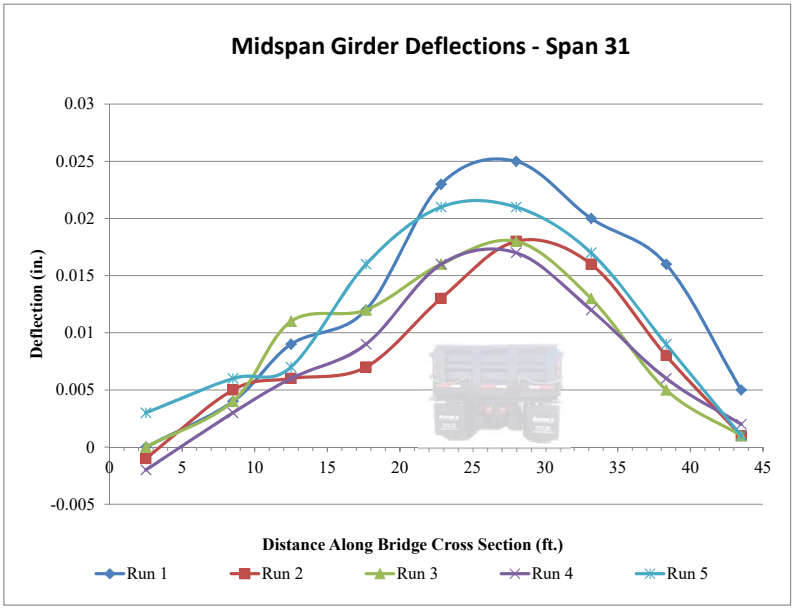

* The contact adhesive didn't hold on the strain transducer of the bottom flange of Girder 6. Values above are shown in red. They are not included in the strain distribution plot above.

NOTES:

1. Girders are numbered from the east in accordance with widened bridge plans
2. Spans are numbered starting at the South Island and end at Willoughby Spit
3. Traffic flows from Willoughby Spit to the South Island on the WB Structure
4. Girders 7 and 8 have considerable damage as shown in the Inspection Mapping
5. Deflection values are given assuming downwards is (+) and upwards is (-)

REFERENCES:

1. Contract Drawings 171-20G dated July 17, 1995 (South Approach Bridge WBL Widening)
2. VDOT Inspection Report and Damage Mapping Details - WB Structure Dated June 2015

Live Load Testing Results	VirginiaTech Invent the Future®	Made	JJR	Date	7/11/2016	Job Number	449462
HRBT WESTBOUND STRUCTURE SPAN 31		Checked	EAE	Date	7/21/2016	Connection	
For Hampton Roads Bridge Tunnel		Backchk'd	JJR	Date	7/22/2016	Sheet No.	1

Truck Configuration 3

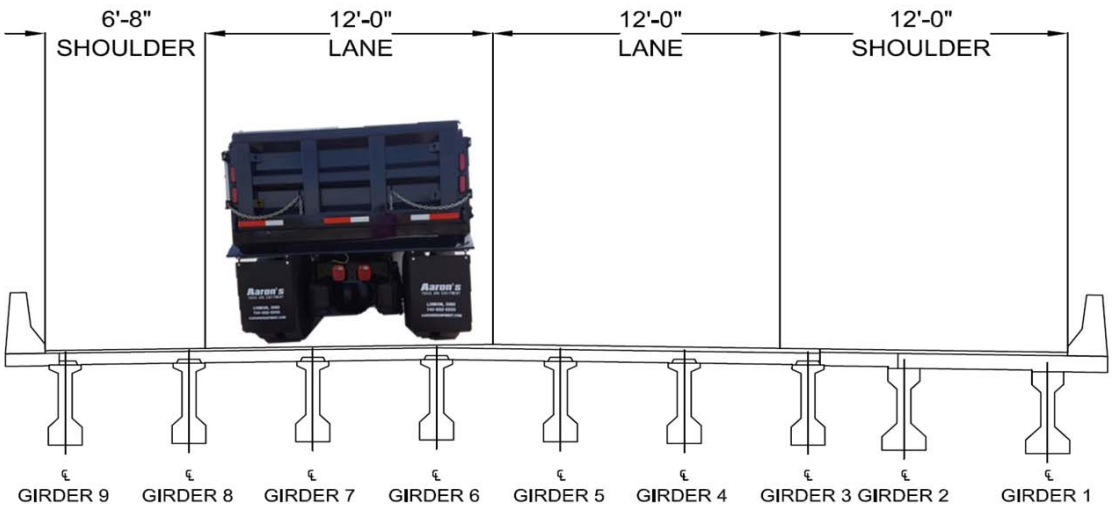

1. Midspan Measurements - Span 31

		Girder 9	Girder 8	Girder 7	Girder 6*	Girder 5	Girder 4	Girder 3	Girder 2	Girder 1
Run 1	Bottom Face of Flange Strain (με) :	13.31	18.27	34.91	8.21	10.71	7.28	2.75	2.42	1.52
	Deflection (in.) :	0.024	0.032	0.033	0.023	0.012	0.006	0.001	0	-0.002
Run 2	Bottom Face of Flange Strain (με) :	13.80	18.53	33.40	7.88	9.46	6.38	1.80	1.70	0.14
	Deflection (in.) :	0.018	0.022	0.026	0.018	0.012	0.008	0.002	0.002	0
Run 3	Bottom Face of Flange Strain (με) :	13.61	18.06	33.52	8.47	9.76	6.46	1.79	1.69	0.00
	Deflection (in.) :	0.02	0.029	0.03	0.026	0.015	0.008	0.003	0.001	-0.002
Run 4	Bottom Face of Flange Strain (με) :	12.02	15.09	33.05	8.79	10.86	7.49	2.62	2.29	0.28
	Deflection (in.) :	0.014	0.021	0.023	0.025	0.015	0.007	0.003	0.002	-0.001
Run 5	Bottom Face of Flange Strain (με) :	13.57	17.95	34.45	8.98	11.31	7.62	2.83	2.75	2.13
	Deflection (in.) :	0.02	0.023	0.026	0.015	0.013	0.007	0.002	0.001	-0.003

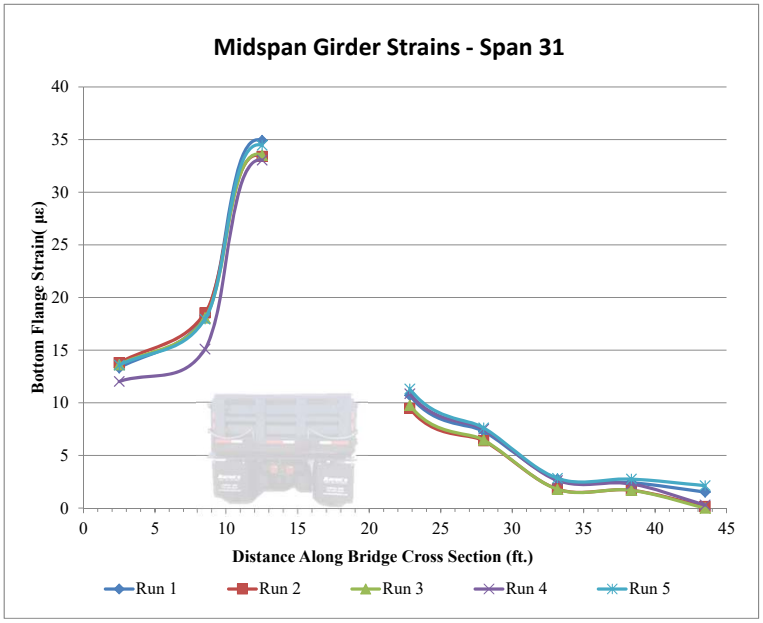

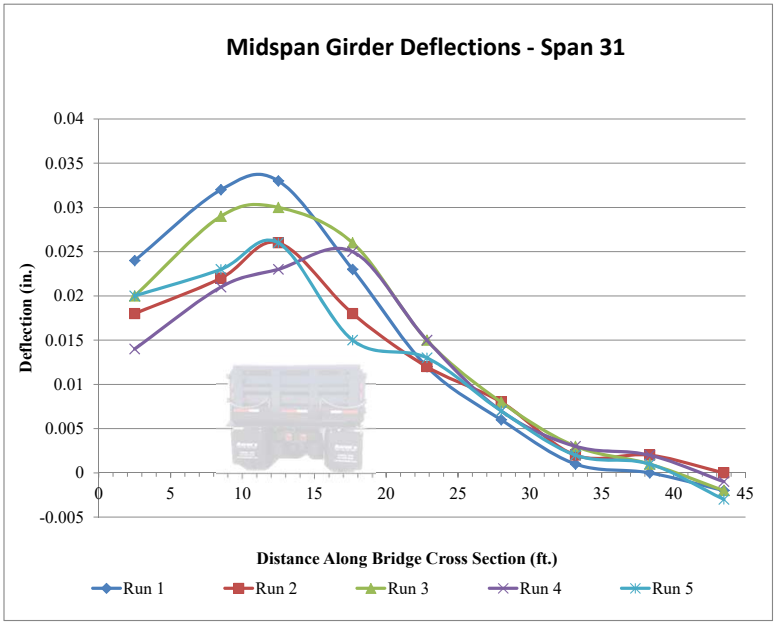

* The contact adhesive didn't hold on the strain transducer of the bottom flange of Girder 6. The above numbers don't capture the full strain value. They are not included in the strain distribution plot above.

NOTES:

1. Girders are numbered from the east in accordance with widened bridge plans
2. Spans are numbered starting at the South Island and end at Willoughby Spit
3. Traffic flows from the Willoughby Spit to the South Island on the WB Structure
4. Girders 7 and 8 have considerable damage as shown in the Inspection Mapping
5. Deflection values are given assuming downwards is (+) and upwards is (-)

REFERENCES:

1. Contract Drawings 171-20G dated July 17, 1995 (South Approach Bridge WBL Widening)
2. VDOT Inspection Report and Damage Mapping Details - WB Structure Dated June 2015

Truck Configuration 3 Continued

2. Girder 7 Strain Distribution at Midspan - Span 31

	Strain Transducer Readings (με)					
Location	Run 1	Run 2	Run 3	Run 4	Run 5	Height (in.)
midheight of top flange	-6.17	-6.16	-5.87	-6.11	-4.59	41.5
1" below top of CT web	-2.47	-2.79	-2.43	-2.86	-1.38	37
1" above bottom of CT web	14.79	14.05	14.10	13.50	14.74	14
midheight of bottom flange	24.24	23.67	23.38	21.74	23.58	3.5
Bot. Face of Flange	34.91	33.37	33.49	33.02	34.45	0

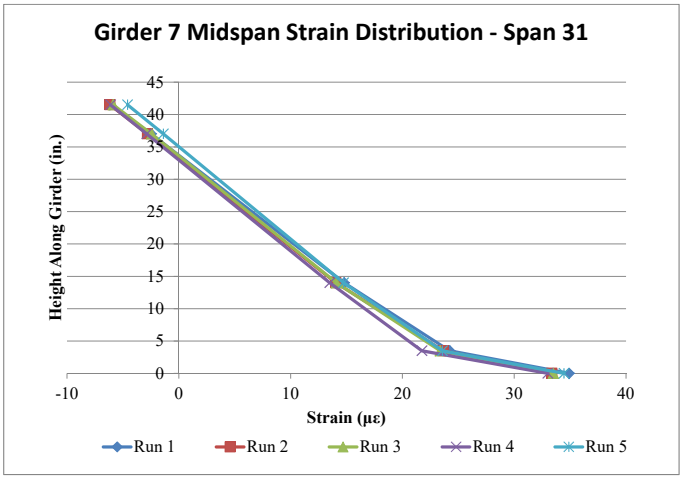

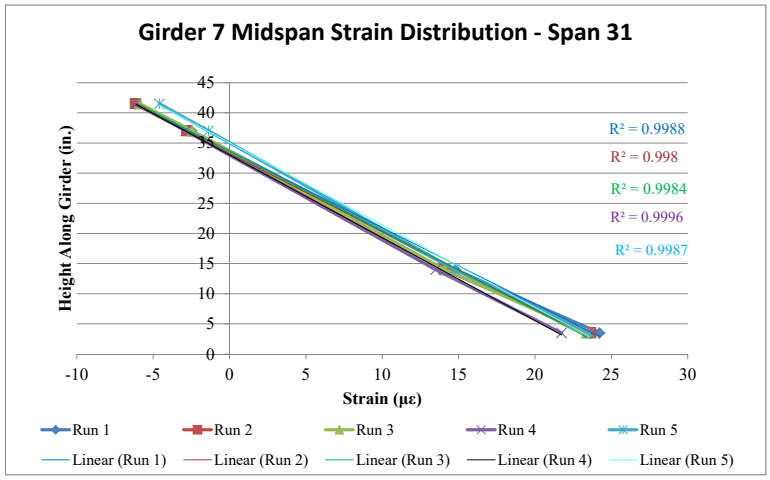

The damaged strands at the bottom of Girder 7 cause a bilinear strain distribution . The concrete is forced to carry higher strains because of the damaged strands at the same height in the cross section. The plot to the right shows the top 4 strain readings to prove a linear strain distribution in the undamaged area of the cross section.

3. Girder 8 Strain Distribution at Midspan - Span 31

	Strain Transducer Readings (με)					
Location	Run 1	Run 2	Run 3	Run 4	Run 5	Height (in.)
midheight of top flange	N/A	N/A	N/A	N/A	-1.40	41.5
1" below top of CT web	N/A	N/A	N/A	N/A	-0.58	37
1" above bottom of CT web	N/A	N/A	N/A	N/A	13.77	14
midheight of bottom flange	26.73	26.67	26.29	23.03	25.79	3.5
Bot. Face of Flange	18.27	18.53	18.06	15.09	17.95	0

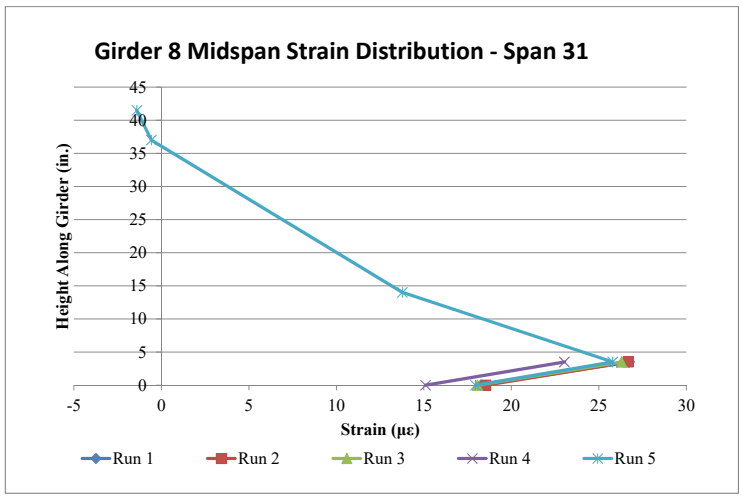

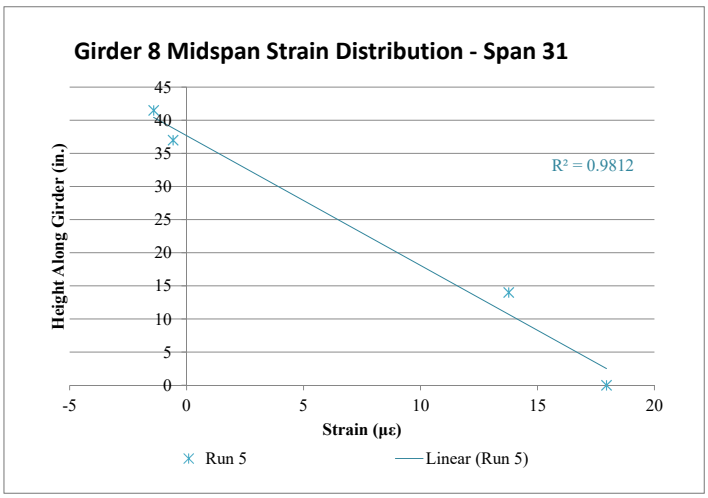

Similar to Girder 7, the damaged strands in Girder 8 are causing the forces to redistribute to the intact strands and the surrounding concrete. In girder 8, layers 2-4 are most damaged causing the the concrete strains at this location to be higher than at the bottom face of the flange. The plot on the right excludes the strain value at midheight of the

NOTES:

1. Girders 7 and 8 have considerable damage as shown in the Inspection Mapping

2. The red highlighetd cells with N/A are from wireless connections problems with a node during the load test.

3. Height of Girder is with respect to soffitt of bottom flange of girder

REFERENCES:

1. Contract Drawings 171-20G dated July 17, 1995 (South Approach Bridge WBL Widening)
2. VDOT Inspection Report and Damage Mapping Details - WB Structure Dated June 2015

Truck Configuration 3 Continued

4. Girder 8 Strain Distribution at ~L/5 - Span 31

	Strain Transducer Readings (με)					
Location	Run 1	Run 2	Run 3	Run 4	Run 5	Height (in.)
midheight of top flange	-1.04	-1.26	-1.04	-0.08	1.28	41.5
1" below top of CT web	-1.54	-2.72	-2.58	-2.31	0.18	37
1" above bottom of CT web	6.96	5.66	5.74	4.45	7.44	14
midheight of bottom flange	14.30	12.62	12.55	10.25	13.86	3.5
Bot. Face of Flange	15.46	14.19	14.04	10.51	14.18	0

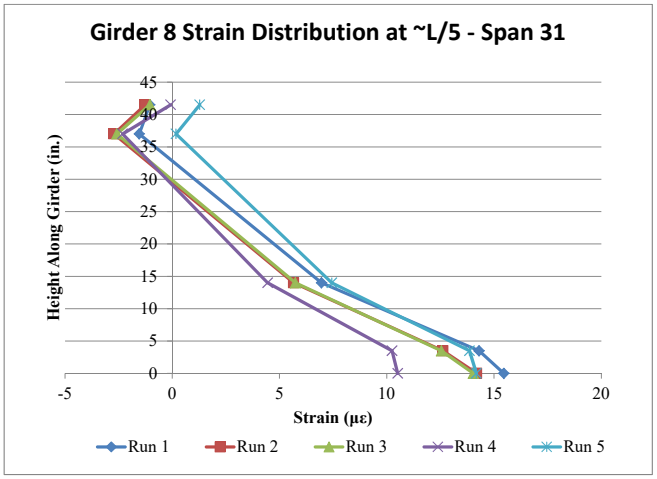

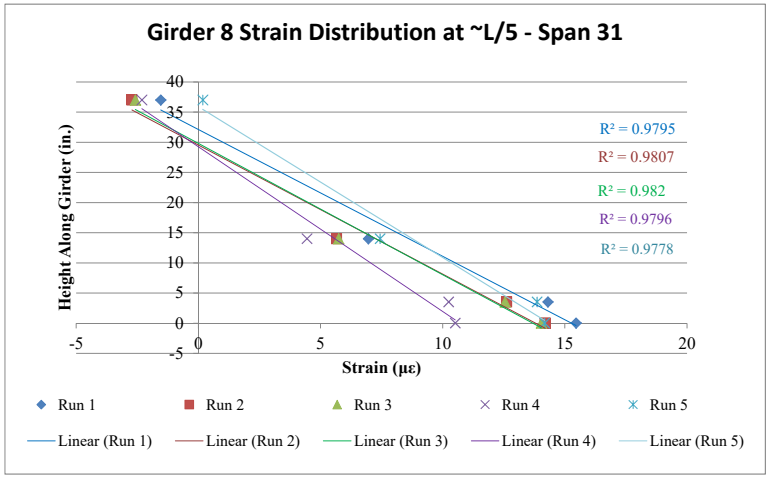

The plot on the right only includes the bottom four strain readings for each run in an attempt to prove a linear strain distribution. Due to the damage at this location, there is some strain redistribution between neighboring strands and the concrete causing the distribution to stray from being exactly linear.

5. Girder 8 Strain Distribution at ~9L/10 - Span 31

	Strain Transducer Readings (με)					
Location	Run 1	Run 2	Run 3	Run 4	Run 5	Height (in.)
midheight of top flange	-0.47	0.55	0.79	0.94	-0.18	41.5
1" below top of CT web	0.61	1.18	1.31	1.12	0.81	37
1" above bottom of CT web	10.37	11.05	10.46	8.79	10.53	14
**midheight of bottom flange	8.30	8.29	7.95	6.92	8.47	3.5
Bot. Face of Flange	N/A	N/A	N/A	N/A	17.13	0

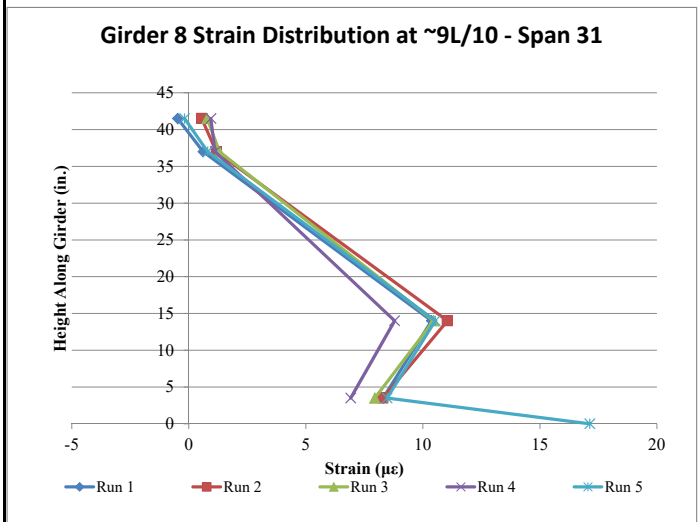

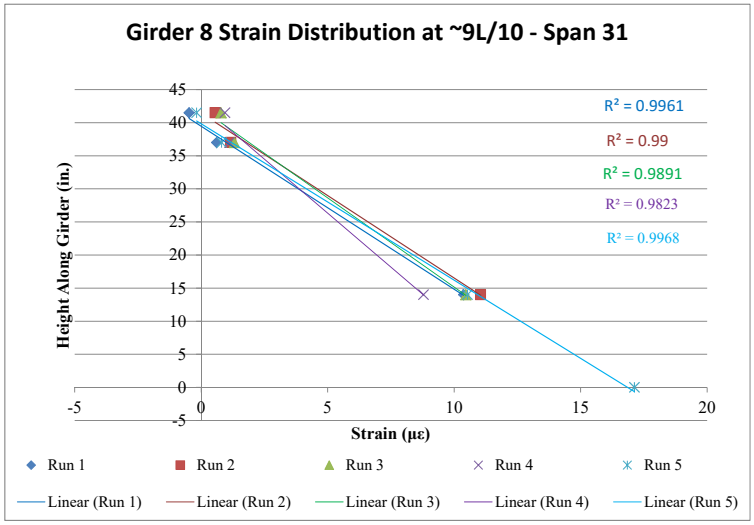

**The plot on the right doesn't include the strain readings at the mid height of the bottom flange. This gauge wasn't attached fully.

NOTES:

1. Girders 7 and 8 have considerable damage as shown in the Inspection Mapping
2. The red highlighted cells with N/A are from wireless connection problems with a node during the load test
3. Height of Girder is with respect to soffitt of bottom flange of girder

REFERENCES:

1. Contract Drawings 171-20G dated July 17, 1995 (South Approach Bridge WBL Widening)
2. VDOT Inspection Report and Damage Mapping Details - WB Structure Dated June 2015

Live Load Testing Results	VirginiaTech Invent the Future	Made	JJR	Date	7/11/2016	Job Number	449462
HRBT WESTBOUND STRUCTURE SPAN 31		Checked	EAE	Date	7/21/2016	Connection	
For Hampton Roads Bridge Tunnel		Backchk'd	JJR	Date	7/22/2016	Sheet No.	1

Truck Configuration 4

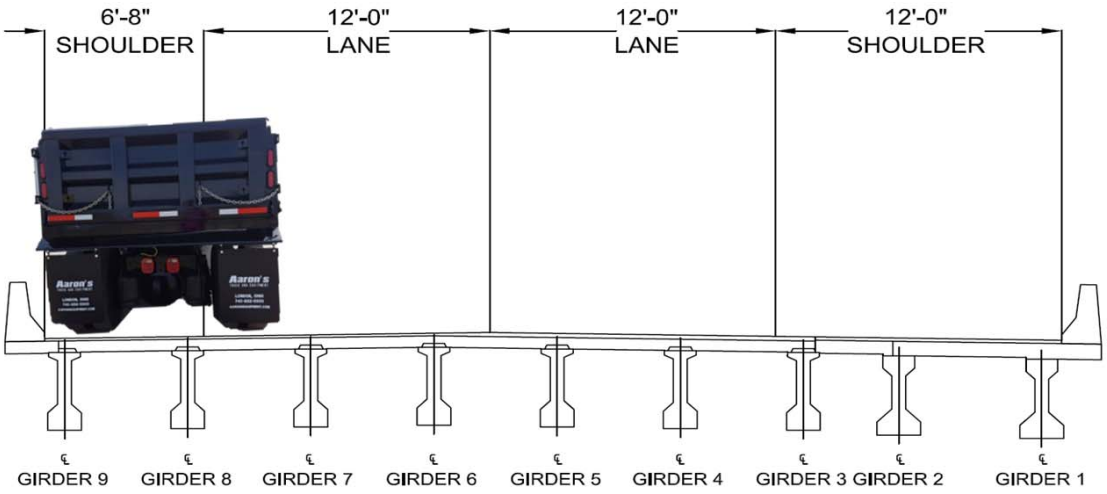

1. Midspan Measurements - Span 31

		Girder 9	Girder 8	Girder 7	Girder 6*	Girder 5	Girder 4	Girder 3	Girder 2	Girder 1
Run 1	Bottom Face of Flange Strain (με) :	33.86	24.08	25.71	4.44	6.84	4.04	0.67	0.92	1.11
	Deflection (in.) :	0.036	0.033	0.028	0.024	0.014	0.002	0.004	0.001	0
Run 2	Bottom Face of Flange Strain (με) :	34.16	23.71	22.65	3.95	5.38	2.95	-0.40	-0.04	-0.46
	Deflection (in.) :	0.039	0.032	0.021	0.013	0.007	0.002	0.001	0	-0.003
Run 3	Bottom Face of Flange Strain (με) :	34.39	23.10	23.15	3.98	5.26	2.90	-0.52	-0.11	-0.50
	Deflection (in.) :	0.042	0.039	0.029	0.018	0.012	0.003	0	-0.001	0
Run 4	Bottom Face of Flange Strain (με) :	33.31	23.48	23.65	3.98	5.53	2.76	-0.55	-0.23	-0.68
	Deflection (in.) :	0.035	0.028	0.019	0.012	0.005	0.001	0	0.001	-0.001
Run 5	Bottom Face of Flange Strain (με) :	35.04	24.42	24.65	4.22	6.62	3.92	0.61	0.97	1.73
	Deflection (in.) :	0.044	0.039	0.027	0.022	0.013	0.009	0.003	0.002	-0.001

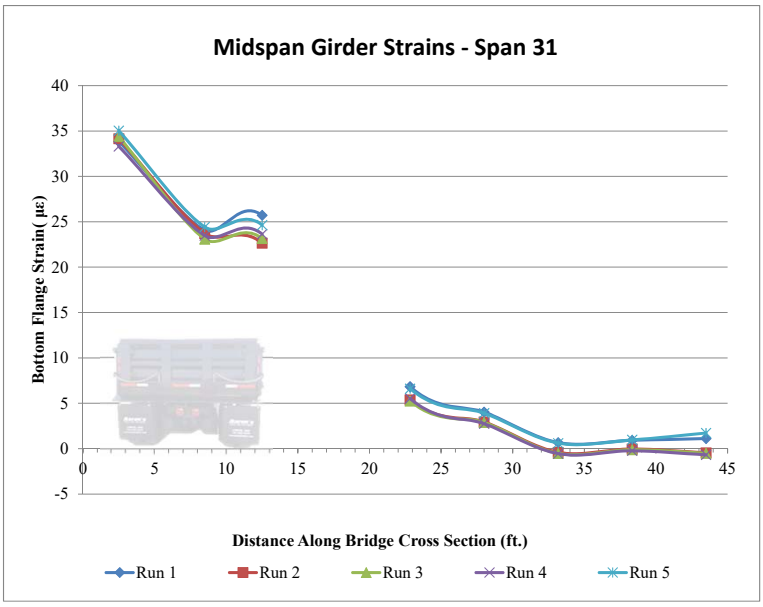

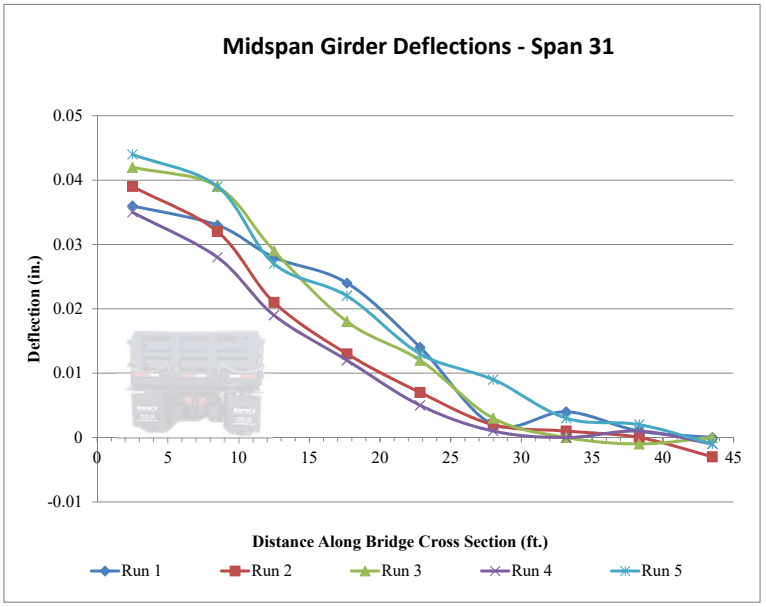

* The contact adhesive didn't hold on the strain transducer of the bottom flange of Girder 6. The above numbers don't capture the full strain value. They are not included in the strain distribution plot above.

NOTES:

1. Girders are numbered from the east in accordance with widened bridge plans
2. Spans are numbered starting at the South Island and end at Willoughby Spit
3. Traffic flows from the Willoughby Spit to the South Island on the WB Structure
4. Girders 7 and 8 have considerable damage as shown in the Inspection Mapping
5. Deflection values are given assuming downwards is (+) and upwards is (-)

REFERENCES:

1. Contract Drawings 171-20G dated July 17, 1995 (South Approach Bridge WBL Widening)
2. VDOT Inspection Report and Damage Mapping Details - WB Structure Dated June 2015

Truck Configuration 4 Continued

2. Girder 7 Strain Distribution at Midspan - Span 31

	Strain Transducer Readings (με)					
Location	Run 1	Run 2	Run 3	Run 4	Run 5	Height (in.)
midheight of top flange	-5.79	-5.30	-5.46	-5.45	-3.87	41.5
1" below top of CT web	-2.12	-2.19	-2.26	-2.26	-0.92	37
1" above bottom of CT web	11.53	9.75	9.68	9.93	11.13	14
midheight of bottom flange	16.10	13.77	13.84	14.09	15.41	3.5
Bot. Face of Flange	25.71	22.62	23.12	23.62	24.65	0

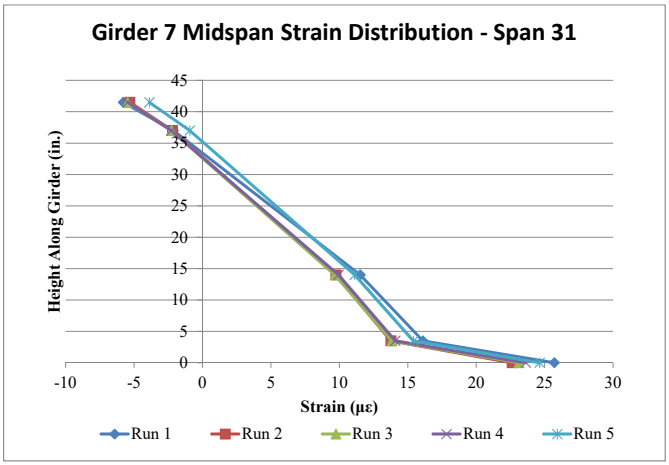

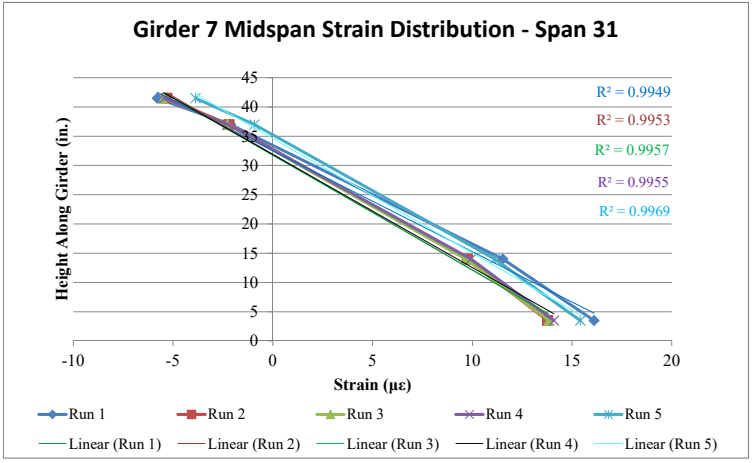

The damaged strands at the bottom of Girder 7 cause a bilinear strain distribution . The concrete is forced to carry higher strains because of the damaged strands at the same height in the cross section. The plot to the right shows the top 4 strain readings to prove a linear strain distribution in the undamaged area of the cross section.

3. Girder 8 Strain Distribution at Midspan - Span 31

	Strain Transducer Readings (με)					
Location	Run 1	Run 2	Run 3	Run 4	Run 5	Height (in.)
midheight of top flange	N/A	N/A	N/A	N/A	-1.39	41.5
1" below top of CT web	N/A	N/A	N/A	N/A	0.43	37
1" above bottom of CT web	N/A	N/A	N/A	N/A	17.94	14
midheight of bottom flange	30.43	29.54	29.78	29.56	30.38	3.5
Bot. Face of Flange	24.08	23.71	23.10	23.48	24.42	0

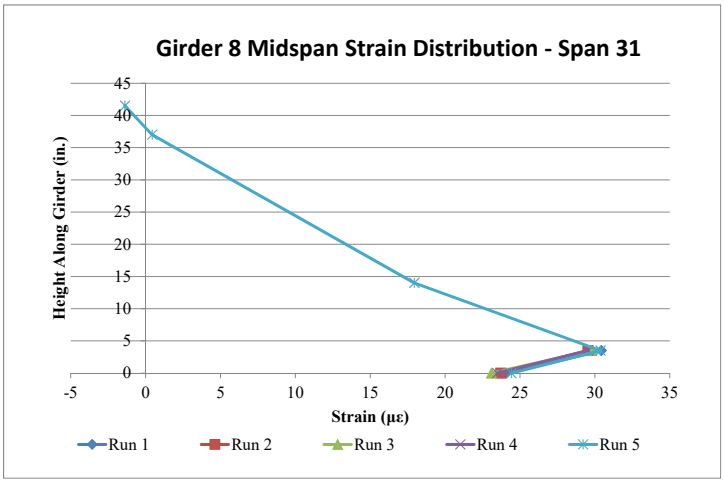

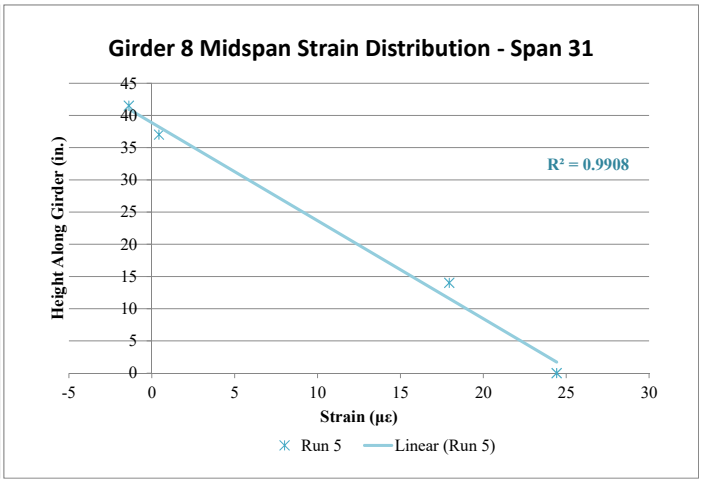

Similar to Girder 7, the damaged strands in Girder 8 are causing the forces to redistribute to the intact strands and the surrounding concrete. In girder 8, layers 2-4 are most damaged causing the the concrete strains at this location to be higher than at the bottom face of the flange. The plot to the right excludes the strain value at midheight of the bottom flange

NOTES:

1. Girders 7 and 8 have considerable damage as shown in the Inspection Mapping

2. The red highlighetd cells with N/A are from wireless connection problems with a node during the load test.

3. Height of Girder is with respect to soffitt of bottom flange of girder

REFERENCES:

1. Contract Drawings 171-20G dated July 17, 1995 (South Approach Bridge WBL Widening)

2. VDOT Inspection Report and Damage Mapping Details - WB Structure Dated June 2015

Truck Configuration 4 Continued

4. Girder 8 Strain Distribution at ~L/5 - Span 31

	Strain Transducer Readings (με)					
Location	Run 1	Run 2	Run 3	Run 4	Run 5	Height (in.)
midheight of top flange	-2.44	-2.15	-1.92	-1.98	-1.08	41.5
1" below top of CT web	-2.38	-3.53	-3.41	-3.70	-1.25	37
1" above bottom of CT web	9.47	7.60	7.67	7.49	9.73	14
midheight of bottom flange	15.94	13.42	13.46	12.91	15.76	3.5
Bot. Face of Flange	21.75	18.82	19.04	18.58	20.82	0

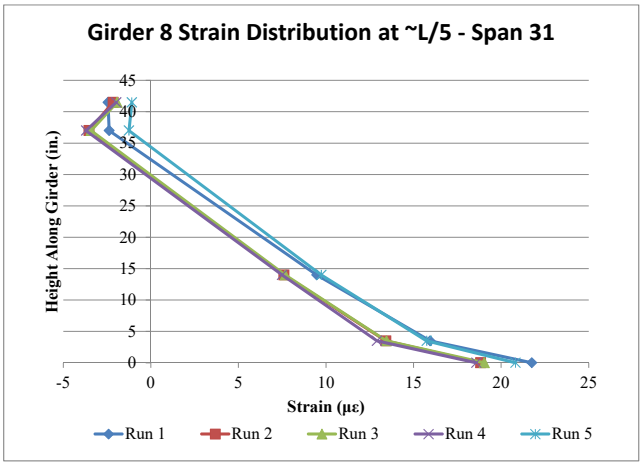

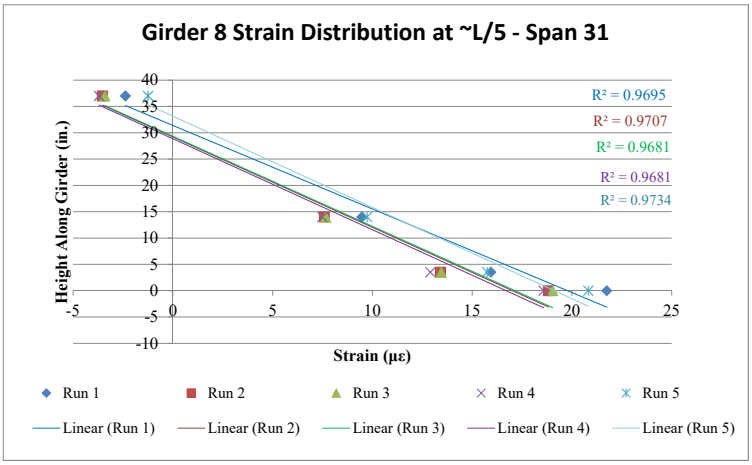

The plot on the right only includes the bottom four strain readings for each run in an attempt to prove a linear strain distribution. Due to the damage at this location, there is some strain redistribution between neighboring strands and the concrete causing the distribution to stray from being exactly linear.

5. Girder 8 Strain Distribution at ~9L/10 - Span 31

	Strain Transducer Readings (με)					
Location	Run 1	Run 2	Run 3	Run 4	Run 5	Height (in.)
midheight of top flange	-1.44	-0.24	-0.44	-1.09	-0.75	41.5
1" below top of CT web	-0.35	0.16	-0.79	-0.70	0.25	37
1" above bottom of CT web	14.75	14.45	13.75	13.87	15.34	14
**midheight of bottom flange	8.83	8.64	8.33	8.36	9.22	3.5
Bot. Face of Flange	N/A	N/A	N/A	N/A	25.97	0

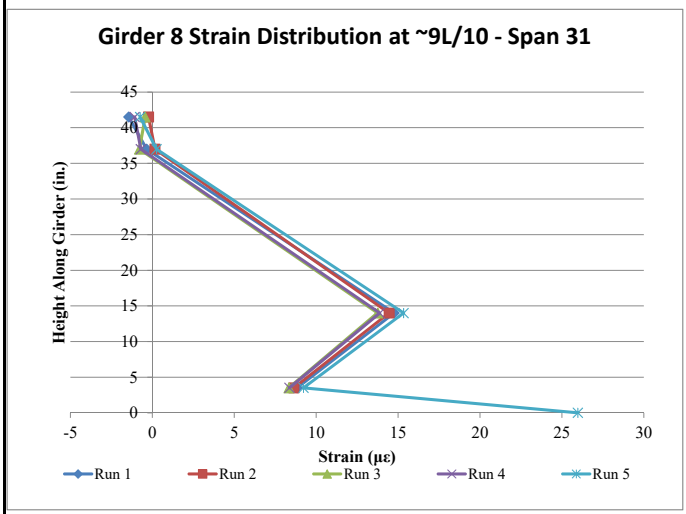

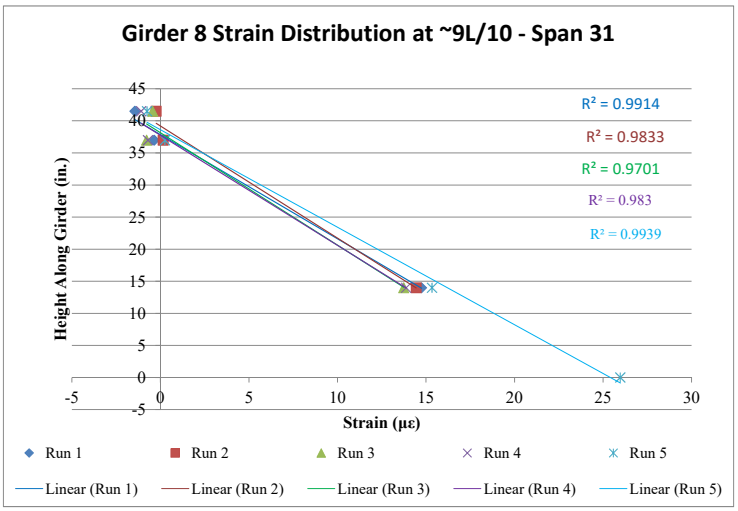

**The plot on the right doesn't include the strain readings at the mid height of the bottom flange. This gauge wasn't attached fully.

NOTES:

1. Girders 7 and 8 have considerable damage as shown in the Inspection Mapping
2. The red highlighted cells with N/A are from wireless connection problems with a node during a load test
3. Height of Girder is with respect to soffitt of bottom flange of girder

REFERENCES:

1. Contract Drawings 171-20G dated July 17, 1995 (South Approach Bridge WBL Widening)
2. VDOT Inspection Report and Damage Mapping Details - WB Structure Dated June 2015

Live Load Testing Results		Made	JJR	Date	7/11/2016	Job Number	449462
HRBT WESTBOUND STRUCTURE SPAN 31	VirginiaTech Invent the Future®	Checked	EAE	Date	7/21/2016	Connection	
For Hampton Roads Bridge Tunnel		Backchk'd	JJR	Date	7/22/2016	Sheet No.	1

Truck Configuration 5

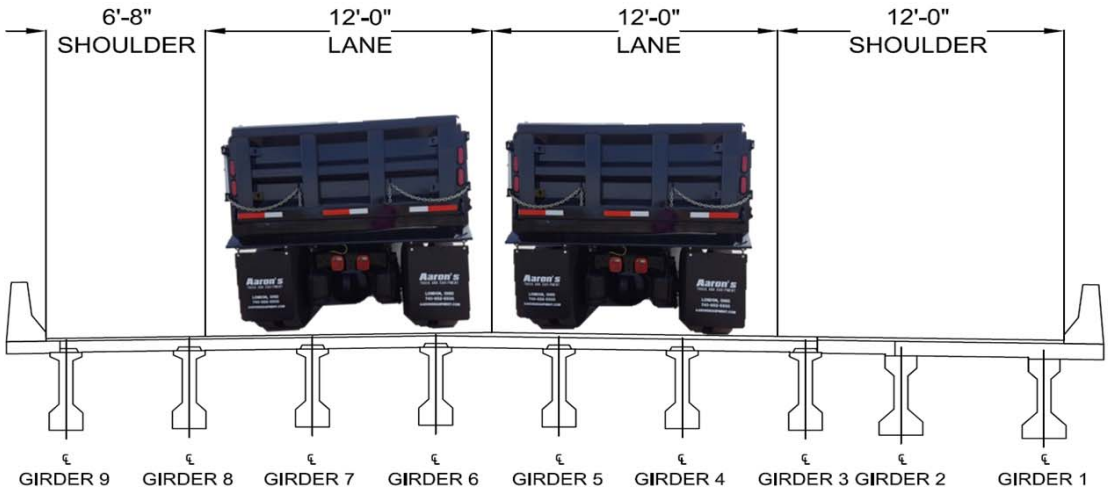

1. Midspan Measurements - Span 31

		Girder 9	Girder 8	Girder 7	Girder 6*	Girder 5	Girder 4	Girder 3	Girder 2	Girder 1
Run 1	Bottom Face of Flange Strain (με) :	18.81	25.27	47.92	11.92	30.41	32.52	19.02	13.98	5.09
	Deflection (in.) :	0.02	0.032	0.039	0.036	0.031	0.025	0.017	0.01	0.003
Run 2	Bottom Face of Flange Strain (με) :	17.44	23.85	44.16	11.89	28.39	30.78	18.26	12.25	2.38
	Deflection (in.) :	0.024	0.034	0.042	0.04	0.032	0.026	0.018	0.011	0.001
Run 3	Bottom Face of Flange Strain (με) :	14.58	13.91	32.49	10.12	30.61	32.60	19.43	13.18	3.08
	Deflection (in.) :	0.026	0.035	0.044	0.045	0.04	0.03	0.018	0.006	-0.004
Run 4	Bottom Face of Flange Strain (με) :	15.27	21.01	41.97	10.58	27.43	30.75	18.58	12.43	2.49
	Deflection (in.) :	0.018	0.026	0.035	0.041	0.034	0.024	0.016	0.009	-0.001
Run 5	Bottom Face of Flange Strain (με) :	18.16	24.49	46.31	13.34	31.52	32.64	18.69	13.73	5.05
	Deflection (in.) :	0.023	0.038	0.038	0.038	0.035	0.029	0.015	0.009	0.002

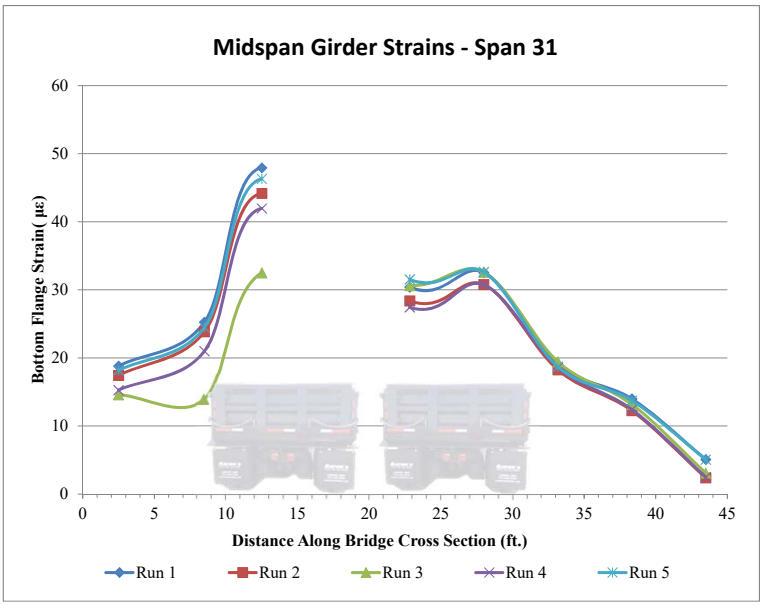

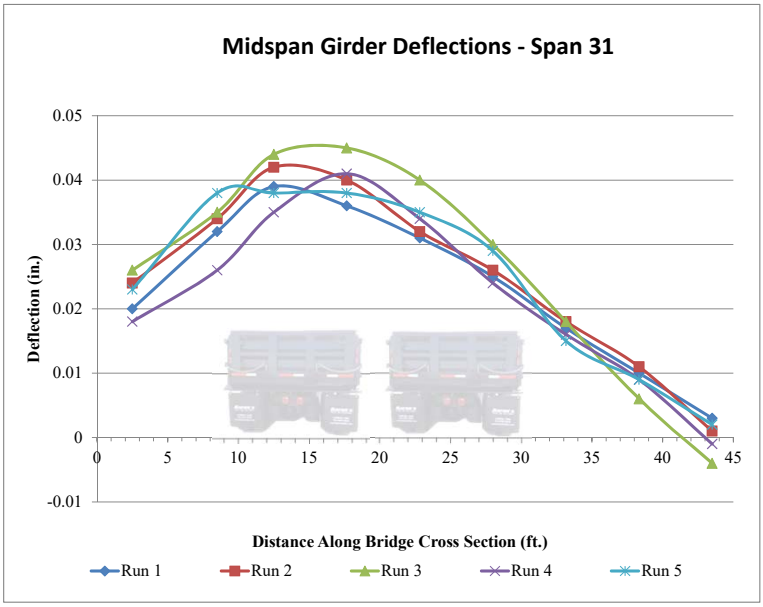

* The contact adhesive didn't hold on the strain transducer of the bottom flange of Girder 6. The above numbers don't capture the full strain value. They are not included in the strain distribution plot above.

NOTES:

1. Girders are numbered from the east in accordance with widened bridge plans
2. Spans are numbered starting at the South Island and end at Willoughby Spit
3. Traffic flows from the Willoughby Spit to the South Island on the WB Structure
4. Girders 7 and 8 have considerable damage as shown in the Inspection Mapping
5. Deflection values are given assuming downwards is (+) and upwards is (-)

REFERENCES:

1. Contract Drawings 171-20G dated July 17, 1995 (South Approach Bridge WBL Widening)
2. VDOT Inspection Report and Damage Mapping Details - WB Structure Dated June 2015

Truck Configuration 5 Continued

2. Girder 7 Strain Distribution at Midspan - Span 31

	Strain Transducer Readings (με)					
Location	Run 1	Run 2	Run 3	Run 4	Run 5	Height (in.)
midheight of top flange	-9.10	-8.88	-7.72	-6.62	-6.24	41.5
1" below top of CT web	-4.09	-4.64	-3.28	-2.49	-1.58	37
1" above bottom of CT web	20.71	18.44	14.12	17.15	20.77	14
midheight of bottom flange	35.41	32.48	23.83	30.21	34.46	3.5
Bot. Face of Flange	47.92	44.13	32.46	41.94	46.31	0

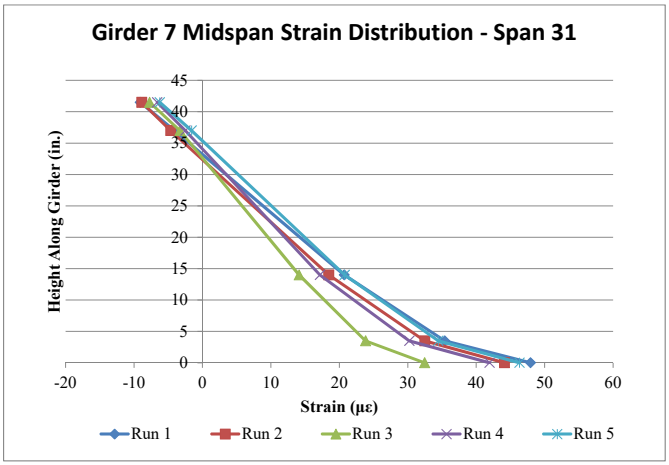

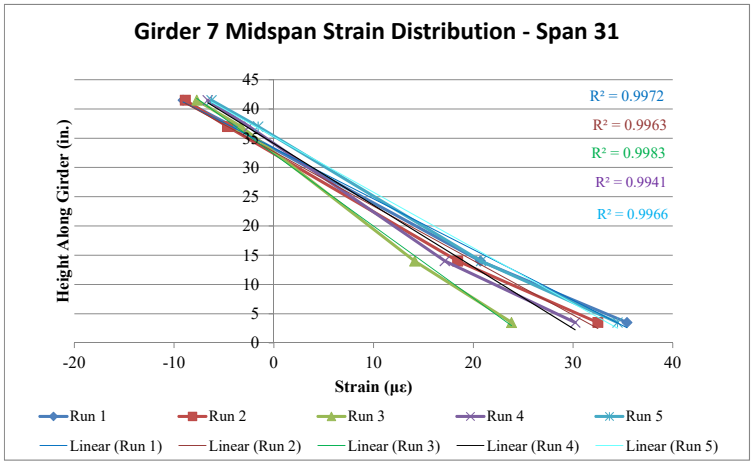

The damaged strands at the bottom of Girder 7 cause a bilinear strain distribution . The concrete is forced to carry higher strains because of the damaged strands at the same height in the cross section. The plot to the right shows the top 4 strain readings to prove a linear strain distribution in the undamaged area of the cross section.

3. Girder 8 Strain Distribution at Midspan - Span 31

	Strain Transducer Readings (με)					
Location	Run 1	Run 2	Run 3	Run 4	Run 5	Height (in.)
midheight of top flange	N/A	N/A	N/A	N/A	-1.26	41.5
1" below top of CT web	N/A	N/A	N/A	N/A	0.06	37
1" above bottom of CT web	N/A	N/A	N/A	N/A	19.26	14
midheight of bottom flange	35.33	33.00	20.82	30.48	34.69	3.5
Bot. Face of Flange	25.27	23.85	13.91	21.01	24.49	0

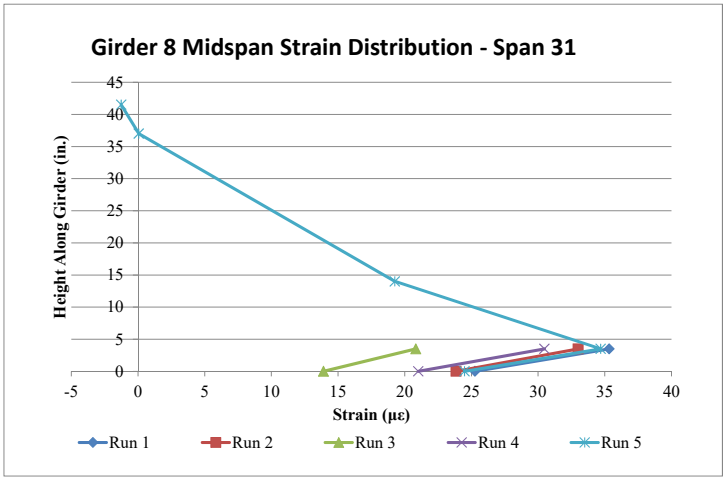

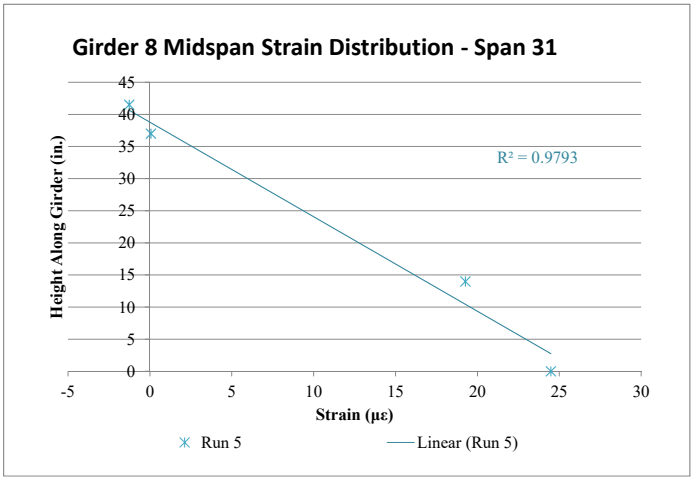

Similar to Girder 7, the damaged strands in Girder 8 are causing the forces to redistribute to the intact strands and the surrounding concrete. In girder 8, layers 2-4 are most damaged causing the the concrete strains at this location to be higher than at the bottom face of the flange. The plot on the right excludes the strain value at midheight of the

NOTES:

1. Girders 7 and 8 have considerable damage as shown in the Inspection Mapping

2. The red highlighetd cells with N/A are from wireless connections problems with a node during the load test.

3. Height of Girder is with respect to soffitt of bottom flange of girder

REFERENCES:

1. Contract Drawings 171-20G dated July 17, 1995 (South Approach Bridge WBL Widening)

2. VDOT Inspection Report and Damage Mapping Details - WB Structure Dated June 2015

Truck Configuration 5 Continued

4. Girder 8 Strain Distribution at ~L/5 - Span 31

	Strain Transducer Readings (με)					
Location	Run 1	Run 2	Run 3	Run 4	Run 5	Height (in.)
midheight of top flange	-3.23	-3.44	-0.41	-2.07	-0.18	41.5
1" below top of CT web	-2.01	-3.78	-2.80	-3.64	-0.53	37
1" above bottom of CT web	10.29	7.78	7.13	7.22	10.14	14
midheight of bottom flange	17.94	14.84	14.50	14.98	18.09	3.5
Bot. Face of Flange	22.09	18.75	16.52	17.35	20.12	0

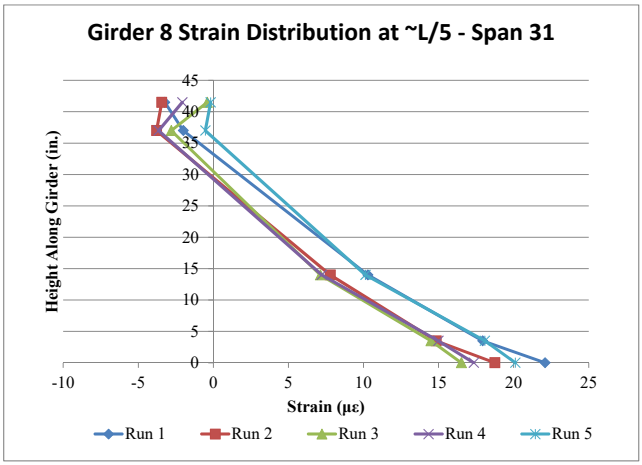

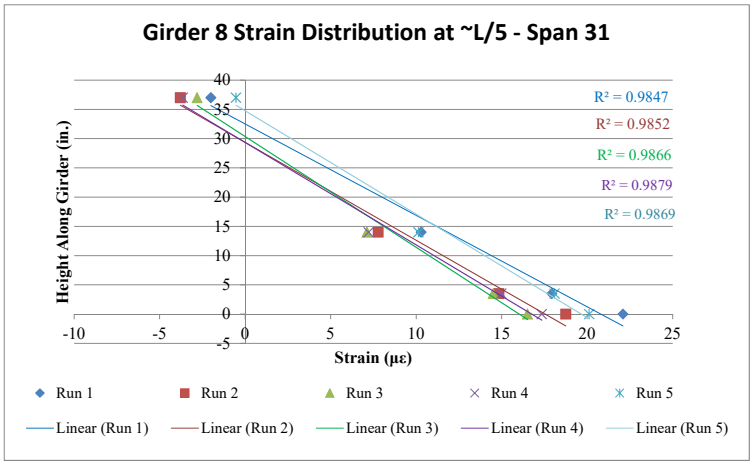

The plot on the right only includes the bottom four strain readings for each run in an attempt to prove a linear strain distribution. Due to the damage at this location, there is some strain redistribution between neighboring strands and the concrete causing the distribution to stray from being exactly linear.

5. Girder 8 Strain Distribution at ~9L/10 - Span 31

	Strain Transducer Readings (με)					
Location	Run 1	Run 2	Run 3	Run 4	Run 5	Height (in.)
midheight of top flange	-0.07	0.72	0.14	-0.03	1.20	41.5
1" below top of CT web	1.14	0.97	0.32	0.38	2.31	37
1" above bottom of CT web	13.36	12.65	9.35	11.75	13.88	14
**midheight of bottom flange	10.12	9.54	7.76	9.20	10.30	3.5
Bot. Face of Flange	N/A	N/A	N/A	N/A	22.09	0

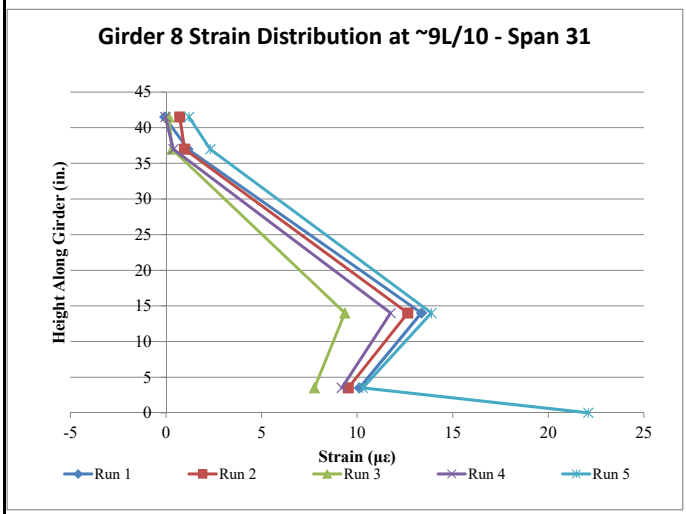

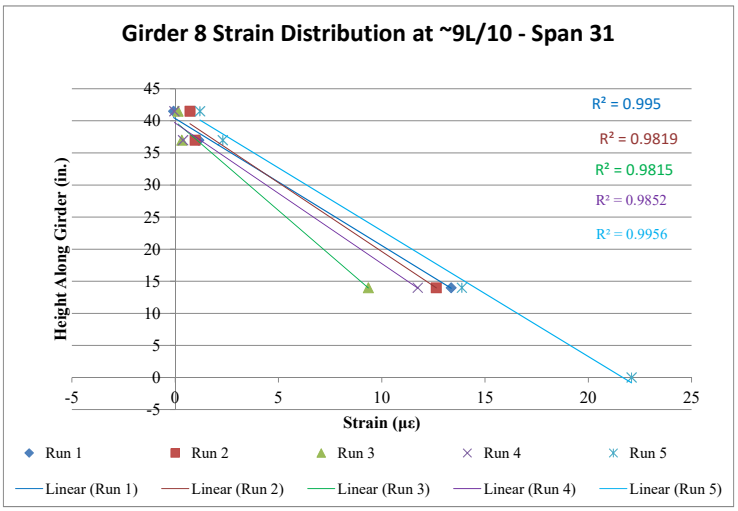

** The plot on the right doesn't include the strain readings at the mid height of the bottom flange. This gauge wasn't attached fully.

NOTES:

1. Girders 7 and 8 have considerable damage as shown in the Inspection Mapping
2. The red highlighted cells with N/A are from wireless connection problems with a node during the load test
3. Height of Girder is with respect to soffitt of bottom flange of girder

REFERENCES:

1. Contract Drawings 171-20G dated July 17, 1995 (South Approach Bridge WBL Widening)
2. VDOT Inspection Report and Damage Mapping Details - WB Structure Dated June 2015

APPENDIX C-4:

WESTBOUND SPAN 32

Live Load Testing Results	VirginiaTech Invent the Future®	Made	JJR	Date	7/11/2016	Job Number	449462
HRBT WESTBOUND STRUCTURE SPAN 32		Checked	EAE	Date	7/21/2016	Connection	
For Hampton Roads Bridge Tunnel		Backchk'd	JJR	Date	7/22/2016	Sheet No.	1

Truck Configuration 1

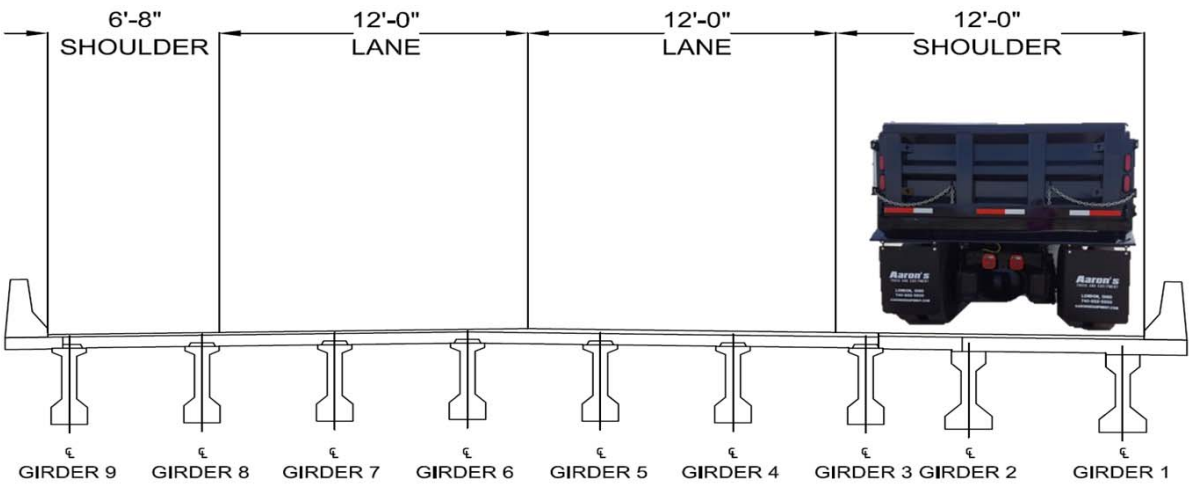

6. Midspan Measurements - Span 32

		Girder 9	Girder 8	Girder 7*	Girder 6	Girder 5	Girder 4	Girder 3	Girder 2	Girder 1
Run 1	Bottom Face of Flange Strain (με) :	-1.45	-0.92	0.56	3.42	6.55	12.12	19.72	23.41	17.57
	String Pot Deflection (in.) :	-0.005	0.001	0.005	0.008	0.014	0.018	0.023	0.027	0.022
	DIC Deflection (in.) :		0.0006	0.0011	0.0040	0.0080				
Run 2	Bottom Face of Flange Strain (με) :	-1.44	-0.34	0.85	3.37	6.62	12.02	19.44	24.01	19.52
	String Pot Deflection (in.) :	-0.004	-0.006	-0.006	0.003	0.004	0.008	0.018	0.02	0.016
	DIC Deflection (in.) :		0.0009	0.0007	0.0044	0.0081				
Run 3	Bottom Face of Flange Strain (με) :	-1.19	-0.41	0.84	3.34	6.61	12.20	19.64	24.03	19.11
	String Pot Deflection (in.) :	0.001	0.002	-0.001	0	0.003	0.01	0.021	0.023	0.017
	DIC Deflection (in.) :		-0.0001	0.0002	0.0022	0.0046				
Run 4	Bottom Face of Flange Strain (με) :	-1.31	-0.53	0.83	3.18	6.33	12.22	19.65	24.34	19.53
	String Pot Deflection (in.) :	-0.004	-0.004	0.002	0.002	0.01	0.018	0.022	0.025	0.017
	DIC Deflection (in.) :		0.0015	0.0019	0.0035	0.0074				
Run 5	Bottom Face of Flange Strain (με) :	-1.30	-0.38	0.68	3.29	6.55	12.11	19.61	24.16	19.47
	String Pot Deflection (in.) :	-0.005	-0.006	-0.004	-0.002	0	0.005	0.016	0.018	0.014
	DIC Deflection (in.) :		0.0009	0.0005	0.0039	0.0061				

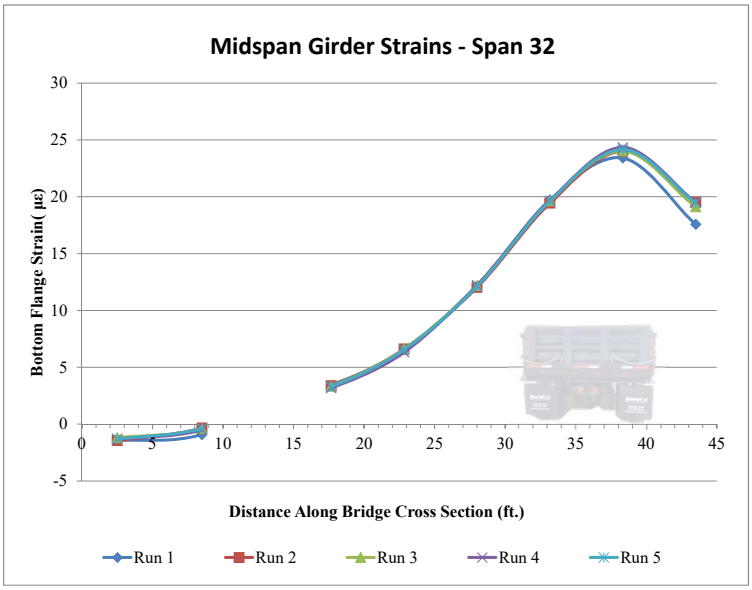

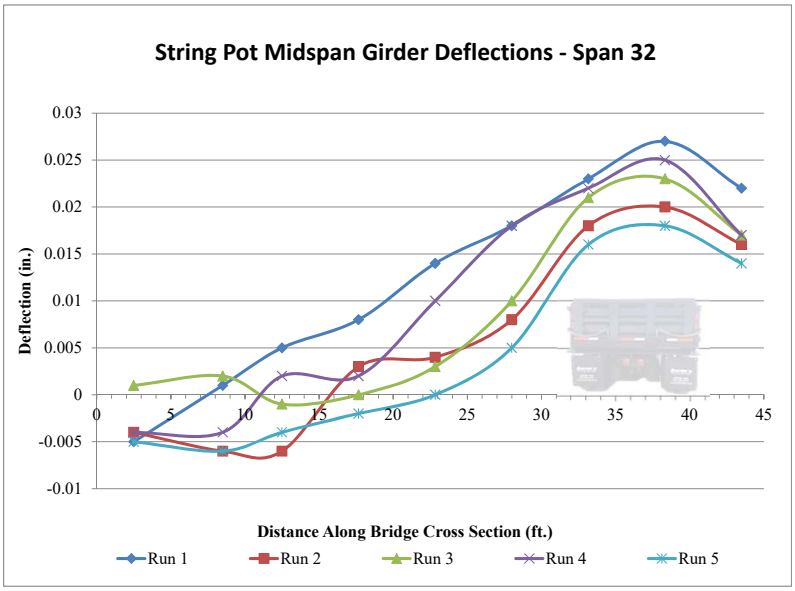

* Girder 7 strain values are low for each configuration. The contact adhesive most likely was not fully adhered. These values are excluded from the girder strain plot.

NOTES:

1. Girders are numbered from the east in accordance with widened bridge plans
2. Spans are numbered starting at the South Island and end at Willoughby Spit
3. Traffic flows from Willoughby Spit to the South Island on the WB Structure
4. Deflection values are given assuming downwards is (+) and upwards is (-)

REFERENCES:

1. Contract Drawings 171-20G dated July 17, 1995 (South Approach Bridge WBL Widening)
2. VDOT Inspection Report and Damage Mapping Details - WB Structure Dated June 2015

Live Load Testing Results HRBT WESTBOUND STRUCTURE SPAN 32 For Hampton Roads Bridge Tunnel	VirginiaTech Invent the Future	Made	JJR	Date	7/11/2016	Job Number	449462
		Checked	EAE	Date	7/21/2016	Connection	
		Backchk'd	JJR	Date	7/22/2016	Sheet No.	1

Truck Configuration 2

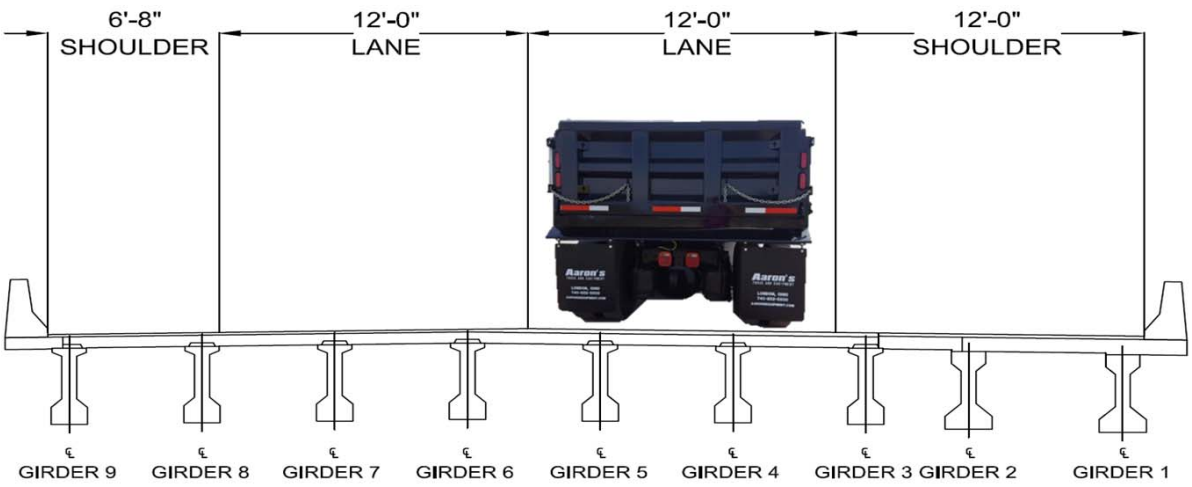

6. Midspan Measurements - Span 32

		Girder 9	Girder 8	Girder 7*	Girder 6	Girder 5	Girder 4	Girder 3	Girder 2	Girder 1
Run 1	Bottom Face of Flange Strain (με) :	0.20	3.18	4.91	12.36	24.04	27.50	15.32	12.61	3.30
	String Pot Deflection (in.) :	-0.001	0.01	0.018	0.027	0.028	0.033	0.024	0.016	0.003
	DIC Deflection (in.) :		0.0045	0.0065	0.0125	0.0175				
Run 2	Bottom Face of Flange Strain (με) :	0.41	2.41	4.24	10.24	21.34	27.24	17.20	13.53	3.79
	String Pot Deflection (in.) :	-0.002	0.008	0.014	0.021	0.022	0.028	0.023	0.015	0.001
	DIC Deflection (in.) :		0.0020	0.0059	0.0097	0.0178				
Run 3	Bottom Face of Flange Strain (με) :	0.68	2.67	4.65	11.30	22.71	27.29	15.71	13.09	4.01
	String Pot Deflection (in.) :	-0.003	0	0.006	0.013	0.018	0.021	0.023	0.016	0.003
	DIC Deflection (in.) :		0.0054	0.0087	0.0115	0.0170				
Run 4	Bottom Face of Flange Strain (με) :	0.69	2.84	4.52	11.64	22.91	27.17	15.38	13.09	4.09
	String Pot Deflection (in.) :	-0.002	0	0.005	0.013	0.021	0.023	0.017	0.01	-0.002
	DIC Deflection (in.) :		0.0051	0.0097	0.0137	0.0190				
Run 5	Bottom Face of Flange Strain (με) :	0.26	2.51	4.33	11.06	21.96	27.14	16.49	13.24	3.86
	String Pot Deflection (in.) :	0.002	0.008	0.009	0.017	0.02	0.021	0.016	0.012	0.003
	DIC Deflection (in.) :		0.0053	0.0068	0.0109	0.0180				

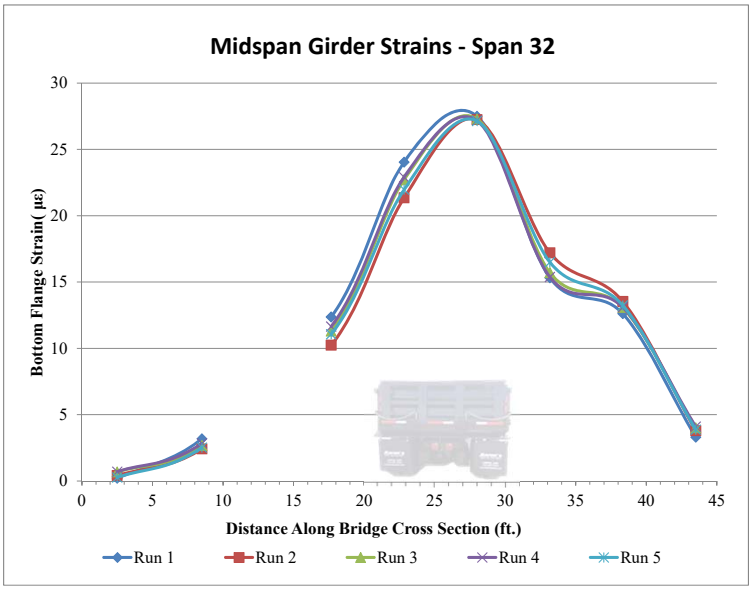

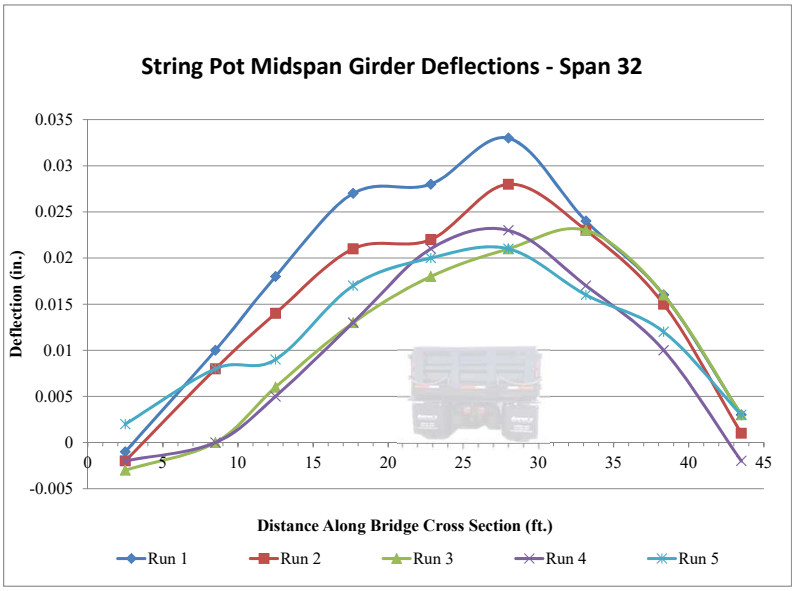

* Girder 7 strain values are low for each configuration. The contact adhesive most likely was not fully adhered. These values are excluded from the girder strain plot.

NOTES:

1. Girders are numbered from the east in accordance with widened bridge plans
2. Spans are numbered starting at the South Island and end at Willoughby Spit
3. Traffic flows from Willoughby Spit to the South Island on the WB Structure
4. Deflection values are given assuming downwards is (+) and upwards is (-)

REFERENCES:

1. Contract Drawings 171-20G dated July 17, 1995 (South Approach Bridge WBL Widening)
2. VDOT Inspection Report and Damage Mapping Details - WB Structure Dated June 2015

Live Load Testing Results	VirginiaTech Invent the Future®	Made	JJR	Date	7/11/2016	Job Number	449462
HRBT WESTBOUND STRUCTURE SPAN 32		Checked	EAE	Date	7/21/2016	Connection	
For Hampton Roads Bridge Tunnel		Backchk'd	JJR	Date	7/22/2016	Sheet No.	1

Truck Configuration 3

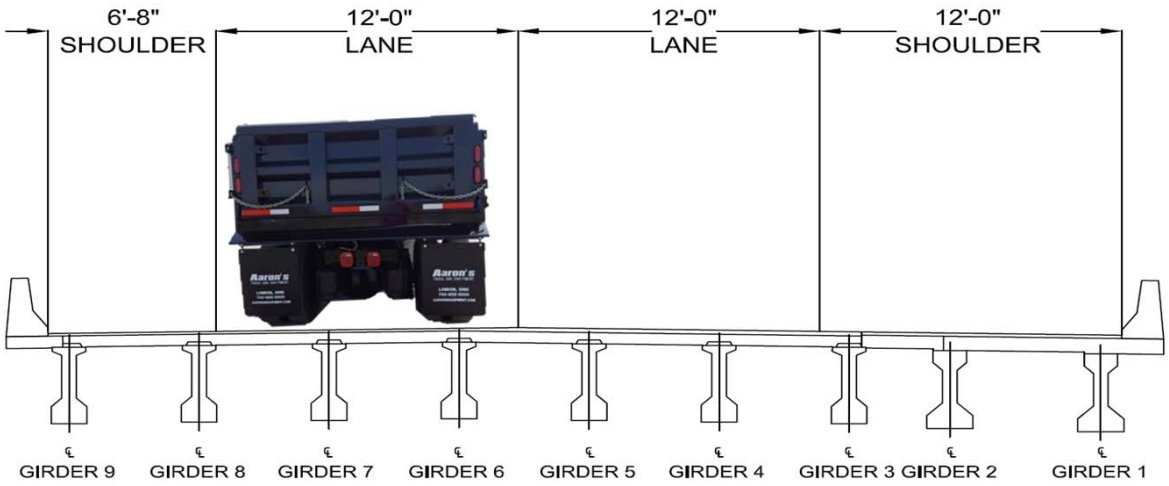

6. Midspan Measurements - Span 32

		Girder 9	Girder 8	Girder 7*	Girder 6	Girder 5	Girder 4	Girder 3	Girder 2	Girder 1
Run 1	Bottom Face of Flange Strain (με) :	11.84	18.05	17.41	21.04	11.96	8.76	4.72	4.39	1.93
	String Pot Deflection (in.) :	0.016	0.023	0.028	0.021	0.017	0.007	-0.002	-0.005	-0.008
	DIC Deflection (in.) :		0.0183	0.0189	0.0168	0.0125				
Run 2	Bottom Face of Flange Strain (με) :	12.30	17.65	16.61	18.60	10.02	7.34	3.67	3.27	0.97
	String Pot Deflection (in.) :	0.022	0.024	0.029	0.028	0.017	0.008	0.001	-0.001	-0.003
	DIC Deflection (in.) :		0.0190	0.0198	0.0176	0.0128				
Run 3	Bottom Face of Flange Strain (με) :	11.64	17.00	16.77	18.80	10.03	7.21	3.79	3.38	1.03
	String Pot Deflection (in.) :	0.015	0.021	0.027	0.025	0.014	0.007	0	-0.003	-0.005
	DIC Deflection (in.) :		0.0181	0.0185	0.0148	0.0101				
Run 4	Bottom Face of Flange Strain (με) :	11.02	15.59	16.48	20.02	11.02	7.86	4.08	3.73	1.20
	String Pot Deflection (in.) :	0.015	0.026	0.03	0.027	0.017	0.013	0.005	0.003	-0.002
	DIC Deflection (in.) :		0.0179	0.0199	0.0164	0.0125				
Run 5	Bottom Face of Flange Strain (με) :	12.65	18.17	17.47	20.79	11.74	8.95	4.76	5.10	3.04
	String Pot Deflection (in.) :	0.011	0.018	0.024	0.021	0.011	0.002	-0.001	-0.003	-0.006
	DIC Deflection (in.) :		0.0174	0.0189	0.0157	0.0114				

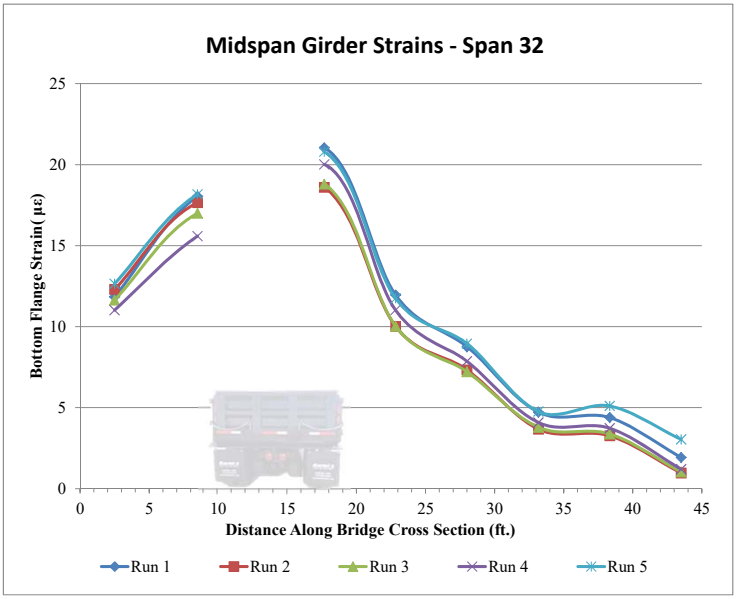

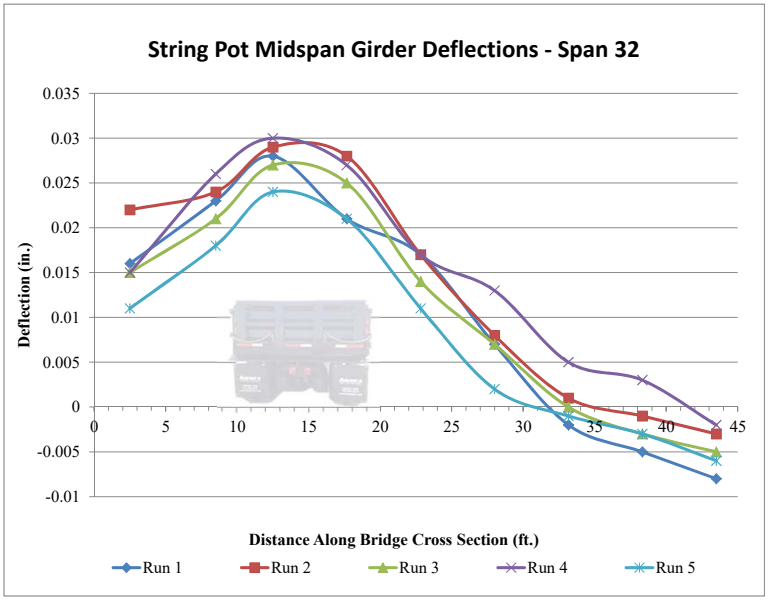

* Girder 7 strain values are low for each configuration. The contact adhesive most likely was not fully adhered. These values are excluded from the girder strain plot.

NOTES:

1. Girders are numbered from the east in accordance with widened bridge plans
2. Spans are numbered starting at the South Island and end at Willoughby Spit
3. Traffic flows from Willoughby Spit to the South Island on the WB Structure
4. Deflection values are given assuming downwards is (+) and upwards is (-)

REFERENCES:

1. Contract Drawings 171-20G dated July 17, 1995 (South Approach Bridge WBL Widening)
2. VDOT Inspection Report and Damage Mapping Details - WB Structure Dated June 2015

Truck Configuration 3 Continued

7. Girder 7 Strain Distribution at Midspan - Span 32

	Strain Transducer Readings (με)					
Location	Run 1	Run 2	Run 3	Run 4	Run 5	Height (in.)
midheight of top flange	-3.74	-5.02	-5.61	-4.99	-1.36	41.5
1" above bottom of CT web	14.33	12.65	12.57	12.22	15.40	14
**Bot. Face of Flange	17.41	16.61	16.77	16.48	17.47	0

** This is the same problematic gauge from the previous page. The contact adhesive most likely was not fully adhered making the strain values "softened" and not fully capturing

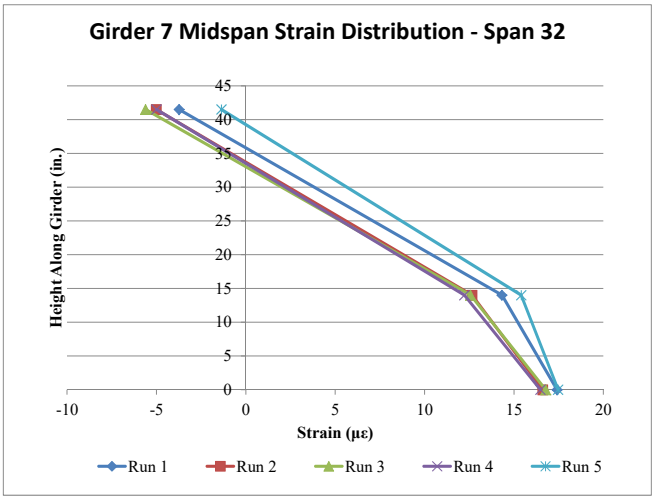

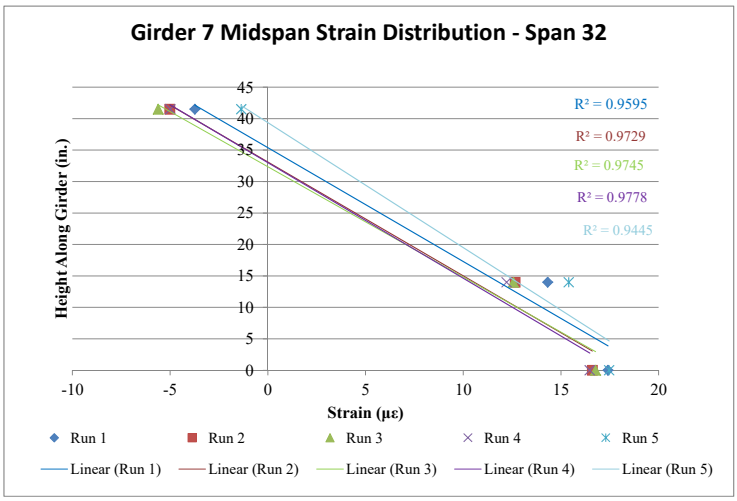

8. Girder 8 Strain Distribution at Midspan - Span 32

	Strain Transducer Readings (με)					
Location	Run 1	Run 2	Run 3	Run 4	Run 5	Height (in.)
midheight of top flange	-2.84	-2.53	-2.53	-2.10	-1.31	41.5
1" above bottom of CT web	13.09	12.07	11.56	11.05	13.62	14
Bot. Face of Flange	18.05	13.85	13.20	11.79	18.17	0

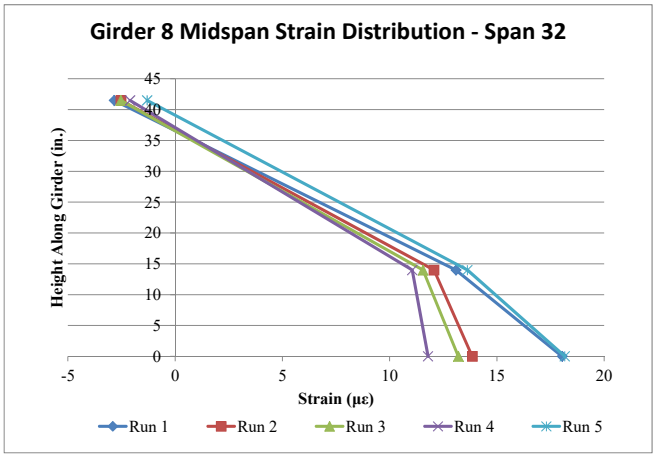

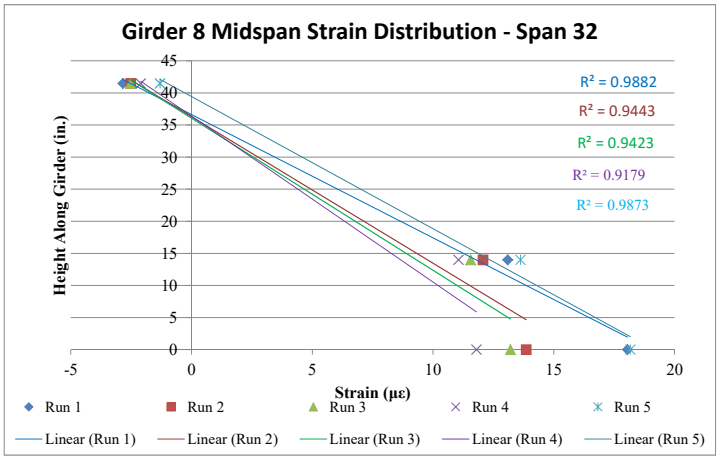

NOTES:

1. Height of Girder is with respect to soffitt of bottom flange of girder

REFERENCES:

1. Contract Drawings 171-20G dated July 17, 1995 (South Approach Bridge WBL Widening)
2. VDOT Inspection Report and Damage Mapping Details - WB Structure Dated June 2015

Truck Configuration 3 Continued

7. Girder 8 Strain Distribution at ~9L/10 - Span 32

	Strain Transducer Readings (με)					
Location	Run 1	Run 2	Run 3	Run 4	Run 5	Height (in.)
midheight of top flange	0.40	1.08	1.66	1.92	0.85	41.5
1" above bottom of CT web	3.62	3.66	3.73	3.68	3.25	14
Bot. Face of Flange	7.16	5.94	5.89	5.39	7.79	0

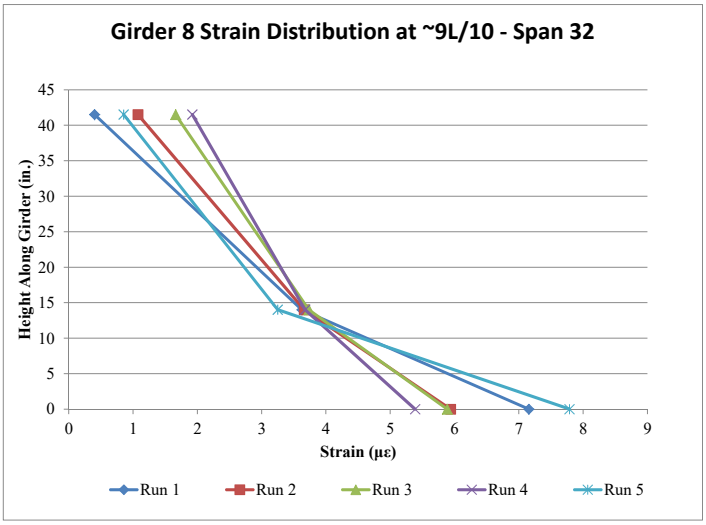

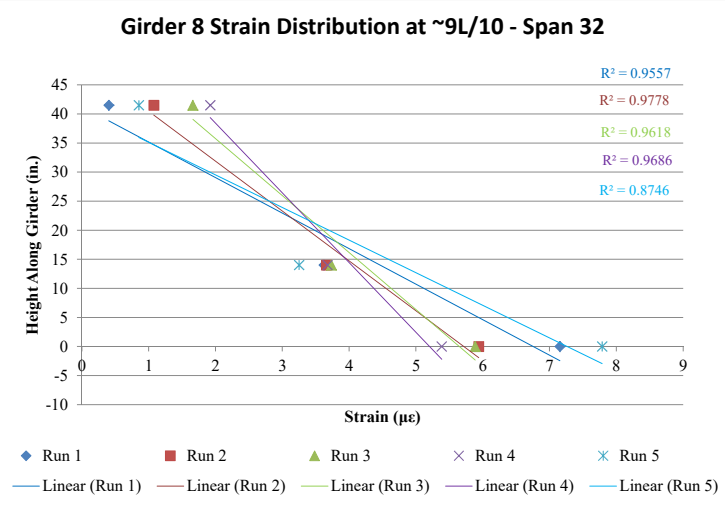

NOTES:

1. Height of Girder is with respect to soffitt of bottom flange of girder

REFERENCES:

1. Contract Drawings 171-20G dated July 17, 1995 (South Approach Bridge WBL Widening)
2. VDOT Inspection Report and Damage Mapping Details - WB Structure Dated June 2015

Live Load Testing Results	VirginiaTech Invent the Future®	Made	JJR	Date	7/11/2016	Job Number	449462
HRBT WESTBOUND STRUCTURE SPAN 32		Checked	EAE	Date	7/21/2016	Connection	
For Hampton Roads Bridge Tunnel		Backchk'd	JJR	Date	7/22/2016	Sheet No.	1

Truck Configuration 4

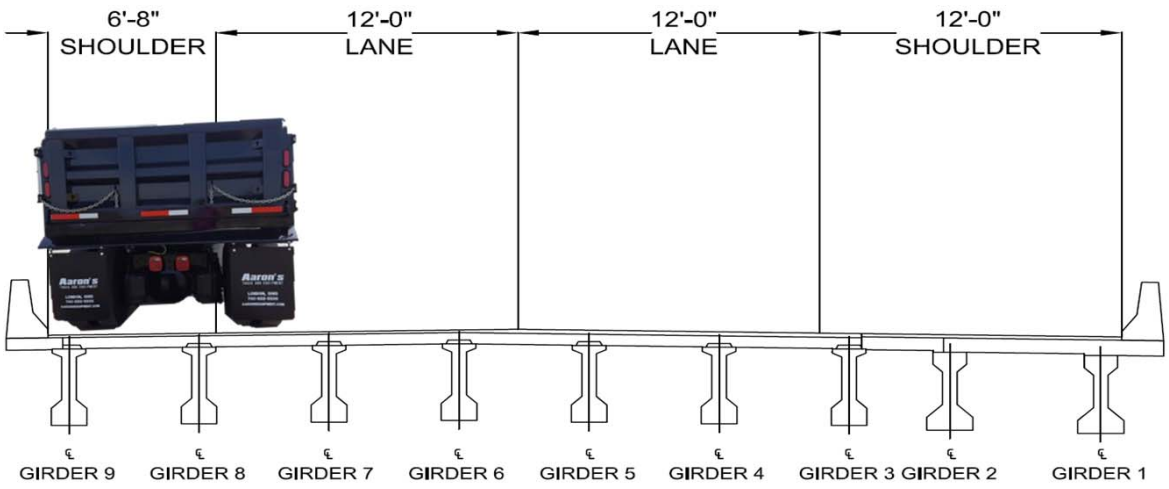

6. Midspan Measurements - Span 32

		Girder 9	Girder 8	Girder 7*	Girder 6	Girder 5	Girder 4	Girder 3	Girder 2	Girder 1
Run 1	Bottom Face of Flange Strain (με) :	31.62	27.70	14.33	11.02	7.55	5.12	2.86	3.15	2.34
	String Pot Deflection (in.) :	0.04	0.032	0.023	0.01	0.007	0.006	-0.001	-0.002	-0.004
	DIC Deflection (in.) :		0.0241	0.0177	0.0106	0.0071				
Run 2	Bottom Face of Flange Strain (με) :	34.16	23.71	22.65	3.95	5.38	2.95	-0.40	-0.04	-0.46
	String Pot Deflection (in.) :	0.035	0.028	0.021	0.006	0.002	-0.003	-0.001	-0.005	-0.009
	DIC Deflection (in.) :		0.0259	0.0195	0.0123	0.0060				
Run 3	Bottom Face of Flange Strain (με) :	34.39	23.10	23.15	3.98	5.26	2.90	-0.52	-0.11	-0.50
	String Pot Deflection (in.) :	0.036	0.027	0.019	0.015	0.011	0.006	-0.001	0	-0.003
	DIC Deflection (in.) :		0.0246	0.0164	0.0107	0.0065				
Run 4	Bottom Face of Flange Strain (με) :	33.31	23.48	23.65	3.98	5.53	2.76	-0.55	-0.23	-0.68
	String Pot Deflection (in.) :	0.037	0.032	0.027	0.016	0.003	0	-0.002	-0.003	-0.004
	DIC Deflection (in.) :		0.0255	0.0184	0.0110	0.0057				
Run 5	Bottom Face of Flange Strain (με) :	32.86	27.13	14.53	11.13	7.16	5.05	2.49	3.36	2.92
	String Pot Deflection (in.) :	0.037	0.027	0.022	0.012	0.005	0	-0.003	-0.004	-0.006
	DIC Deflection (in.) :		0.0255	0.0191	0.0133	0.0086				

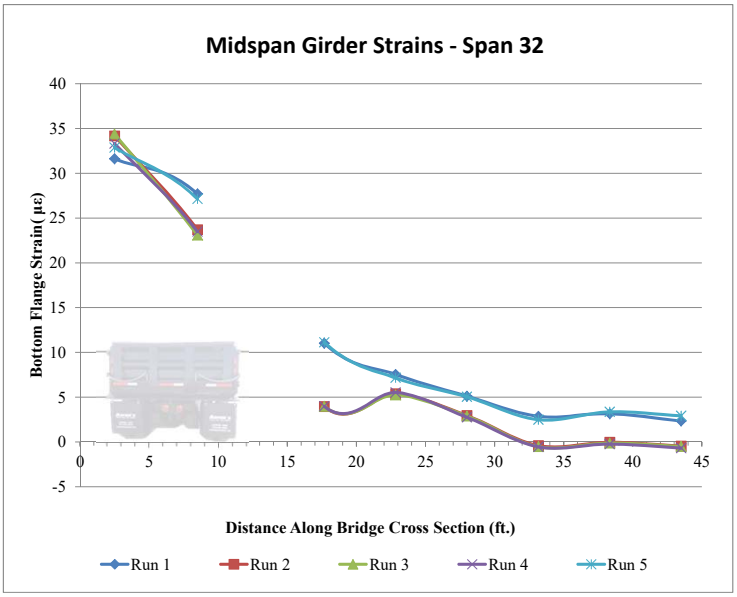

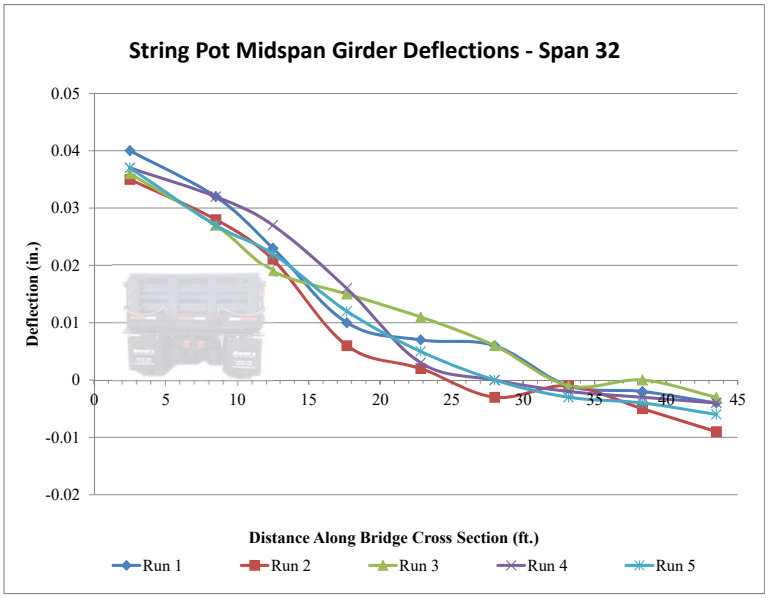

* Girder 7 strain values are low for each configuration. The contact adhesive most likely was not fully adhered. These values are excluded from the girder strain plot.

NOTES:

1. Girders are numbered from the east in accordance with widened bridge plans
2. Spans are numbered starting at the South Island and end at Willoughby Spit
3. Traffic flows from Willoughby Spit to the South Island on the WB Structure
4. Deflection values are given assuming downwards is (+) and upwards is (-)

REFERENCES:

1. Contract Drawings 171-20G dated July 17, 1995 (South Approach Bridge WBL Widening)
2. VDOT Inspection Report and Damage Mapping Details - WB Structure Dated June 2015

Truck Configuration 4 Continued

7. Girder 7 Strain Distribution at Midspan - Span 32

	Strain Transducer Readings (με)					
Location	Run 1	Run 2	Run 3	Run 4	Run 5	Height (in.)
midheight of top flange	-4.17	-5.73	-5.92	-5.32	-1.51	41.5
1" above bottom of CT web	11.30	9.32	8.77	14.85	12.25	14
**Bot. Face of Flange	14.33	13.66	12.45	25.32	14.53	0

** This is the same problematic gauge from the previous page. The contact adhesive most likely was not fully adhered making the strain values "softened" and not fully capturing

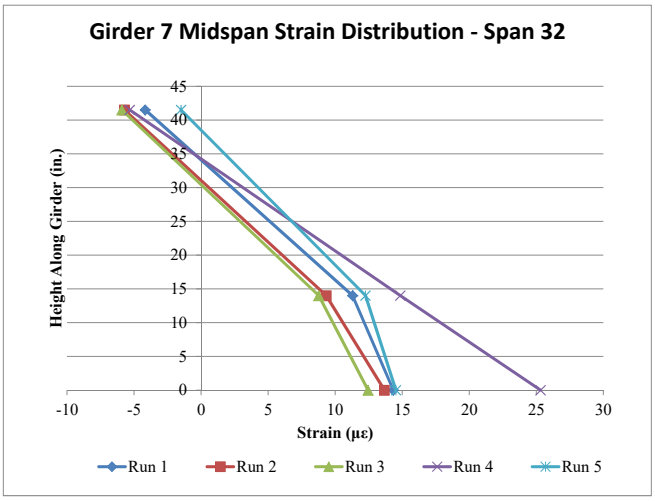

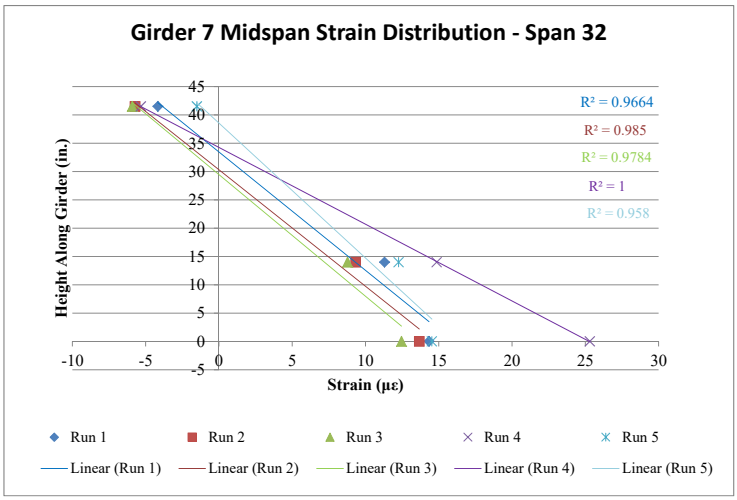

8. Girder 8 Strain Distribution at Midspan - Span 32

	Strain Transducer Readings (με)					
Location	Run 1	Run 2	Run 3	Run 4	Run 5	Height (in.)
midheight of top flange	-3.99	-2.74	-2.78	-3.27	-2.48	41.5
1" above bottom of CT web	18.18	16.32	16.35	16.27	18.48	14
Bot. Face of Flange	27.70	22.12	21.90	21.72	27.13	0

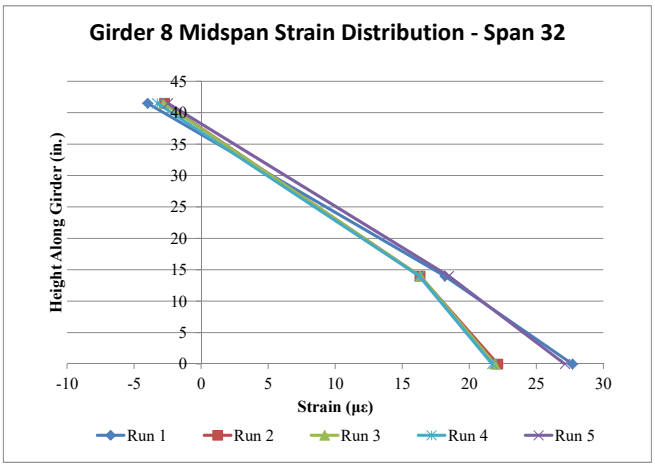

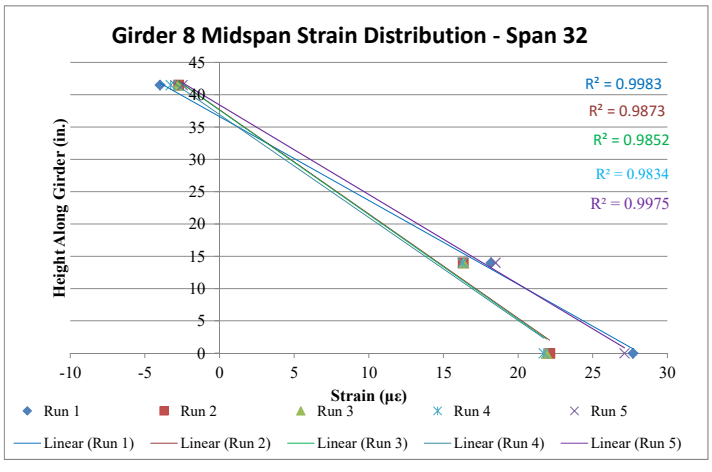

NOTES:

1. Height of Girder is with respect to soffitt of bottom flange of girder

REFERENCES:

1. Contract Drawings 171-20G dated July 17, 1995 (South Approach Bridge WBL Widening)
2. VDOT Inspection Report and Damage Mapping Details - WB Structure Dated June 2015

Truck Configuration 4 Continued

7. Girder 8 Strain Distribution at ~9L/10 - Span 32

	Strain Transducer Readings (με)					
Location	Run 1	Run 2	Run 3	Run 4	Run 5	Height (in.)
midheight of top flange	-0.62	0.84	-0.07	-0.23	-0.15	41.5
1" above bottom of CT web	5.12	4.71	5.02	4.92	4.13	14
Bot. Face of Flange	12.58	10.02	10.66	10.60	11.84	0

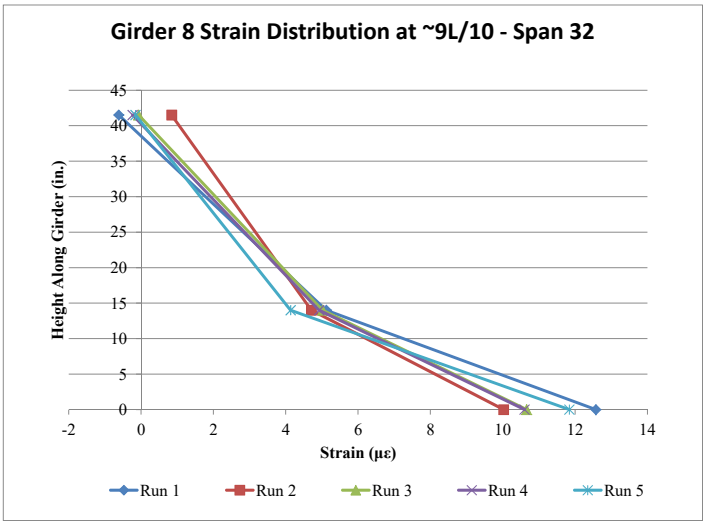

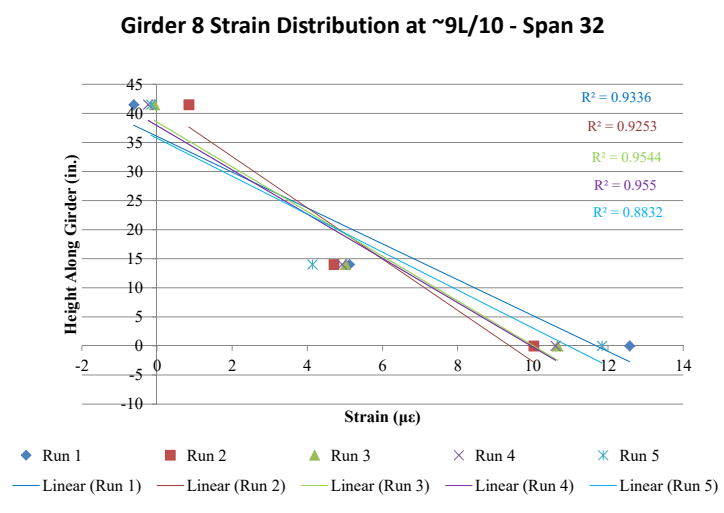

NOTES:

1. Height of Girder is with respect to soffitt of bottom flange of girder

REFERENCES:

1. Contract Drawings 171-20G dated July 17, 1995 (South Approach Bridge WBL Widening)
2. VDOT Inspection Report and Damage Mapping Details - WB Structure Dated June 2015

Live Load Testing Results	VirginiaTech Invent the Future®	Made	JJR	Date	7/11/2016	Job Number	449462
HRBT WESTBOUND STRUCTURE SPAN 32		Checked	EAE	Date	7/21/2016	Connection	
For Hampton Roads Bridge Tunnel		Backchk'd	JJR	Date	7/22/2016	Sheet No.	1

Truck Configuration 5

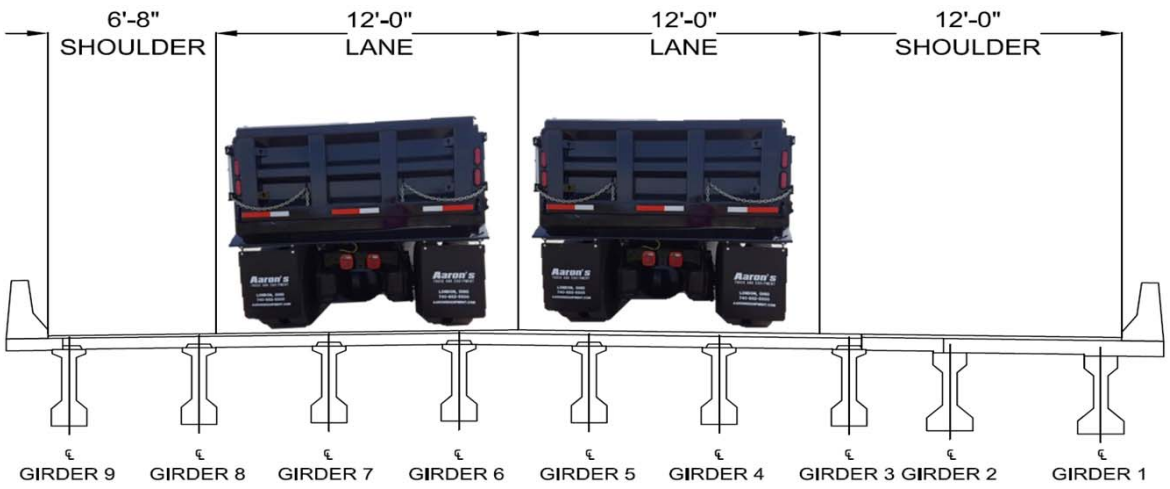

6. Midspan Measurements - Span 32

		Girder 9	Girder 8	Girder 7*	Girder 6	Girder 5	Girder 4	Girder 3	Girder 2	Girder 1
Run 1	Bottom Face of Flange Strain (με) :	13.33	22.52	23.88	34.41	34.11	34.07	20.53	16.95	5.70
	String Pot Deflection (in.) :	0.008	0.015	0.028	0.037	0.029	0.026	0.018	0.011	-0.004
	DIC Deflection (in.) :		0.0221	0.0278	0.0306	0.0308				
Run 2	Bottom Face of Flange Strain (με) :	12.23	19.91	22.38	30.93	31.20	32.44	19.62	14.72	3.31
	String Pot Deflection (in.) :	0.01	0.024	0.038	0.037	0.035	0.03	0.013	0.001	-0.005
	DIC Deflection (in.) :		0.0212	0.0257	0.0292	0.0287				
Run 3	Bottom Face of Flange Strain (με) :	10.90	18.65	22.27	32.09	31.83	32.69	19.63	14.98	3.43
	String Pot Deflection (in.) :	0.015	0.023	0.037	0.036	0.031	0.022	0.01	0.002	-0.006
	DIC Deflection (in.) :		0.0195	0.0250	0.0266	0.0249				
Run 4	Bottom Face of Flange Strain (με) :	11.50	19.36	21.07	30.03	30.35	32.10	19.18	14.61	3.30
	String Pot Deflection (in.) :	0.012	0.025	0.038	0.038	0.036	0.03	0.023	0.011	-0.006
	DIC Deflection (in.) :		0.0225	0.0291	0.0315	0.0317				
Run 5	Bottom Face of Flange Strain (με) :	14.62	22.71	24.50	33.42	34.67	33.32	18.21	15.37	5.40
	String Pot Deflection (in.) :	0.014	0.026	0.035	0.038	0.037	0.024	0.015	0.006	-0.006
	DIC Deflection (in.) :		0.0212	0.0288	0.0310	0.0284				

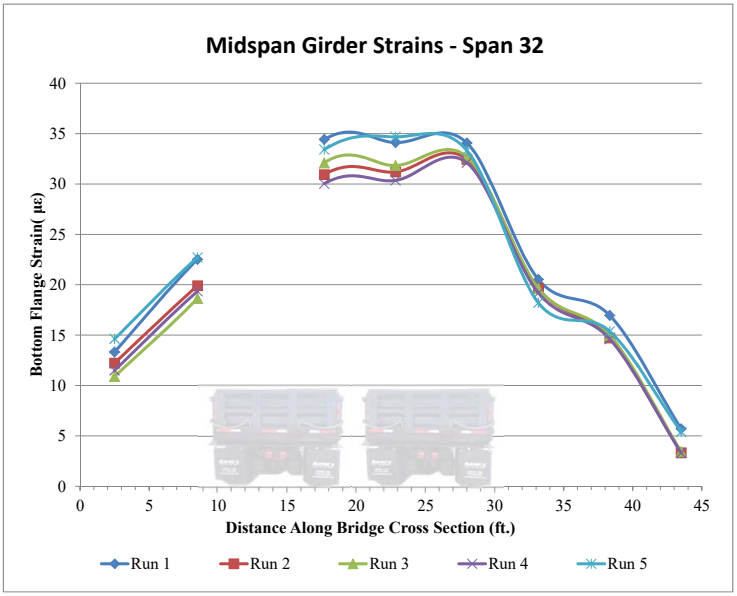

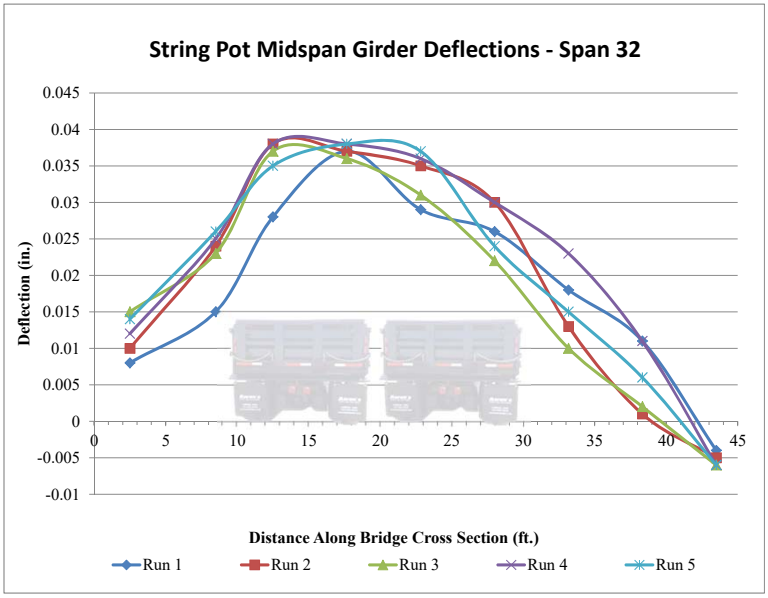

* Girder 7 strain values are low for each configuration. The contact adhesive most likely was not fully adhered. These values are excluded from the girder strain plot.

NOTES:

1. Girders are numbered from the east in accordance with widened bridge plans
2. Spans are numbered starting at the South Island and end at Willoughby Spit
3. Traffic flows from Willoughby Spit to the South Island on the WB Structure
4. Deflection values are given assuming downwards is (+) and upwards is (-)

REFERENCES:

1. Contract Drawings 171-20G dated July 17, 1995 (South Approach Bridge WBL Widening)
2. VDOT Inspection Report and Damage Mapping Details - WB Structure Dated June 2015

Truck Configuration 5 Continued

7. Girder 7 Strain Distribution at Midspan - Span 32

	Strain Transducer Readings (με)					
Location	Run 1	Run 2	Run 3	Run 4	Run 5	Height (in.)
midheight of top flange	-5.42	-7.46	-7.92	-7.77	-2.97	41.5
1" above bottom of CT web	20.13	17.53	17.08	17.08	20.99	14
**Bot. Face of Flange	23.88	22.38	22.27	21.07	24.50	0

** This is the same problematic gauge from the previous page. The contact adhesive most likely was not fully adhered making the strain values "softened" and not fully capturing

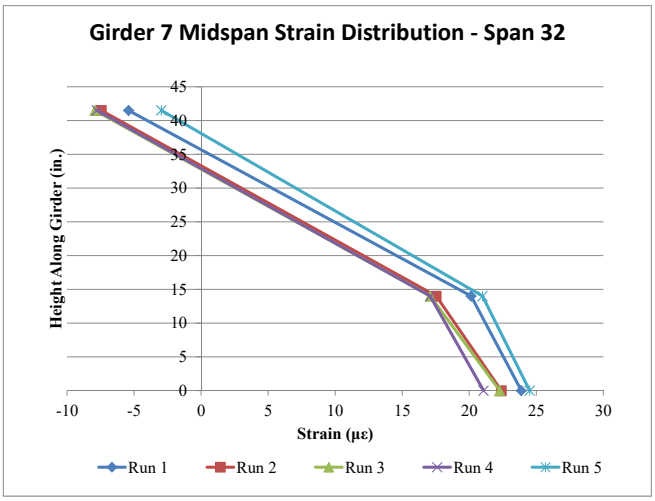

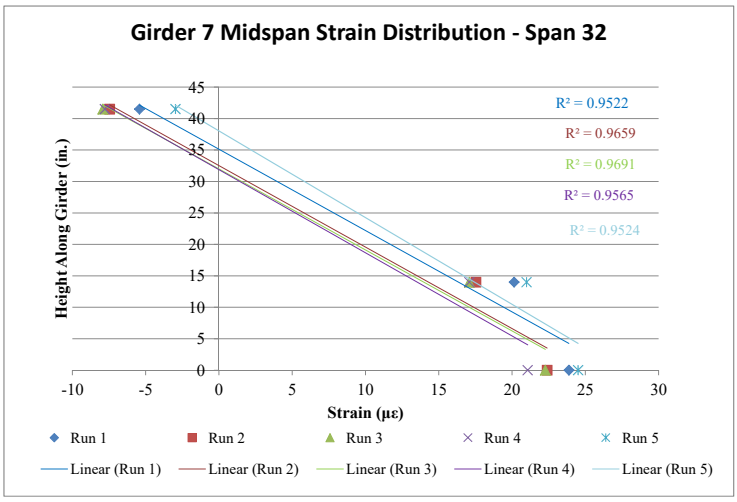

8. Girder 8 Strain Distribution at Midspan - Span 32

	Strain Transducer Readings (με)					
Location	Run 1	Run 2	Run 3	Run 4	Run 5	Height (in.)
midheight of top flange	-3.21	-3.65	-3.08	-3.68	-1.87	41.5
1" above bottom of CT web	16.71	13.82	12.88	13.09	17.07	14
Bot. Face of Flange	22.52	16.11	14.85	15.56	22.71	0

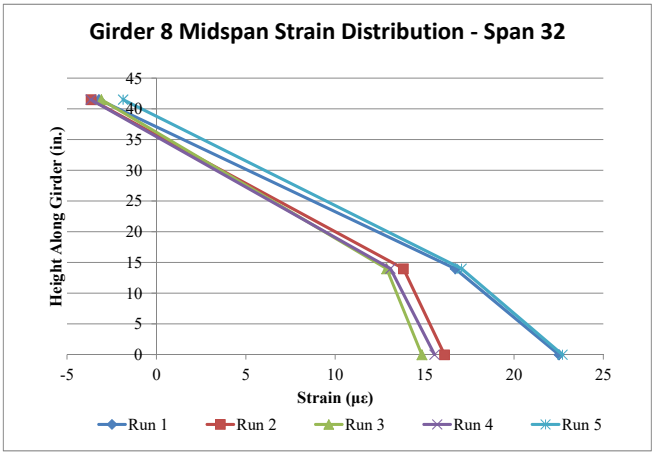

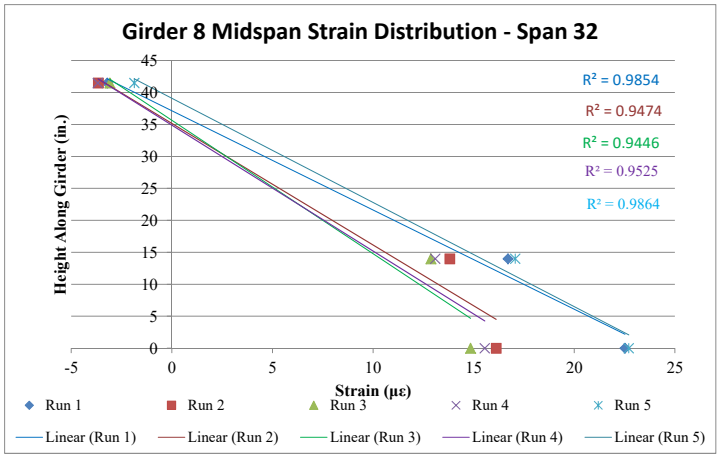

NOTES:

1. Height of Girder is with respect to soffitt of bottom flange of girder

REFERENCES:

1. Contract Drawings 171-20G dated July 17, 1995 (South Approach Bridge WBL Widening)
2. VDOT Inspection Report and Damage Mapping Details - WB Structure Dated June 2015

Truck Configuration 5 Continued

7. Girder 8 Strain Distribution at ~9L/10 - Span 32

	Strain Transducer Readings (με)					
Location	Run 1	Run 2	Run 3	Run 4	Run 5	Height (in.)
midheight of top flange	-0.14	0.91	0.27	-0.07	0.99	41.5
1" above bottom of CT web	5.12	4.00	3.94	4.04	4.39	14
Bot. Face of Flange	9.72	6.34	6.65	7.05	9.17	0

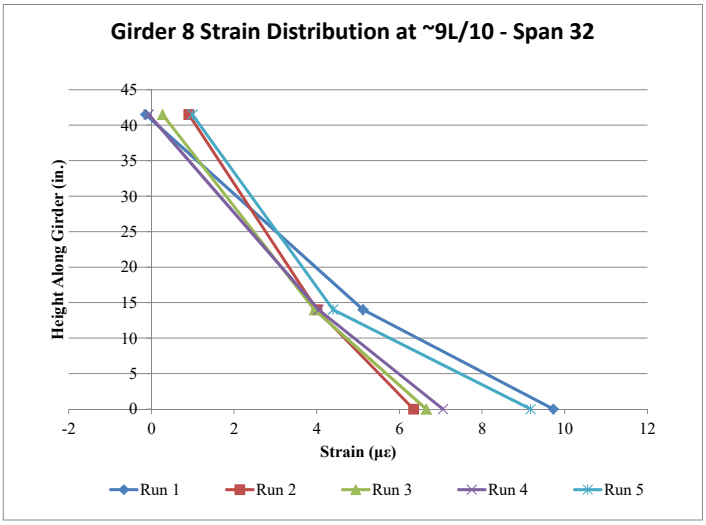

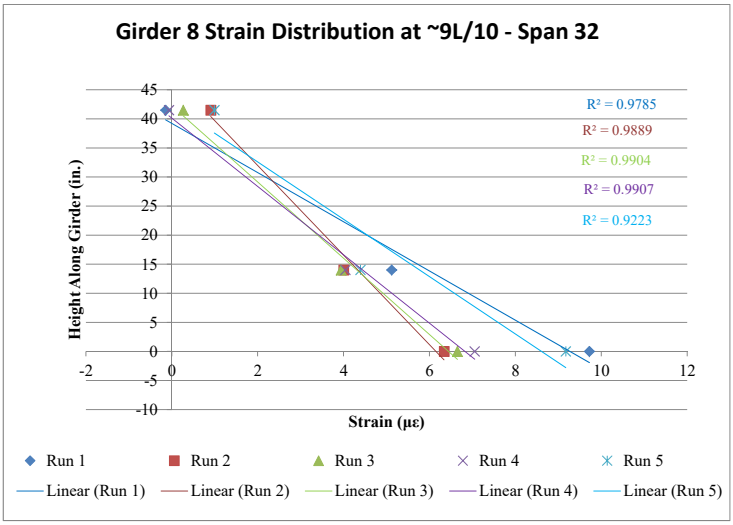

NOTES:

1. Height of Girder is with respect to soffitt of bottom flange of girder

REFERENCES:

1. Contract Drawings 171-20G dated July 17, 1995 (South Approach Bridge WBL Widening)
2. VDOT Inspection Report and Damage Mapping Details - WB Structure Dated June 2015

APPENDIX C-5:

WESTBOUND SPAN 34

Live Load Testing Results HRBT WESTBOUND STRUCTURE SPAN 34 For Hampton Roads Bridge Tunnel	UNIVERSITY of VIRGINIA SCHOOL OF ENGINEERING	Made AB	Date 8/4/2016	Job Number XXXXX
		Checked	Date	Connection
		Backchk'd	Date	Sheet No. 1

Truck Configuration 1

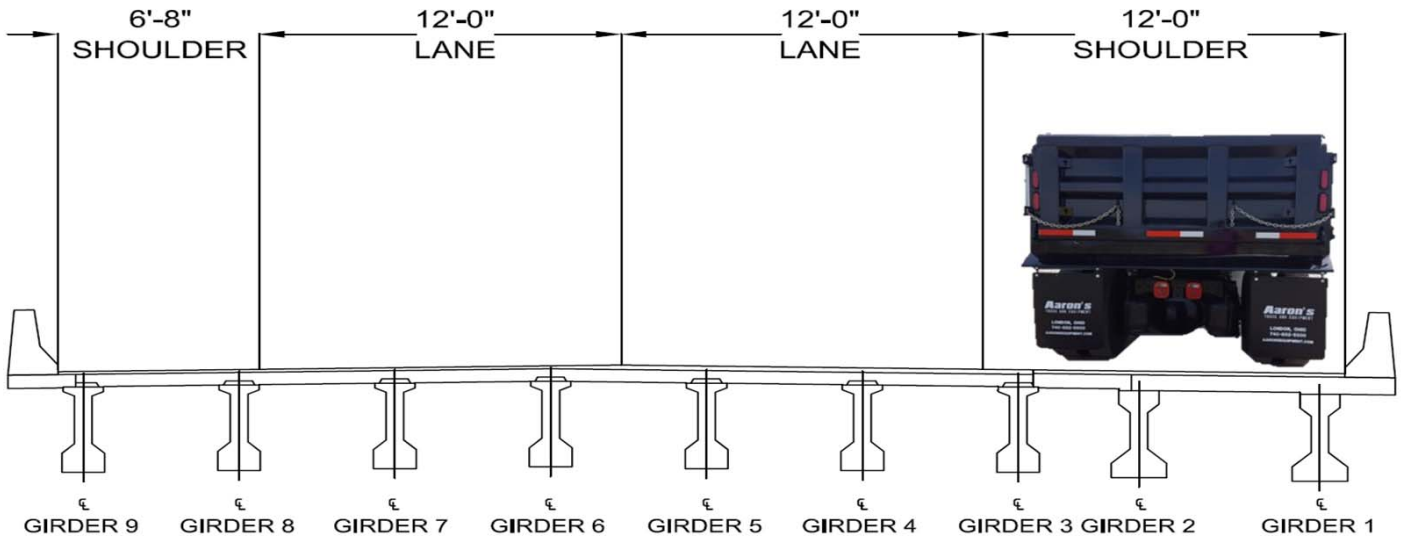

1. Midspan Measurements

		Girder 9*	Girder 8*	Girder 7	Girder 6*	Girder 5*	Girder 4*	Girder 3	Girder 2*	Girder 1
Run 1	Bottom Face of Flange Strain (με) :	-0.05	-0.19	0.97	1.58	3.33	5.33	18.38	11.66	18.81
	Deflection (in.) :	-0.005	-0.002	0.000	0.002	0.007	0.013	0.020	N/A	0.019
Run 2	Bottom Face of Flange Strain (με) :	0.05	-0.65	0.47	1.06	3.04	4.20	15.91	11.24	19.57
	Deflection (in.) :	-0.003	-0.001	0.000	0.000	0.006	0.007	0.013	N/A	0.014
Run 3	Bottom Face of Flange Strain (με) :	-0.67	0.11	1.18	1.37	3.58	5.05	18.59	11.85	18.79
	Deflection (in.) :	-0.003	-0.003	0.000	0.002	0.006	0.013	0.019	N/A	0.018

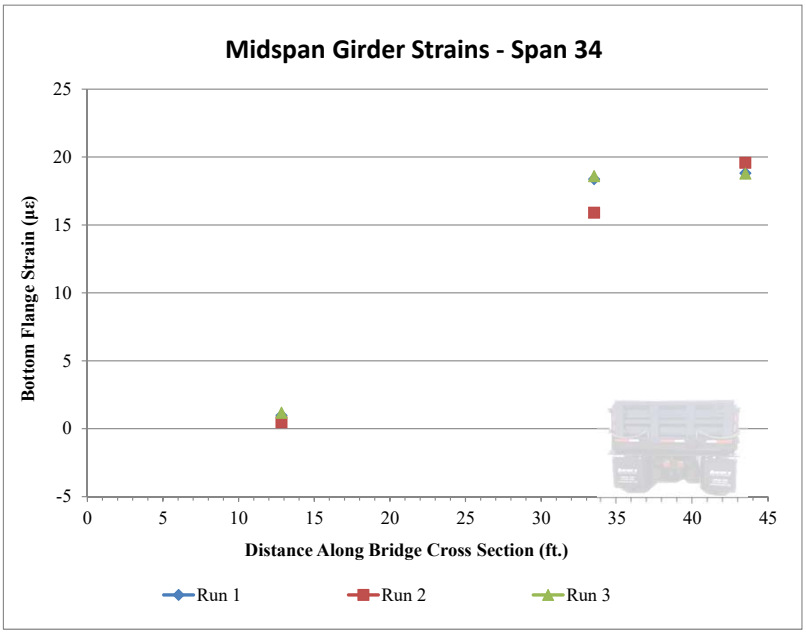

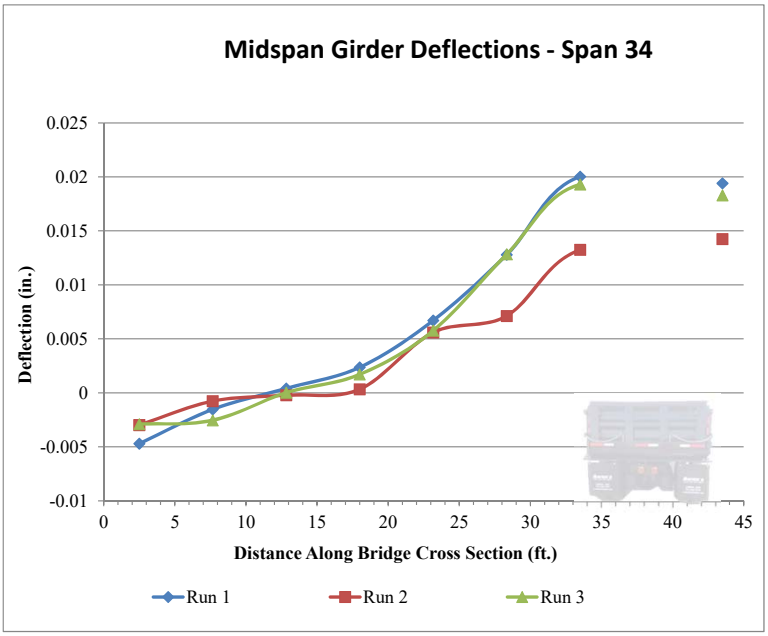

Note: Strain measurments for girder locations 2, 4, 5, 6, 8, and 9 (G2, G4, G5, G6, G8, and G9) not included in figures due to uncertainty surrounding the validity. It was noted during installation of gauges on G8 and G9 that adhesion was difficult; however, the cause of the inconsistency in the other gauges is uncertain and may be attributed to poor calibration.

Note: The midspan deflection of girder 2 is not included in the plots due to low quality images aquired during testing, which could not be resolved.

NOTES:

1. Girders are numbered from the east in accordance with widened bridge plans
2. Spans are numbered starting at the South Island and end at Willoughby Spit
3. Traffic flows from Willoughby Spit to the South Island on the WB Structure
4. Girder 4 has considerable damage as shown in the Inspection Mapping
5. Deflection values are given assuming downwards is (+) and upwards is (-)

REFERENCES:

1. As - Built Contract Drawings T-3 (224-03) dated December 1977
2. VDOT July 2014 Special Inspection Report for EB South Approach Bridge

Truck Configuration 1 Continued

2. Girder 3 Strain Distribution at 6 ft.

	**Strain Transducer Readings (με)			
Location	Run 1	Run 2	Run 3	Height (in.)
9" below top of CT web	0.08	-0.35	-0.39	23.5
Bot. Face of Flange	7.60	8.08	7.89	0

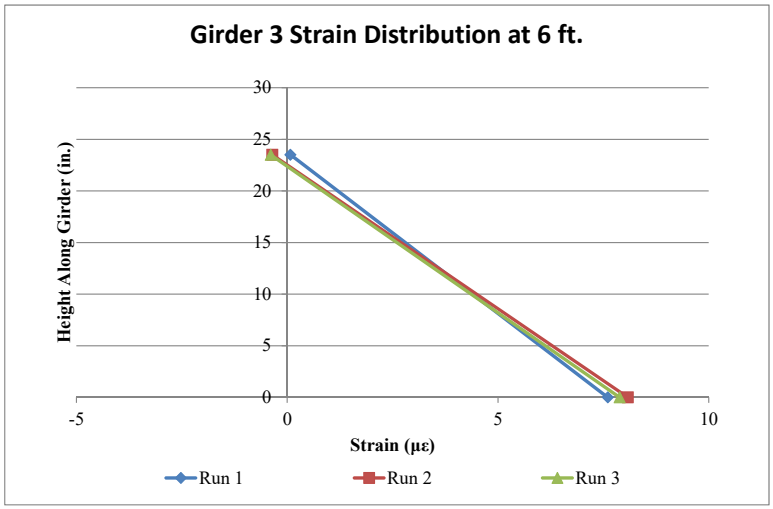

** Raw strain signals were processed for removing residual strain in signals.

3. Girder 4 Strain Distribution at 6 ft.

	**Strain Transducer Readings (με)			
Location	Run 1	Run 2	Run 3	Height (in.)
9" below top of CT web	-0.39	-0.28	0.02	23.5
Bot. Face of Flange	2.24	2.16	2.16	0

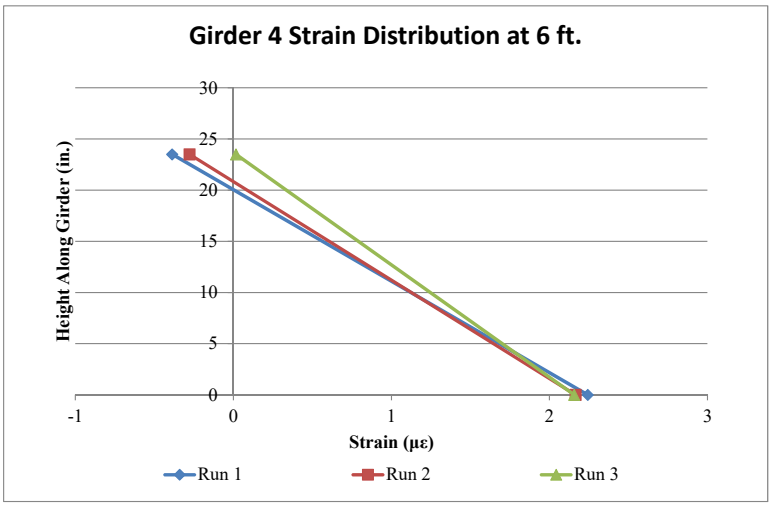

NOTES:

1. Girders are numbered from the east in accordance with widened bridge plans
2. Spans are numbered starting at the South Island and end at Willoughby Spit
3. Traffic flows from Willoughby Spit to the South Island on the WB Structure
4. Girder 4 has considerable damage as shown in the Inspection Mapping
5. Deflection values are given assuming downwards is (+) and upwards is (-)

REFERENCES:

1. As - Built Contract Drawings T-3 (224-03) dated December 1977
2. VDOT July 2014 Special Inspection Report for EB South Approach Bridge

Truck Configuration 1 Continued

4. Girder 5 Strain Distribution at 6 ft.

	**Strain Transducer Readings (με)			
Location	Run 1	Run 2	Run 3	Height (in.)
9" below top of CT web	0.07	0.01	0.12	23.5
Bot. Face of Flange	1.82	2.01	1.90	0

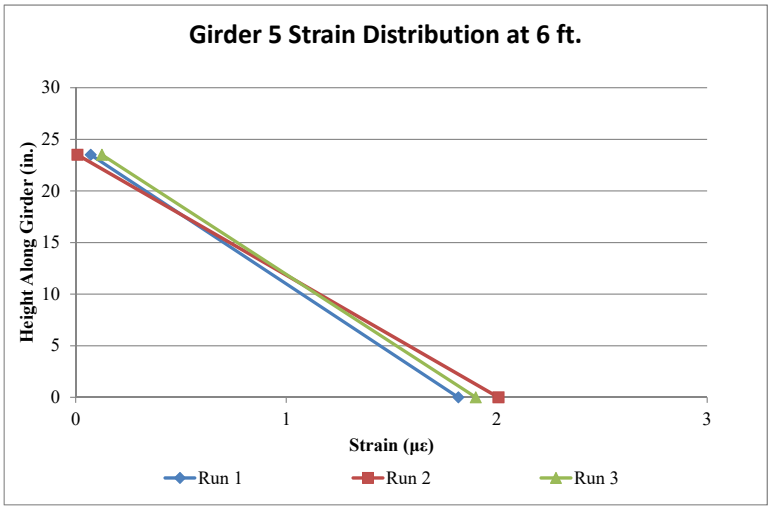

** Raw strain signals were processed for removing residual strain in signals.

NOTES:

1. Girders are numbered from the east in accordance with widened bridge plans
2. Spans are numbered starting at the South Island and end at Willoughby Spit
3. Traffic flows from Willoughby Spit to the South Island on the WB Structure
4. Girder 4 has considerable damage as shown in the Inspection Mapping
5. Deflection values are given assuming downwards is (+) and upwards is (-)

REFERENCES:

1. As - Built Contract Drawings T-3 (224-03) dated December 1977
2. VDOT July 2014 Special Inspection Report for EB South Approach Bridge

Live Load Testing Results		Made	AB	Date	8/4/2016	Job Number	XXXXX
HRBT WESTBOUND STRUCTURE SPAN 34	UNIVERSITY of VIRGINIA SCHOOL OF ENGINEERING	Checked		Date		Connection	
For Hampton Roads Bridge Tunnel		Backchk'd		Date		Sheet No.	1

Truck Configuration 2

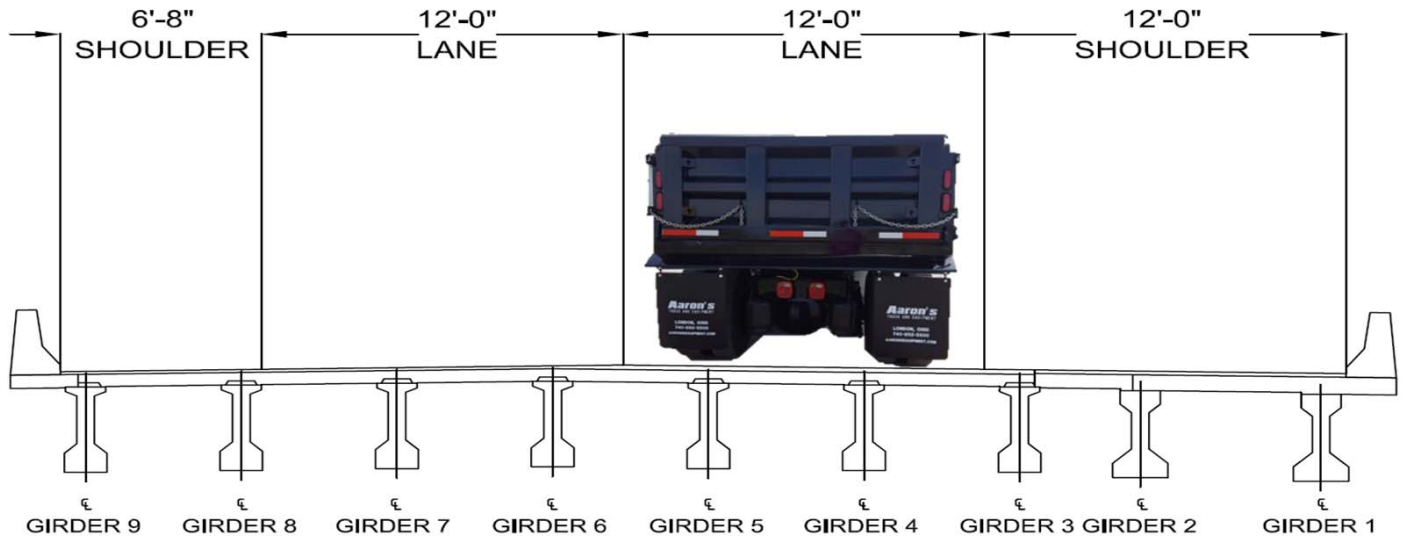

1. Midspan Measurements

		Girder 9*	Girder 8*	Girder 7	Girder 6*	Girder 5*	Girder 4*	Girder 3	Girder 2*	Girder 1
Run 1	Bottom Face of Flange Strain (με) :	0.21	1.35	8.73	6.58	13.67	14.02	17.78	6.34	2.87
	Deflection (in.) :	0.000	0.006	0.009	0.016	0.024	0.025	0.020	N/A	0.002
Run 2	Bottom Face of Flange Strain (με) :	-0.14	0.88	7.00	5.75	12.34	13.42	16.43	5.35	2.18
	Deflection (in.) :	0.000	0.003	0.007	0.011	0.018	0.020	0.015	N/A	0.002
Run 3	Bottom Face of Flange Strain (με) :	-0.08	1.45	8.16	6.15	13.57	13.81	18.52	6.33	2.70
	Deflection (in.) :	-0.001	0.005	0.011	0.016	0.024	0.026	0.019	N/A	0.003

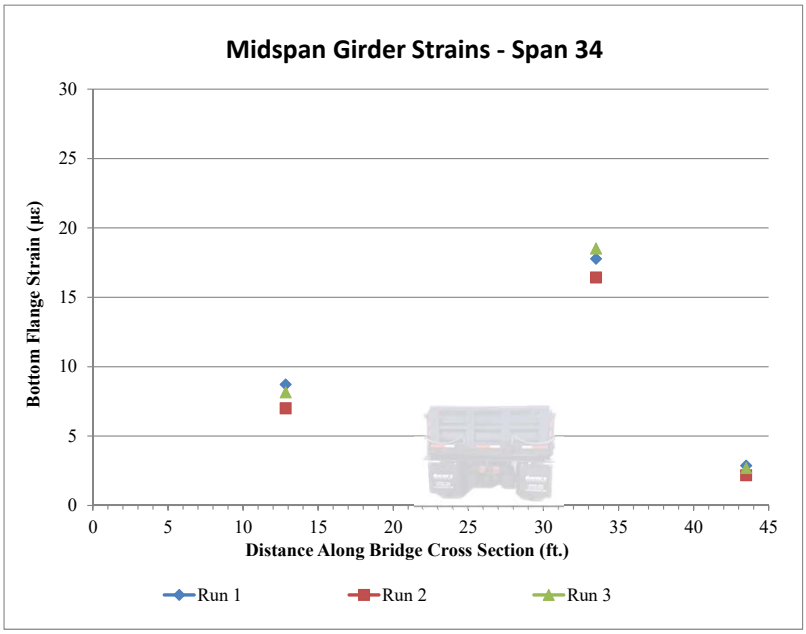

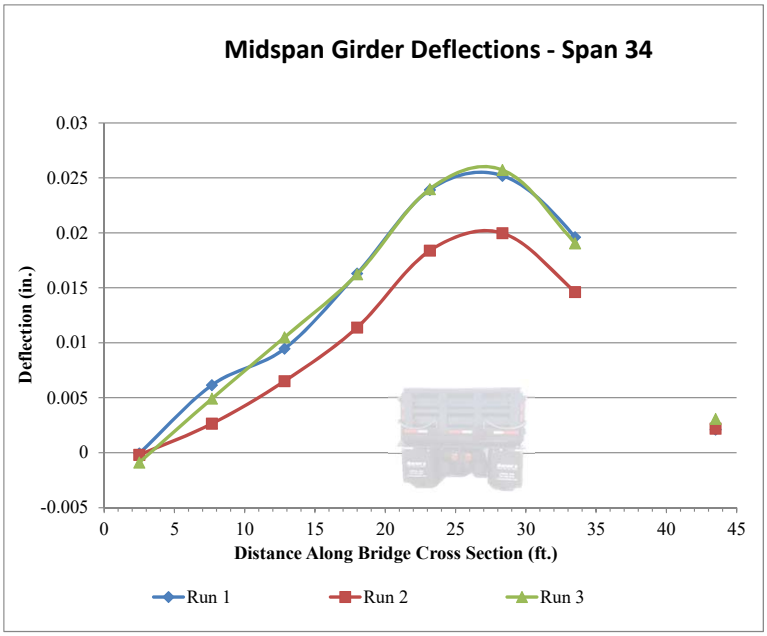

Note: Strain measurments for girder locations 2, 4, 5, 6, 8, and 9 (G2, G4, G5, G6, G8, and G9) not included in figures due to uncertainty surrounding the validity. It was noted during installation of gauges on G8 and G9 that adhesion was difficult; however, the cause of the inconsistency in the other

Note: The midspan deflection of girder 2 is not included in the plots due to low quality images aquired during testing, which could not be resolved.

NOTES:

1. Girders are numbered from the east in accordance with widened bridge plans
2. Spans are numbered starting at the South Island and end at Willoughby Spit
3. Traffic flows from Willoughby Spit to the South Island on the WB Structure
4. Girder 4 has considerable damage as shown in the Inspection Mapping
5. Deflection values are given assuming downwards is (+) and upwards is (-)

REFERENCES:

1. As - Built Contract Drawings T-3 (224-03) dated December 1977
2. VDOT July 2014 Special Inspection Report for EB South Approach Bridge

Truck Configuration 2 Continued

2. Girder 3 Strain Distribution at 6 ft.

	**Strain Transducer Readings (με)			
Location	Run 1	Run 2	Run 3	Height (in.)
9" below top of CT web	-0.24	-0.04	-0.18	23.5
Bot. Face of Flange	7.44	7.92	8.30	0

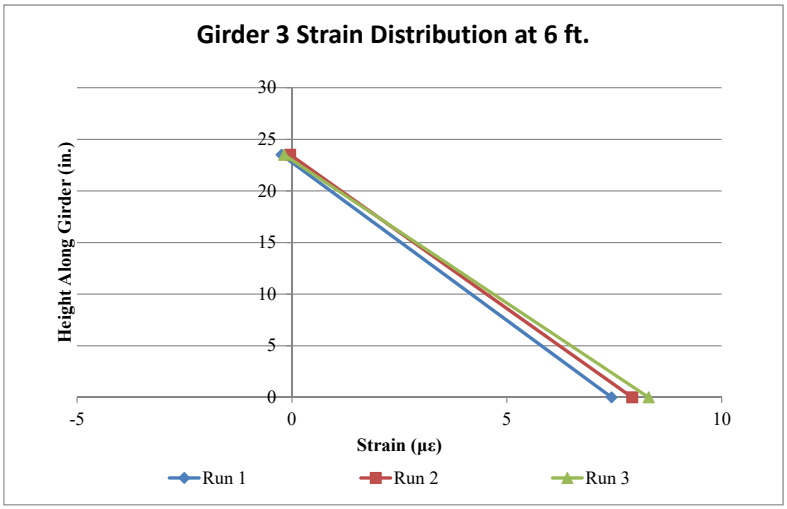

** Raw strain signals were processed for removing residual strain in signals.

3. Girder 4 Strain Distribution at 6 ft.

	**Strain Transducer Readings (με)			
Location	Run 1	Run 2	Run 3	Height (in.)
9" below top of CT web	2.05	1.58	1.17	23.5
Bot. Face of Flange	4.74	5.06	4.91	0

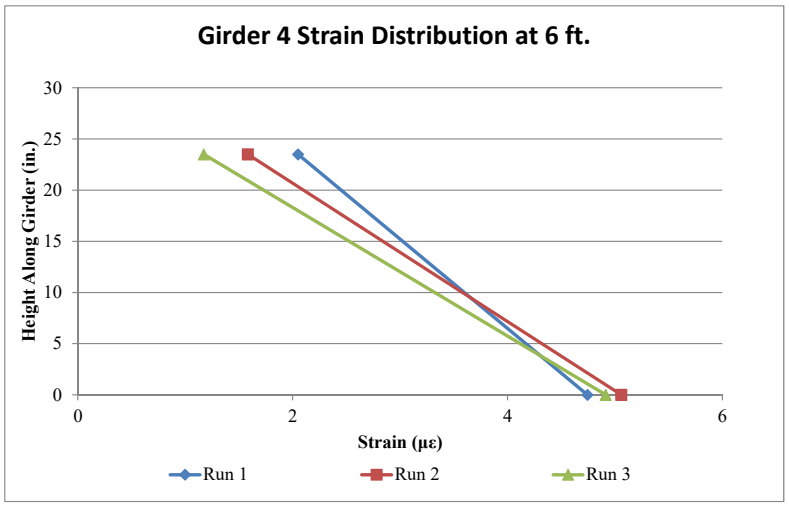

NOTES:

1. Girders are numbered from the east in accordance with widened bridge plans
2. Spans are numbered starting at the South Island and end at Willoughby Spit
3. Traffic flows from Willoughby Spit to the South Island on the WB Structure
4. Girder 4 has considerable damage as shown in the Inspection Mapping
5. Deflection values are given assuming downwards is (+) and upwards is (-)

REFERENCES:

1. As - Built Contract Drawings T-3 (224-03) dated December 1977
2. VDOT July 2014 Special Inspection Report for EB South Approach Bridge

Truck Configuration 2 Continued

4. Girder 5 Strain Distribution at 6 ft.

	**Strain Transducer Readings (με)			
Location	Run 1	Run 2	Run 3	Height (in.)
9" below top of CT web	0.94	0.08	0.56	23.5
Bot. Face of Flange	11.62	11.66	11.74	0

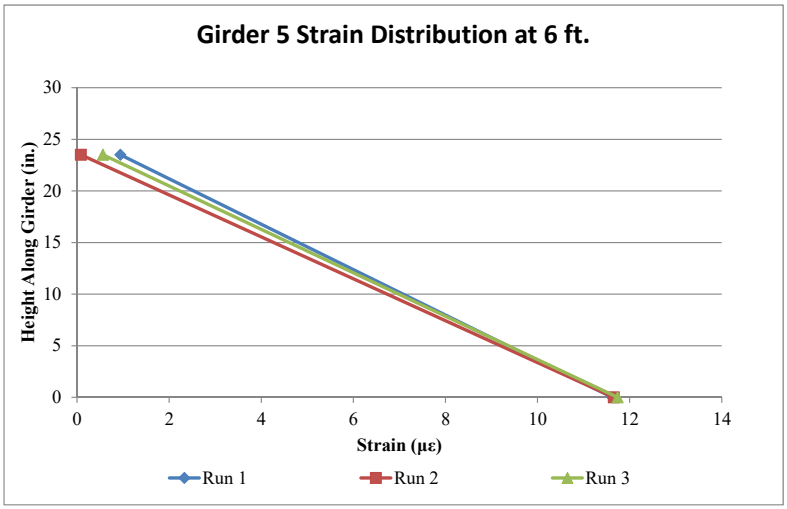

** Raw strain signals were processed for removing residual strain in signals.

NOTES:

1. Girders are numbered from the east in accordance with widened bridge plans
2. Spans are numbered starting at the South Island and end at Willoughby Spit
3. Traffic flows from Willoughby Spit to the South Island on the WB Structure
4. Girder 4 has considerable damage as shown in the Inspection Mapping
5. Deflection values are given assuming downwards is (+) and upwards is (-)

REFERENCES:

1. As - Built Contract Drawings T-3 (224-03) dated December 1977
2. VDOT July 2014 Special Inspection Report for EB South Approach Bridge

Live Load Testing Results		Made	AB	Date	8/4/2016	Job Number	XXXXX
HRBT WESTBOUND STRUCTURE SPAN 34	UNIVERSITY of VIRGINIA SCHOOL OF ENGINEERING	Checked		Date		Connection	
For Hampton Roads Bridge Tunnel		Backchk'd		Date		Sheet No.	1

Truck Configuration 3

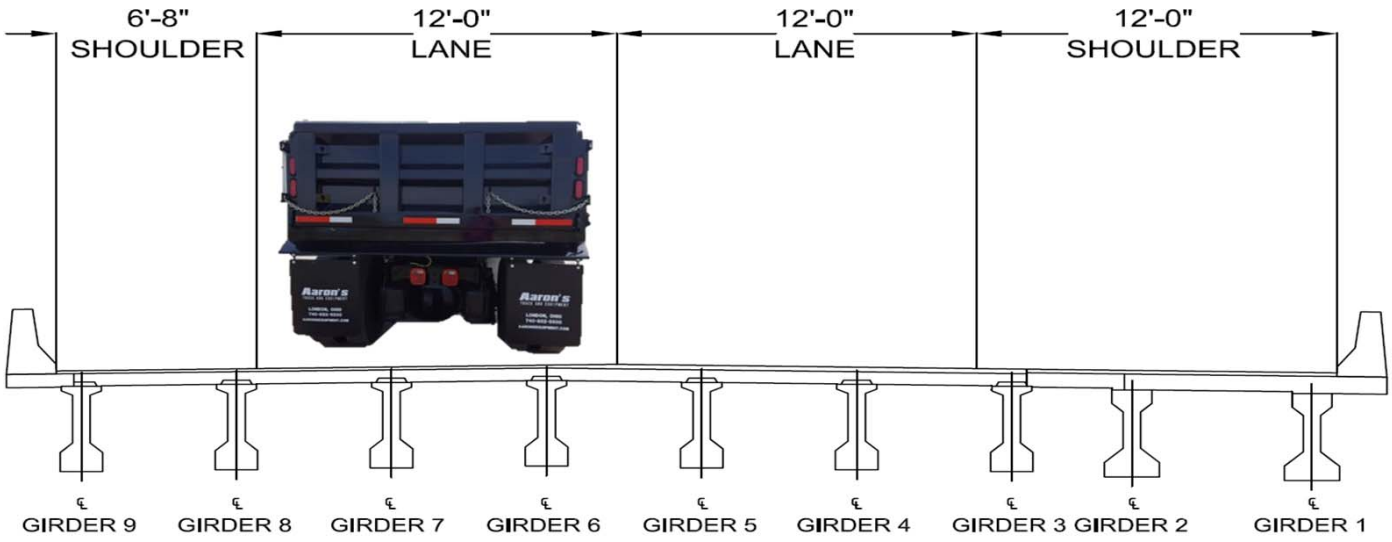

1. Midspan Measurements

		Girder 9*	Girder 8*	Girder 7	Girder 6*	Girder 5*	Girder 4*	Girder 3	Girder 2*	Girder 1
Run 1	Bottom Face of Flange Strain (με) :	3.39	6.57	27.48	10.37	6.61	3.77	2.82	0.97	-0.12
	Deflection (in.) :	0.016	0.020	0.024	0.020	0.014	0.007	0.003	N/A	-0.001
Run 2	Bottom Face of Flange Strain (με) :	3.38	6.21	24.67	9.36	5.82	3.24	2.35	0.90	-0.18
	Deflection (in.) :	0.013	0.018	0.019	0.016	0.010	0.006	0.002	N/A	0.000
Run 3	Bottom Face of Flange Strain (με) :	3.56	6.19	27.07	10.30	6.56	3.50	2.65	0.73	0.00
	Deflection (in.) :	0.016	0.022	0.024	0.021	0.014	0.007	0.003	N/A	-0.002

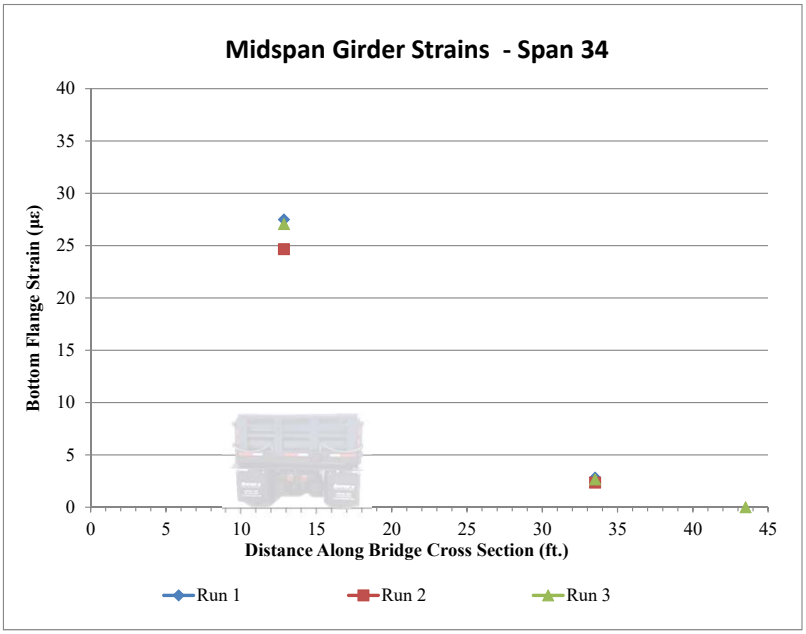

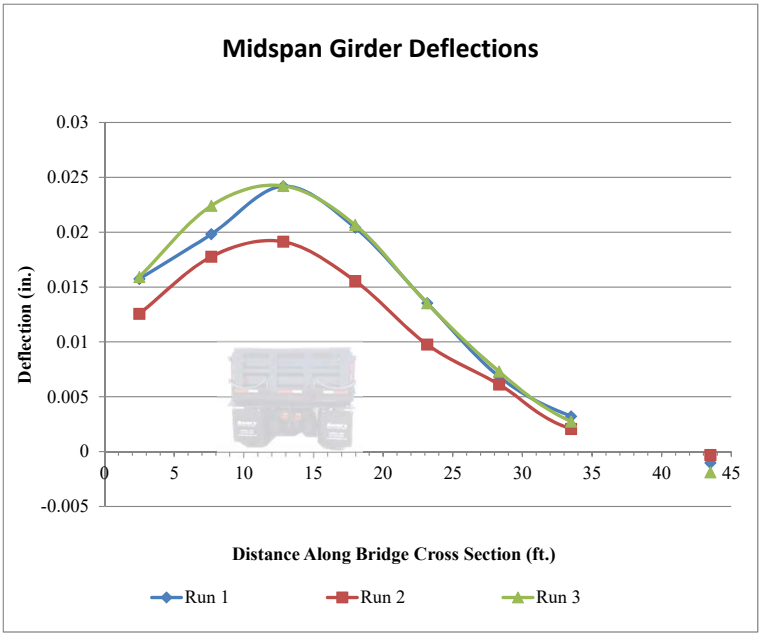

Note: Strain measurments for girder locations 2, 4, 5, 6, 8, and 9 (G2, G4, G5, G6, G8, and G9) not included in figures due to uncertainty surrounding the validity. It was noted during installation of gauges on G8 and G9 that adhesion was difficult; however, the cause of the inconsistency in the other

Note: The midspan deflection of girder 2 is not included in the plots due to low quality images aquired during testing, which could not be resolved.

NOTES:

1. Girders are numbered from the east in accordance with widened bridge plans
2. Spans are numbered starting at the South Island and end at Willoughby Spit
3. Traffic flows from Willoughby Spit to the South Island on the WB Structure
4. Girder 4 has considerable damage as shown in the Inspection Mapping
5. Deflection values are given assuming downwards is (+) and upwards is (-)

REFERENCES:

1. As - Built Contract Drawings T-3 (224-03) dated December 1977
2. VDOT July 2014 Special Inspection Report for EB South Approach Bridge

Truck Configuration 3 Continued

2. Girder 3 Strain Distribution at 6 ft.

	**Strain Transducer Readings (με)			
Location	Run 1	Run 2	Run 3	Height (in.)
9" below top of CT web	-0.10	-0.07	-0.01	23.5
Bot. Face of Flange	1.25	1.20	1.28	0

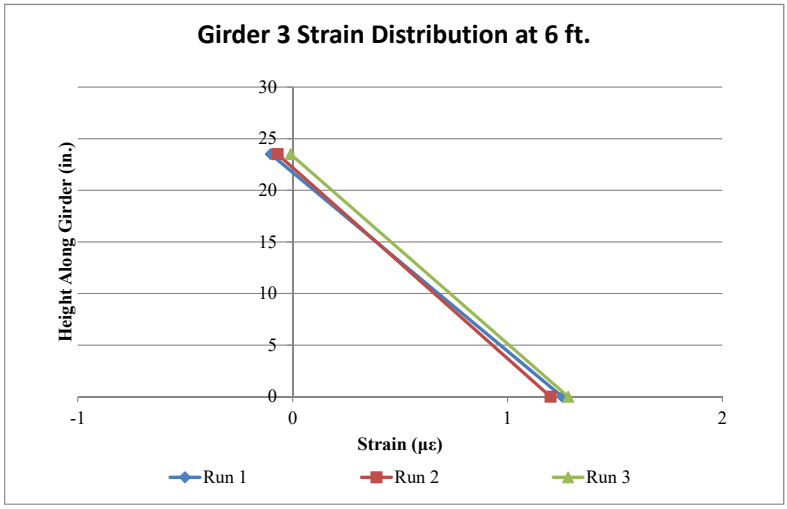

** Raw strain signals were processed for removing residual strain in signals.

3. Girder 4 Strain Distribution at 6 ft.

	**Strain Transducer Readings (με)			
Location	Run 1	Run 2	Run 3	Height (in.)
9" below top of CT web	-0.69	-0.64	-0.63	23.5
Bot. Face of Flange	0.65	0.76	0.74	0

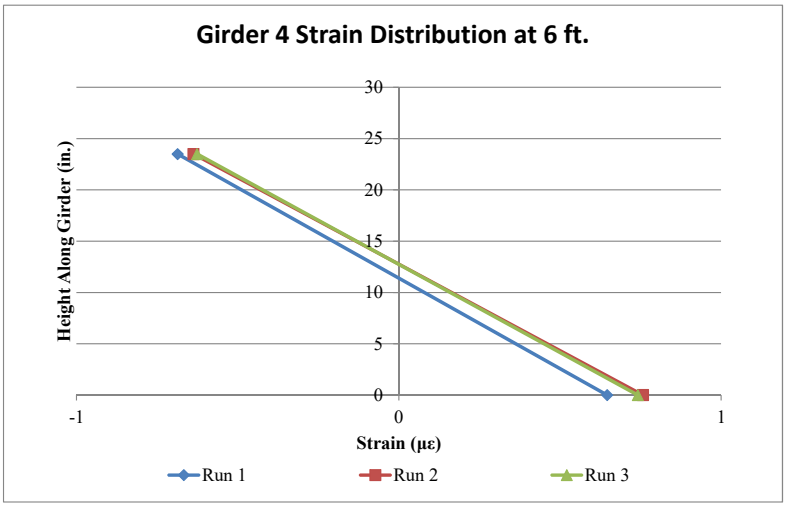

NOTES:

1. Girders are numbered from the east in accordance with widened bridge plans
2. Spans are numbered starting at the South Island and end at Willoughby Spit
3. Traffic flows from Willoughby Spit to the South Island on the WB Structure
4. Girder 4 has considerable damage as shown in the Inspection Mapping
5. Deflection values are given assuming downwards is (+) and upwards is (-)

REFERENCES:

1. As - Built Contract Drawings T-3 (224-03) dated December 1977
2. VDOT July 2014 Special Inspection Report for EB South Approach Bridge

Truck Configuration 3 Continued

4. Girder 5 Strain Distribution at 6 ft.

	**Strain Transducer Readings (με)			
Location	Run 1	Run 2	Run 3	Height (in.)
9" below top of CT web	0.00	-0.06	0.11	23.5
Bot. Face of Flange	3.17	3.31	3.35	0

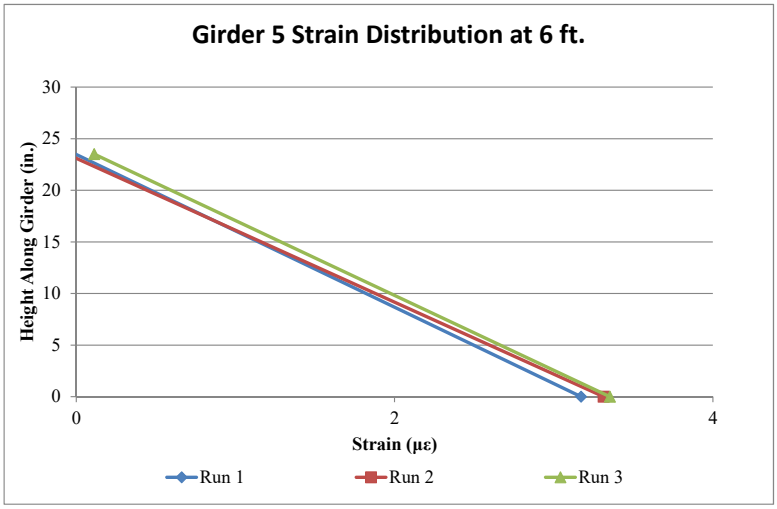

** Raw strain signals were processed for removing residual strain in signals.

NOTES:

1. Girders are numbered from the east in accordance with widened bridge plans
2. Spans are numbered starting at the South Island and end at Willoughby Spit
3. Traffic flows from Willoughby Spit to the South Island on the WB Structure
4. Girder 4 has considerable damage as shown in the Inspection Mapping
5. Deflection values are given assuming downwards is (+) and upwards is (-)

REFERENCES:

1. As - Built Contract Drawings T-3 (224-03) dated December 1977
2. VDOT July 2014 Special Inspection Report for EB South Approach Bridge

Live Load Testing Results		Made	AB	Date	8/4/2016	Job Number	XXXXX
HRBT WESTBOUND STRUCTURE SPAN 34	UNIVERSITY of VIRGINIA SCHOOL OF ENGINEERING	Checked		Date		Connection	
For Hampton Roads Bridge Tunnel		Backchk'd		Date		Sheet No.	1

Truck Configuration 4

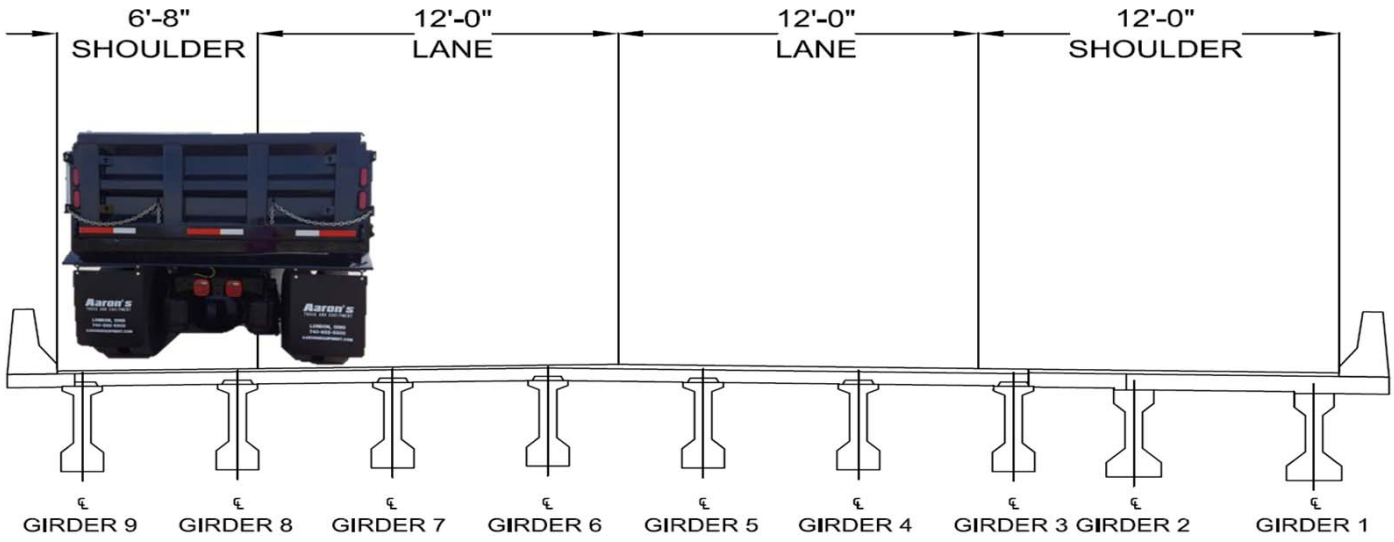

1. Midspan Measurements

		Girder 9*	Girder 8*	Girder 7	Girder 6*	Girder 5*	Girder 4*	Girder 3	Girder 2*	Girder 1
Run 1	Bottom Face of Flange Strain (με) :	8.46	9.50	24.46	5.49	3.86	1.56	-0.01	-0.25	-0.36
	Deflection (in.) :	0.036	0.027	0.020	0.012	0.007	0.001	-0.002	N/A	-0.004
Run 2	Bottom Face of Flange Strain (με) :	7.69	7.94	20.80	4.58	3.14	0.89	-0.23	-0.13	-0.65
	Deflection (in.) :	0.027	0.023	0.017	0.009	0.005	0.002	-0.001	N/A	0.000
Run 3	Bottom Face of Flange Strain (με) :	8.39	9.15	23.24	5.12	3.69	1.54	-0.22	-0.22	-0.58
	Deflection (in.) :	0.037	0.032	0.021	0.012	0.006	0.001	-0.003	N/A	-0.003

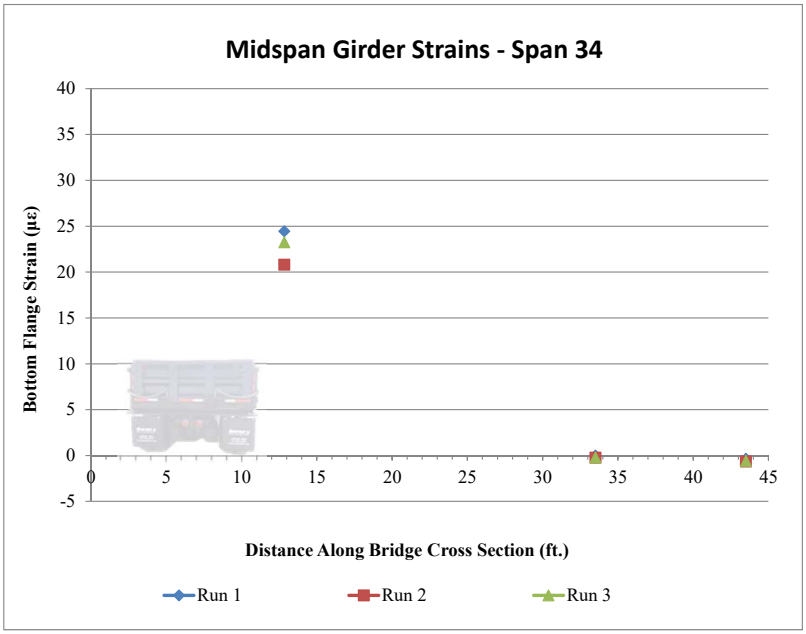

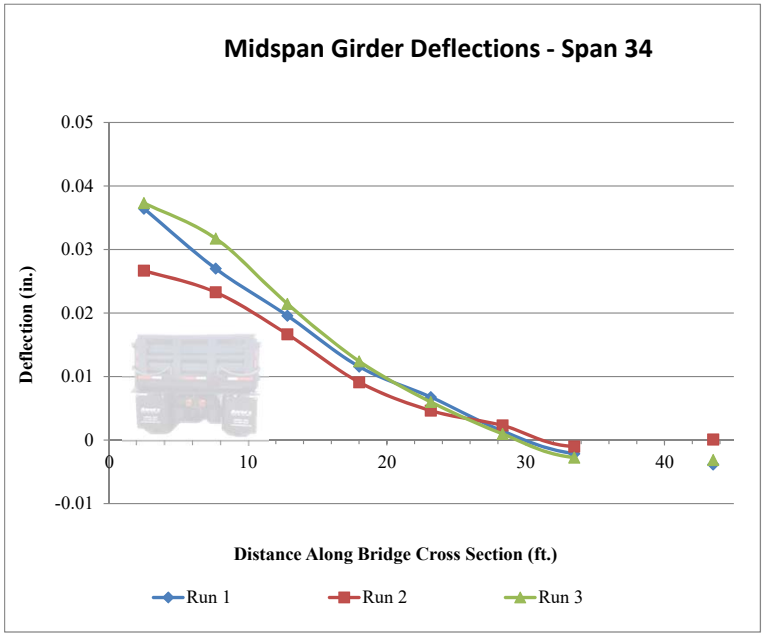

Note: Strain measurments for girder locations 2, 4, 5, 6, 8, and 9 (G2, G4, G5, G6, G8, and G9) not included in figures due to uncertainty surrounding the validity. It was noted during installation of gauges on G8 and G9 that adhesion was difficult; however, the cause of the inconsistency in the other

Note: The midspan deflection of girder 2 is not included in the plots due to low quality images aquired during testing, which could not be resolved.

NOTES:

1. Girders are numbered from the east in accordance with widened bridge plans
2. Spans are numbered starting at the South Island and end at Willoughby Spit
3. Traffic flows from Willoughby Spit to the South Island on the WB Structure
4. Girder 4 has considerable damage as shown in the Inspection Mapping
5. Deflection values are given assuming downwards is (+) and upwards is (-)

REFERENCES:

1. As - Built Contract Drawings T-3 (224-03) dated December 1977
2. VDOT July 2014 Special Inspection Report for EB South Approach Bridge

Truck Configuration 4 Continued

2. Girder 5 Strain Distribution at 6 ft.

	**Strain Transducer Readings (με)			
Location	Run 1	Run 2	Run 3	Height (in.)
9" below top of CT web	-0.18	-0.23	-0.25	23.5
Bot. Face of Flange	1.97	1.69	1.74	0

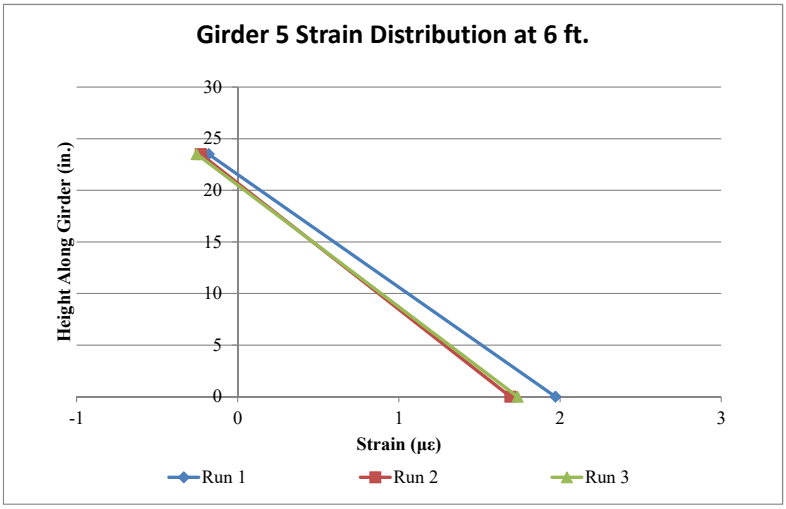

** Raw strain signals were processed for removing residual strain in signals.

3. Girders 3 and 4 Strain Distribution at 6 ft.

Strain distribution for these girders was not ploted due to recording very small strain.

NOTES:

1. Girders are numbered from the east in accordance with widened bridge plans
2. Spans are numbered starting at the South Island and end at Willoughby Spit
3. Traffic flows from Willoughby Spit to the South Island on the WB Structure
4. Girder 4 has considerable damage as shown in the Inspection Mapping
5. Deflection values are given assuming downwards is (+) and upwards is (-)

REFERENCES:

1. As - Built Contract Drawings T-3 (224-03) dated December 1977
2. VDOT July 2014 Special Inspection Report for EB South Approach Bridge

Live Load Testing Results		Made	AB	Date	8/4/2016	Job Number	XXXXX
HRBT WESTBOUND STRUCTURE SPAN 34	UNIVERSITY of VIRGINIA SCHOOL OF ENGINEERING	Checked		Date		Connection	
For Hampton Roads Bridge Tunnel		Backchk'd		Date		Sheet No.	1

Truck Configuration 5

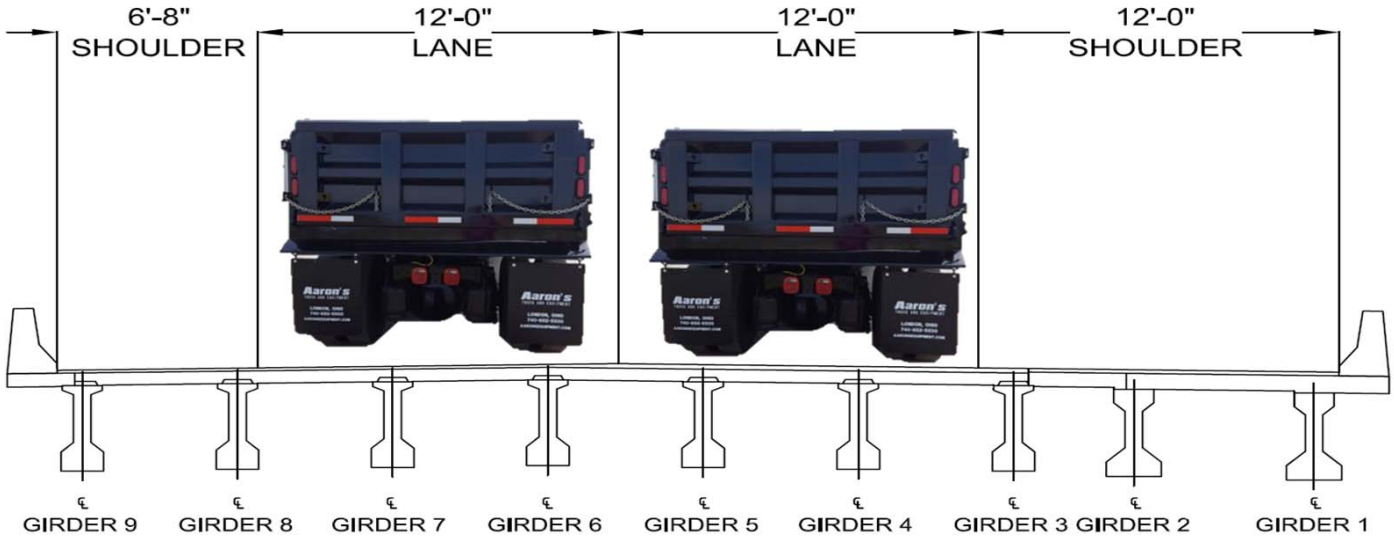

1. Midspan Measurements

		Girder 9*	Girder 8*	Girder 7	Girder 6*	Girder 5*	Girder 4*	Girder 3	Girder 2*	Girder 1
Run 1	Bottom Face of Flange Strain (με) :	4.12	7.90	37.58	17.19	19.96	17.05	19.54	6.87	2.38
	Deflection (in.) :	0.018	0.031	0.038	0.040	0.037	0.037	0.022	N/A	-0.001
Run 2	Bottom Face of Flange Strain (με) :	3.23	7.40	33.05	15.93	18.04	15.59	17.01	5.52	1.65
	Deflection (in.) :	0.012	0.021	0.027	0.029	0.030	0.026	0.018	N/A	0.001
Run 3	Bottom Face of Flange Strain (με) :	3.85	7.49	36.56	16.62	19.56	16.61	19.37	6.59	2.45
	Deflection (in.) :	0.015	0.026	0.034	0.036	0.035	0.032	0.022	N/A	0.000

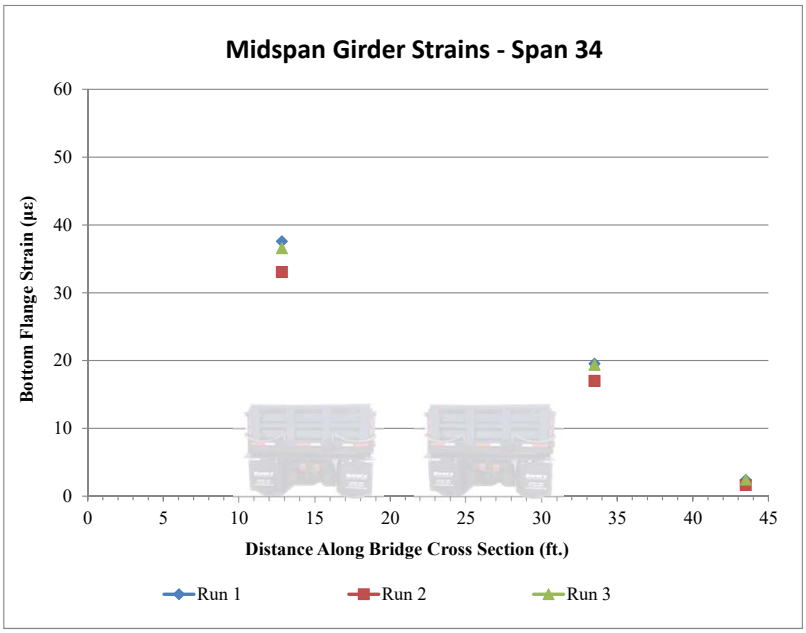

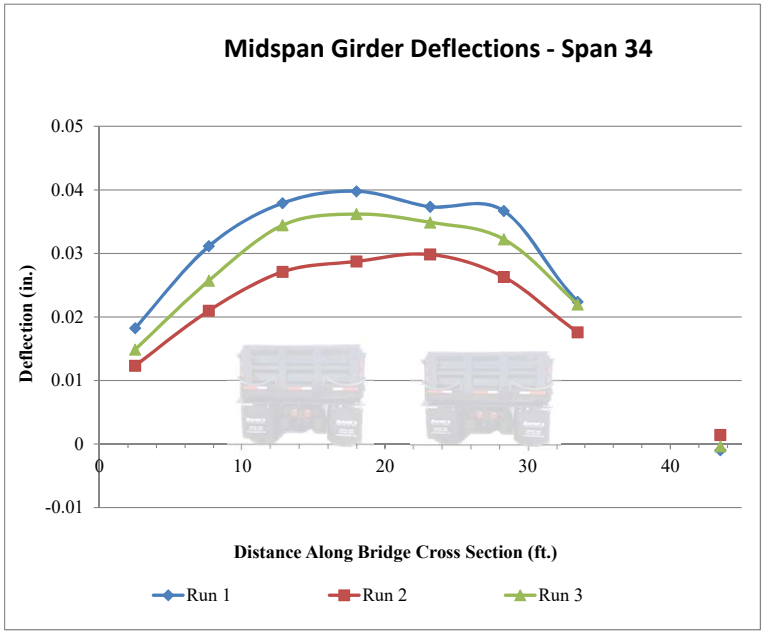

Note: Strain measurments for girder locations 2, 4, 5, 6, 8, and 9 (G2, G4, G5, G6, G8, and G9) not included in figures due to uncertainty surrounding the validity. It was noted during installation of gauges on G8 and G9 that adhesion was difficult; however, the cause of the inconsistency in the other

Note: The midspan deflection of girder 2 is not included in the plots due to low quality images aquired during testing, which could not be resolved.

NOTES:

1. Girders are numbered from the east in accordance with widened bridge plans
2. Spans are numbered starting at the South Island and end at Willoughby Spit
3. Traffic flows from Willoughby Spit to the South Island on the WB Structure
4. Girder 4 has considerable damage as shown in the Inspection Mapping
5. Deflection values are given assuming downwards is (+) and upwards is (-)

REFERENCES:

1. As - Built Contract Drawings T-3 (224-03) dated December 1977
2. VDOT July 2014 Special Inspection Report for EB South Approach Bridge

Truck Configuration 5 Continued

2. Girder 3 Strain Distribution at 6 ft.

	**Strain Transducer Readings (με)			
Location	Run 1	Run 2	Run 3	Height (in.)
9" below top of CT web	-0.23	-0.14	-0.28	23.5
Bot. Face of Flange	8.94	8.43	8.37	0

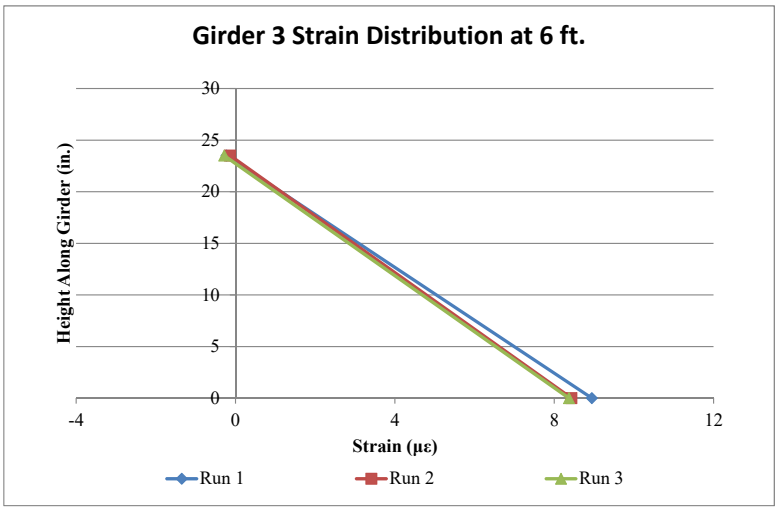

** Raw strain signals were processed for removing residual strain in signals.

3. Girder 4 Strain Distribution at 6 ft.

	**Strain Transducer Readings (με)			
Location	Run 1	Run 2	Run 3	Height (in.)
9" below top of CT web	0.17	0.29	0.16	23.5
Bot. Face of Flange	5.24	5.00	4.70	0

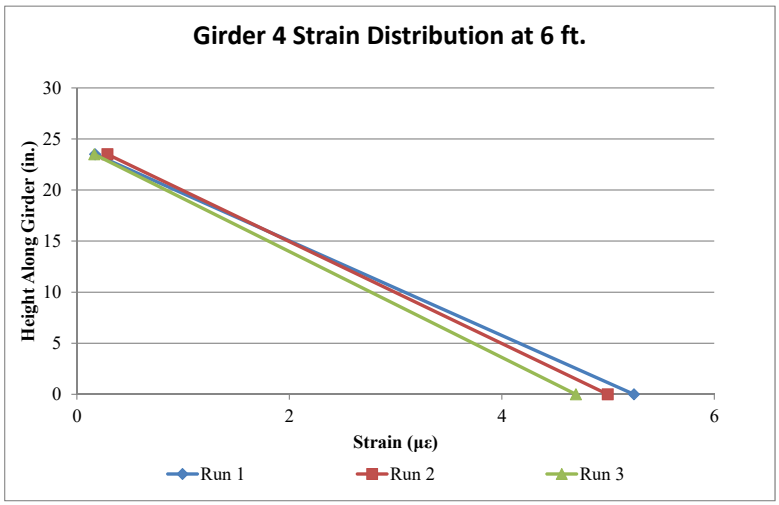

NOTES:

1. Girders are numbered from the east in accordance with widened bridge plans
2. Spans are numbered starting at the South Island and end at Willoughby Spit
3. Traffic flows from Willoughby Spit to the South Island on the WB Structure
4. Girder 4 has considerable damage as shown in the Inspection Mapping
5. Deflection values are given assuming downwards is (+) and upwards is (-)

REFERENCES:

1. As - Built Contract Drawings T-3 (224-03) dated December 1977
2. VDOT July 2014 Special Inspection Report for EB South Approach Bridge

Truck Configuration 5 Continued

4. Girder 5 Strain Distribution at 6 ft.

	**Strain Transducer Readings (με)			
Location	Run 1	Run 2	Run 3	Height (in.)
9" below top of CT web	1.30	0.47	0.89	23.5
Bot. Face of Flange	15.10	15.19	14.40	0

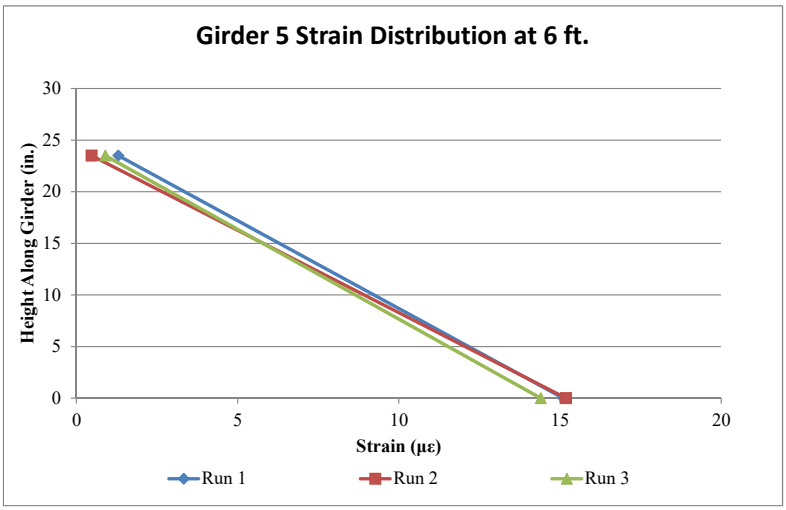

** Raw strain signals were processed for removing residual strain in signals.

NOTES:

1. Girders are numbered from the east in accordance with widened bridge plans
2. Spans are numbered starting at the South Island and end at Willoughby Spit
3. Traffic flows from Willoughby Spit to the South Island on the WB Structure
4. Girder 4 has considerable damage as shown in the Inspection Mapping
5. Deflection values are given assuming downwards is (+) and upwards is (-)

REFERENCES:

1. As - Built Contract Drawings T-3 (224-03) dated December 1977
2. VDOT July 2014 Special Inspection Report for EB South Approach Bridge

APPENDIX D

COMPARISON PLOTS

APPENDIX D-1:

EASTBOUND STRAIN COMPARISON PLOTS

Live Load Testing Results HRBT EB Strain Comparisons For Hampton Roads Bridge Tunnel	VirginiaTech Invent the Future®	Made JJR	Date 8/14/2016	Job Number 449462
		Checked	Date	Connection
		Backchk'd	Date	Sheet No. 1

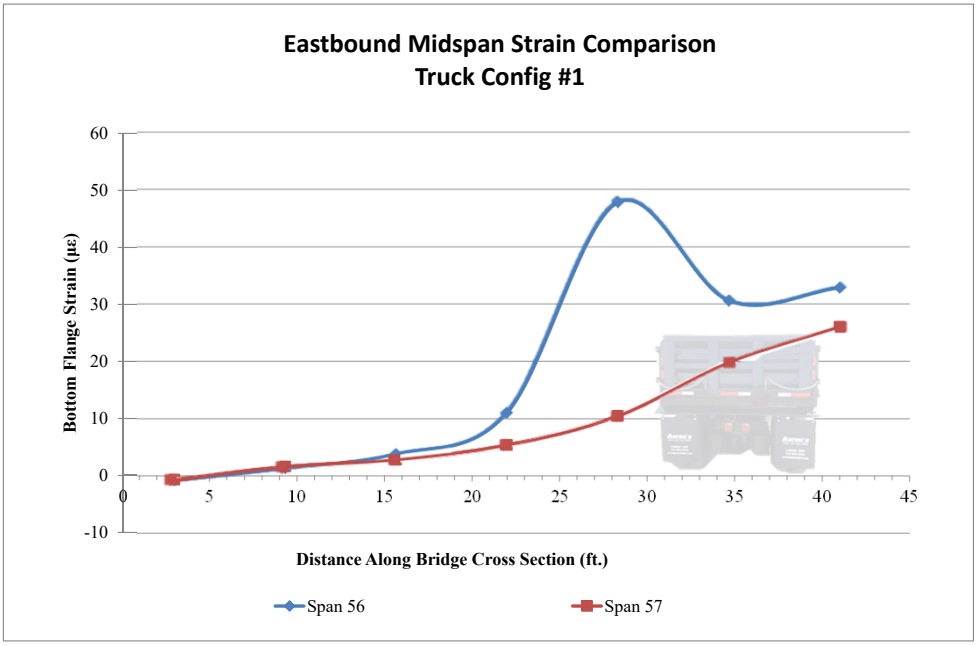

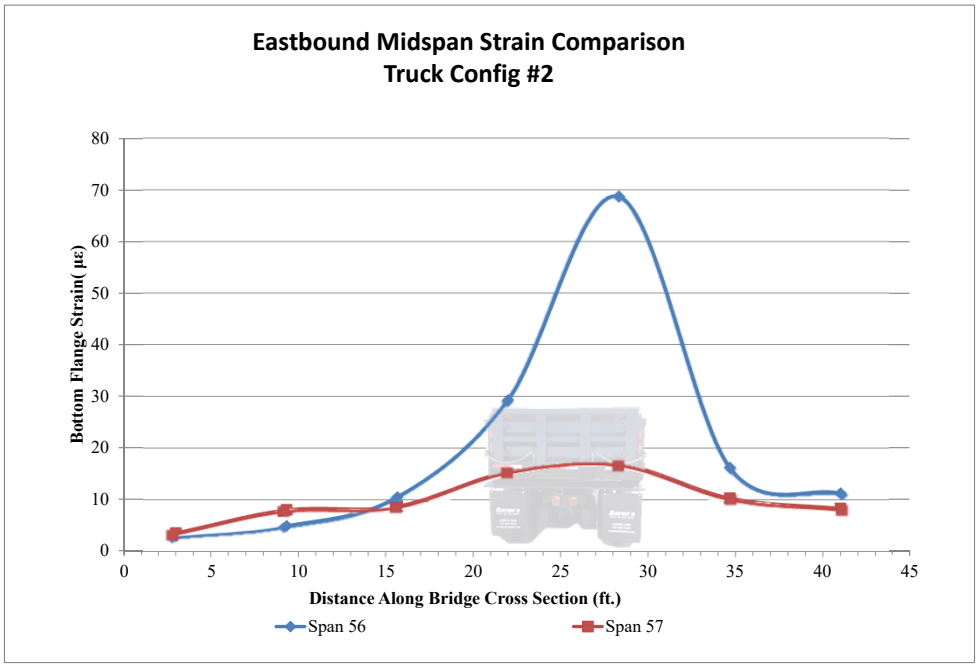

NOTES:

1. Girders are numbered from the east in accordance with original bridge plans
2. Span 56 is the small craft navigation span as seen in the contract drawings
3. Girder 5 has considerable damage as shown in Inspection Report

REFERENCES:

1. As - Built Contract Drawings T-3 (224-03) dated December 1977
2. VDOT July 2014 Special Inspection Report for EB South Approach Bridge

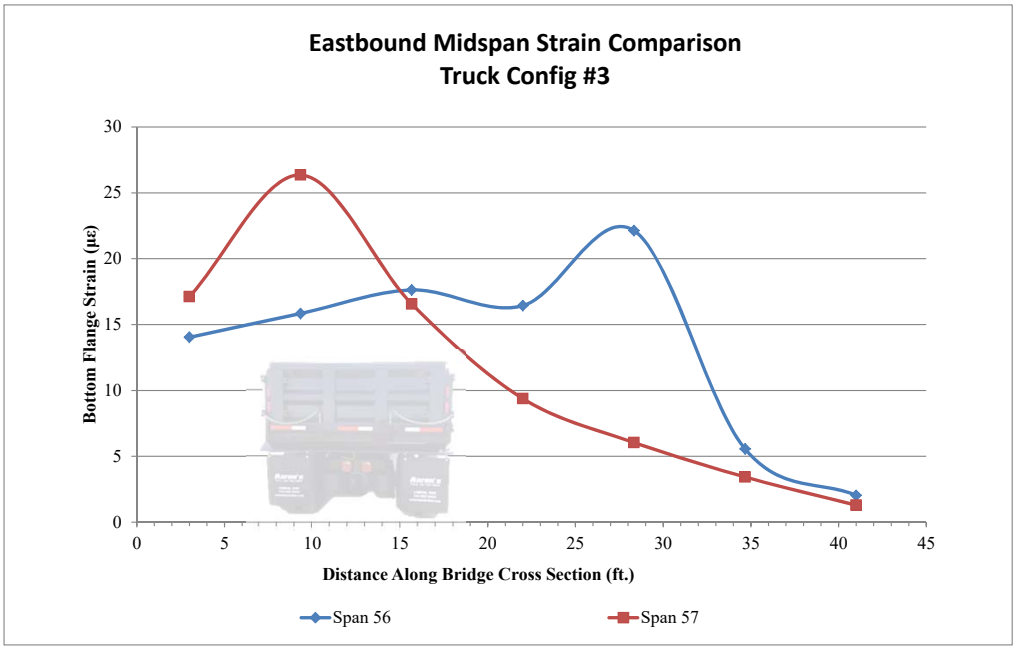

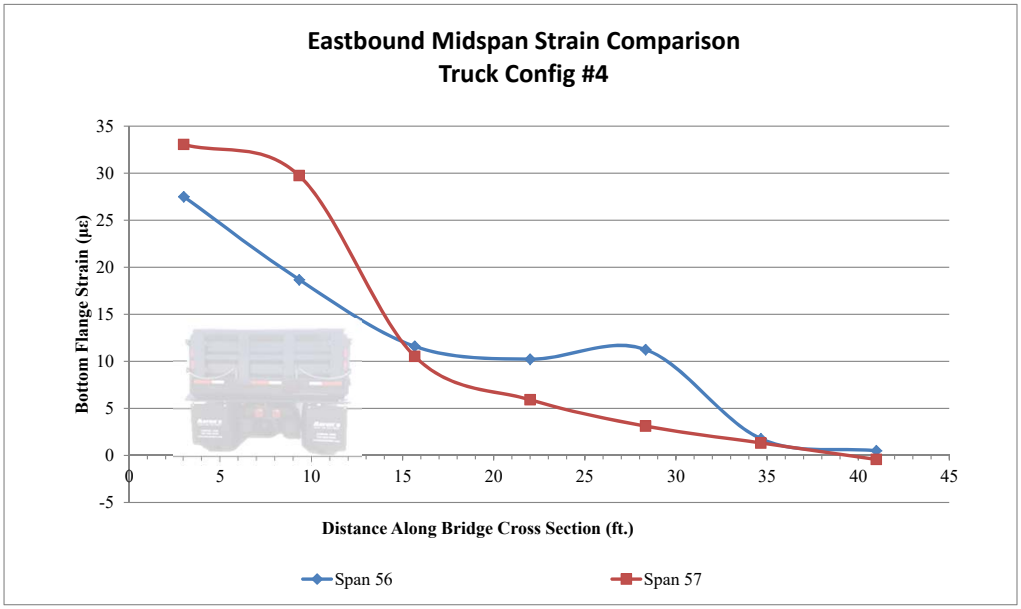

NOTES:
1. Girders are numbered from the east in accordance with original bridge plans
2. Span 56 is the small craft navigation span as seen in the contract drawings
3. Girder 5 has considerable damage as shown in Inspection Report

REFERENCES:
1. As - Built Contract Drawings T-3 (224-03) dated December 1977
2. VDOT July 2014 Special Inspection Report for EB South Approach Bridge

Live Load Testing Results	VirginiaTech Invent the Future®	Made	JJR	Date	8/14/2016	Job Number	449462
HRBT EB Strain Comparisons		Checked		Date		Connection	
For Hampton Roads Bridge Tunnel		Backchk'd		Date		Sheet No.	3

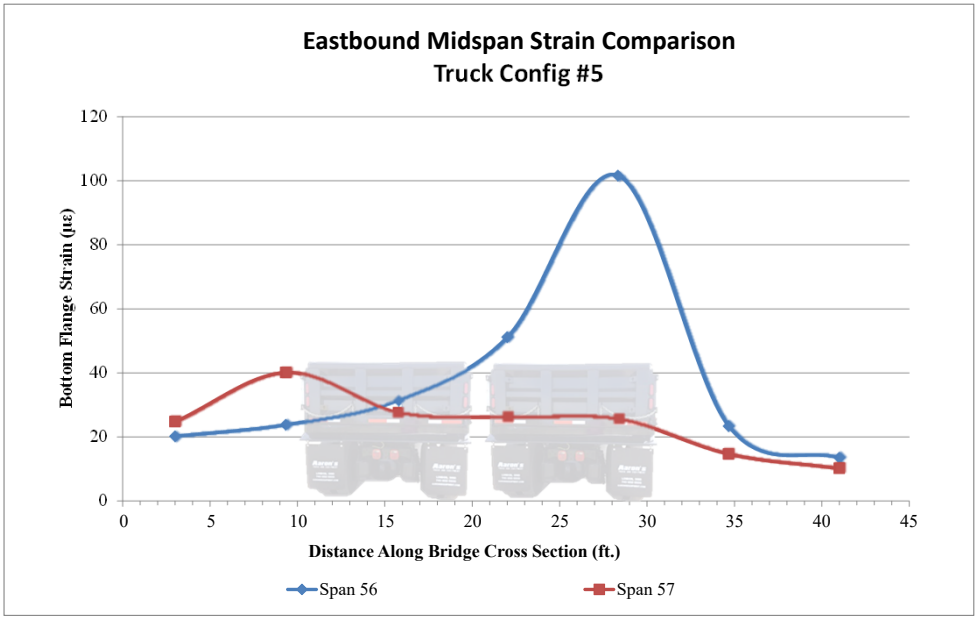

NOTES:

1. Girders are numbered from the east in accordance with original bridge plans
2. Span 56 is the small craft navigation span as seen in the contract drawings
3. Girder 5 has considerable damage as shown in Inspection Report

REFERENCES:

1. As - Built Contract Drawings T-3 (224-03) dated December 1977
2. VDOT July 2014 Special Inspection Report for EB South Approach Bridge

APPENDIX D-2:

WESTBOUND STRAIN COMPARISON PLOTS

Live Load Testing Results HRBT WESTBOUND STRAIN COMPARISONS For Hampton Roads Bridge Tunnel	VirginiaTech Invent the Future®	Made JJR	Date 8/14/2016	Job Number 449462
		Checked	Date	Connection
		Backchk'd	Date	Sheet No. 1

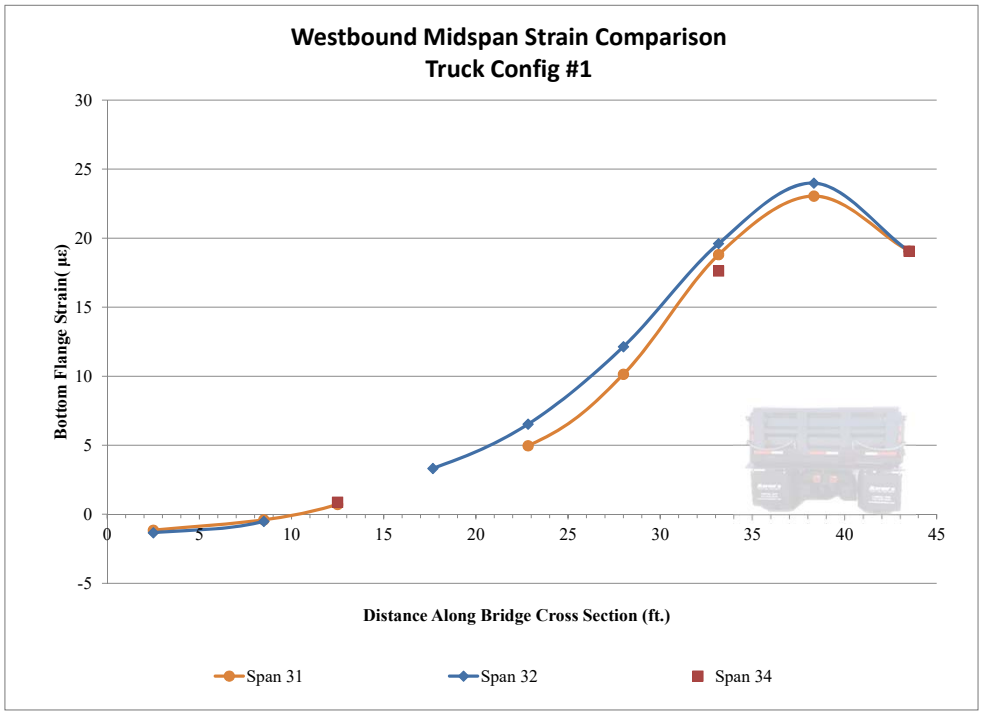

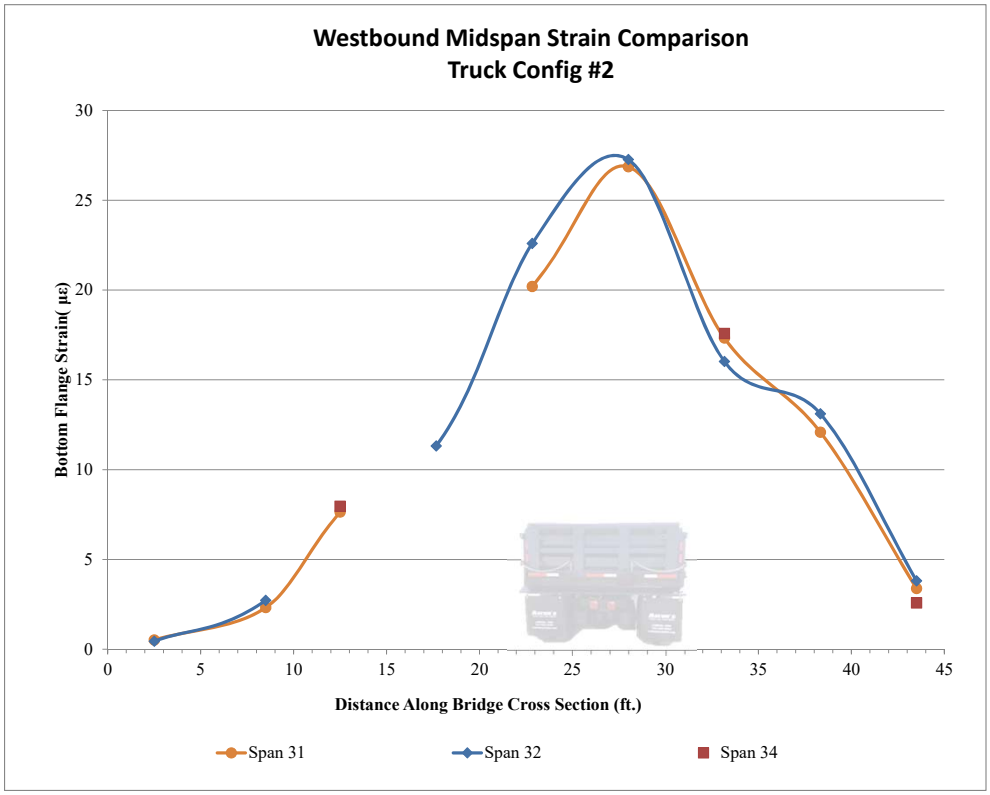

NOTES:
1. Girders are numbered from the east in accordance with widened bridge plans
2. Spans are numbered starting at the South Island and end at Willoughby Spit
3. Traffic flows from Willoughby Spit to the South Island on the WB Structure
4. Missing data points are due to bad contact between gauge and concrete girder

REFERENCES:
1. Contract Drawings 171-20G dated July 17, 1995 (South Approach Bridge WBL Widening)
2. VDOT Inspection Report and Damage Mapping Details - WB Structure Dated June 2015

Live Load Testing Results HRBT WESTBOUND STRAIN COMPARISONS For Hampton Roads Bridge Tunnel	VirginiaTech Invent the Future®	Made JJR	Date 8/14/2016	Job Number 449462
		Checked	Date	Connection
		Backchk'd	Date	Sheet No. 2

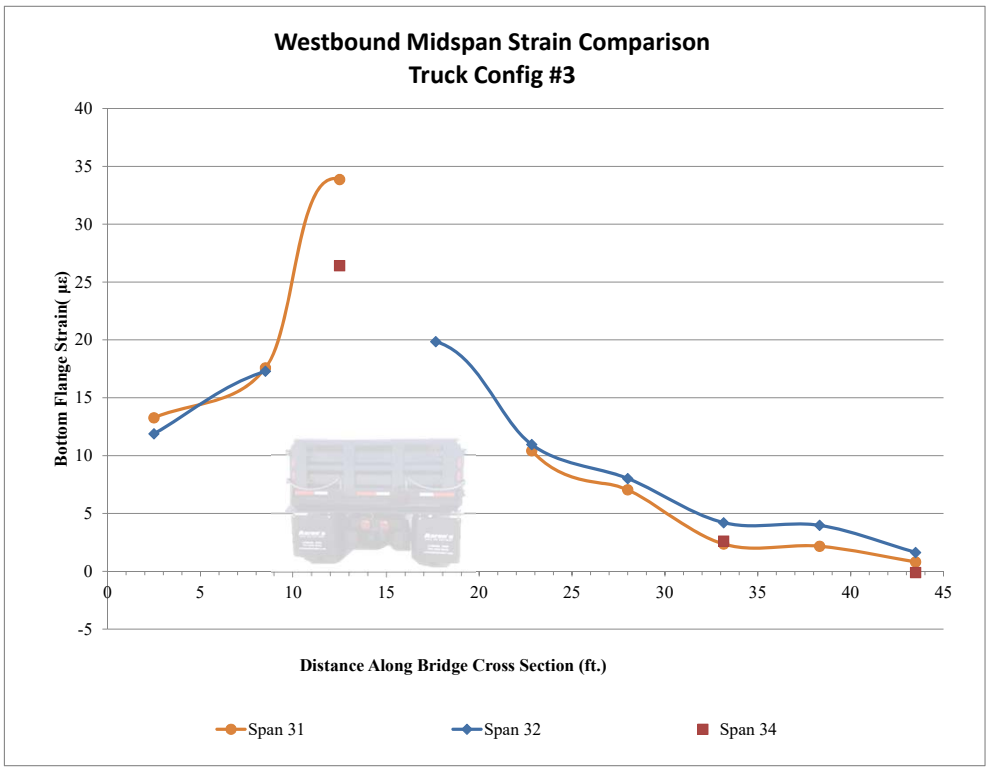

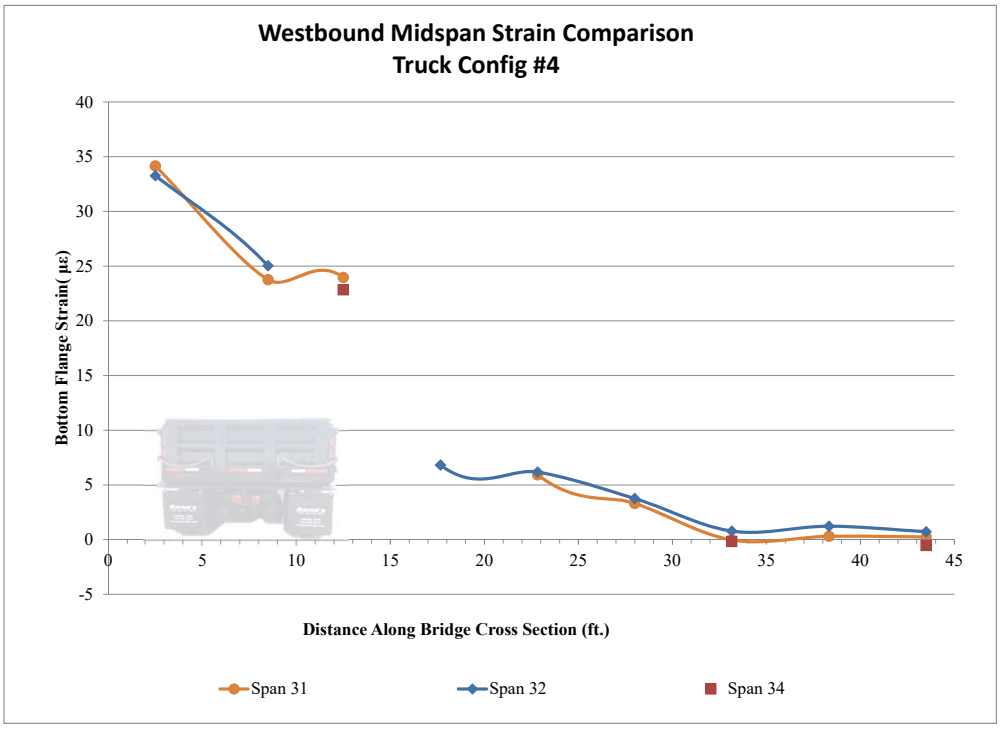

NOTES:
1. Girders are numbered from the east in accordance with widened bridge plans
2. Spans are numbered starting at the South Island and end at Willoughby Spit
3. Traffic flows from Willoughby Spit to the South Island on the WB Structure
4. Missing data points are due to bad contact between gauge and concrete girder

REFERENCES:
1. Contract Drawings 171-20G dated July 17, 1995 (South Approach Bridge WBL Widening)
2. VDOT Inspection Report and Damage Mapping Details - WB Structure Dated June 2015

Live Load Testing Results		Made	JJR	Date	8/14/2016	Job Number	449462
HRBT WESTBOUND STRAIN COMPARISONS		Checked		Date		Connection	
For Hampton Roads Bridge Tunnel		Backchk'd		Date		Sheet No.	3

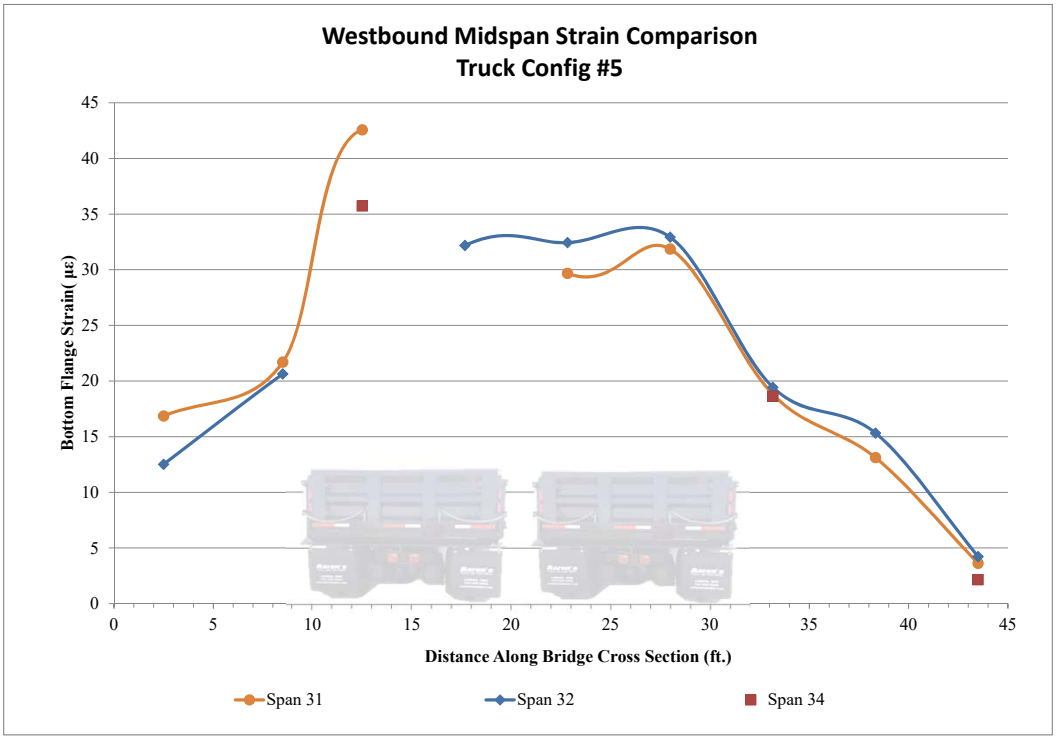

NOTES:

1. Girders are numbered from the east in accordance with widened bridge plans
2. Spans are numbered starting at the South Island and end at Willoughby Spit
3. Traffic flows from Willoughby Spit to the South Island on the WB Structure
4. Missing data points are due to bad contact between gauge and concrete girder

REFERENCES:

1. Contract Drawings 171-20G dated July 17, 1995 (South Approach Bridge WBL Widening)
2. VDOT Inspection Report and Damage Mapping Details - WB Structure Dated June 2015

APPENDIX D-3:

WESTBOUND DEFLECTION COMPARISON PLOTS

Live Load Testing Results	VirginiaTech Invent the Future®	Made	JJR	Date	8/14/2016	Job Number	449462
HRBT WB DEFLECTION COMPARISONS		Checked		Date		Connection	
For Hampton Roads Bridge Tunnel		Backchk'd		Date		Sheet No.	1

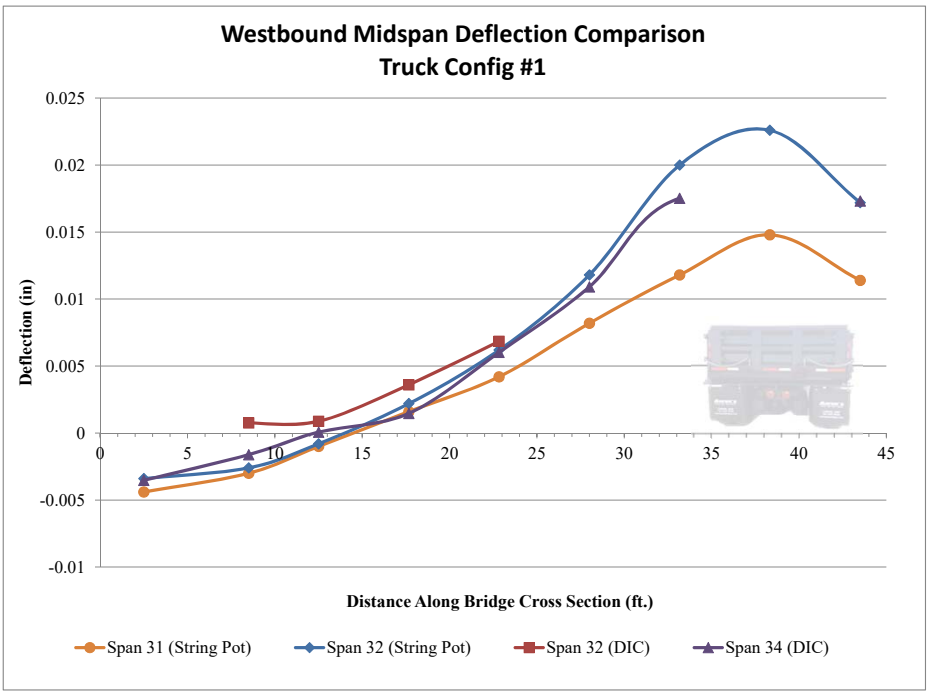

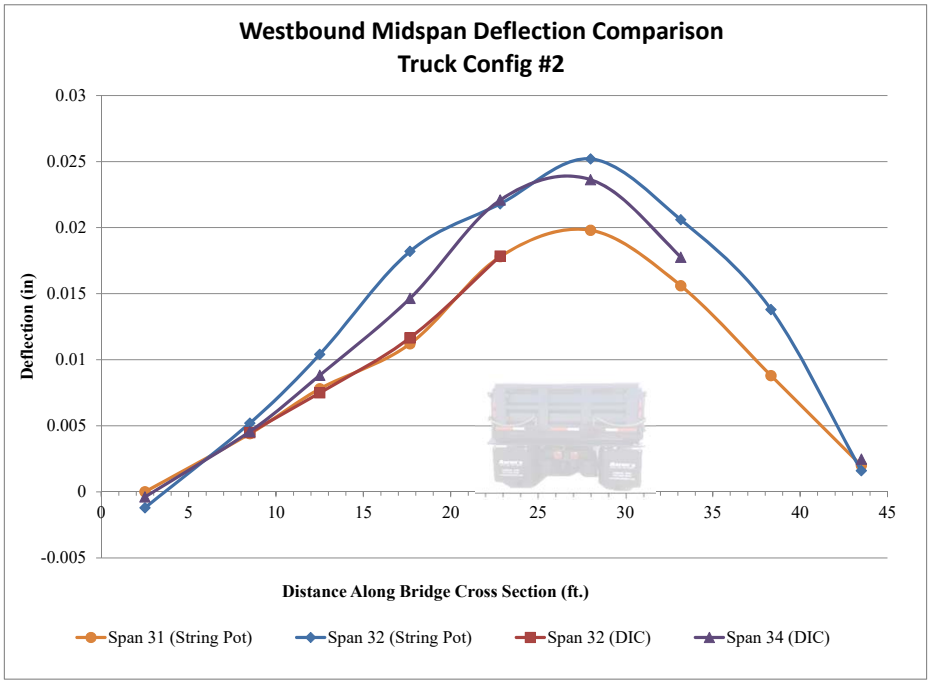

NOTES:

1. Girders are numbered from the east in accordance with widened bridge plans
2. Spans are numbered starting at the South Island and end at Willoughby Spit
3. Traffic flows from Willoughby Spit to the South Island on the WB Structure
4. Missing data points are from malfunctioning equipment

REFERENCES:

1. Contract Drawings 171-20G dated July 17, 1995 (South Approach Bridge WBL Widening)
2. VDOT Inspection Report and Damage Mapping Details - WB Structure Dated June 2015

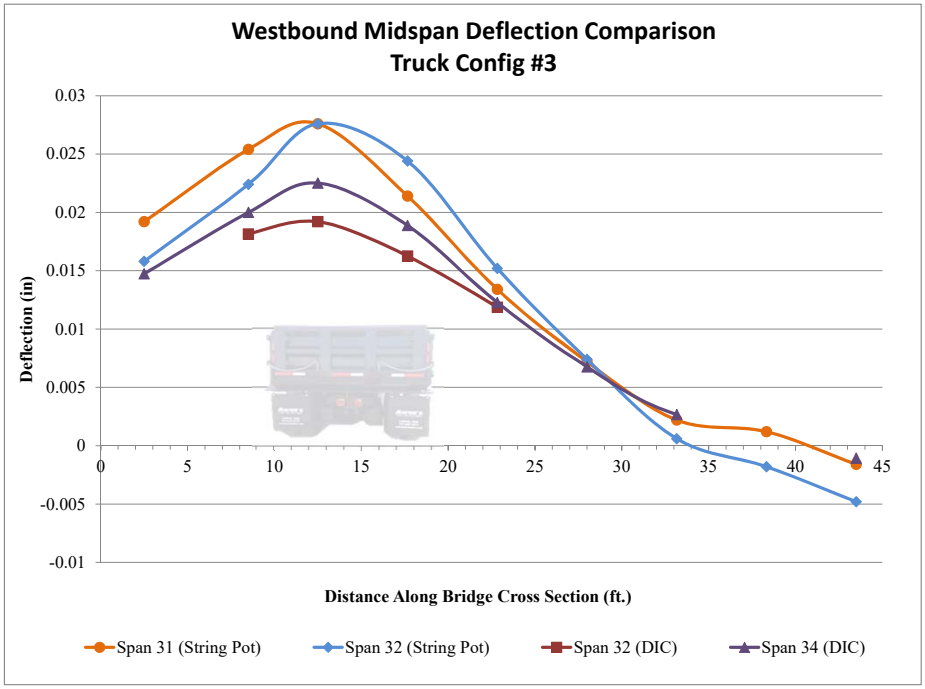

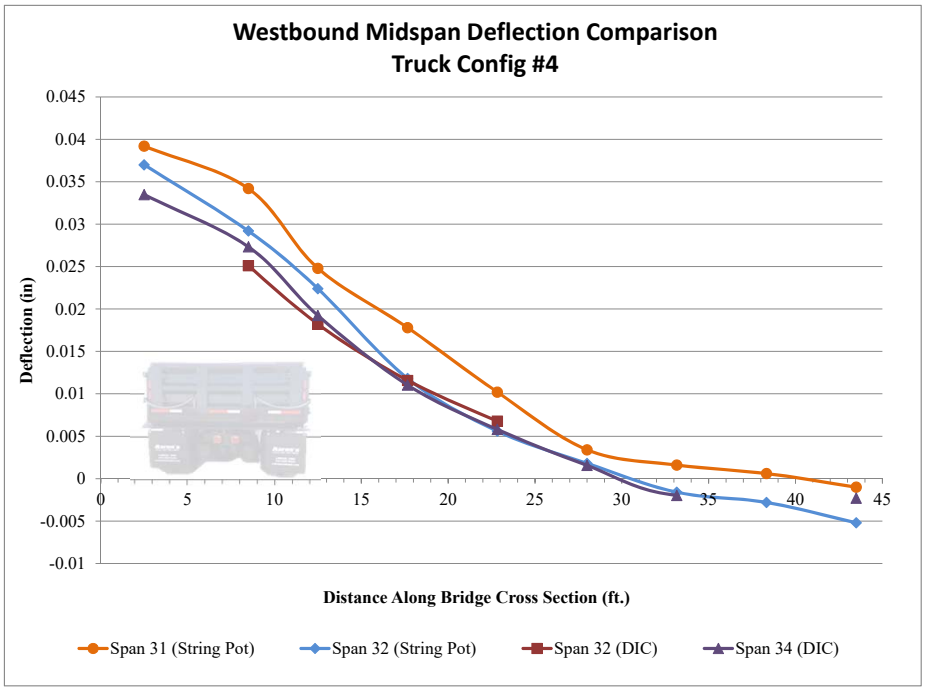

NOTES:

1. Girders are numbered from the east in accordance with widened bridge plans
2. Spans are numbered starting at the South Island and end at Willoughby Spit
3. Traffic flows from Willoughby Spit to the South Island on the WB Structure
4. Missing data points are from malfunctioning equipment

REFERENCES:

1. Contract Drawings 171-20G dated July 17, 1995 (South Approach Bridge WBL Widening)
2. VDOT Inspection Report and Damage Mapping Details - WB Structure Dated June 2015

Live Load Testing Results HRBT WB DEFLECTION COMPARISONS For Hampton Roads Bridge Tunnel	VirginiaTech Invent the Future®	Made JJR	Date 8/14/2016	Job Number 449462
		Checked	Date	Connection
		Backchk'd	Date	Sheet No. 3

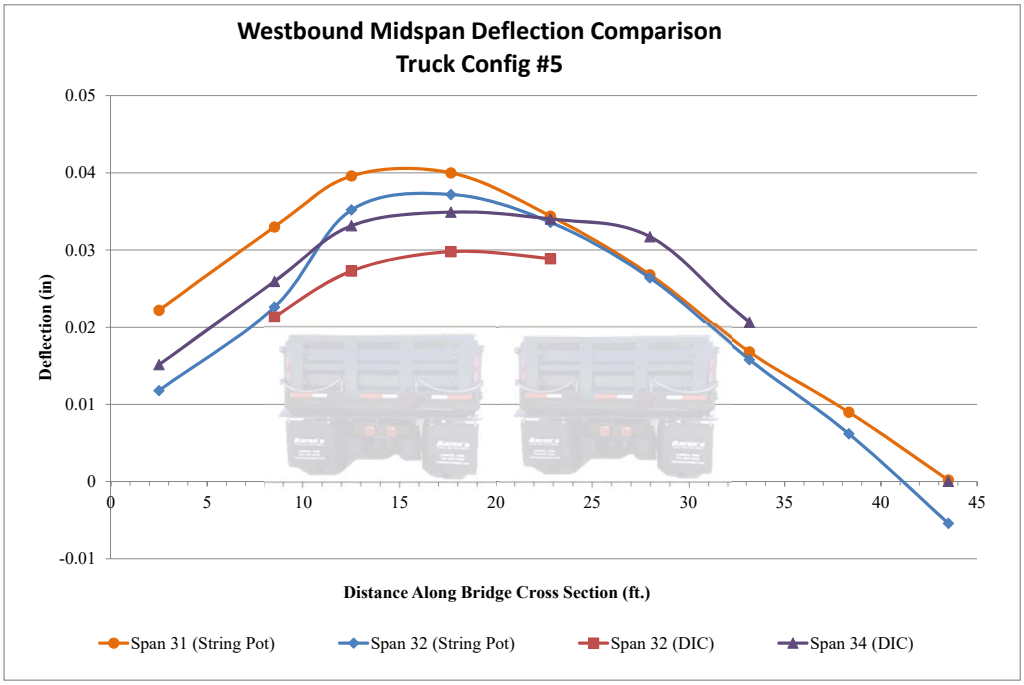

NOTES:

1. Girders are numbered from the east in accordance with widened bridge plans
2. Spans are numbered starting at the South Island and end at Willoughby Spit
3. Traffic flows from Willoughby Spit to the South Island on the WB Structure
4. Missing data points are from malfunctioning equipment

REFERENCES:

1. Contract Drawings 171-20G dated July 17, 1995 (South Approach Bridge WBL Widening)
2. VDOT Inspection Report and Damage Mapping Details - WB Structure Dated June 2015

APPENDIX D-4:

WESTBOUND STRAIN & DEFLECTION TREND COMPARISONS

Live Load Testing Results HRBT WB STRAIN & DEFLECTION TRENDS For Hampton Roads Bridge Tunnel	Made JJR	Date 8/14/2016	Job Number 449462
	Checked	Date	Connection
	Backchk'd	Date	Sheet No. 1

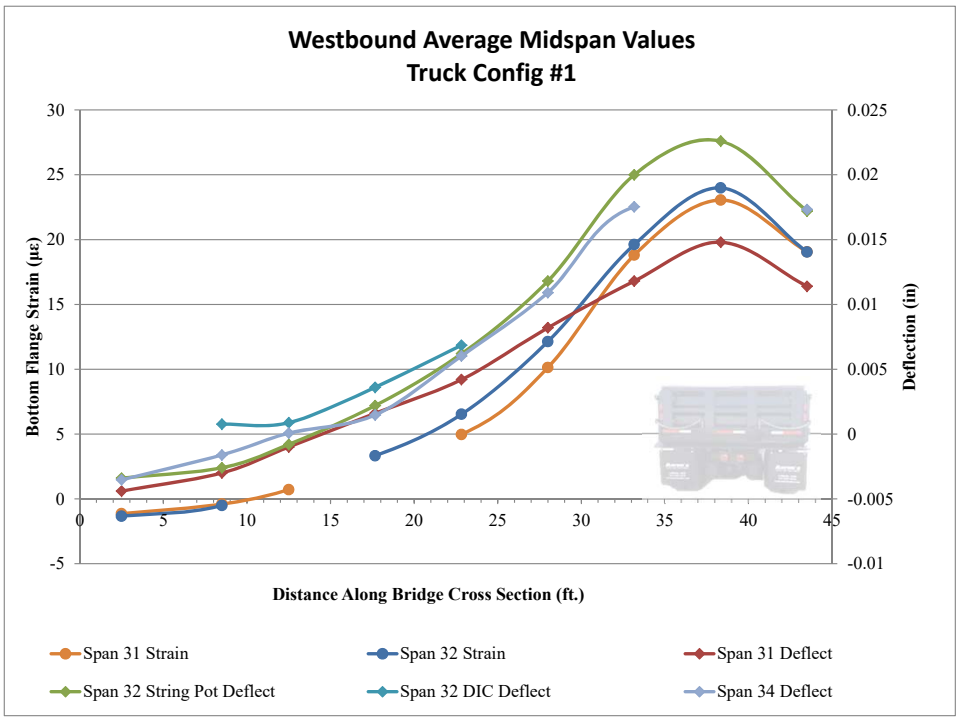

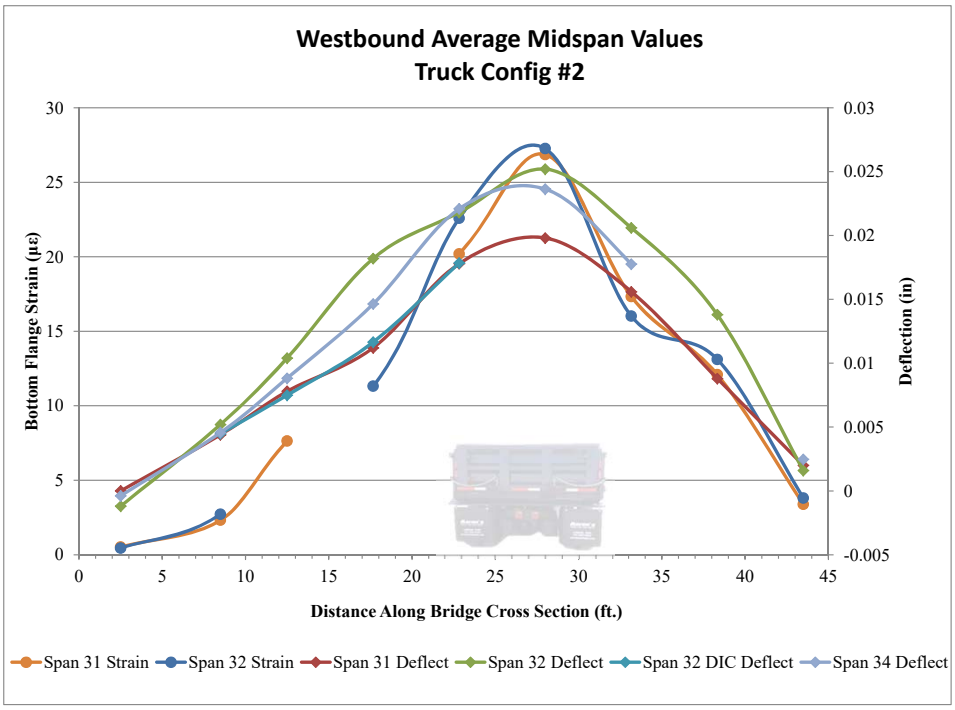

NOTES:
1. Girders are numbered from the east in accordance with widened bridge plans
2. Spans are numbered starting at the South Island and end at Willoughby Spit
3. Traffic flows from Willoughby Spit to the South Island on the WB Structure
4. Missing data points are from malfunctioning equipment

REFERENCES:
1. Contract Drawings 171-20G dated July 17, 1995 (South Approach Bridge WBL Widening)
2. VDOT Inspection Report and Damage Mapping Details - WB Structure Dated June 2015

Live Load Testing Results HRBT WB STRAIN & DEFLECTION TRENDS For Hampton Roads Bridge Tunnel	Made JJR	Date 8/14/2016	Job Number 449462
	Checked	Date	Connection
	Backchk'd	Date	Sheet No. 2

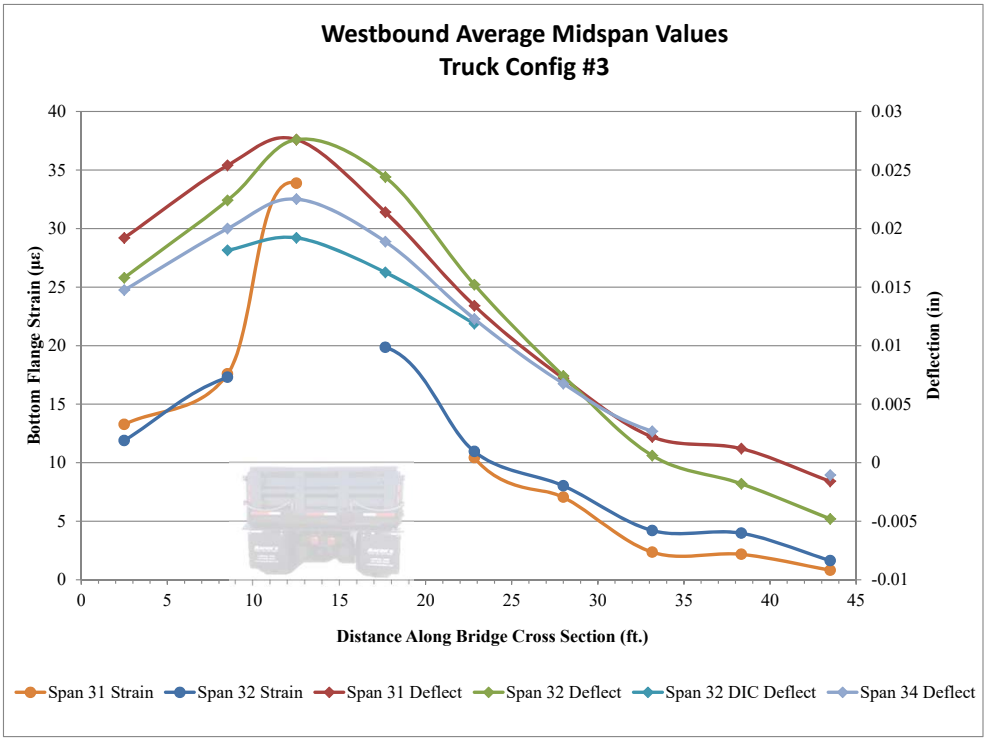

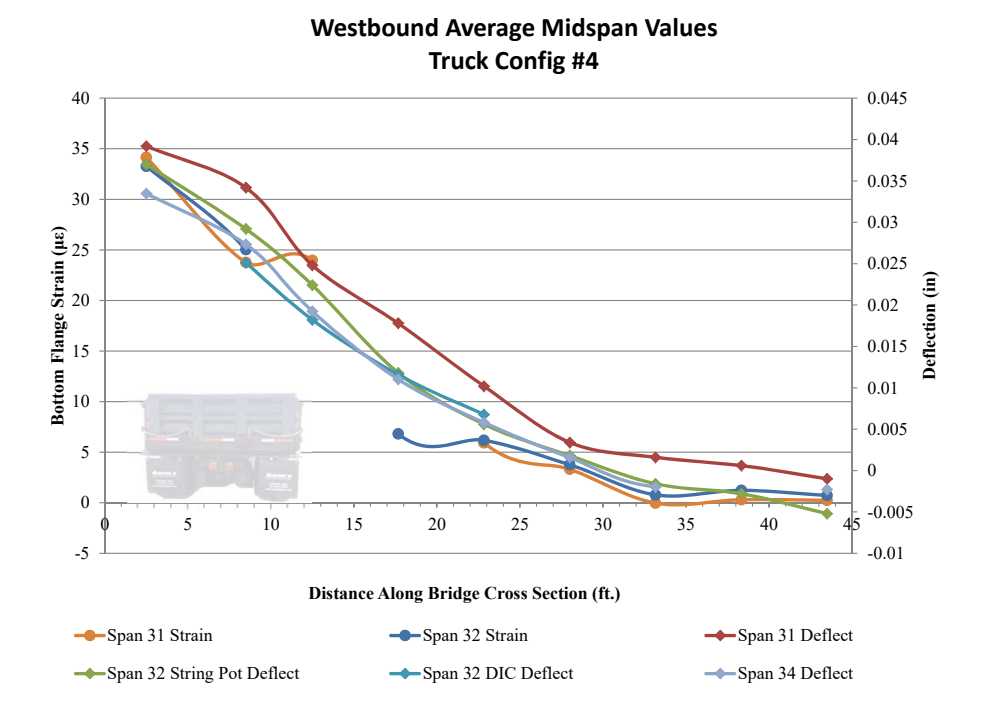

NOTES:
1. Girders are numbered from the east in accordance with widened bridge plans
2. Spans are numbered starting at the South Island and end at Willoughby Spit
3. Traffic flows from Willoughby Spit to the South Island on the WB Structure
4. Missing data points are from malfunctioning equipment

REFERENCES:
1. Contract Drawings 171-20G dated July 17, 1995 (South Approach Bridge WBL Widening)
2. VDOT Inspection Report and Damage Mapping Details - WB Structure Dated June 2015

Live Load Testing Results HRBT WB STRAIN & DEFLECTION TRENDS For Hampton Roads Bridge Tunnel	Made JJR	Date 8/14/2016	Job Number 449462
	Checked	Date	Connection
	Backchk'd	Date	Sheet No. 3

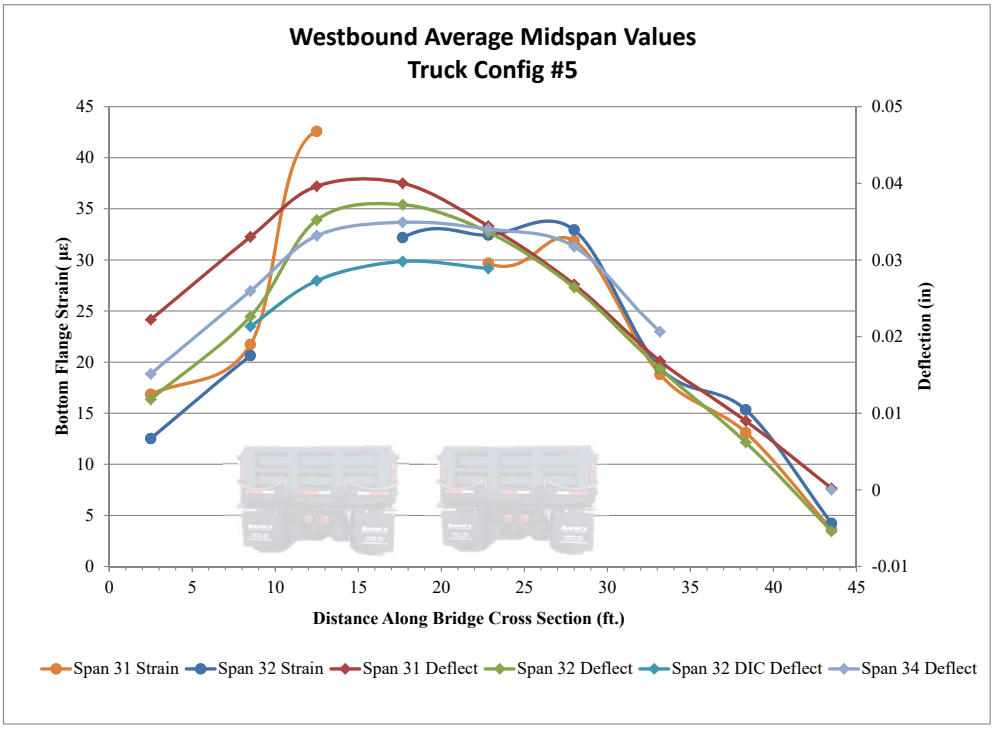

NOTES:
1. Girders are numbered from the east in accordance with widened bridge plans
2. Spans are numbered starting at the South Island and end at Willoughby Spit
3. Traffic flows from Willoughby Spit to the South Island on the WB Structure
4. Missing data points are from malfunctioning equipment

REFERENCES:
1. Contract Drawings 171-20G dated July 17, 1995 (South Approach Bridge WBL Widening)
2. VDOT Inspection Report and Damage Mapping Details - WB Structure Dated June 2015

APPENDIX E

LLDF AND EXPECTED STRAIN CALCULATIONS

Eastbound Girders - Distribution Factors

1. Eastbound Structure Plans

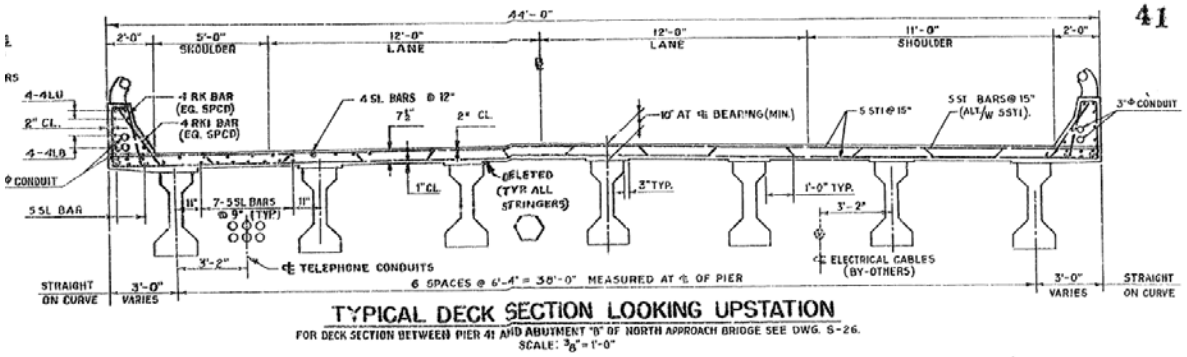

TYPICAL DECK SECTION LOOKING UPSTATION

FOR DECK SECTION BETWEEN PIER 41 AND ABUTMENT "B" OF NORTH APPROACH BRIDGE SEE DWG. S-26.

SCALE: 3/8" = 1'-0"

Girder 1 Girder 2 Girder 3 Girder 4 Girder 5 Girder 6 Girder 7

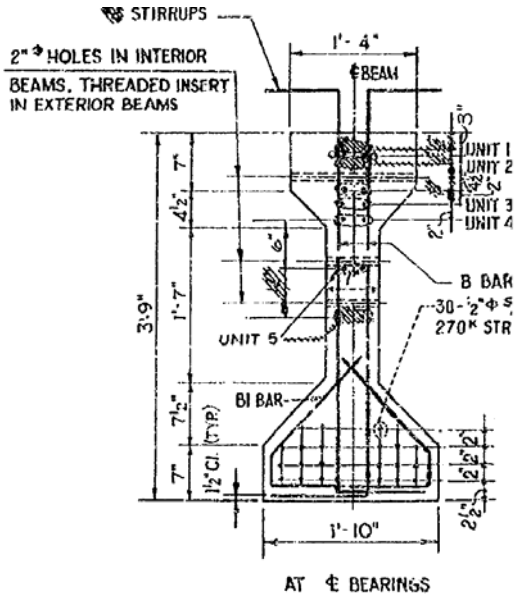

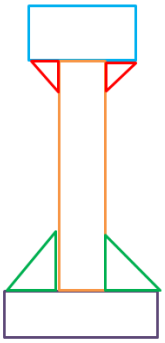

2. Bridge Cross Section Properties (Per As Built Drawings)

$f'c\_girders := 5$ ksi $\quad w := 145$ pcf $\quad t_{haunch} := 0$ in $\quad S := 6 + \frac{4}{12}$ ft

$f'c\_deck := 4$ ksi $\quad L := 75$ ft $\quad t_s := 7.5$ inches

$$E_{c\_deck} := 33000 \cdot \left(\frac{w}{1000}\right)^{1.5} \cdot \sqrt{f'c\_deck} \qquad E_{c\_deck} = 3644.1 \text{ ksi}$$

Eqn. 5.4.2.4-1 pg. 5-18 (362)

$$E_{c\_girders} := 33000 \cdot \left(\frac{w}{1000}\right)^{1.5} \cdot \sqrt{f'c\_girders} \qquad E_{c\_girders} = 4074.3 \text{ ksi}$$

Eqn. 5.4.2.4-1 pg. 5-18 (362)

$$n := \frac{E_{c\_girders}}{E_{c\_deck}} \qquad n = 1.118$$

Eqn. 6.10.1.1b-1 pg. 6-104 (731)

2.1 Girder Section Properties

	Width (in)	Height (in)	Area (in^2)	y (in)	Ay (in^3)	Ix (in^4)	d (in)	I+Ad^2 (in^4)
Light Blue Box	16	7	112	41.5	4648	457.3	21.23	50920.7
Red Triangle	4.5	4.5	20.25	36.5	739.125	22.8	16.23	5354.6
Orange Box	7	31	217	22.5	4882.5	17378.1	2.23	18453.9
Green Triangles	7.5	7.5	56.25	9.5	534.375	175.8	10.77	6704.6
Purple Box	22	7	154	3.5	539	628.8	16.77	43956.6
			559.5		11343			125390.3

y_bot 20.273 in

$I_x := 125390.3 \ in^4$ $A := 559.5 \ in^2$ $y_{bot} := 20.273 \ in$ $h := 45 \ in$

$t_w := 7 \ in$ $b_w := 16 \ in$

$$e_g := \frac{t_s}{2} + t_{haunch} + \left(h - y_{bot}\right) \qquad e_g = 28.477 \ in$$

$$K_g := n \cdot \left(I_x + A \cdot e_g^{\,2}\right) \qquad K_g = 647466 \ in^4$$

Eqn. 4.6.2.2.1-1
pg. 4-32 (266)

2.2 Short Term Composite (n) Section Properties

$$b_{eff} := \min\left(\frac{L \cdot 12}{4}, 12 \cdot t_s + t_w, 12 \cdot t_s + \frac{b_w}{2}, S \cdot 12\right) \qquad b_{eff} = 76 \ in$$

$$b_{eff} := \frac{b_{eff}}{n} \qquad b_{eff} = 67.976 \ in$$

	Width (in)	Height (in)	Area (in^2)	y (in)	Ay (in^3)	Ix (in^4)	d (in)	I+Ad^2 (in^4)
Girder	--------	----------	559.5	20.273	11343	125390.3	13.58	228522
Slab	67.976	7.5	509.82	48.75	24853.73	2389.781	14.90	115571
			1069.32		36196.73			344094

y_bot 33.850 in

$I_{x\_comp} := 344094 \ in^4$ $y_{bot\_comp} := 33.85 \ in$ $A_{comp} := 1069.32 \ in$

3. AASHTO Girder Distribution Factors

Note: For the Tables referenced below, all conditions are satisfied:

$3.5 \le S \le 16.0$
$4.5 \le t_s \le 12.0$
$20 \le L \le 240$

$N_b \ge 4$
$10{,}000 \le K_g \le 7{,}000{,}000$

MOMENT DISTRIBUTION FACTORS - INTERIOR GIRDER

Two or more Design Lanes:

MOMENT DISTRIBUTION FACTORS - INTERIOR GIRDER

Two or more Design Lanes:

$$g\_m := 0.075 + \left(\frac{S}{9.5}\right)^{0.6} \cdot \left(\frac{S}{L}\right)^{0.2} \cdot \left(\frac{K_g}{12 \cdot L \cdot t_s^{\,3}}\right)^{0.1}$$

$g\_m = 0.579$ lanes

Table 4.6.2.2.2b-1 pg 4-37 (271)

One Lane Loaded:

$$g\_m\_one := 0.06 + \left(\frac{S}{14}\right)^{0.4} \cdot \left(\frac{S}{L}\right)^{0.3} \cdot \left(\frac{K_g}{12 \cdot L \cdot t_s^{\,3}}\right)^{0.1}$$

$g\_m\_one = 0.426$ lanes

Table 4.6.2.2.2b-1 pg 4-37 (271)

$g\_moment := \max(g\_m, g\_m\_one)$ $g\_moment = 0.579$ lanes Girders 2-6

MOMENT DISTRIBUTION FACTORS - EXTERIOR GIRDER

Two or more Design Lanes:

$d_e := 1$ ft

$$e := 0.77 + \frac{d_e}{9.1}$$

$e = 0.88$

Table 4.6.2.2.2d-1 p. 4-40 (274)

$g\_m := e \cdot g\_moment$ $g\_m = 0.51$ lanes

Table 4.6.2.2.2d-1 p. 4-40 (274)

One Lane Loaded (Lever Rule):

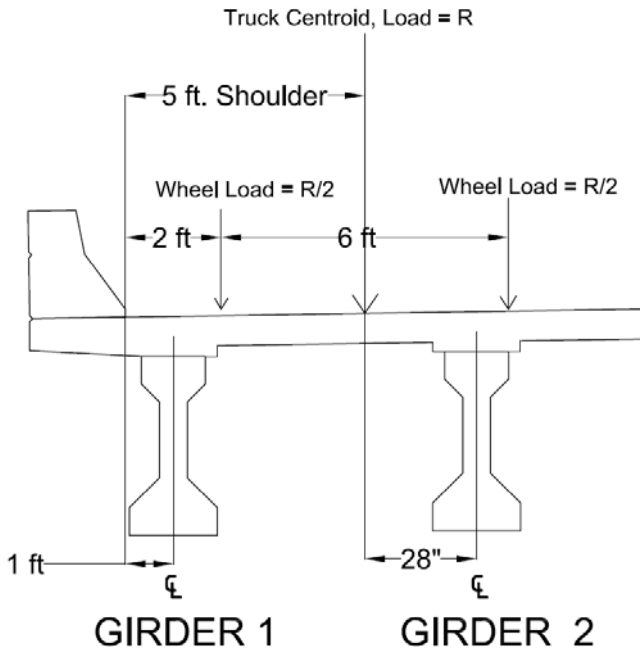

$m := 1.2$ multiple presence factor for one lane

Table 3.6.1.1.2-1
p. 3-20 (77)

$$g\_m\_lever := \frac{(5 \cdot 12 + 4)}{(6 \cdot 12 + 4)} \cdot \frac{1}{2} \cdot m$$

$g\_m\_lever = 0.505$ lanes

$g\_moment := \max(g\_m, g\_m\_lever)$ $g\_moment = 0.51$ lanes Girders 1 and 7

Original Westbound Girders - Distribution Factors

1. Westbound Structure Plans

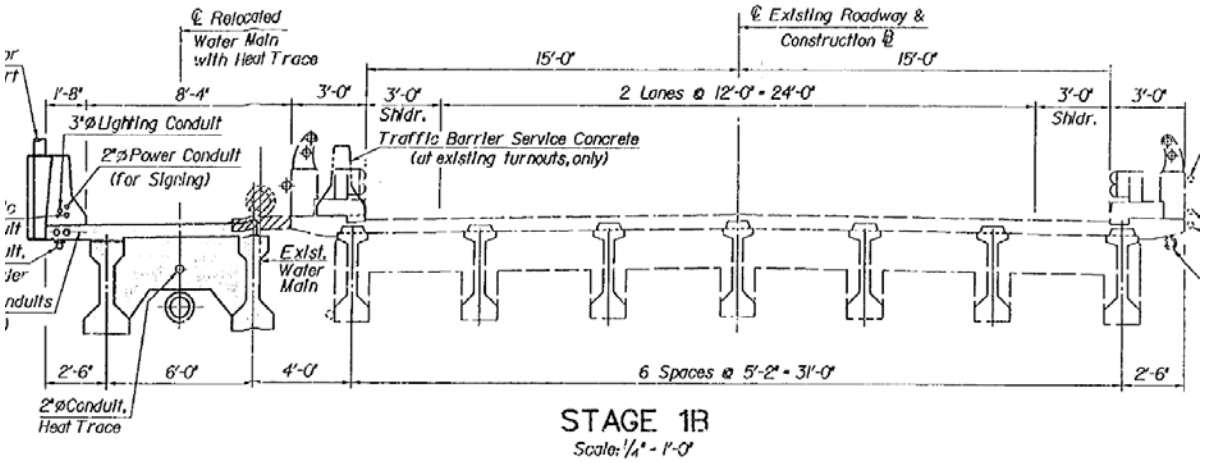

Girder 3 Girder 4 Girder 5 Girder 6 Girder 7 Girder 8 Girder 9

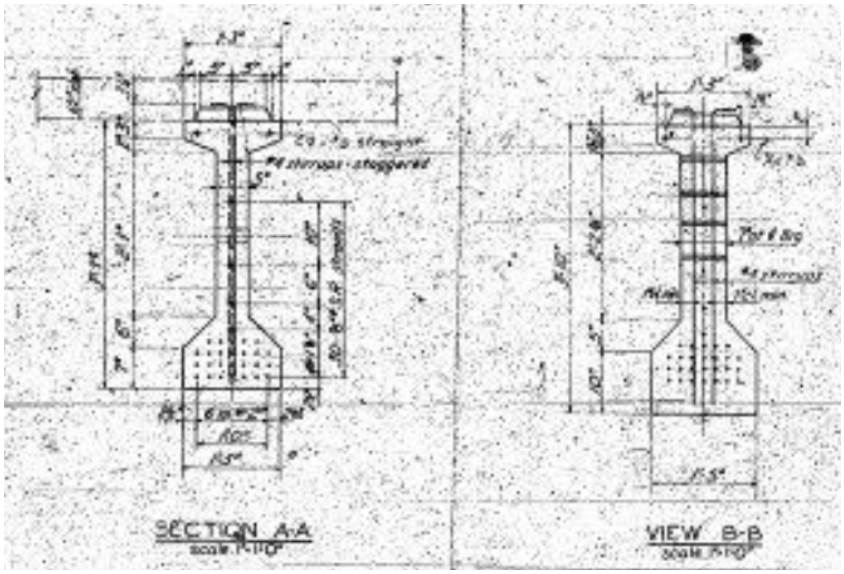

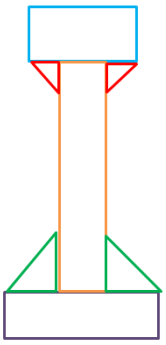

2. Bridge Cross Section Properties (Per As Built Drawings)

$f'c\_girders := 5$ ksi $\quad w := 145$ pcf $\quad t_{haunch} := 0$ in $\quad S := 5 + \frac{2}{12}$ ft

$f'c\_deck := 4$ ksi $\quad L := 50$ ft $\quad t_s := 6.5$ inches

$$E_{c\_deck} := 33000 \cdot \left(\frac{w}{1000}\right)^{1.5} \cdot \sqrt{f'c\_deck} \qquad E_{c\_deck} = 3644.1 \text{ ksi}$$

Eqn. 5.4.2.4-1 pg. 5-18 (362)

$$E_{c\_girders} := 33000 \cdot \left(\frac{w}{1000}\right)^{1.5} \cdot \sqrt{f'c\_girders} \qquad E_{c\_girders} = 4074.3 \text{ ksi}$$

Eqn. 5.4.2.4-1 pg. 5-18 (362)

$$n := \frac{E_{c\_girders}}{E_{c\_deck}} \qquad n = 1.118$$

Eqn. 6.10.1.1b-1
pg. 6-104 (731)

2.1 Girder Section Properties

Noncomposite Girder

	Width (in)	Height (in)	Area (in^2)	y (in)	Ay (in^3)	Ix (in^4)	d (in)	I+Ad^2 (in^4)
Light Blue Box	15	3	45	41.5	1867.5	33.8	23.16	24163.7
Red Triangle	5	2	10	39.33333	393.3333	2.2	20.99	4407.9
Orange Box	5	33	165	23.5	3877.5	14973.8	5.16	19360.9
Green Triangles	6	6	36	9	324	72.0	9.34	3214.9
Purple Box	17	7	119	3.5	416.5	485.9	14.84	26705.3
			375		6878.833			77852.7

y_bot 18.344 in

$Ix := 77852.7 \ in^4$ $A := 375 \ in^2$ $y_{bot} := 18.344 \ in$ $h := 43 \ in$

$t_w := 5 \ in$ $b_w := 15 \ in$

$$e_g := \frac{t_s}{2} + t_{haunch} + (h - y_{bot}) \qquad e_g = 27.906 \ in$$

$$K_g := n \cdot (Ix + A \cdot e_g^2) \qquad K_g = 413541 \ in^4$$

Eqn. 4.6.2.2.1-1
pg. 4-32 (266)

2.2 Short Term Composite (n) Section Properties

$$b_{eff} := \min\left(\frac{L \cdot 12}{4}, 12 \cdot t_s + t_w, 12 \cdot t_s + \frac{b_w}{2}, S \cdot 12\right) \qquad b_{eff} = 62 \ in$$

$$b_{eff} := \frac{b_{eff}}{n} \qquad b_{eff} = 55.454 \ in$$

Composite Girder

	Width (in)	Height (in)	Area (in^2)	y (in)	Ay (in^3)	Ix (in^4)	d (in)	I+Ad^2 (in^4)
Girder	--------	----------	375	18.344	6878.833	77852.7	13.68	148002
Slab	55.454	6.5	360.451	46.25	16670.86	1269.088	14.23	74250
			735.451		23549.69			222253

y_bot 32.021 in

$I_{x\_comp} := 222253 \ in^4$ $y_{bot\_comp} := 32.021 \ in$ $A_{comp} := 735.451 \ in$

3. AASHTO Girder Distribution Factors

Note: For the Tables referenced below, all conditions are satisfied:

$3.5 \le S \le 16.0$
$4.5 \le t_s \le 12.0$
$20 \le L \le 240$

$N_b \ge 4$
$10{,}000 \le K_g \le 7{,}000{,}000$

MOMENT DISTRIBUTION FACTORS - INTERIOR GIRDERS

Two or more Design Lanes:

$$g\_m := 0.075 + \left(\frac{S}{9.5}\right)^{0.6} \cdot \left(\frac{S}{L}\right)^{0.2} \cdot \left(\frac{K_g}{12 \cdot L \cdot t_s^{\,3}}\right)^{0.1}$$

$g\_m = 0.558$ lanes

Table 4.6.2.2.2b-1 pg 4-37 (271)

One Lane Loaded:

$$g\_m\_one := 0.06 + \left(\frac{S}{14}\right)^{0.4} \cdot \left(\frac{S}{L}\right)^{0.3} \cdot \left(\frac{K_g}{12 \cdot L \cdot t_s^{\,3}}\right)^{0.1}$$

$g\_m\_one = 0.432$ lanes

Table 4.6.2.2.2b-1 pg 4-37 (271)

$g\_moment := \max(g\_m, g\_m\_one)$ $g\_moment = 0.558$ lanes Girders 4-8

MOMENT DISTRIBUTION FACTORS - EXTERIOR GIRDER

Two or more Design Lanes:

$d_e := \frac{10}{12}$ ft

$e := 0.77 + \frac{d_e}{9.1}$ $e = 0.862$

Table 4.6.2.2.2d-1 p. 4-40 (274)

$g\_m := e \cdot g\_moment$ $g\_m = 0.481$ lanes

Table 4.6.2.2.2d-1 p. 4-40 (274)

One Lane Loaded (Lever Rule):

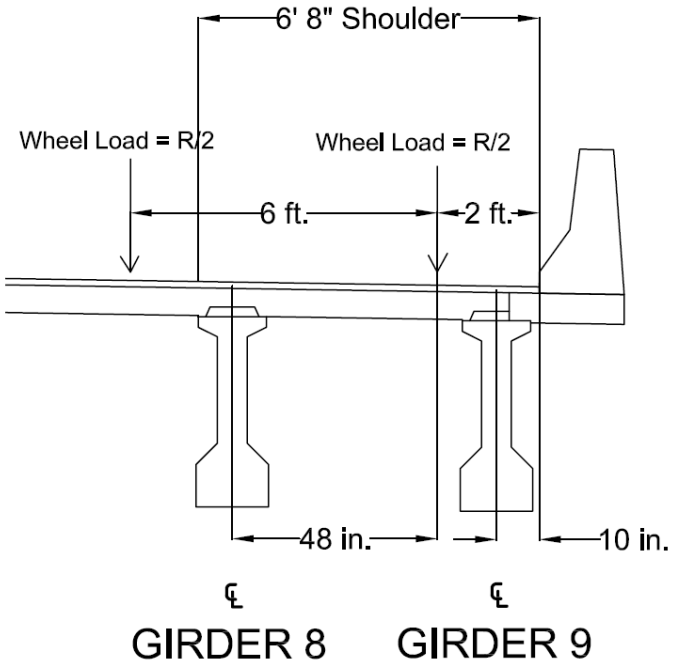

$m := 1.2$ multiple presence factor for one lane

Table 3.6.1.1.2-1
p. 3-20 (77)

$$g\_m\_lever := \frac{(48)}{(5\cdot 12 + 2)}\cdot\frac{1}{2}\cdot m \qquad g\_m\_lever = 0.465 \text{ lanes}$$

$g\_moment := \max(g\_m, g\_m\_lever)$ $g\_moment = 0.481$ lanes Girder 9

Modifications Made for Girder 3

2.2 Short Term Composite (n) Section Properties

$$S := \frac{5 + \frac{2}{12} + 4}{2}$$ Note: Spacing is 5'2" on Right, 4' on Left $S = 4.583$ ft

$$b_{eff} := \min\left(\frac{L\cdot 12}{4}, 12\cdot t_s + t_w, 12\cdot t_s + \frac{b_w}{2}, S\cdot 12\right) \qquad b_{eff} = 55 \text{ in}$$

$$b_{eff} := \frac{b_{eff}}{n} \qquad b_{eff} = 49.193 \text{ in}$$

Composite Girder

	Width (in)	Height (in)	Area (in^2)	y (in)	Ay (in^3)	Ix (in^4)	d (in)	I+Ad^2 (in^4)
Girder	--------	----------	375	18.344	6878.833	77852.7	12.84	139713
Slab	49.193	6.5	319.7545	46.25	14788.65	1125.802	15.06	73674
			694.7545		21667.48			213387

y_bot 31.187 in

$I_{x\_comp} := 213387\ in^4$ $y_{bot\_comp} := 31.387\ in$ $A_{comp} := 694.75\ in$

3. AASHTO Girder Distribution Factors

Note: For the Tables referenced below, all conditions are satisfied:

$3.5 \le S \le 16.0$ $N_b \ge 4$

$4.5 \le t_s \le 12.0$ $10{,}000 \le K_g \le 7{,}000{,}000$

$20 \le L \le 240$

MOMENT DISTRIBUTION FACTORS - INTERIOR GIRDERS

Two or more Design Lanes:

$$g\_m := 0.075 + \left(\frac{S}{9.5}\right)^{0.6} \cdot \left(\frac{S}{L}\right)^{0.2} \cdot \left(\frac{K_g}{12 \cdot L \cdot t_s^{\,3}}\right)^{0.1}$$

$g\_m = 0.514$ lanes

Table 4.6.2.2.2b-1 pg 4-37 (271)

One Lane Loaded:

$$g\_m\_one := 0.06 + \left(\frac{S}{14}\right)^{0.4} \cdot \left(\frac{S}{L}\right)^{0.3} \cdot \left(\frac{K_g}{12 \cdot L \cdot t_s^{\,3}}\right)^{0.1}$$

$g\_m\_one = 0.402$ lanes

Table 4.6.2.2.2b-1 pg 4-37 (271)

$g\_moment := \max(g\_m, g\_m\_one)$ $g\_moment = 0.514$ lanes Girder 3

Westbound Widened Girders - Distribution Factors

1. Westbound Structure Plans

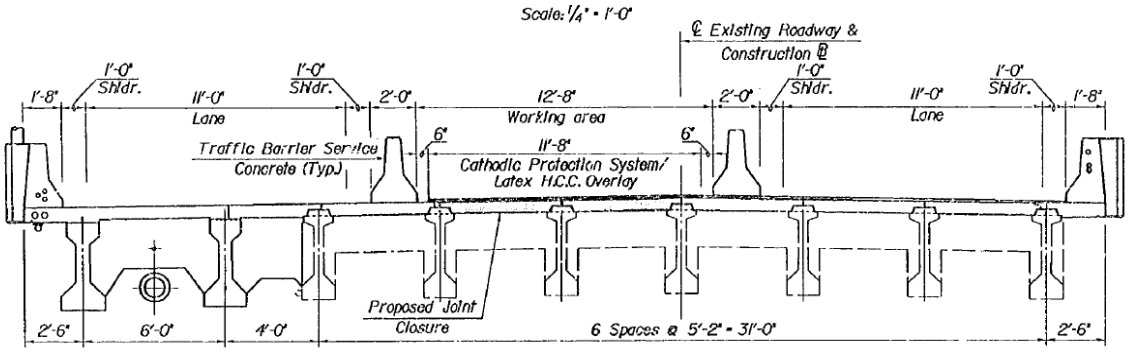

Girder 1 Girder 2

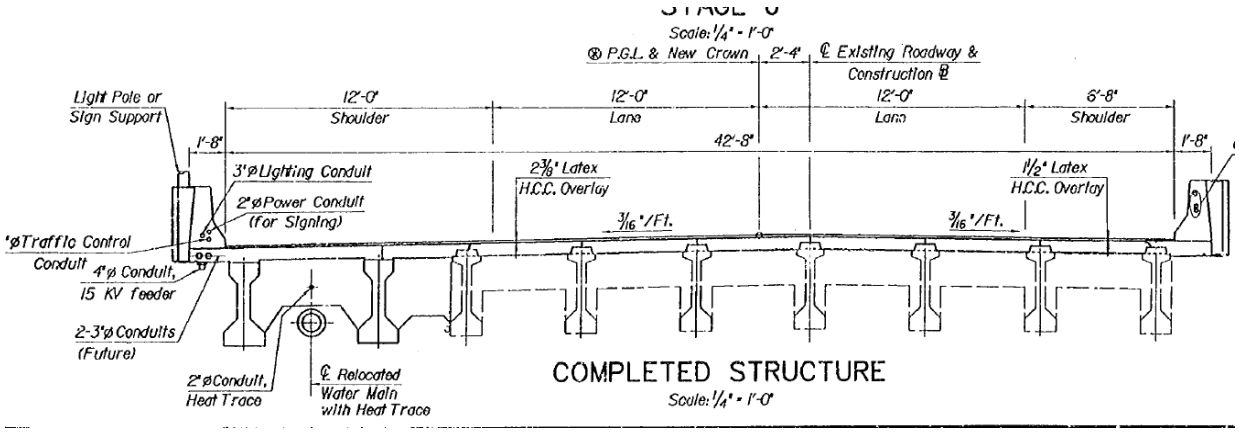

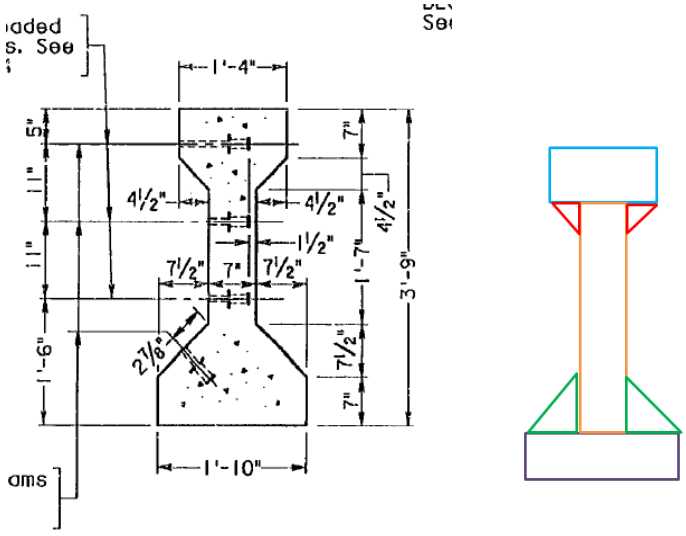

SECTION A-A

2. Bridge Cross Section Properties (Per As Built Drawings)

Left Right

$f'c\_girders := 5$ ksi $\quad w := 145$ pcf $\quad t_{haunch} := 0$ in $\quad S := 3 + 2$ ft

$f'c\_deck := 4$ ksi $\quad L := 50$ ft $\quad t_s := 7.5$ inches

$$E_{c\_deck} := 33000 \cdot \left(\frac{w}{1000}\right)^{1.5} \cdot \sqrt{f'c\_deck} \qquad E_{c\_deck} = 3644.1 \text{ ksi}$$ Eqn. 5.4.2.4-1 pg. 5-18 (362)

$$E_{c\_girders} := 33000 \cdot \left(\frac{w}{1000}\right)^{1.5} \cdot \sqrt{f'c\_girders} \qquad E_{c\_girders} = 4074.3 \text{ ksi}$$ Eqn. 5.4.2.4-1 pg. 5-18 (362)

$$n := \frac{E_{c\_girders}}{E_{c\_deck}} \qquad n = 1.118$$ Eqn. 6.10.1.1b-1 pg. 6-104 (731)

2.1 Girder Section Properties

	Width (in)	Height (in)	Area (in^2)	y (in)	Ay (in^3)	Ix (in^4)	d (in)	I+Ad^2 (in^4)
Light Blue Box	16	7	112	41.5	4648	457.3	21.23	50920.7
Red Triangle	4.5	4.5	20.25	36.5	739.125	22.8	16.23	5354.6
Orange Box	7	31	217	22.5	4882.5	17378.1	2.23	18453.9
Green Triangles	7.5	7.5	56.25	9.5	534.375	175.8	10.77	6704.6
Purple Box	22	7	154	3.5	539	628.8	16.77	43956.6
			559.5		11343			125390.3
		y_bot	20.273 in					

$Ix := 125390.3$ in^4 $\quad A := 559.5$ in^2 $\quad y_{bot} := 20.273$ in $\quad h := 45$ in

$t_w := 7$ in $\quad b_w := 16$ in

$$e_g := \frac{t_s}{2} + t_{haunch} + \left(h - y_{bot}\right) \qquad e_g = 28.477 \text{ in}$$

$$K_g := n \cdot \left(Ix + A \cdot e_g^{\,2}\right) \qquad K_g = 647466 \text{ } in^4$$ Eqn. 4.6.2.2.1-1 pg. 4-32 (266)

2.2 Short Term Composite (n) Section Properties

$$b_{eff} := \min\left(\frac{L \cdot 12}{4}, 12 \cdot t_s + t_w, 12 \cdot t_s + \frac{b_w}{2}, S \cdot 12\right) \qquad b_{eff} = 60 \text{ in}$$

$$b_{eff} := \frac{b_{eff}}{n} \qquad b_{eff} = 53.666 \text{ in}$$

Composite Girder

	Width (in)	Height (in)	Area (in^2)	y (in)	Ay (in^3)	Ix (in^4)	d (in)	I+Ad^2 (in^4)
Girder	--------	----------	559.5	20.273	11343	125390.3	11.91	204815
Slab	53.66666	7.5	402.49995	48.75	19621.87	1886.719	16.56	112292
			961.99995		30964.87			317107

y_bot 32.188 in

$I_{x\_comp} := 317107\ in^4$ $y_{bot\_comp} := 32.188\ in$ $A_{comp} := 962\ in$

3. AASHTO Girder Distribution Factors

Note: For the Tables referenced below, all conditions are satisfied: $3.5 \le S \le 16.0$, $4.5 \le t_s \le 12.0$, $20 \le L \le 240$, $N_b \ge 4$, $10{,}000 \le K_g \le 7{,}000{,}000$

MOMENT DISTRIBUTION FACTORS - INTERIOR GIRDER

Two or more Design Lanes:

$$g\_m := 0.075 + \left(\frac{S}{9.5}\right)^{0.6} \cdot \left(\frac{S}{L}\right)^{0.2} \cdot \left(\frac{K_g}{12 \cdot L \cdot t_s^{\,3}}\right)^{0.1}$$

$g\_m = 0.547$ lanes — Table 4.6.2.2.2b-1 pg 4-37 (271)

One Lane Loaded:

$$g\_m\_one := 0.06 + \left(\frac{S}{14}\right)^{0.4} \cdot \left(\frac{S}{L}\right)^{0.3} \cdot \left(\frac{K_g}{12 \cdot L \cdot t_s^{\,3}}\right)^{0.1}$$

$g\_m\_one = 0.425$ lanes — Table 4.6.2.2.2b-1 pg 4-37 (271)

$g\_moment := \max(g\_m, g\_m\_one)$ $g\_moment = 0.547$ lanes — Girder 2

MOMENT DISTRIBUTION FACTORS - EXTERIOR GIRDER

Two or more Design Lanes:

$d_e := \frac{10}{12}$ ft

$e := 0.77 + \frac{d_e}{9.1}$ $e = 0.862$ — Table 4.6.2.2.2d-1 p. 4-40 (274)

$g\_m := e \cdot g\_moment$ $g\_m = 0.471$ lanes — Table 4.6.2.2.2d-1 p. 4-40 (274)

One Lane Loaded (Lever Rule):

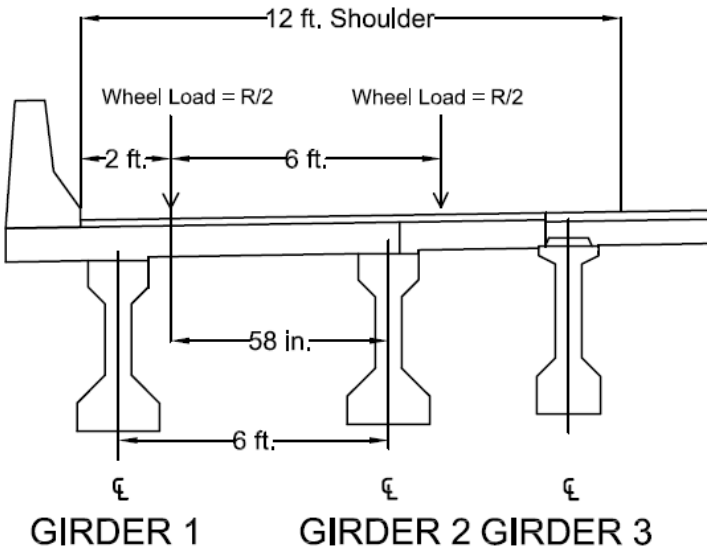

$m := 1.2$ multiple presence factor for one lane

Table 3.6.1.1.2-1
p. 3-20 (77)

$$g\_m\_lever := \frac{(58)}{(6 \cdot 12)} \cdot \frac{1}{2} \cdot m$$

$g\_m\_lever = 0.483$ lanes

$g\_moment := \max(g\_m, g\_m\_lever)$ $g\_moment = 0.483$ lanes Girder 1

Strain Distribution Comparison Calculations

1. Given Information

Structure: Eastbound
Span: 56
Girder: 5
Truck Configuration: 5

From the Experimental Strain Live Load Distribution Factors:

$LLDF_{RL} := 0.2589$ $LLDF_{LL} := 0.1137$

2. Truck Loads

Left Lane Axle Loads

$P_{LL\_front\_D} := 8200\ lbs$ $P_{LL\_front\_P} := 7800\ lbs$

$P_{LL\_back1\_D} := 8960\ lbs$ $P_{LL\_back1\_P} := 9260\ lbs$

$P_{LL\_back2\_D} := 9280\ lbs$ $P_{LL\_back2\_P} := 9520\ lbs$

$P_{LL\_front} := P_{LL\_front\_D} + P_{LL\_front\_P}$ $P_{LL\_front} = 16000\ lbs$

$P_{LL\_back1} := P_{LL\_back1\_D} + P_{LL\_back1\_P}$ $P_{LL\_back1} = 18220\ lbs$

$P_{LL\_back2} := P_{LL\_back2\_D} + P_{LL\_back2\_P}$ $P_{LL\_back2} = 18800\ lbs$

Right Lane Truck Axle Loads

$P_{RL\_front\_D} := 7980\ lbs$ $P_{RL\_front\_P} := 7640\ lbs$

$P_{RL\_back1\_D} := 9320\ lbs$ $P_{RL\_back1\_P} := 8000\ lbs$

$P_{RL\_back2\_D} := 9600\ lbs$ $P_{RL\_back2\_P} := 8220\ lbs$

$P_{RL\_front} := P_{RL\_front\_D} + P_{RL\_front\_P}$ $P_{RL\_front} = 15620\ lbs$

$P_{RL\_back1} := P_{RL\_back1\_D} + P_{RL\_back1\_P}$ $P_{RL\_back1} = 17320\ lbs$

$P_{RL\_back2} := P_{RL\_back2\_D} + P_{RL\_back2\_P}$ $P_{RL\_back2} = 17820\ lbs$

3. Load Taken By Gider of Interest

$P_{front} := LLDF_{LL} \cdot P_{LL\_front} + LLDF_{RL} \cdot P_{RL\_front}$ $P_{front} = 5863$ lbs

$P_{back1} := LLDF_{LL} \cdot P_{LL\_back1} + LLDF_{RL} \cdot P_{RL\_back2}$ $P_{back1} = 6685$ lbs

$P_{back2} := LLDF_{LL} \cdot P_{LL\_back2} + LLDF_{RL} \cdot P_{RL\_back2}$ $P_{back2} = 6751$ lbs

4. Determine Moment In Girder

Using an influence line for the moment at 1.50, the max influence can be found by applying a unit load at midspan and calculating the corresponding moment:

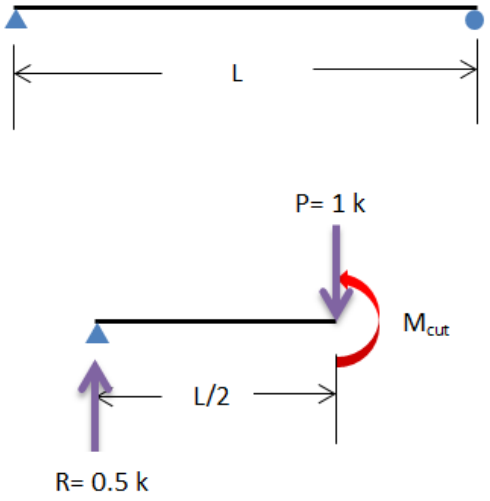

$L := 75 \ ft$

Sum moments about the cut:

$M_{cut} := 0.5 \cdot 0.5 \cdot L$ $M_{cut} = 18.75 \ \frac{k - ft}{k}$

Influence Line:

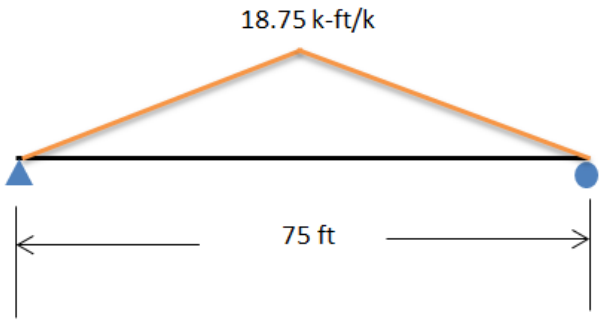

Determine Truck Moment:

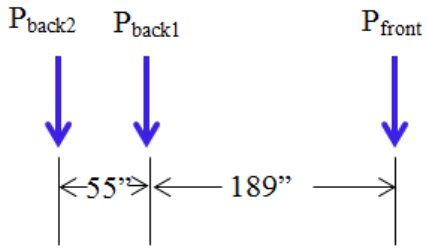

$$influence_{back2} := 0.5\cdot\left(\frac{L}{2} - \frac{55}{12}\right) \qquad influence_{back2} = 16.458 \ \frac{k-ft}{k}$$

$$influence_{back1} := 0.5\cdot\frac{L}{2} \qquad influence_{back1} = 18.75 \ \frac{k-ft}{k}$$

$$influence_{front} := -0.5\cdot\left(\frac{L}{2} + \frac{189}{12}\right) + M_{cut}\cdot 2 \qquad influence_{front} = 10.875 \ \frac{k-ft}{k}$$

$$M_{truck} := influence_{back2}\cdot\frac{P_{back2}}{1000} + influence_{back1}\cdot\frac{P_{back1}}{1000} + influence_{front}\cdot\frac{P_{front}}{1000}$$

$M_{truck} = 300$ k – ft

5. Compare to Cracking Moment

$f_c := 5500$ psi

Note: The As-Built drawings specify 5000 psi concrete for the girders but it is assumed the contractor ordered a slightly stronger mix

$$f_r := 7.5\cdot\sqrt{f_c} \qquad f_r = 556 \ psi$$

From Excel Sheet Section Properties: $I_{tr} := 366025$ in^4 $y_{bot} := 33.128$ in

$$M_{cr} := \frac{f_r\cdot I_{tr}}{y_{bot}}\cdot\frac{1}{12000} \qquad M_{cr} = 512 \ k-ft$$

$M_{truck} = 300$ k – ft < $M_{cr} = 512$ k – ft

6. Determine Strain at Bottom of Girder:

$$E_c := 57\cdot\sqrt{f_c} \qquad E_c = 4227 \ ksi$$

$$\varepsilon_{bot} := \frac{(M_{truck}\cdot 12)\cdot y_{bot}}{I_{tr}\cdot E_c}\cdot 10^6$$

$\varepsilon_{bot} = 77.1$ microstrain

7. Compare to Actual Experimental Strains

Strain value for damaged girder: $\varepsilon_{bot\_exp} := 101.5$ microstrain

Undamaged extrapolation value for bottom of girder: $\varepsilon_{bot\_extrapolated} := 40$ microstrain

Strain Distribution Comparison Calculations

1. Given Information

Structure: Westbound
Span: 31
Girder: 7
Truck Configuration: 5

From the Experimental Strain Live Load Distribution Factors:

$LLDF_{RL} := 0.07032$ $LLDF_{LL} := 0.25256$

2. Truck Loads

Left Lane Axle Loads

$P_{LL\_front\_D} := 8220\ lbs$ $P_{LL\_front\_P} := 7840\ lbs$

$P_{LL\_back1\_D} := 9240\ lbs$ $P_{LL\_back1\_P} := 9380\ lbs$

$P_{LL\_back2\_D} := 9240\ lbs$ $P_{LL\_back2\_P} := 8920\ lbs$

$P_{LL\_front} := P_{LL\_front\_D} + P_{LL\_front\_P}$ $P_{LL\_front} = 16060\ lbs$

$P_{LL\_back1} := P_{LL\_back1\_D} + P_{LL\_back1\_P}$ $P_{LL\_back1} = 18620\ lbs$

$P_{LL\_back2} := P_{LL\_back2\_D} + P_{LL\_back2\_P}$ $P_{LL\_back2} = 18160\ lbs$

Right Lane Truck Axle Loads

$P_{RL\_front\_D} := 7960\ lbs$ $P_{RL\_front\_P} := 7300\ lbs$

$P_{RL\_back1\_D} := 9980\ lbs$ $P_{RL\_back1\_P} := 9800\ lbs$

$P_{RL\_back2\_D} := 9920\ lbs$ $P_{RL\_back2\_P} := 9640\ lbs$

$P_{RL\_front} := P_{RL\_front\_D} + P_{RL\_front\_P}$ $P_{RL\_front} = 15260\ lbs$

$P_{RL\_back1} := P_{RL\_back1\_D} + P_{RL\_back1\_P}$ $P_{RL\_back1} = 19780\ lbs$

$P_{RL\_back2} := P_{RL\_back2\_D} + P_{RL\_back2\_P}$ $P_{RL\_back2} = 19560\ lbs$

3. Load Taken By Gider of Interest

$P_{front} := LLDF_{LL} \cdot P_{LL\_front} + LLDF_{RL} \cdot P_{RL\_front}$ $P_{front} = 5129$ lbs

$P_{back1} := LLDF_{LL} \cdot P_{LL\_back1} + LLDF_{RL} \cdot P_{RL\_back2}$ $P_{back1} = 6078$ lbs

$P_{back2} := LLDF_{LL} \cdot P_{LL\_back2} + LLDF_{RL} \cdot P_{RL\_back2}$ $P_{back2} = 5962$ lbs

4. Determine Moment In Girder

Using an influence line for the moment at 1.50, the max influence can be found by applying a unit load at midspan and calculating the corresponding moment:

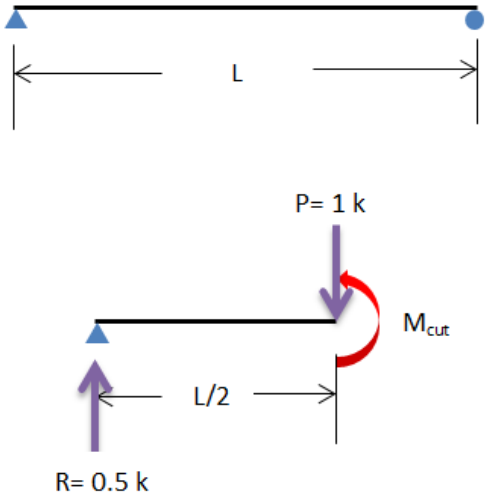

$L := 50 \ ft$

Sum moments about the cut:

$M_{cut} := 0.5 \cdot 0.5 \cdot L$ $M_{cut} = 12.5 \ \frac{k - ft}{k}$

Influence Line:

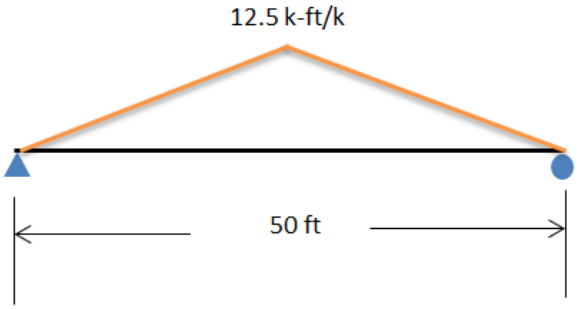

Determine Truck Moment:

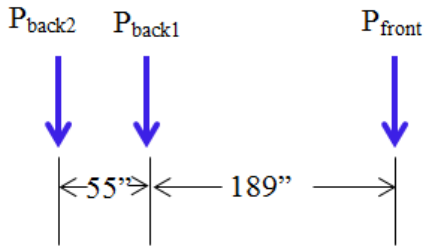

$$influence_{back2} := 0.5\cdot\left(\frac{L}{2} - \frac{55}{12}\right) \qquad influence_{back2} = 10.208 \quad \frac{k-ft}{k}$$

$$influence_{back1} := 0.5\cdot\frac{L}{2} \qquad influence_{back1} = 12.5 \quad \frac{k-ft}{k}$$

$$influence_{front} := -0.5\cdot\left(\frac{L}{2} + \frac{189}{12}\right) + 25 \qquad influence_{front} = 4.625 \quad \frac{k-ft}{k}$$

$$M_{truck} := influence_{back2}\cdot\frac{P_{back2}}{1000} + influence_{back1}\cdot\frac{P_{back1}}{1000} + influence_{front}\cdot\frac{P_{front}}{1000}$$

$M_{truck} = 161$ k – ft

5. Compare to Cracking Moment

$f_c := 5500$ psi

Note: The As-Built drawings specify 5000 psi concrete for the girders but it is assumed the contractor ordered a slightly stronger mix

$$f_r := 7.5\cdot\sqrt{f_c} \qquad f_r = 556 \quad psi$$

From Excel Sheet Section Properties: $I_{tr} := 254604$ in^4 $y_{bot} := 32.575$ in

$$M_{cr} := \frac{f_r\cdot I_{tr}}{y_{bot}}\cdot\frac{1}{12000} \qquad M_{cr} = 362 \quad k-ft$$

$M_{truck} = 161$ k – ft < $M_{cr} = 362$ k – ft

6. Determine Strain at Bottom of Girder:

$$E_c := 57\cdot\sqrt{f_c} \qquad E_c = 4227 \quad ksi$$

$$\varepsilon_{bot} := \frac{(M_{truck}\cdot 12)\cdot y_{bot}}{I_{tr}\cdot E_c}\cdot 10^6$$

$\varepsilon_{bot} = 58.3$ microstrain

7. Compare to Actual Experimental Strains

Strain value for damaged girder: $\varepsilon_{bot\_exp} := 42.55$ microstrain

Undamaged extrapolation value for bottom of girder: $\varepsilon_{bot\_extrapolated} := 33.84$ microstrain